HYDRODYNAMIC FORCES AND MOMENTS ON A SUBMERGED BODY OF REVOLUTION RESULTING FROM A FAIRWATER AND CONTROL SURFACES

Joseph James Luckard, Jr.

Massachusetts Institute of Technology

Prepared for:

Naval Ship Research and Development Center

June 1973

Security Classification

i

DOCUMENT CONTROL DATA - R & D AD-776 196

(Security classification of title, body of abstract and indexing annotation must be entered when the overall report is classified)

1. ORIGINATING ACTIVITY (Corporate author)
DEPARTMENT OF OCEAN ENGINEERING
MASSACHUSETTS INSTITUTE OF TECHNOLOGY
CAMBRIDGE, MASSACHUSETTS 02139

2a. REPORT SECURITY CLASSIFICATION
UNCL

2b. GROUP
N/A

3. REPORT TITLE
HYDRODYNAMIC FORCES AND MOMENTS ON A SUBMERGED BODY OF REVOLUTION RESULTING FROM A FAIRWATER AND CONTROL SURFACES

4. DESCRIPTIVE NOTES (Type of report and inclusive dates)
THESIS

5. AUTHOR(S) (First name, middle initial, last name)
JOSEPH JAMES LUCKARD, JR.

6. REPORT DATE
MAY 1973

7a. TOTAL NO. OF PAGES
198

7b. NO. OF REFS
15

8a. CONTRACT OR GRANT NO.
N00014-67-A-0204-0058 new

b. PROJECT NO.
SR 023 01 01

c.

d.

9a. ORIGINATOR'S REPORT NUMBER(S)
N/A

9b. OTHER REPORT NO(S) (Any other numbers that may be assigned this report)

10. DISTRIBUTION STATEMENT
APPROVED FOR PUBLIC RELEASE: DISTRIBUTION UNLIMITED

11. SUPPLEMENTARY NOTES

12. SPONSORING MILITARY ACTIVITY
Naval Ship Research & Development Center
Bethesda, Maryland 20034

13. ABSTRACT

This thesis involves an investigation of the hydrodynamic forces and moments on a submerged body of revolution, resulting from the addition of an asymmetric fairwater, and hull-control surfaces, and the results of their interactions.

This investigation involved both experimental and numerical models. Experimental tests were perfromed in the M.I.T. Variable Pressure Water Tunnel on a fairwater model, with independently-controlled hydroplanes, and on a sub mersible model, whose configuration was systematically altered by the addition of a fairwater and control surfaces. Graphical results for both of these models are presented. Flow visualization tests were also performed on the submersible model in order to observe the change in flow past the body of revolution and control surfaces caused by the asymmetric fairwater and its resulting downwash. Photographic results of these tests are presented.

A preliminary numerical model (Fortran language) for the prediction of forces and moments, based on potential theory and vorticity distributions, is presented and its results compared with those obtained experimentally.

DD FORM 1 NOV 65 1473 (PAGE 1)

S/N 0101-807-6801

Security Classification

ia

14 KEY WORDS	LINK A		LINK B		LINK C	
	ROLE	WT	ROLE	WT	ROLE	WT
HYDRODYNAMIC FORCES HULL CONTROL SURFACES						

"HYDRODYNAMIC FORCES AND MOMENTS ON A SUBMERGED BODY OF REVOLUTION RESULTING FROM A FAIRWATER AND CONTROL SURFACES"

By Joseph James Luckard, Jr.

B.S., United States Naval Academy

1965

Department of Ocean Engineering
Massachusetts Institute of Technology

Supported by:

Naval Ship Systems Command General Hydromechanics Research Program, administered by the Naval Ship Research and Development Center, Office of Naval Research Contract N00014-67-A-0204-0058

June 1973

(Submitted in partial Fulfillment of the Requirements for the Degree of Naval Architect at M.I.T. THESIS)

ic

HYDRODYNAMIC FORCES AND MOMENTS ON A SUBMERGED BODY OF REVOLUTION RESULTING FROM A FAIRWATER AND CONTROL SURFACES

by

JOSEPH JAMES LUCKARD JR.

B.S., United States Naval Academy

1965

SUBMITTED IN PARTIAL FULFILLMENT

OF THE REQUIREMENTS FOR THE

DEGREE OF NAVAL ARCHITECT

at the

MASSACHUSETTS INSTITUTE OF

TECHNOLOGY

June, 1973

Signature of Author.....Joseph James Luckard Jr.....
Department of Ocean Engineering
May 11, 1973

Certified by.....Damon E. Wilson Cummings.....
Thesis Supervisor

Accepted by.....
Chairman, Departmental Committee
on Graduate Students

HYDRODYNAMIC FORCES AND MOMENTS ON A SUBMERGED BODY OF REVOLUTION RESULTING FROM A FAIRWATER AND CONTROL SURFACES

by

Joseph James Luckard Jr.

Submitted to the Department of Ocean Engineering on May 11, 1973 in partial fulfillment of the requirements for the degree of Naval Architect.

ABSTRACT

This thesis involves an investigation of the hydrodynamic forces and moments on a submerged body of revolution, resulting from the addition of an asymmetric fairwater, and hull-control surfaces, and the results of their interactions.

This investigation involved both experimental and numerical models. Experimental tests were performed in the M.I.T. Variable Pressure Water Tunnel on a fairwater model, with independently-controlled hydroplanes, and on a submersible model, whose configuration was systematically altered by the addition of a fairwater and control surfaces. Graphical results for both of these models are presented. Flow visualization tests were also performed on the submersible model in order to observe the change in flow past the body of revolution and control surfaces caused by the asymmetric fairwater and its resulting downwash. Photographic results of these tests are presented.

A preliminary numerical model (Fortran language) for the prediction of forces and moments, based on potential theory and vorticity distributions, is presented and its results compared with those obtained experimentally.

Thesis Supervisor: Dr. Damon E. Cummings
Title: Visiting Lecturer

ACKNOWLEDGEMENT

The author would like to express his appreciation for assistance, support, and advice throughout this project to Dr. Damon E. Cummings, project supervisor, whose proposal initiated this project, sponsored by the General Hydrodynamics Research Program of NSRDC; and to Dr. J. N. Newman, whose participation helped to broaden my background in hydrodynamics.

Thanks are also extended to Dean Lewis, Engineer in charge of the Hydrodynamics Laboratory (water tunnel), for his time, effort and interest expended during the experimental portion of this project; and to Alice Pobuda for her perseverance in the expert typing of this thesis.

Finally, I would like to extend my appreciation to my wife Kathi, not only for the proofreading of this thesis, but also for her understanding throughout the last two and one half years, so that this culmination could be achieved.

TABLE OF CONTENTS

LIST OF FIGURES

I. INTRODUCTION

In March 1971, a technical proposal was submitted by the Department of Naval Architecture and Marine Engineering, now the Department of Ocean Engineering, Massachusetts Institute of Technology, to the General Hydrodynamics Research Program of the Naval Ship Research and Development Center to investigate hull-control surface interactions on submerged bodies, to include the effects imposed on the body by the fairwater and rudders (1). This proposal was divided into two problem areas: the constant yaw angle case, and the unsteady (time dependent) state case. This thesis will cover investigation performed in the first problem area of the project, that of the steady angle of attack in the horizontal plane. Particular items of interest are:

A. The geometry of the trailing vortex sheet shed from the fairwater when operating at an angle of attack. Where is the sheet with respect to the hull, and control surfaces downstream, such as the rudder? What velocities are induced on the hull and rudder by the trailing vortex sheet, and what forces and moments result from this interaction?

B. The lift generated on the fairwater due to side (sway) velocity when operating at an angle of attack. Besides the external trailing vortex sheet described above in A, an image system of trailing vorticity is required within the hull

surface to satisfy the boundary condition of zero velocity normal to the hull surface, and Kelvin's theorem of conservation of circulation. A net circulation around the hull of a submersible, aft of the fairwater, is implied by this reasoning. The combination of this net circulation and sway velocity leads to a net lift on the hull. This resultant lift resolves itself into a heave force and pitch moment excitation, which must either be compensated for by the vehicle control system, or result in an unanticipated coupling between yaw, heave and pitch motions of the vehicle. Nonsymmetric design of most submersibles, caused by the single fairwater, also combines with this resultant side force (lift component) into a roll moment on the vehicle.

Quantitative assessment of these forces and moments were investigated by experimental, analytical and numerical procedures. Experimental results were necessary to determine actual forces and moments experienced on a submerged body, to visually observe resulting hydrodynamic effects, and to be used as a basis of comparison for numerical results. To satisfy the primary objective of the project, a general and useable motion control prediction model, both analytical and numerical modeling were used.

Experimental results are presented for a fairwater model and a submersible model of different configurations.

Theoretical results, based on another part of this GHR project in which Newman and Rodriguez investigated a linearized low-aspect ratio slender body theory, are compared with the applicable experimental results of this project.

Some numerical results are presented also, but are not final. Continuing modifications are being made to the computer program for the most realistic results, before a final project report is submitted to the Navy in early fall 1973.

Dr. Damon E. Cummings was the project supervisor and Dr. J. N. Newman was a participating faculty member throughout this investigation.

II. BACKGROUND

The design of submersible vehicles has changed drastically since the first successful American military submarine was built in the 19th century by the Holland Torpedo Boat Company. This first vessel, the HOLLAND, had many basic design features which eventually were reinstituted into present day research and military submersible designs, especially since the development and design of the ALBACORE in 1950. This latter vessel was designed purposely to maximize submerged features at the expense of surface capabilities, emphasizing high submerged speed and maneuverability.

Particular hydrodynamic points of interest of HOLLAND to this investigation are:

1. A body of revolution hull form;
2. Little superstructure and no fairwater (sail), to minimize submerged resistance;
3. Stern planes and rudder surface located at the vertical centerline; and
4. Forward hydroplanes not employed.

The only features in military submarine and some research submersible design which have not returned to the HOLLAND configuration are the retention of the fairwater (sail) and forward hydroplanes, which are presently located on the fairwater (sail planes) for both military and hydrodynamic per-

formance purposes. Some research and test submersible vehicles have returned to the basic HOLLAND design in all aspects in an attempt to achieve an optimum submersible design.

Drag force components on a submersible resulting from appendages such as control surfaces, fairwater, shafts, and struts are of extreme importance when obtaining propulsion requirements for a particular vessel, but are of relatively minor importance when investigating stability and control. Much effort has been placed in this area for the last two decades to obtain an efficient design. This aspect will not be pursued in this report.

Present day submersible design has put an extraordinary requirement on stability and control. Although the military and research submersibles have vastly different performance capabilities, particularly the speed spectrums, the requirements of precise control and retention of stability remain. In particular, this is true for motions in the vertical plane, where a submersible must have the ability to operate, at slow or high speeds, within a relatively narrow vertical range. Full employment of a vessel's depth capabilities is desirable, but accidental penetration of depths beyond its maximum operating depth might lead to disaster. Nor is accidental broaching of the surface of the water a desirable maneuver in both the military and the research submersibles. Although

the horizontal plane is usually not as narrow ranged as the vertical, horizontal motions are important, especially in restricted waterways.

In the vertical (and horizontal) plane there are basically four performance criteria: (2)

1. Ability to maintain constant depth (course) with minimum plane movement and minimum depth (course) error;
2. Ability to enter into a maneuver as rapidly as possible;
3. Ability to exit from a maneuver as rapidly as possible;
4. Ability to return to equilibrium as quickly as possible when the controls are returned to zero.

An additional performance criterion only in the horizontal plane is the ability to execute a steady-turning maneuver with minimum tactical diameter, advance, transfer, loss of speed, and with minimum cross-coupled motions such as roll.

Most recent submarines have been equipped with fairwater (sail) planes, rather than bow planes, to reduce noise, alleviate the requirement for retraction, and to gain larger span dimensions within the submarine block dimensions. It has been shown on operational submarines that the drag of the fairwater planes compares favorably with previously used bow planes, even though fairwater planes have about 75% more

relative area. This same comparison shows 85% more relative vertical force, although only 20% more moment for fairwater planes than bow planes, because of the reduction in length of the moment arm (2).

For high speed maneuvering, forward hydroplanes are redundant. Depth changes can more readily be obtained by adjusting the angle on the stern planes, rather than applying a force close to the center of gravity. At low speeds, forward hydroplanes do make depth control somewhat easier.

Forward hydroplanes are desirable to help compensate for the nonsymmetrical hull form in the vertical plane, re-resulting from the fairwater, and to create a hydrodynamic vertical force and hydrodynamic moment in the vertical plane.

The hydrodynamic effects caused by asymmetry occur even when the hull body axis is parallel to the inflow velocity due to drag on the fairwater. In order to compensate for this effect and maintain constant depth, a hull angle of attack and a stern plane angle must be present, and are referred to as neutral angles of a particular vessel. These angles depend on the size of the fairwater and inflow velocity vector. If inflow velocity is assumed to be maintained horizontal, these angles introduce a pitch angle on the vessel equal to the hull angle of attack. This pitch angle in turn introduces a speed-dependent longitudinal metacentric moment, which is

the reason why the hull angle of attack and stern plane angle are speed-dependent. A critical range occurs at very slow speeds, in which the required angles for constant depth are too great to be accomplished by the stern planes only. Forward planes become a necessity at this time to reduce the magnitude of the requirements on the stern planes.

In the horizontal plane, the performance criterion that a vessel have the ability to execute a steady-turning maneuver with minimum tactical diameter, advance, transfer, loss of speed, and, in particular, minimum crosscoupled motions is of extreme importance and will require the major portion of this investigation for a valid understanding.

Of particular interest are the effects that a fairwater has on the above performance criterion concerning the steady-turning maneuver. The fairwater causes an increase in roll angle during a turn. One reason for this effect lies in the positions of the center of gravity (G), and center of buoyancy (B) of the vessel with respect to the axis of revolution of the hull body. When a submersible with a body of revolution, whose metacenter (M) is at the axis of symmetry because of wrap-around ballast tanks, is submerged completely, the waterplane area disappears. When this occurs, the location of the center of buoyancy (B) shifts from a position below the center of gravity (G) to one above. The location of the center of gravity (G), which has always been located below

the metacenter for the surfaced situation, is lowered even more by the added ballast. This low center of gravity, although increasing the roll stability of the vessel, introduces an asymmetry when the body of revolution is acted upon by hydrodynamic forces, in particular during a steady-turning maneuver. This occurs whether a fairwater is present or not, although it is more pronounced with a fairwater.

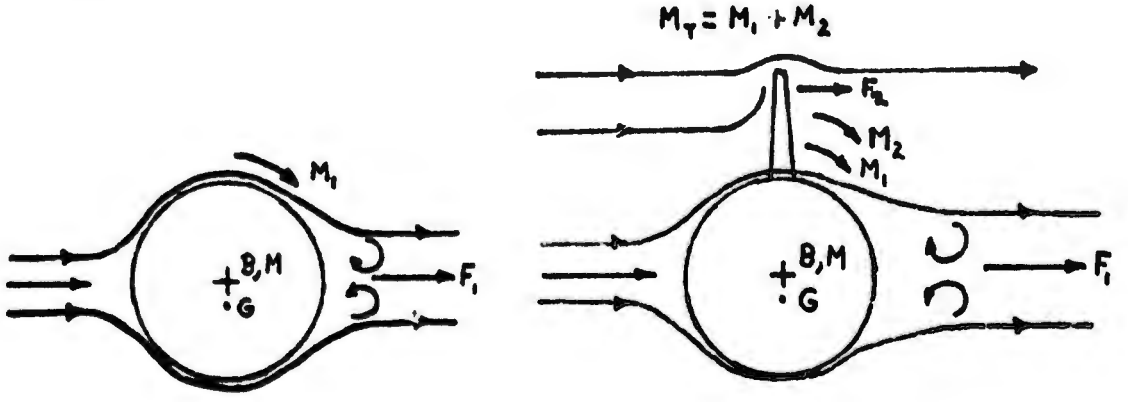

Fairwaters are located forward of the center of gravity; therefore, the hydrodynamic effects resulting in the horizontal plane during a steady turn are both stabilizing and destabilizing. Since the fairwater is essentially a lifting surface, it develops an effective lift force which is directed towards the turning circle center. This force, when combined with the vessel's velocity vector components, tends to decrease the angle of attack, which would be a stabilizing effect.

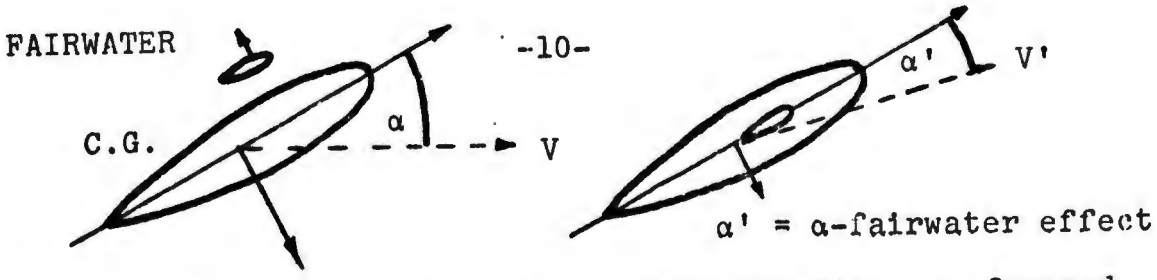

Yet, when this force is combined with the distance forward of the center of gravity, the resulting moment is destabilizing. It tends to increase the yaw moment on the vessel in the horizontal plane, thus effectively reducing the turning diameter, which is desirable. However, in the roll-heave plane, the point of action of the lift force on the fairwater induces a roll moment on the vessel that is undesirable. The total roll moment experienced by the submersible is not entirely due to the fairwater. Part of this roll moment results from the hydrodynamic side force acting on the body of revolution above the center of gravity (G), which is below the body axis, for stability reasons. Table 5 of reference 2 reports of a model tested with a fairwater at a speed of 20 knots, rudder angle of 35 degrees and in a steady turn, which resulted in an angle of heel of 11.3 degrees. When this same model was tested without the fairwater, the angle of heel was reduced, but still present at 2.5 degrees. It was also shown during these tests that removal of the fairwater increased the turning diameter by about 25 per cent.

Although this investigation is pursuing the hydrodynamic effects at constant angles of attack, a brief statement on

the transient phenomenon of "snap-roll" is of interest. Snap-roll describes what occurs shortly after the initiation of a turn, corresponds to the amplitude of the first half cycle of roll and is believed to be an overshoot phenomenon. After the snap-roll occurs, the roll angle decreases to the steady-roll value. Values for snap-roll in the model tests described in the last paragraph were 39 degrees for the model with fairwater, and 12.5 degrees when the fairwater was removed. As before, the effect of the location of the center of gravity below the axis of symmetry is evident (2).

Since snap-roll is so immediate and of such a large magnitude on high-speed submersibles, control response time and knowledge of a submersible's particular characteristics are of extreme importance. When the snap-roll occurs, in combination with a rudder angle on for the turn, a cross-coupling results in an effective diving attitude for the vessel. Although this effect can be alleviated by judicious handling of available control surfaces, a problem of overshoot can arise. As previously mentioned, snap-roll only lasts for a relatively short period of a turn, after which the steady-turn phase is incurred. As a result, the effective diving attitude decreases. If the correction imposed for snap-roll is not reduced accordingly, the vessel's attitude will be one of decreasing depth, with an extreme result of broaching.

III. METHODOLOGY

The purposes of the experiments reported on in this project were to investigate the hydrodynamic forces and moments that act on a submerged body in a steady flow both on a symmetrical slender body and on one to which appendages were added.

Possible methods were also investigated to redistribute the forces and moments to alleviate undesirable hydrodynamic effects caused by asymmetry, which is present in most submersible designs.

Measurement of Hydrodynamic Effects

Tests were conducted in the Variable Pressure Water Tunnel (see Appendix A) located in the Hydrodynamics Laboratory at M.I.T., see Figure 1. Measurement of the forces and moments on a particular model is accomplished through the application of a dynamometer which has six degrees of freedom, see Figures 2 and 3. These six degrees of freedom can be measured with respect to any point along the height of the test area. A computer program is used to deduce the three forces and three moments on the model being evaluated (see Appendix B). For the model tests covered in this project, coordinate systems were located at the center of the test area, along the axis of revolution of the submersible model,

see Figure 2, and at the tunnel wall, base of the fairwater model, see Figure 3.

Hydrodynamic Notation of Dynamometer Coordinate System

(With respect to model, about end of shaft)

FX - Surge - applied force on longitudinal axis

FY - Heave - applied force on vertical axis

FZ - Sway - applied force on transverse axis

MX - Roll - moment applied about the longitudinal axis

MY - Yaw - moment applied about the vertical axis

MZ - Pitch - moment applied about the transverse axis

Note: FXO, MXO, FZO, MZO, FYO, MYO are simultaneously-computed hydrodynamic effects from "general" dynamometer program for evaluation of model test in which results are desired with respect to water tunnel flow (free stream flow).

Experimental Models

Two different models were designed and built to measure the hydrodynamic forces and moments on a submerged body after symmetry to tunnel water flow is lost by the addition of appendages (fairwaters, control surfaces) and increased angle of attack (angular difference between free stream flow and body of appendage line of symmetry).

The two models include:

A) A streamlined body of revolution (tear-drop shape), with detachable fairwater sail and stern section, see Figures 4a, 5a and 6, to investigate the interaction effects of hydrodynamic forces and moments between a submersible hull, fairwater and control surfaces at various angles of attack and velocities (model hull and fairwater were constructed out of lucite; stern section and control surfaces were constructed out of brass).

The hull was constructed with a length (L) of 24.5 inches, a maximum diameter (D) of 3.5 inches occurring at a distance of 9.8 inches from the bow, resulting in a L/D ratio of 7.0. This slenderness and a fine stern should prevent most separation, and also enhance the applicability of slender body theory. The support shaft was located at a distance, from the bow, of 40 per cent of the model length; and

B) A fairwater with detachable and independent control surfaces, see Figures 4b, 5b, 6 and 7.

Construction of Fairwater and Control Surfaces

In conjunction with both model experiments, foil shapes were required for fairwater and control surfaces. The lucite fairwater (submersible model) and planes (fairwater model) were produced on a manual milling machine, from offsets developed from a computer program for this particular project (see Appendix C). This computer program is in a general form to meet any particular designs of thickness, chord length, taper, setback and foil design (NACA___). This program calculates steps of thickness along the length of chord and span to be milled. These depths of cut are determined by foil geometry, end mill size and step size between milling runs. After milling of the step functions, the foil is finished by hand.

The stern control surfaces (submersible model) were produced on the Gugger Profile machine, located in the Gas Turbine laboratory shop of Building 31 (Sloan Laboratories). This machine requires a 4:1, plus 1/2 inch, scale model of surface to be developed, and is limited in the width of model fed between cam follower surface. Extra 1/2 inch is added on to compensate for abrupt changes in model shape (trailing edge).

Since the rudders used for the submersible were of foil shape, with no taper or setback, a simplified model (cam) was

made of an NACA foil shape, see Figure 8. Extended lengths of the foil shape can be produced and divided into various lengths of span. Cam followers are adjustable, so foil chord and thickness dimensions can be varied within limits, while using the same model (cam).

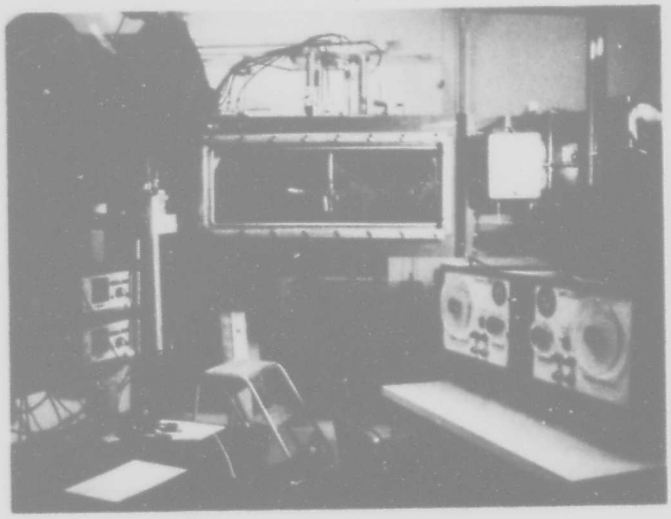

Figure 1 Variable Pressure Water Tunnel control and test section.

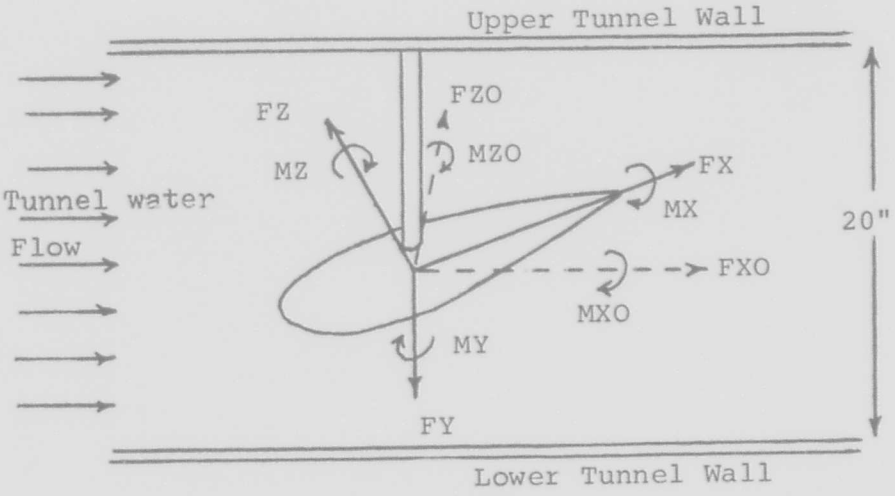

Figure 2 Dynamometer Coordinate System at center of model axis, center of tunnel.

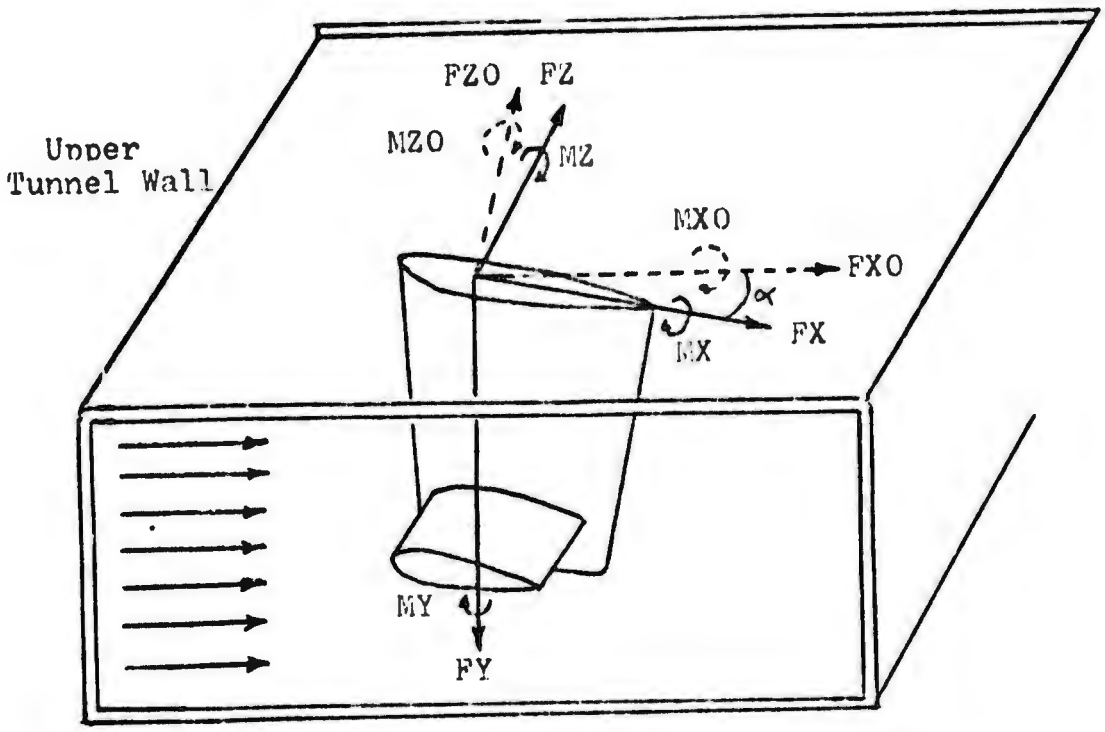

a. Dynamometer Coordinate System at base of model, against upper tunnel wall, at an angle of attack (α).

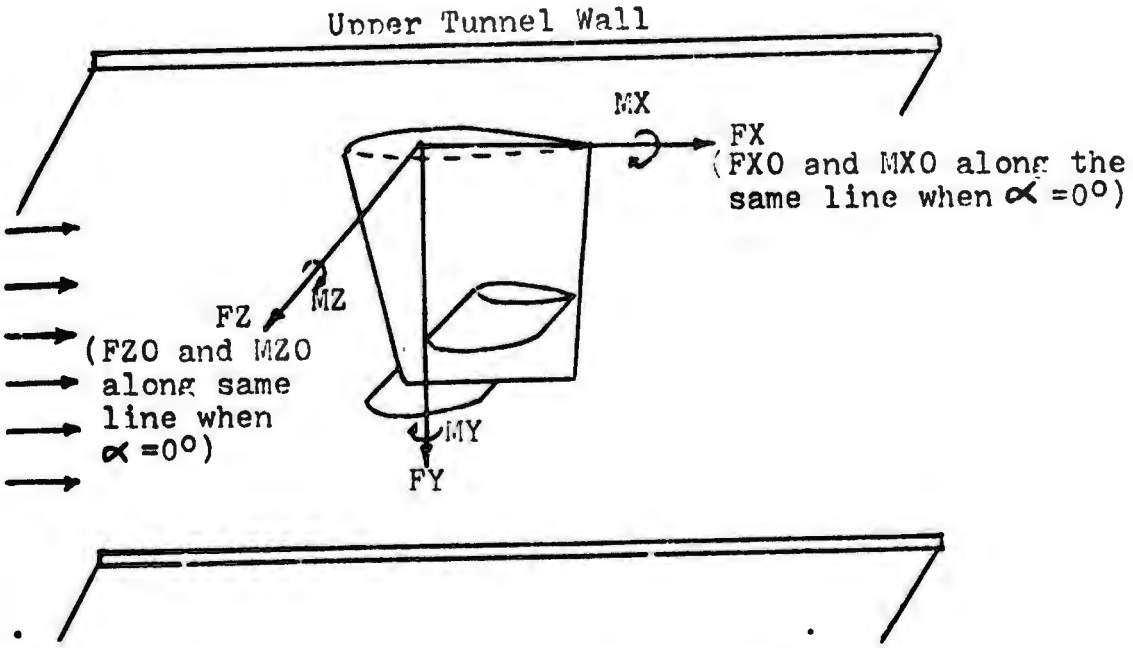

b. Dynamometer Coordinate System at base of model, against upper tunnel wall, parallel to tunnel flow.

Figure 3 Fairwater Coordinate System

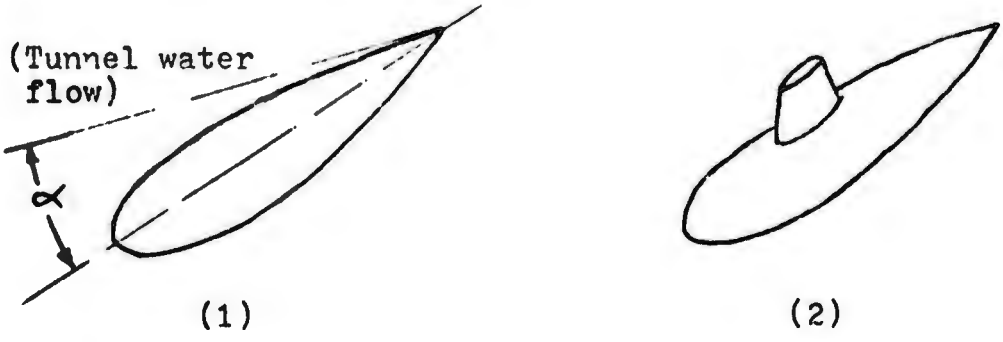

a. Streamlined body of revolution (tear-drop shape)

(1) without fairwater
(2) with fairwater

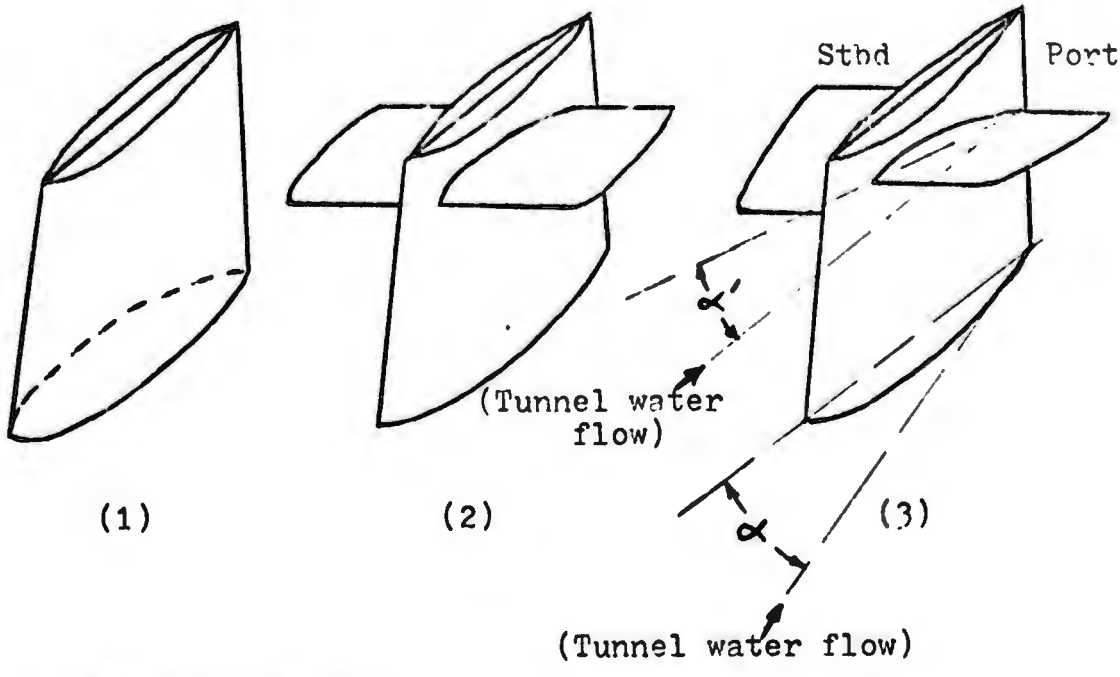

b. Fairwater design

(1) without control surfaces
(2) with control surfaces, at same angle of attack (α')
(3) with independent control surfaces, port side positive, and starboard(stbd) side negative angle of attack (α').

Figure 4 Model orientation

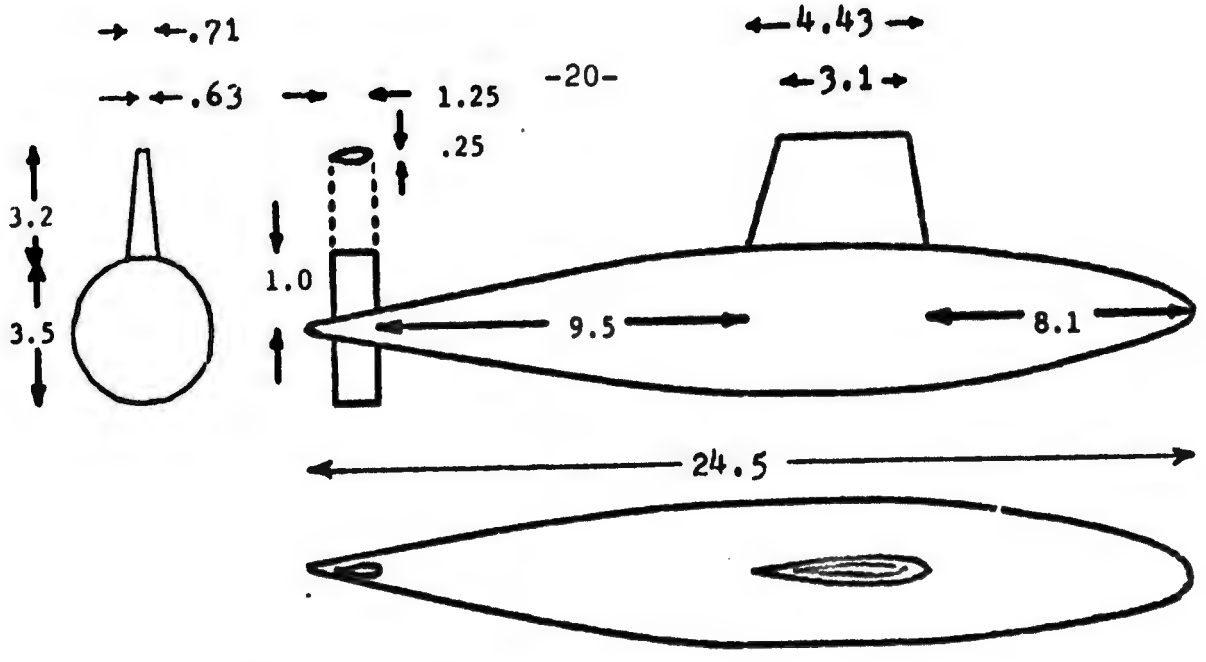

a. Submersible with fairwater

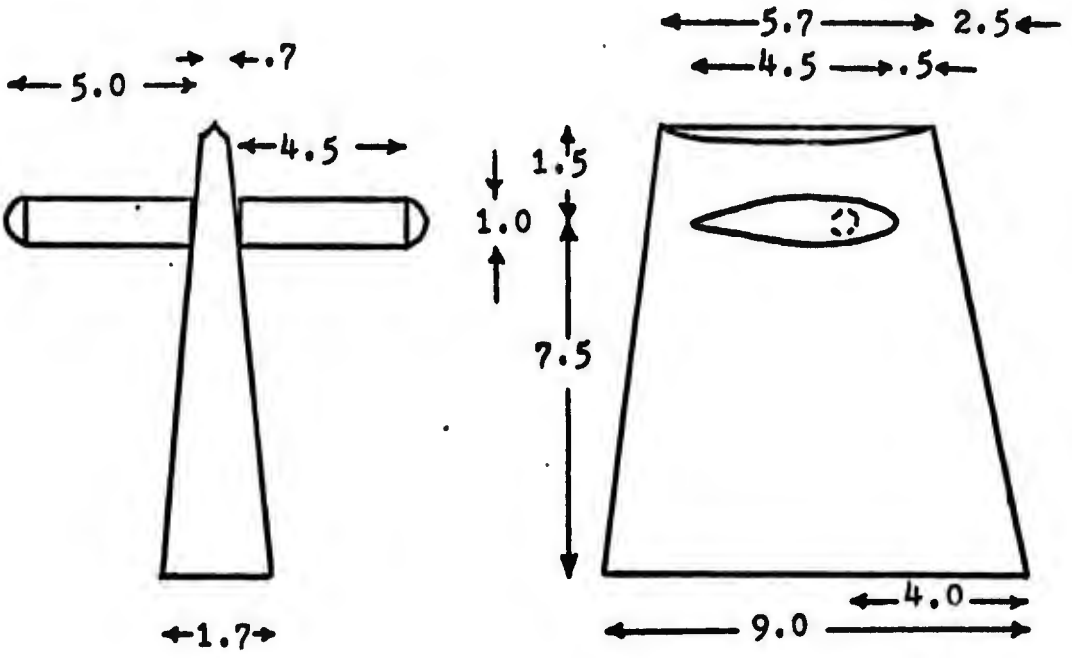

b.Fairwater with control surfaces

Figure 5 Model dimensions (inches)

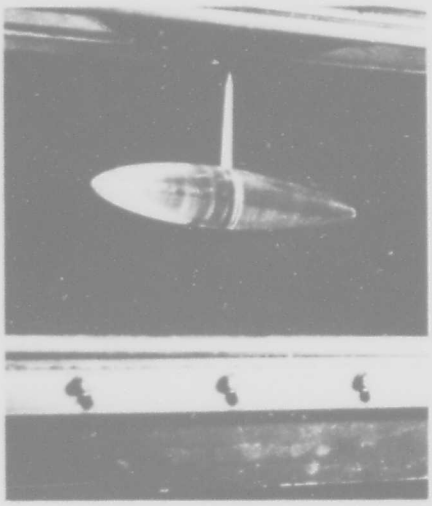

a. Oblique view without fairwater (Clean Hull).

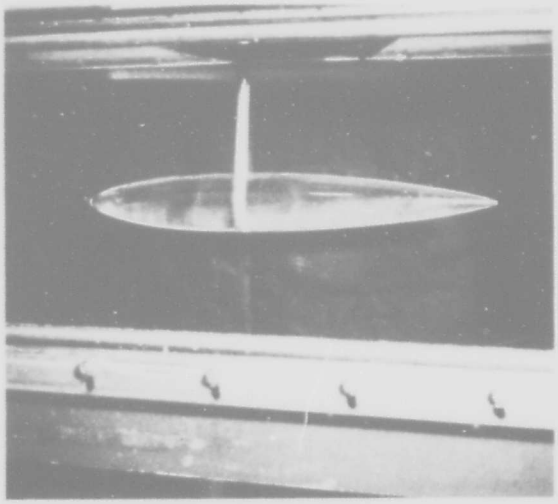

b. Side view without fairwater (Clean Hull).

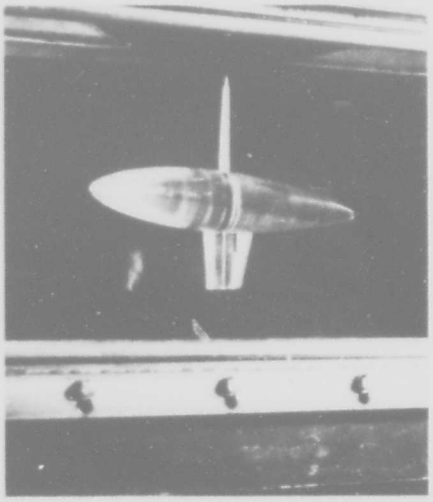

c. Oblique view with fairwater.

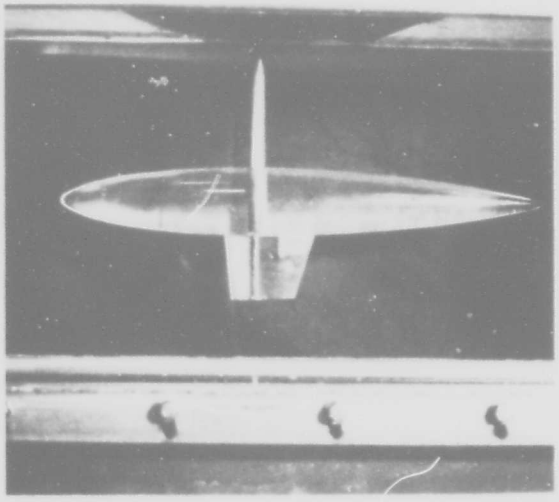

d. Side view with fairwater.

Figure 6 Submersible model

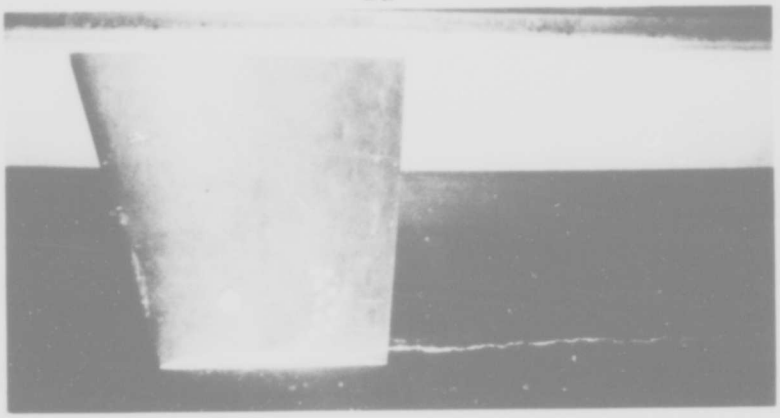

a. Side view of fairwater, without control surfaces. (Note support and guide locations used with control surfaces)

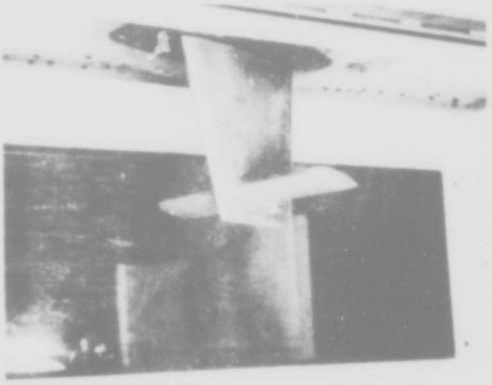

b. Oblique view, with control surfaces at $\alpha' = 0^{o}$.

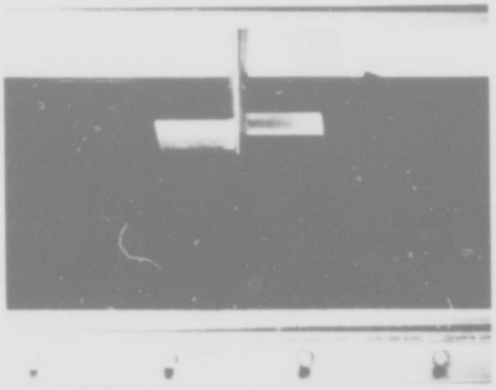

c. Front view, with control surfaces at $\alpha' = \pm 20^{o}$.

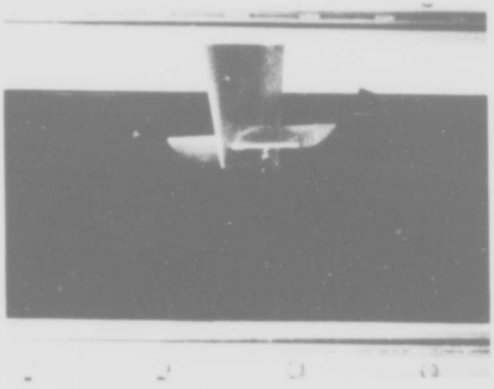

d. Oblique front view, with control surfaces at $\alpha' = \pm 20^{o}$.

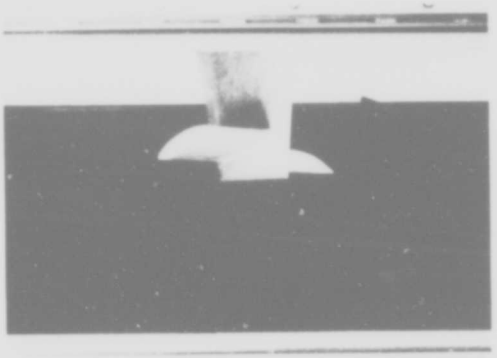

e. Oblique rear view, with control surfaces at $\alpha' = \pm 20^{o}$.

Figure 7 Fairwater model

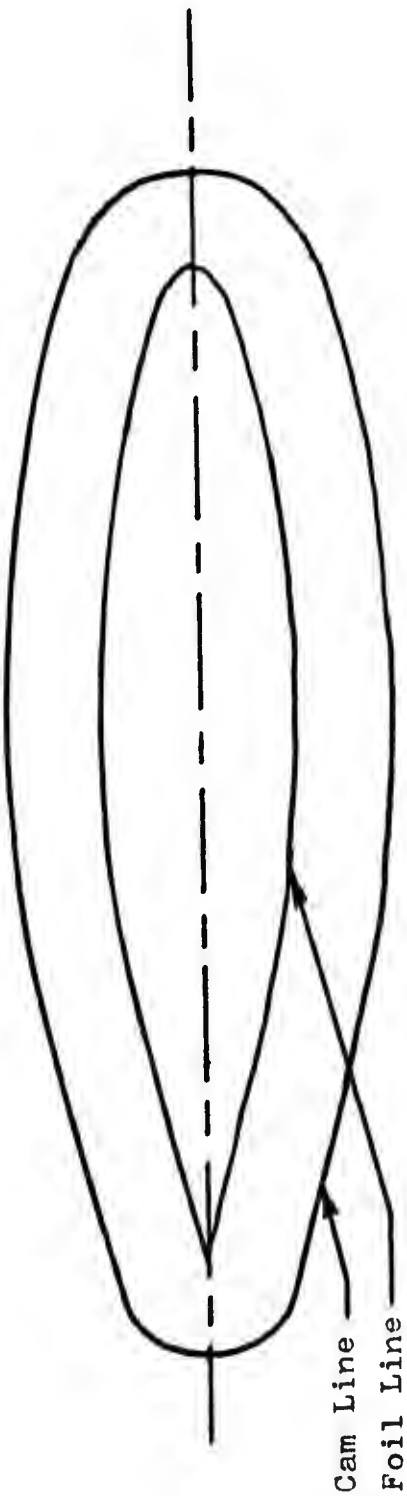

Cam pattern for rudders of submersible model
NACA 66-010
Chord = 1.25 inches
Thickness = .25 inches
Figure 8

IV. SUBMERSIBLE MODEL EXPERIMENTAL RESULTS

To experimentally investigate the hydrodynamic forces and moments on a submerged body of revolution, and how these effects are altered by the addition of appendages, the following different model configurations were tested:

1. clean hull (no appendages)
2. with fairwater
3. with fairwater and upper rudder
4. with fairwater, upper rudder and lower rudder.

Flow velocities of 10, 15 and 20 feet per second were used, and angles of attack in the yaw-sway plane were varied between $\pm$ 25 degrees for tests evaluated at 10 feet per second, and $\pm$ 15 degrees for tests evaluated at 15 and 20 feet per second.

Caution must be used when interpreting the experimental results obtained during this investigation. All photographs and graphical displays of the results are shown according to the coordinate system previously described. Therefore, it must be kept in mind at all times that the model and results are inverted, since the model is mounted upside down on the top of the tunnel.

The support shaft used during the submersible model testing was evaluated by testing a bare shaft to determine

the forces and moments it would experience in the water tunnel. These effects were then deducted from the model test, to obtain results representing only the model. The interactions caused by the shaft on the hull and control surfaces were not investigated, but must be considered when interpreting the experimental results. Also, the lower pressure at the exposed end of the base shaft, caused by the flow pattern past the shaft, was not considered.

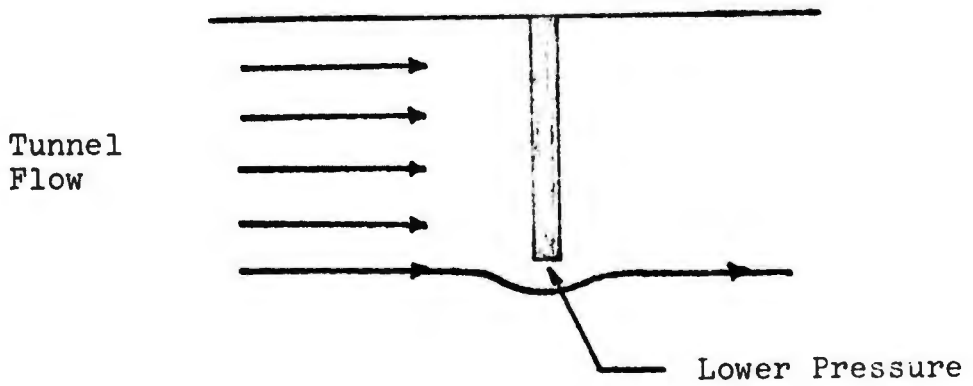

Heave Force (FYO)

1. Shaft Effect

Although the heave force on a bare support shaft, vertical and perpendicular to the flow, should have a constant value with respect to angle of yaw, the results obtained fluctuated and decreased for negative angles, see Figure 9. This is most likely a result of measuring accuracy of the dynamometer load cells used. An approximation was made to obtain a constant value of heave to be deducted from each model results, to alleviate the shaft effect. These values

were:

1) 1 lb, for a velocity of 15 ft/sec

2) 1.7 lb, for a velocity of 20 ft/sec

2. Model Results

When configuration 1 (clean hull) is tested, an initial negative heave force is registered at zero angle of yaw. According to the coordinate system used, this would appear as a downward force if the model were right side up. As the model is adjusted for both positive and negative angles of yaw, a symmetrical increasingly more positive result occurs, see Figures 10 and 11. There should not be any heave force on this symmetrical model configuration, but the results could possibly be caused by the model not being perfectly aligned in the tunnel test area, or support shaft interaction with the flow around the body.

Configuration 2 (with fairwater) induces a drastic change in the pattern of the heave force imposed on the model. The results follow that of configuration 1 up to $\pm$ 5 degrees yaw. After $\pm$ 5 degrees, the slope decreases rapidly, reversing and producing a heave force at $\pm$ 10 to $\pm$ 15 degrees yaw comparable to that experienced at zero angle of yaw, see Figures 10 and 11. Thus it would appear that the addition of the fairwater and its resulting trailing wake induces a circulation and velocity on the hull body which generates a

decreasing slope of heave force per degree yaw in the coordinate system used. This is comparable to an increasingly large force downward, if the model were in an upright position.

The sensitivity of the results can be seen from Figure 12, in which results of tests 3 and 5, conducted on different days, were compared to see if they were compatible. The magnitude of test 5 varied, but the curve followed the same characteristic pattern as test 3. This difference in magnitude could result from a small difference in model alignment in the water tunnel or variation in the calibration of the dynamometer system on different days.

When configuration 3 (fairwater and upper rudder) and configuration 4 (fairwater plus both rudders) were tested, there appeared to be no effective change from the result of configuration 2, see Figures 13 and 14. The circulation and trailing wake off the rudders did not have any afterbody on which to induce a heave force component.

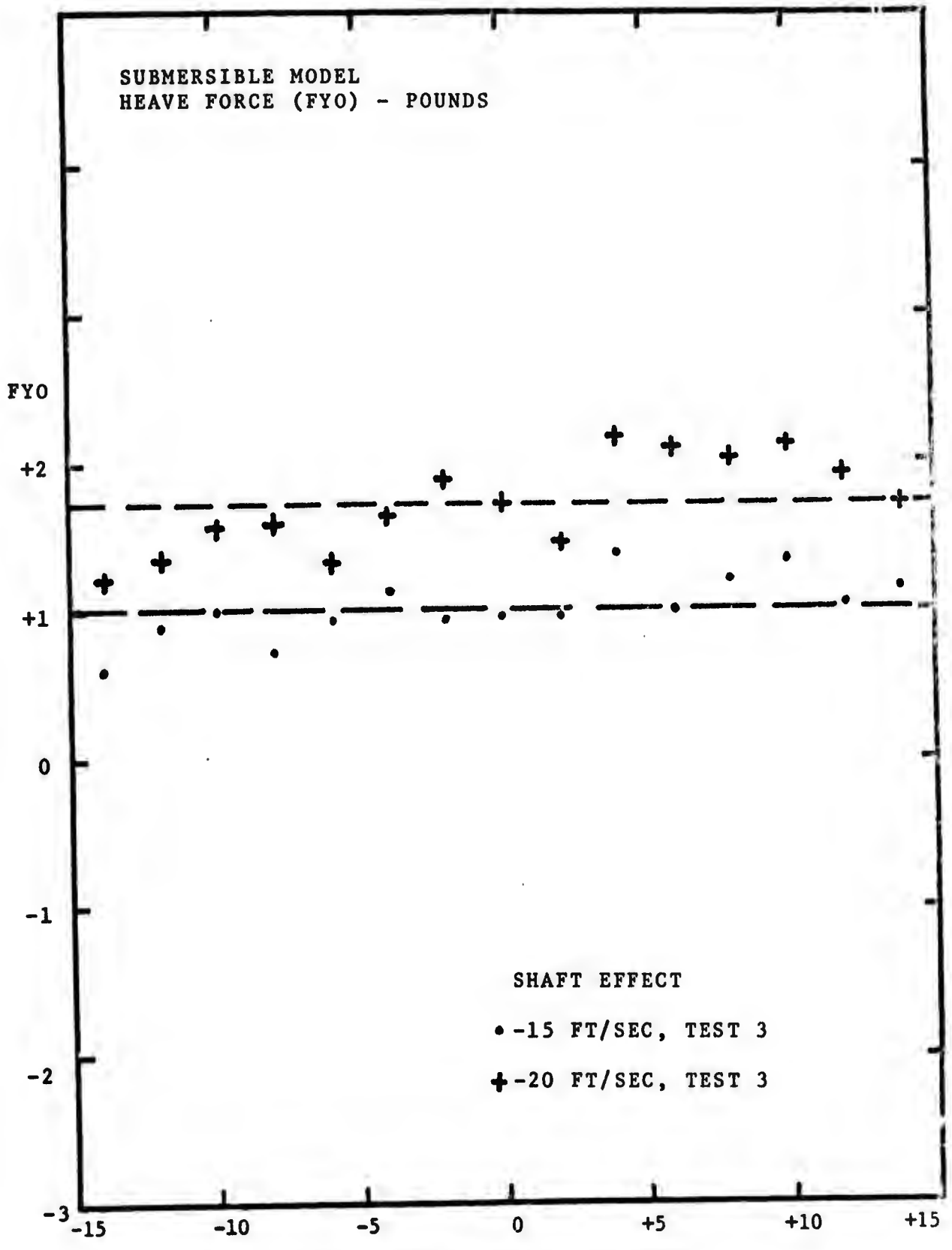
SUBMERSIBLE MODEL
HEAVE FORCE (FYO) - POUNDS
FYO
+2
+1
0
-1
-2
-3
-15
-10
-5
0
+5
+10
+15
SHAFT EFFECT
• -15 FT/SEC, TEST 3
+ -20 FT/SEC, TEST 3
Angle of Attack- (Degrees-Yaw)

Figure 9

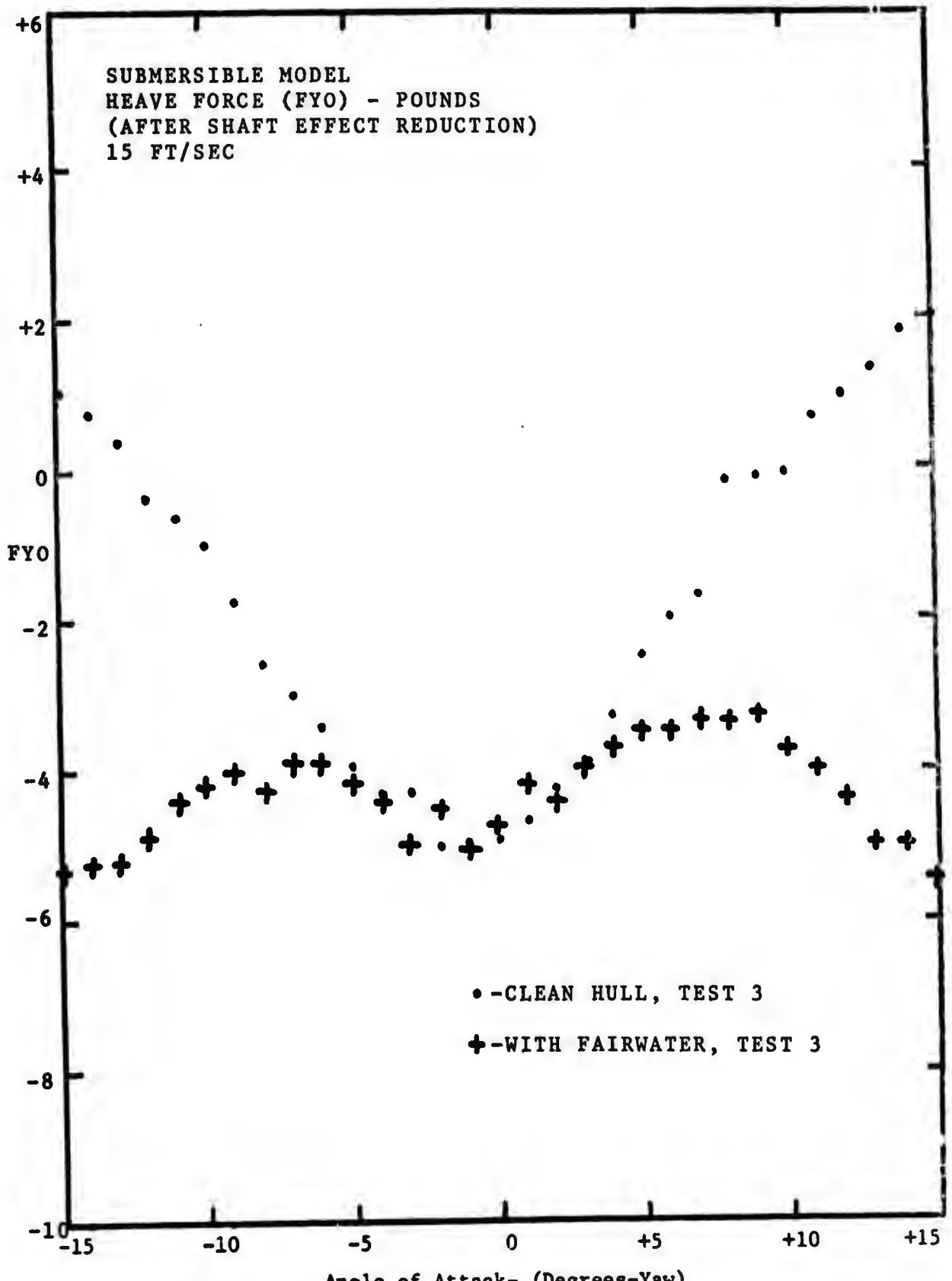
SUBMERSIBLE MODEL
HEAVE FORCE (FYO) - POUNDS
(AFTER SHAFT EFFECT REDUCTION)
15 FT/SEC
+6
+4
+2
0
-2
-4
-6
-8
-10
FYO
-15
-10
-5
0
+5
+10
+15
•-CLEAN HULL, TEST 3
✚-WITH FAIRWATER, TEST 3
Angle of Attack- (Degrees-Yaw)

Figure 10

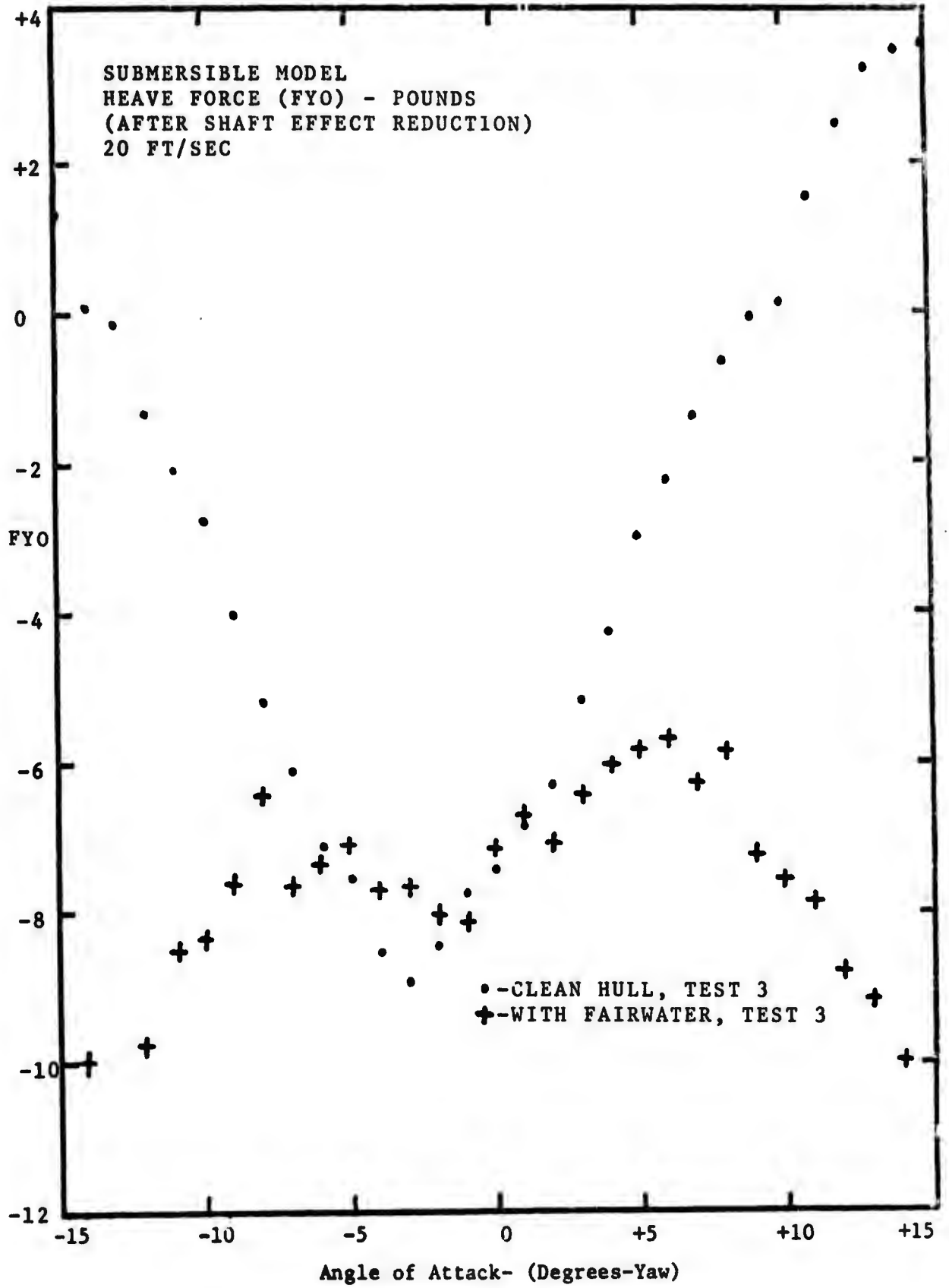
SUBMERSIBLE MODEL
HEAVE FORCE (FYO) - POUNDS
(AFTER SHAFT EFFECT REDUCTION)
20 FT/SEC
+4
+2
0
-2
FYO
-4
-6
-8
-10
-12
-15
-10
-5
0
+5
+10
+15
•-CLEAN HULL, TEST 3
+-WITH FAIRWATER, TEST 3
Angle of Attack- (Degrees-Yaw)

Figure 11

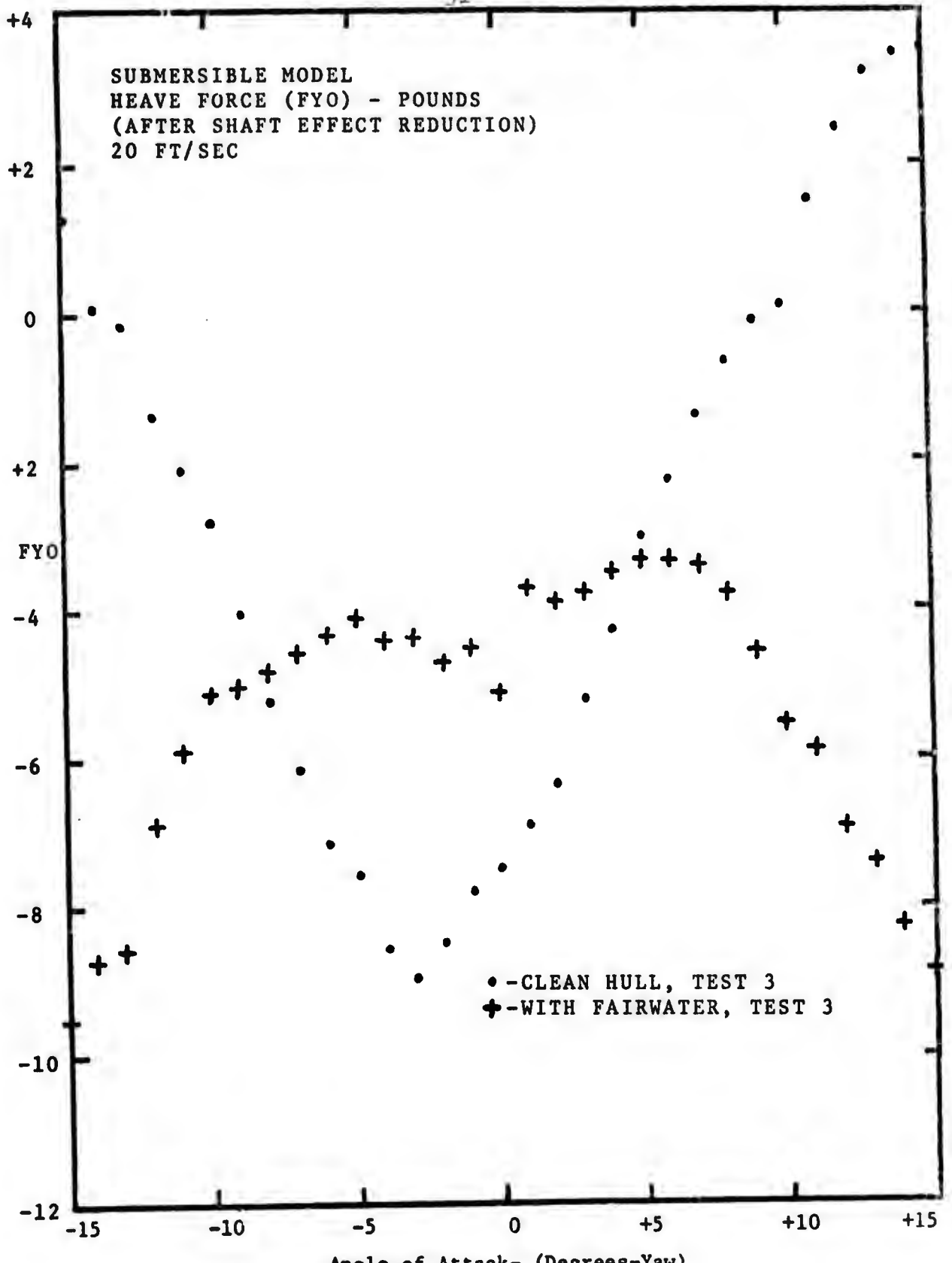
SUBMERSIBLE MODEL
HEAVE FORCE (FYO) - POUNDS
(AFTER SHAFT EFFECT REDUCTION)
20 FT/SEC
+4
+2
0
+2
FYO
-4
-6
-8
-10
-12
-15
-10
-5
0
+5
+10
+15
• -CLEAN HULL, TEST 3
+ -WITH FAIRWATER, TEST 3
Angle of Attack- (Degrees-Yaw)

Figure 12

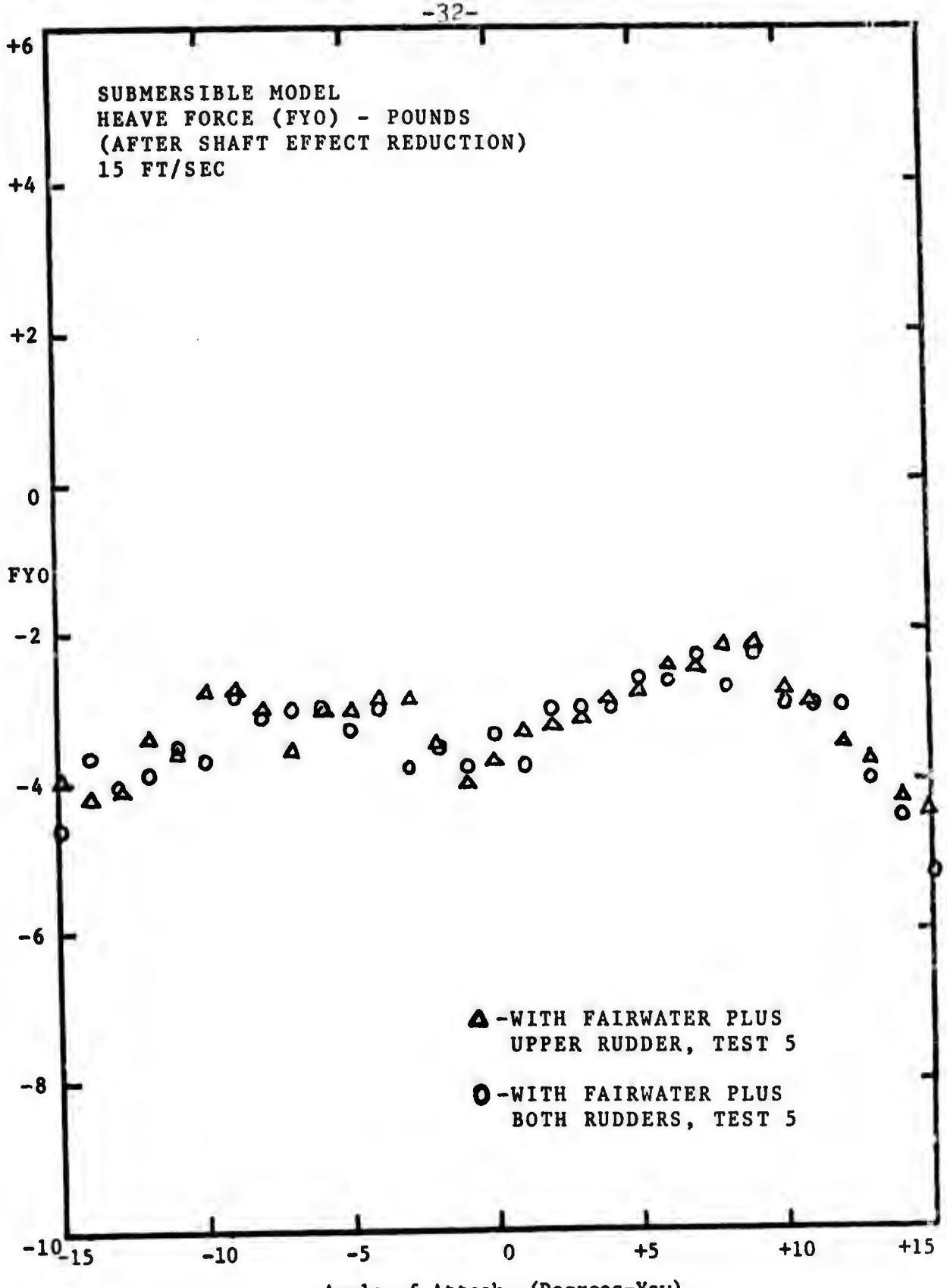
SUBMERSIBLE MODEL
HEAVE FORCE (FYO) - POUNDS
(AFTER SHAFT EFFECT REDUCTION)
15 FT/SEC
+6
+4
+2
0
FYO
-2
-4
-6
-8
-10
-15
-10
-5
0
+5
+10
+15
Δ -WITH FAIRWATER PLUS UPPER RUDDER, TEST 5
O -WITH FAIRWATER PLUS BOTH RUDDERS, TEST 5
Angle of Attack- (Degrees-Yaw)

Figure 13

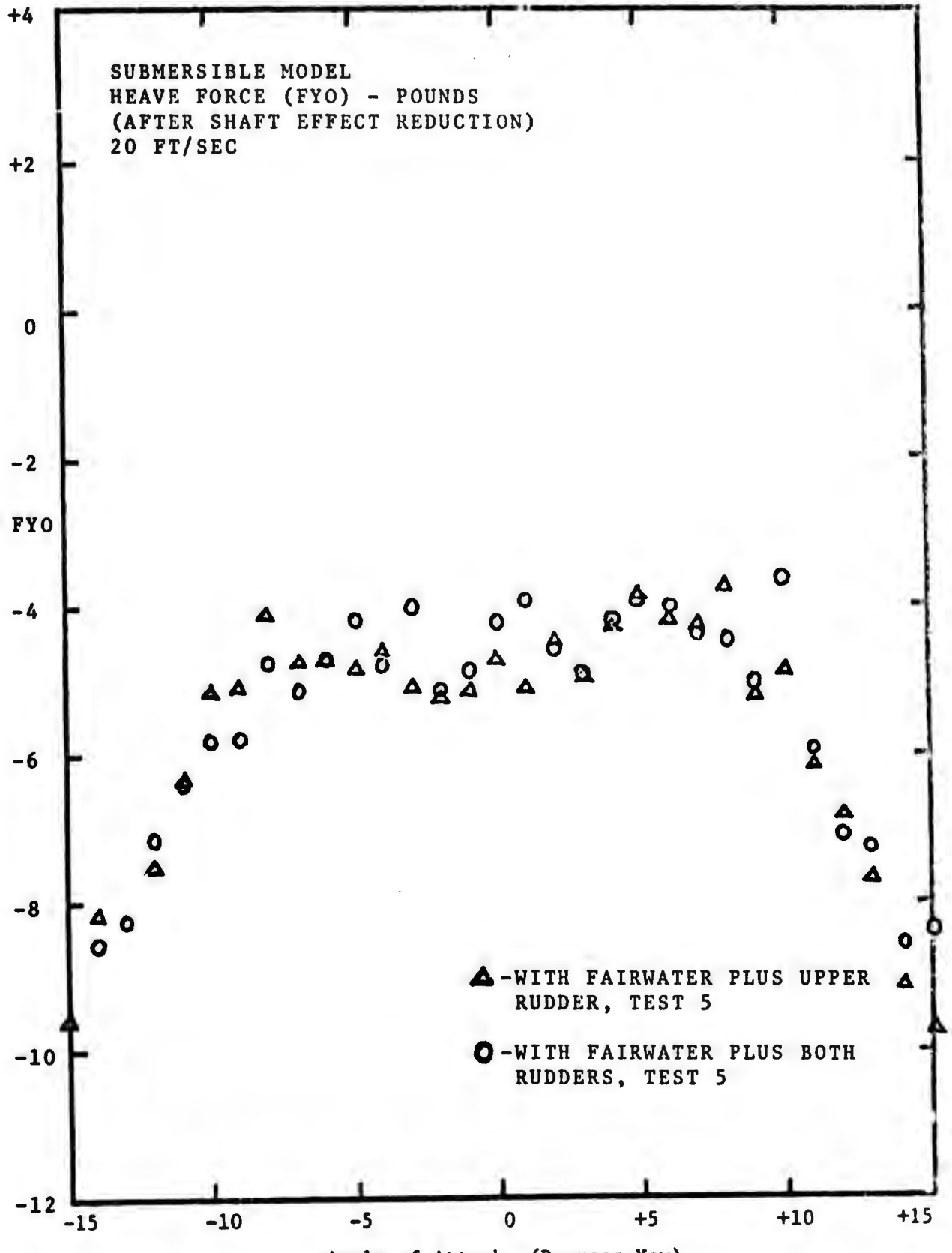
SUBMERSIBLE MODEL
HEAVE FORCE (FYO) - POUNDS
(AFTER SHAFT EFFECT REDUCTION)
20 FT/SEC
+4
+2
0
-2
FYO
-4
-6
-8
-10
-12
-15
-10
-5
0
+5
+10
+15
Angle of Attack- (Degrees-Yaw)
△-WITH FAIRWATER PLUS UPPER RUDDER, TEST 5
O-WITH FAIRWATER PLUS BOTH RUDDERS, TEST 5

Figure 14

Pitch Moment (MZ)

1. Shaft Effect

Since the pitch moment on the base shaft should decrease with increasing angle of yaw (α), the reduction factor ($\cos \alpha$) can be assumed to be unity for the range of deflection at which the shaft was evaluated (zero to $\pm$ 15 degrees). Therefore, the reduction for the shaft effect is assumed to be constant, and a mean value of the experimental results, at different velocities, can be deducted from the model test to arrive at values of pitch moment, for the different model configurations, which approach that of a non-supported model. The resulting mean values were:

1) 40 in-lb, for a velocity of 15 ft/sec, and

2) 71 in-lb, for a velocity of 20 ft/sec, see Figure 15.

2. Model Results

Pitch moment on the various model configurations followed the same pattern of results obtained for heave force. Configuration 1 (clean hull) produced a negative moment at zero angle of yaw and a steadily increasing moment, with a decreasing slope, as yaw angle is increased, see Figures 16 and 17. The negative moment at zero angle of yaw could be caused by model alignment, or shaft interactions. The flow past the shaft causes a high pressure area at the forward stagnation point and a low pressure area on the aft portion

of the circumference. Fairwater drag would also produce a similar effect, but the magnitude of the negative moment was equivalent to that obtained for configuration 1 (clean hull).

Configuration 2 (with fairwater) produced an increasing moment, which followed the results of configuration 1 between about $\pm$ 5 to $\pm$ 10 degrees, after which the pitch moment decreased, as fast as it had increased, see Figures 16 and 17. This result would be comparable to a submersible, in an upright position, experiencing an initial bow up pitch moment at zero angle of yaw. This is due to shaft-hull interaction, a minor model misalignment in the vertical plane, or possibly miscalibration of equipment. This is followed, with increasing angle of attack, by a bow down pitch moment, caused by a lift force on the hull aft of the fairwater. This is finally succeeded by a bow up pitch moment, resulting from the drag component of the fairwater, and the circulation and induced velocity from the fairwater on the aft section of the hull body.

As in the heave force results, pitch moment did not seem to be affected by the addition of the upper rudder (configuration 3), see Figures 18, 19 and 20, or when tested with both rudders attached (configuration 4), see Figures 19 and 21. Their induced velocities have very little effect on the hull, which precedes them in the fluid flow, and their wakes have no afterbody to affect either.

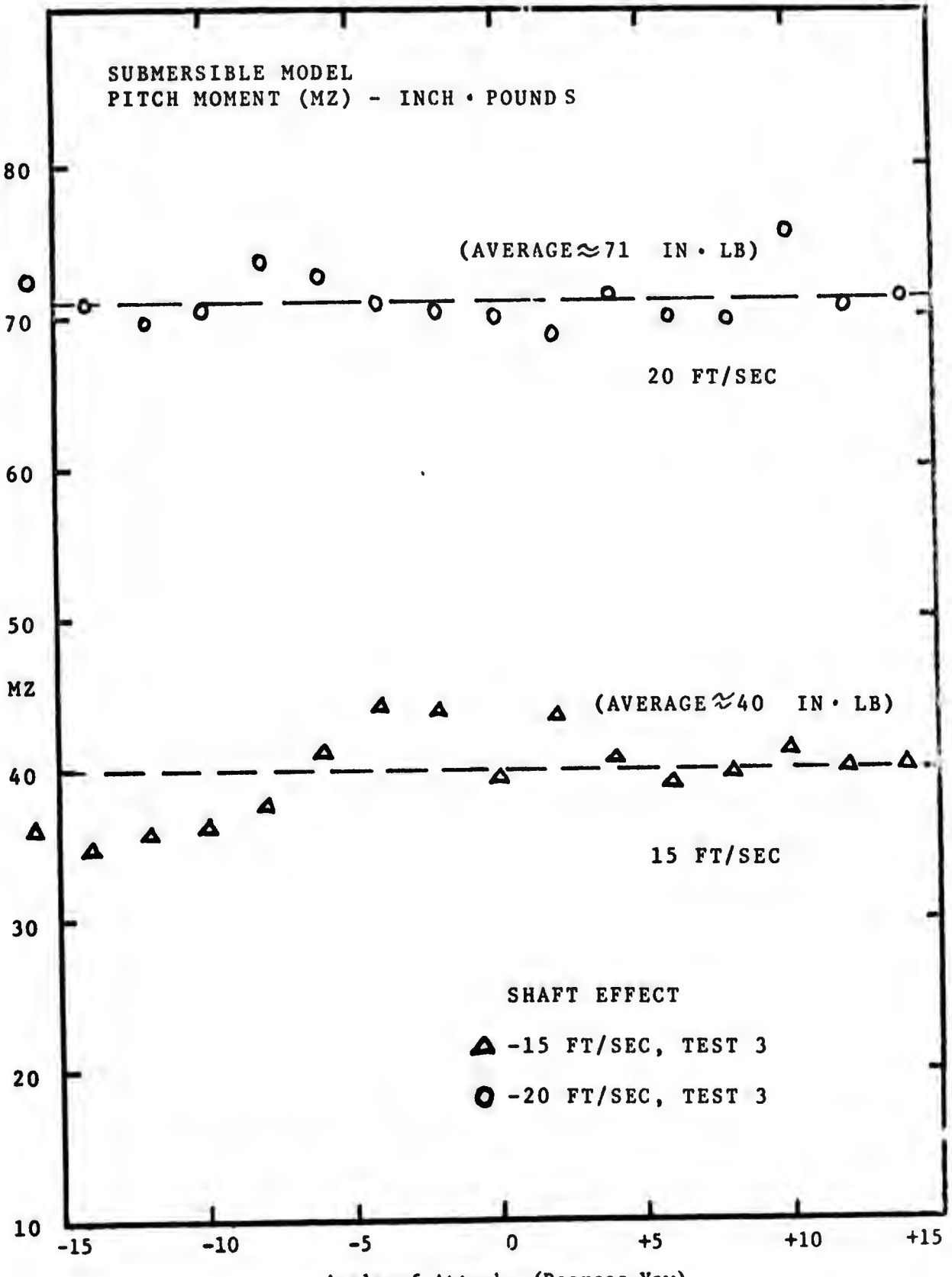
SUBMERSIBLE MODEL
PITCH MOMENT (MZ) - INCH • POUNDS
(AVERAGE≈71 IN • LB)
20 FT/SEC
(AVERAGE≈40 IN • LB)
15 FT/SEC
SHAFT EFFECT
-15 FT/SEC, TEST 3
-20 FT/SEC, TEST 3
MZ
80
70
60
50
40
30
20
10
-15
-10
-5
0
+5
+10
+15
Angle of Attack- (Degrees-Yaw)

Figure 15

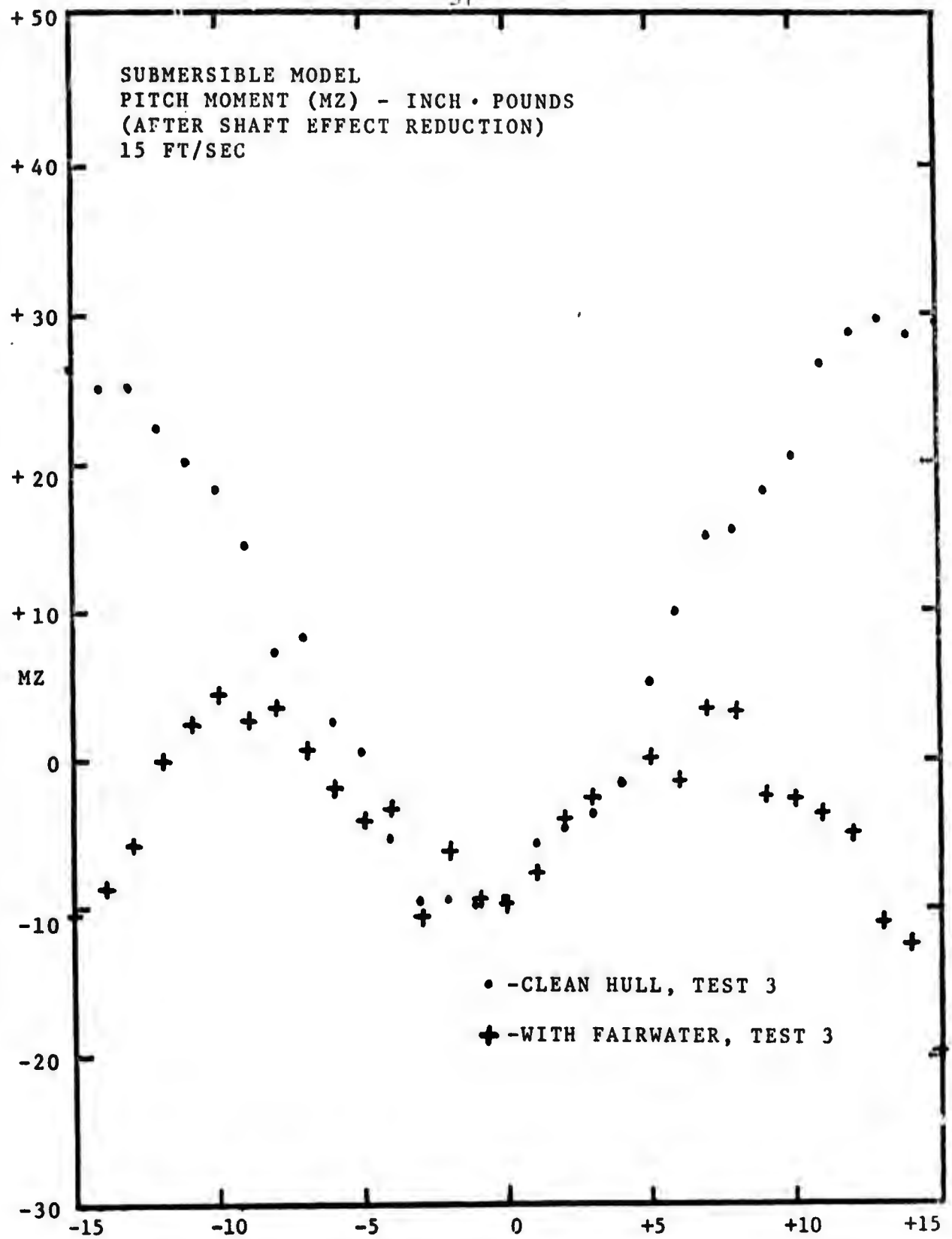
SUBMERSIBLE MODEL
PITCH MOMENT (MZ) - INCH • POUNDS
(AFTER SHAFT EFFECT REDUCTION)
15 FT/SEC
+50
+40
+30
+20
+10
MZ
0
-10
-20
-30
-15
-10
-5
0
+5
+10
+15
• -CLEAN HULL, TEST 3
+ -WITH FAIRWATER, TEST 3
Angle of Attack- (Degrees-Yaw)

Figure 16

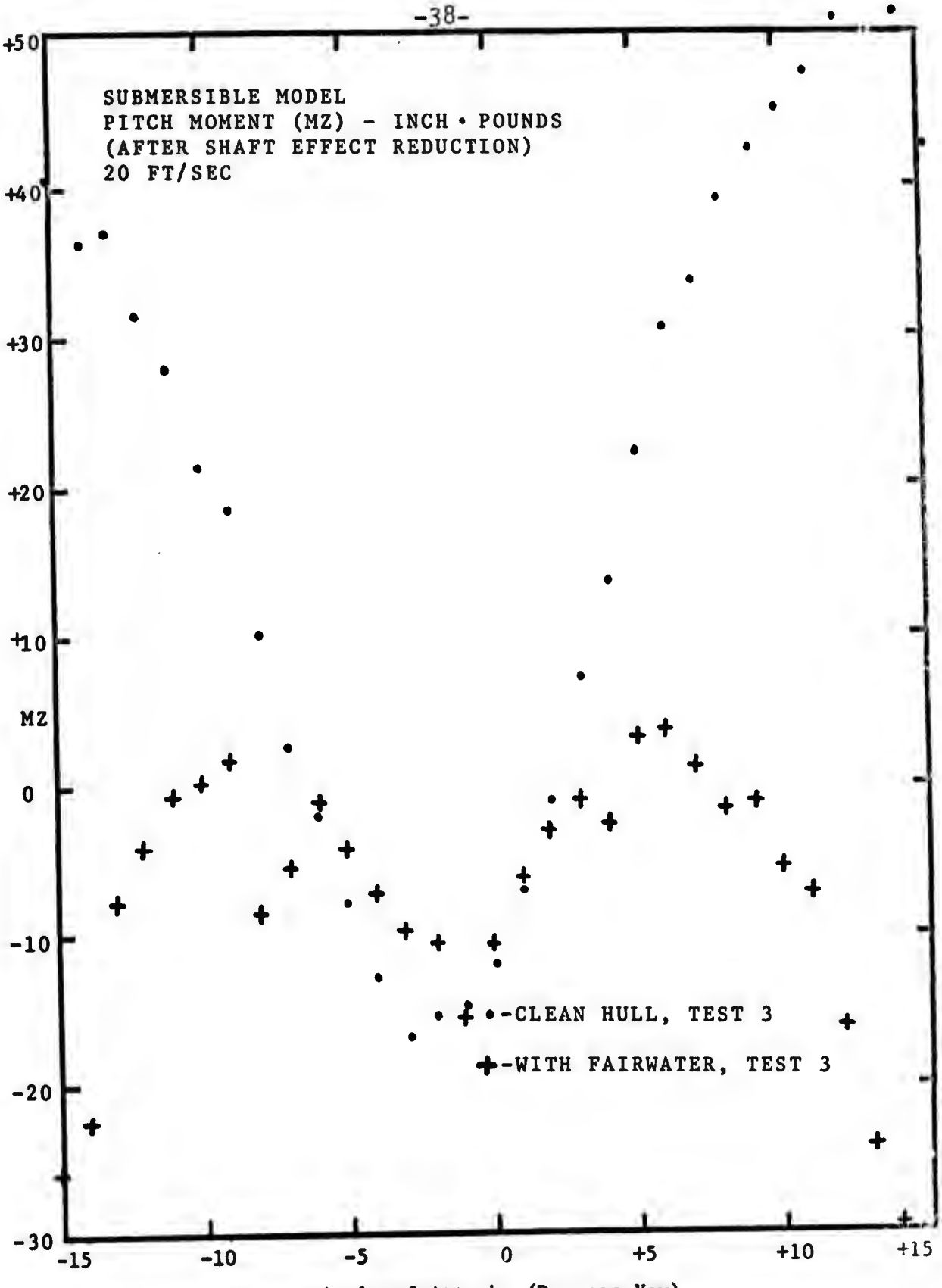
SUBMERSIBLE MODEL
PITCH MOMENT (MZ) - INCH • POUNDS
(AFTER SHAFT EFFECT REDUCTION)
20 FT/SEC
+50
+40
+30
+20
+10
MZ
0
-10
-20
-30
-15
-10
-5
0
+5
+10
+15
•-CLEAN HULL, TEST 3
+-WITH FAIRWATER, TEST 3
Angle of Attack- (Degrees-Yaw)

Figure 17

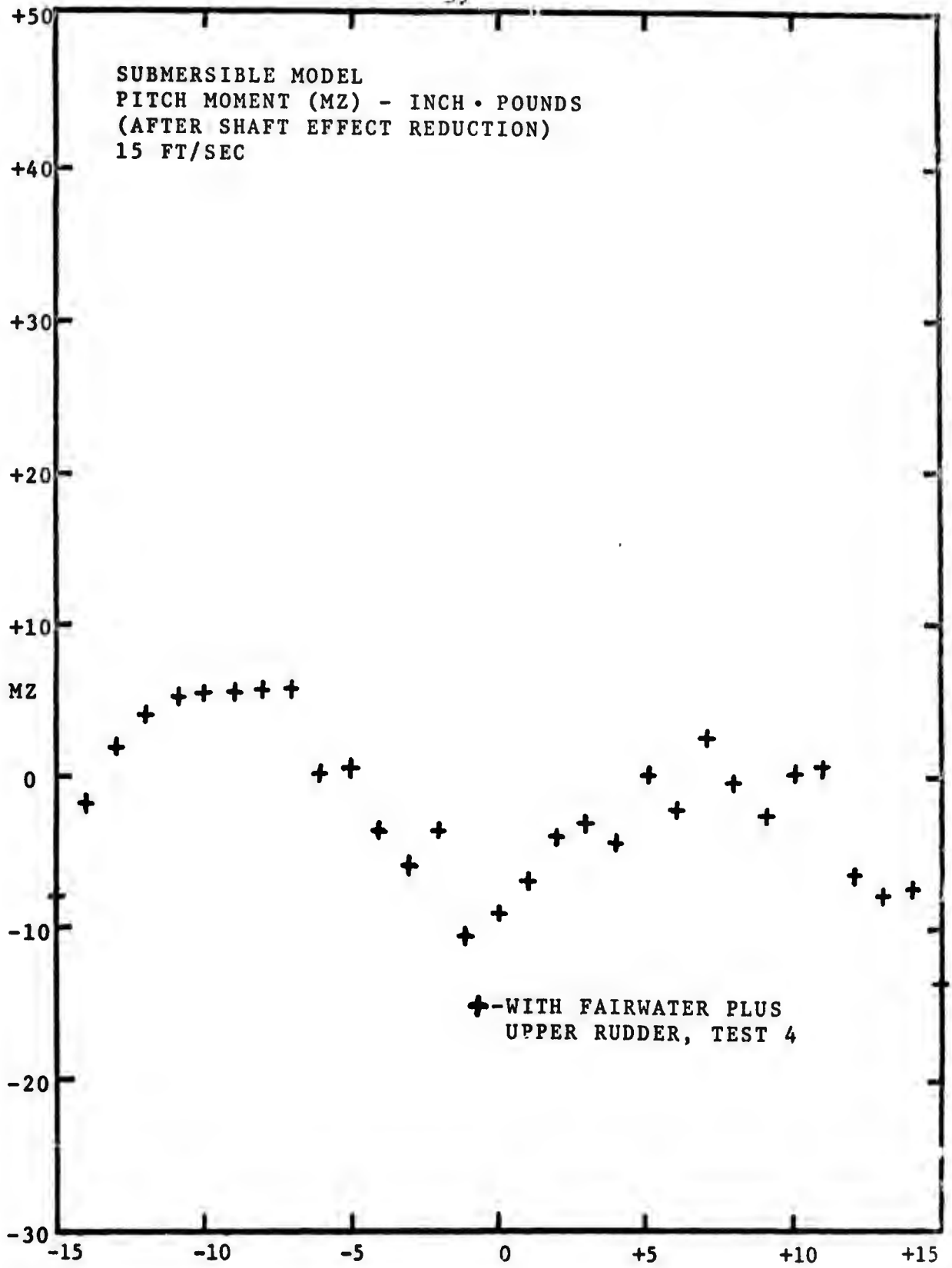
SUBMERSIBLE MODEL
PITCH MOMENT (MZ) - INCH • POUNDS
(AFTER SHAFT EFFECT REDUCTION)
15 FT/SEC
+50
+40
+30
+20
+10
MZ
0
-10
-20
-30
-15
-10
-5
0
+5
+10
+15
+-WITH FAIRWATER PLUS
UPPER RUDDER, TEST 4
Angle of Attack- (Degrees-Yaw)

Figure 18

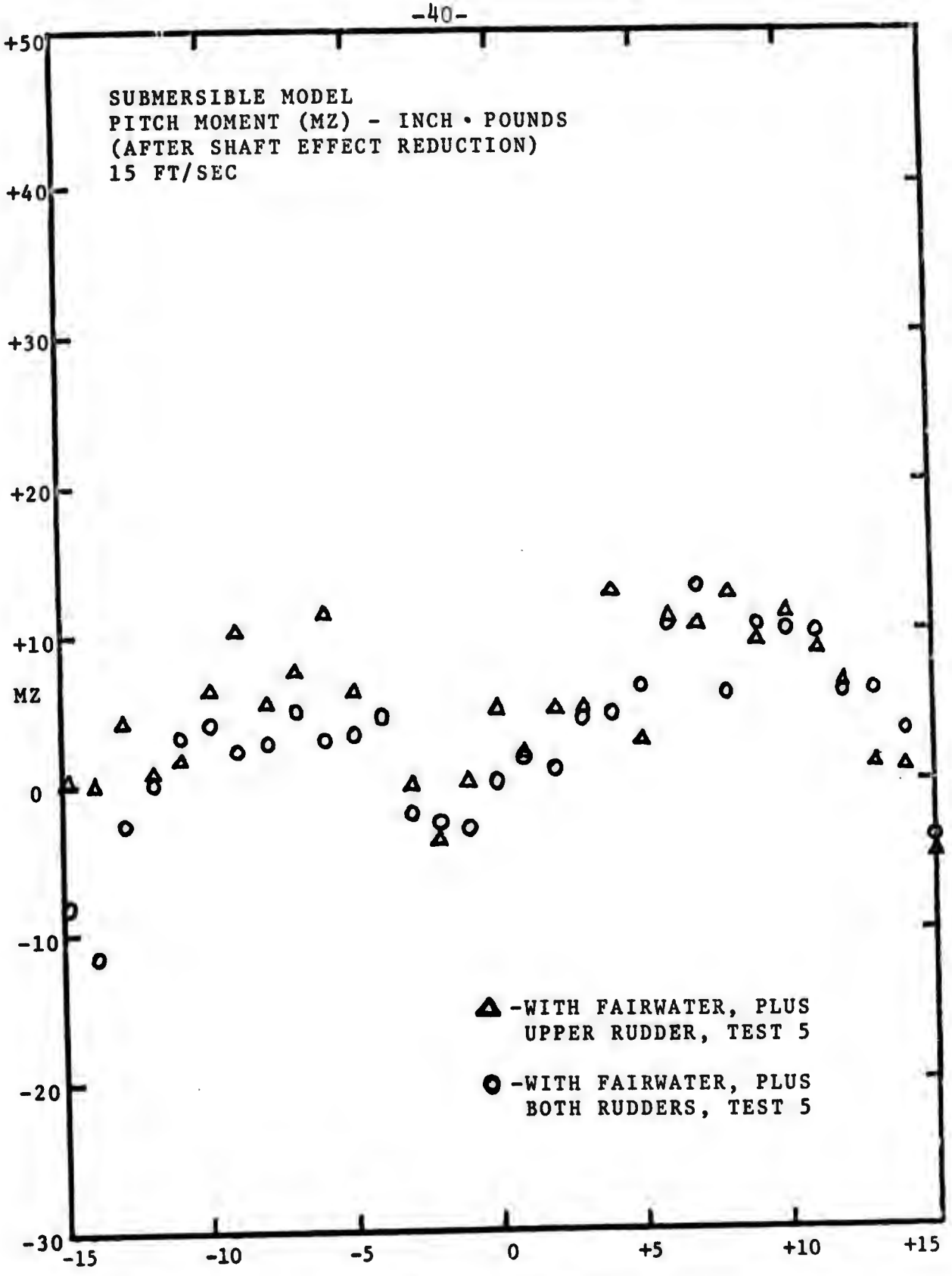

Angle of Attack- (Degrees-Yaw)

Figure 19

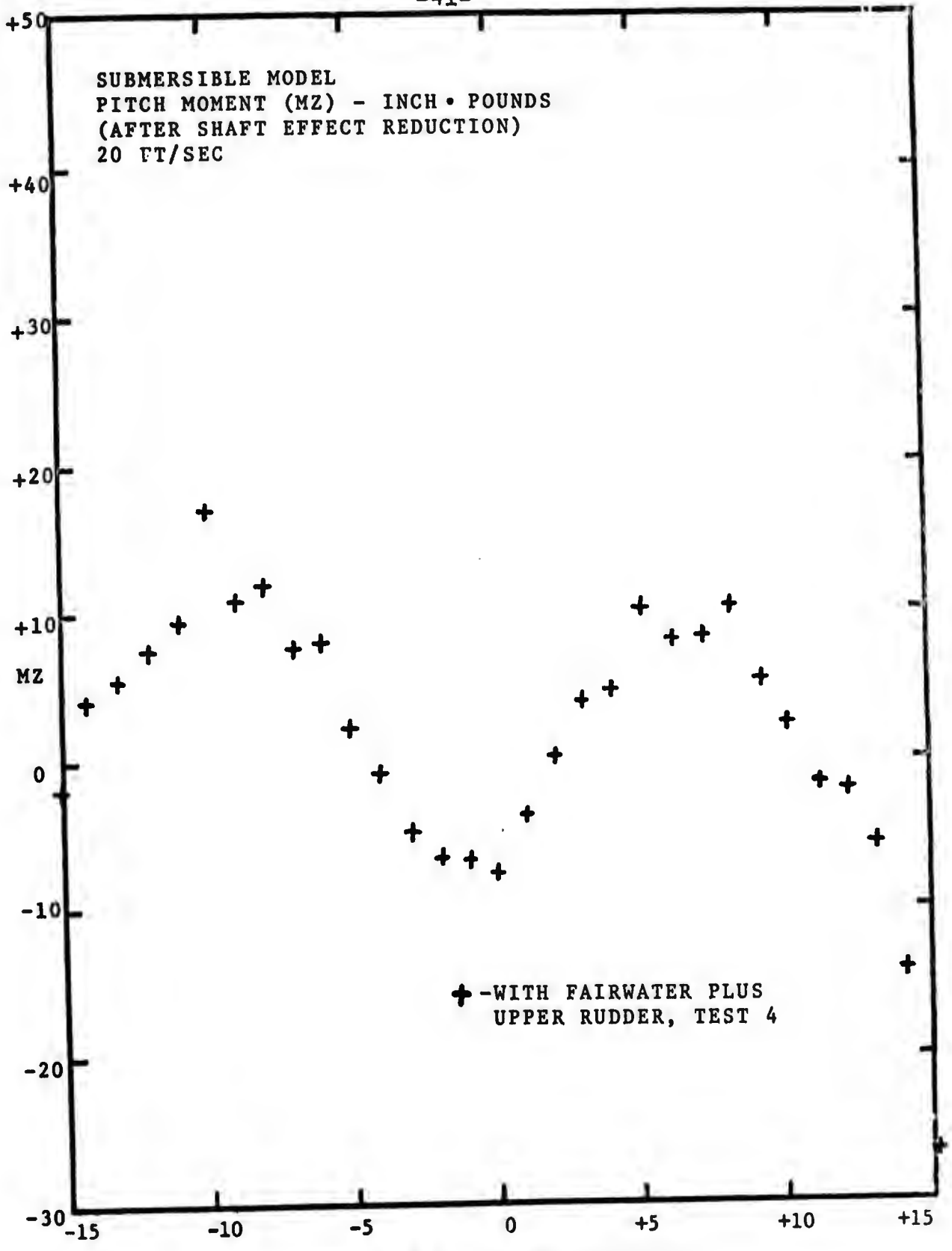
SUBMERSIBLE MODEL
PITCH MOMENT (MZ) - INCH • POUNDS
(AFTER SHAFT EFFECT REDUCTION)
20 FT/SEC
+50
+40
+30
+20
+10
MZ
0
-10
-20
-30
-15
-10
-5
0
+5
+10
+15
+ -WITH FAIRWATER PLUS
UPPER RUDDER, TEST 4
Angle of Attack- (Degrees-Yaw)

Figure 20

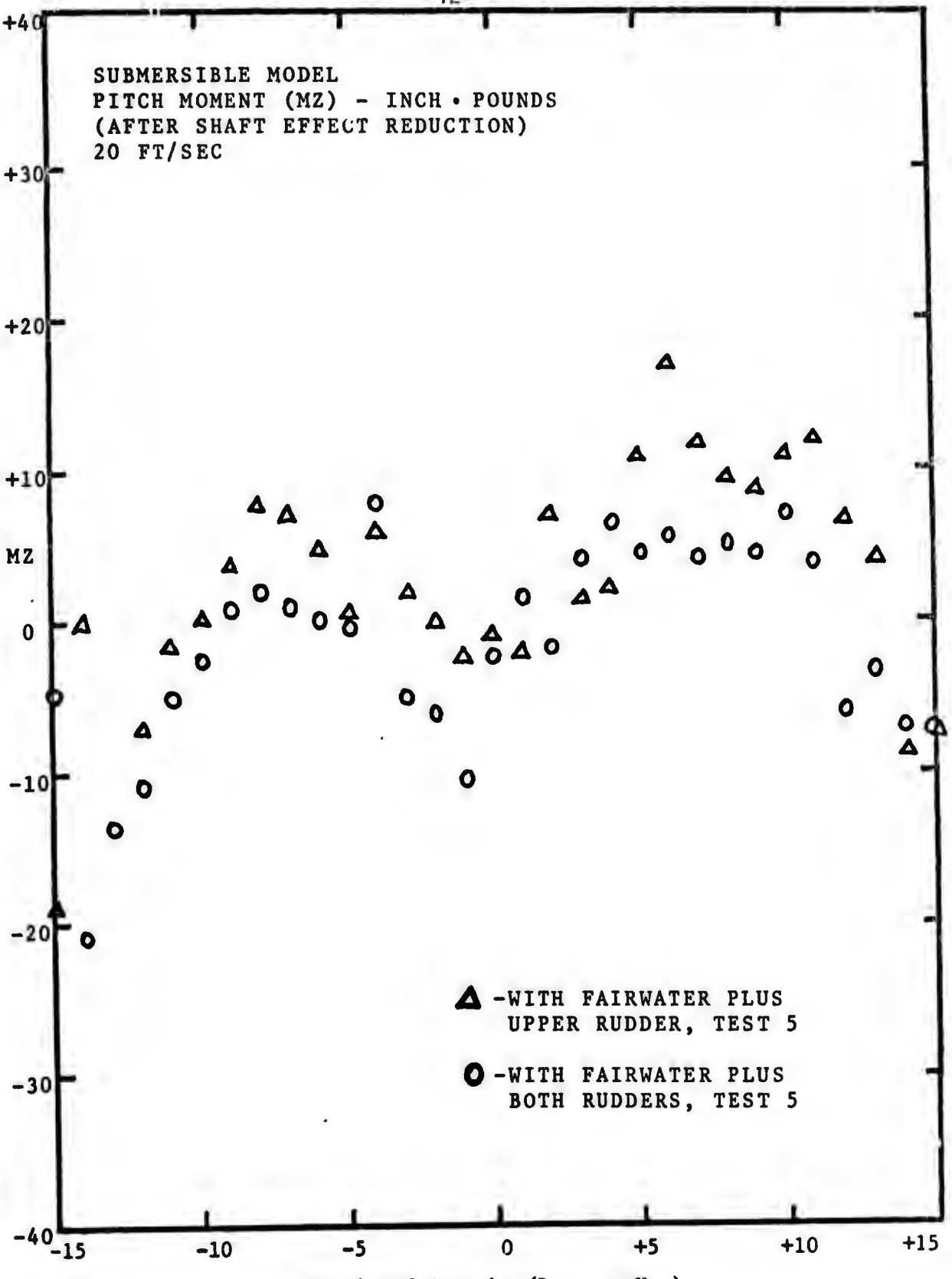

Angle of Attack- (Degrees-Yaw)

Figure 21

SIDE FORCE (FZ)

1. Shaft Effect

The side force on the bare shaft, although relatively small, was a linear function, and increased with angle of yaw and flow velocity, see Figure 22. The slopes of the lines obtained experimentally were:

A. 1.5 lb/10 degrees = .15 lb/degree, for 15 ft/sec,

B. 2.4 lb/10 degrees = .24 lb/degree, for 20 ft/sec.

An approximation of .05 lb/degree was made for the slope expected for a velocity of 10 ft/sec.

2. Model Results

Every model configuration tested resulted in a side force that increased linearly with angle of yaw and flow velocity. The total side force on a configuration was due to appropriate contributions of side force on the symmetric body of revolution, the fairwater and the rudders, see Figure 23. The side force on the body of revolution results from viscous effects, changes in the crossflow pattern along the length of the model, separation of the flow past the body, and interaction with the fairwater. The fairwater and rudders are essentially lifting surfaces that generate a side force component when placed at an angle of incidence to the flow.

The resulting slopes for the configurations tested were:

Configuration	Velocity (ft/sec)	Slope (lb/degree)	Reference Figure Number
1	15	.50	24
1	20	1.05	25
2	15	1.70	24
2	20	3.20	25
3	15	1.90	27
3	20	3.30	28
4	10	.94	26
4	15	2.00	27
4	20	3.40	28

Although the addition of the fairwater (configuration 2) resulted in a step increase of the side force from that of the clean hull (configuration 1), the addition of the upper rudder (configuration 3) and the lower rudder (configuration 4) resulted in relatively no increase of the side force on the body. The reason for the latter result was found by investigation of the flow past the body. A flow visualization method was used in which the hull body, fairwater and

rudders were tufted, in order to observe and photograph the flow at various angles of yaw, see Figures 29, 30, 31 and 32. The flow past the forward portion of the model showed the increasing crossflow component resulting from increasing angle of yaw as seen by the angle of deflection of the tufts from the body axis. Yet, the flow past the aft portion of the model appears as that observed for a reduced angle of yaw. The difference between these two sections is the location of the fairwater. The change in the flow pattern,resulting from the fairwater shedded wake and its induced velocity, reduces the effective angle of yaw on the upper rudder. The upper rudder is defined as that which is on the same side of the submersible as the fairwater.

The lower rudder, on the opposite side from the fairwater, experiences a similar effect due to the presence of the support shaft, but the magnitude is not as great. The flow visualization test was performed at three water tunnel velocities - 10 ft/sec, 15 ft/sec, and 20 ft/sec - and until separation on the fairwater and both rudders occurred. The flow patterns and initiation of separation on the lifting surfaces did not depend on flow velocity, but only on angle of yaw. The initiation of separation occurred at different angles of yaw for each of the three lifting surfaces. Separation on the fairwater was observed at an angle of yaw equal to 16.5 degrees. At this angle, neither of the rudder surfaces showed any

signs of separation. Separation on the lower rudder appeared when the body of the model was placed at 20 degrees yaw angle. The upper rudder still showed no signs of separation. The angle of yaw was increased until separation was observed at a model yaw angle of 29 degrees, see Figure 32c. Figure 32d was included to show the flow pattern along the model at a negative angle of yaw (15 degrees).

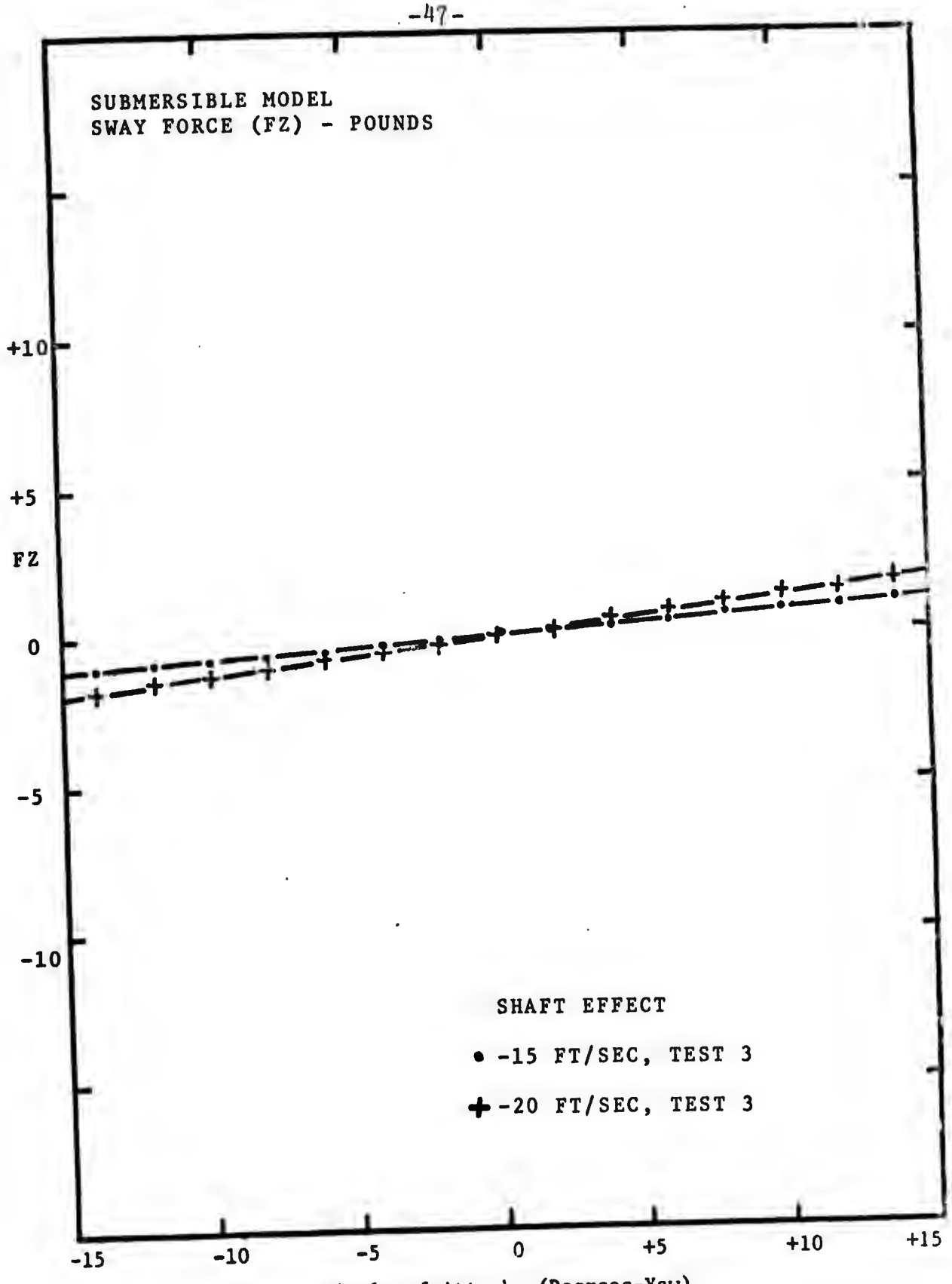
SUBMERSIBLE MODEL
SWAY FORCE (FZ) - POUNDS
+10
+5
FZ
0
-5
-10
SHAFT EFFECT
• -15 FT/SEC, TEST 3
+ -20 FT/SEC, TEST 3
-15
-10
-5
0
+5
+10
+15
Angle of Attack- (Degrees-Yaw)

Figure 22

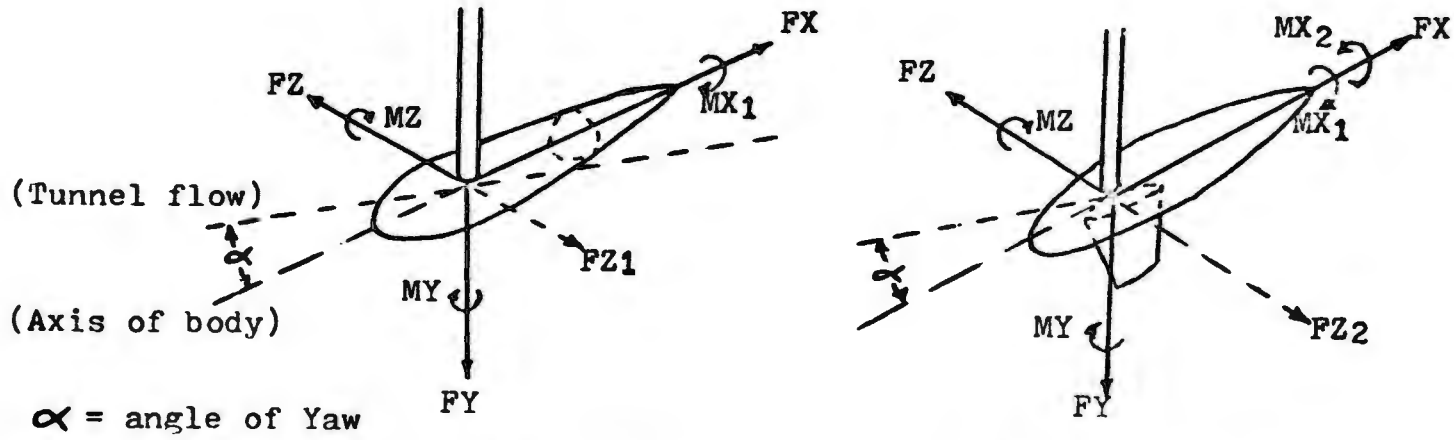

a. Without fairwater b. With fairwater

a. MX_1 = Roll moment about body axis, resulting from non-symmetry of streamlined body, (the supporting shaft)

FZ_1 = Side force on the body, due to form drag at angles of Yaw

b. MX_2 = Roll moment about body axis, resulting from non-symmetry of added fairwater, (Net roll moment on model, $MX=\Sigma MX_i$; in above case, $MX=MX_2-MX_1$)

FZ_2 = Side force resulting from the addition of the fairwater to the body, (Net side force, $FZ=\Sigma FZ_i$; in above case, $FZ=FZ_1+FZ_2$)

Figure 23 Interpretation of hydrodynamic effects for graphic results

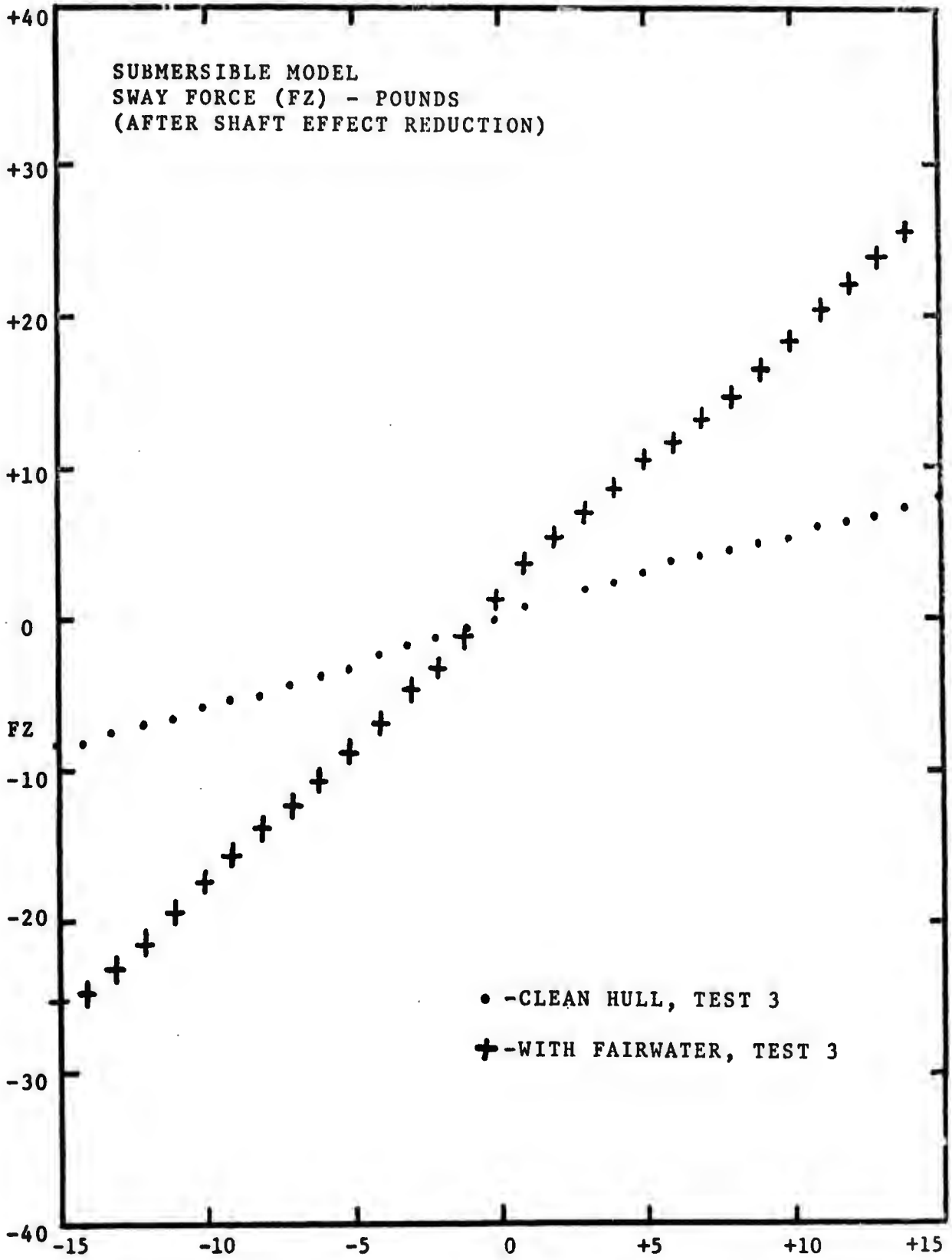
SUBMERSIBLE MODEL
SWAY FORCE (FZ) - POUNDS
(AFTER SHAFT EFFECT REDUCTION)
+40
+30
+20
+10
0
FZ
-10
-20
-30
-40
-15
-10
-5
0
+5
+10
+15
• -CLEAN HULL, TEST 3
+ -WITH FAIRWATER, TEST 3
Angle of Attack- (Degrees-Yaw)

Figure 24

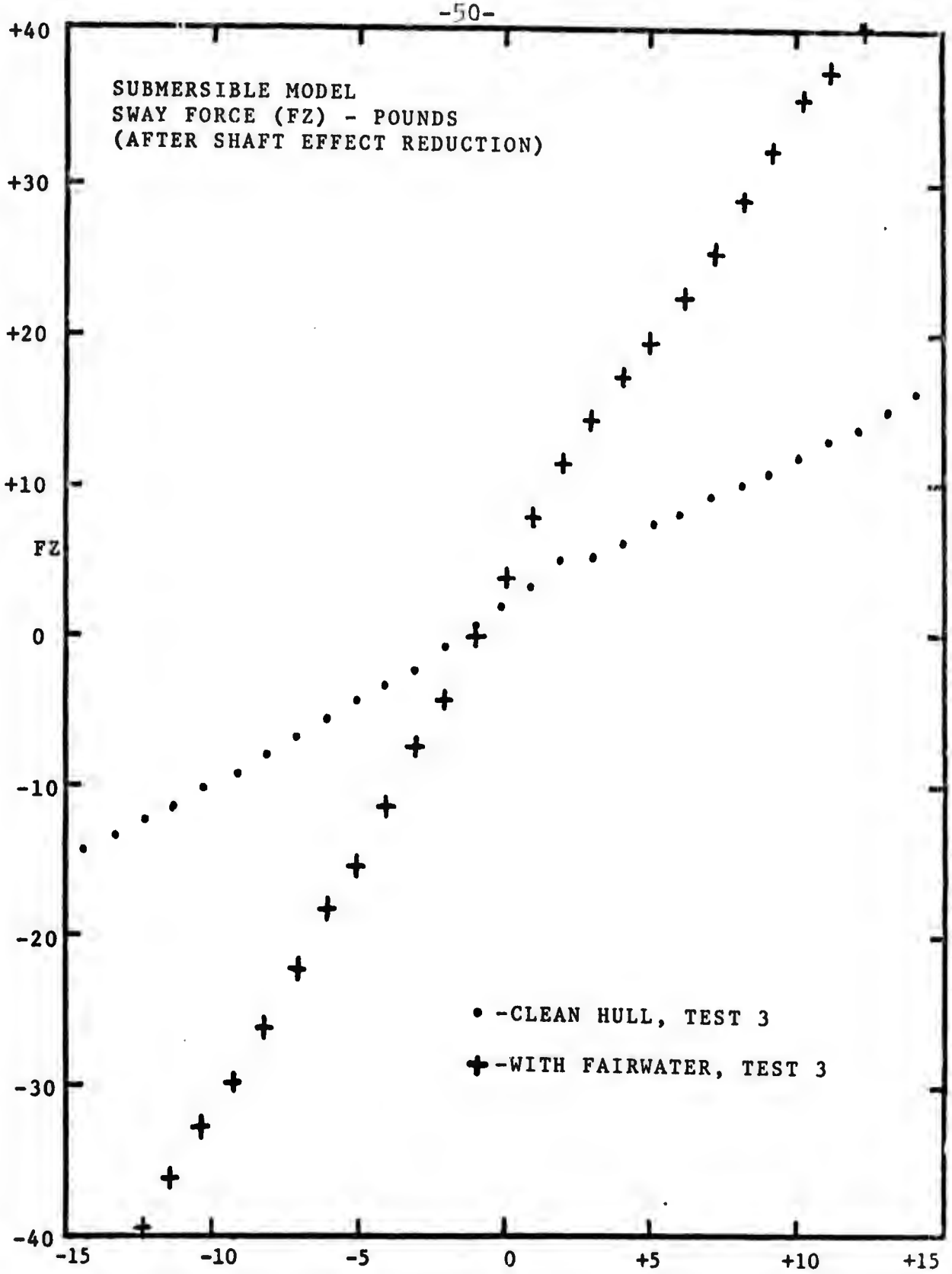
SUBMERSIBLE MODEL
SWAY FORCE (FZ) - POUNDS
(AFTER SHAFT EFFECT REDUCTION)
+40
+30
+20
+10
FZ
0
-10
-20
-30
-40
-15
-10
-5
0
+5
+10
+15
• -CLEAN HULL, TEST 3
+ -WITH FAIRWATER, TEST 3
Angle of Attack- (Degrees-Yaw)

Figure 25

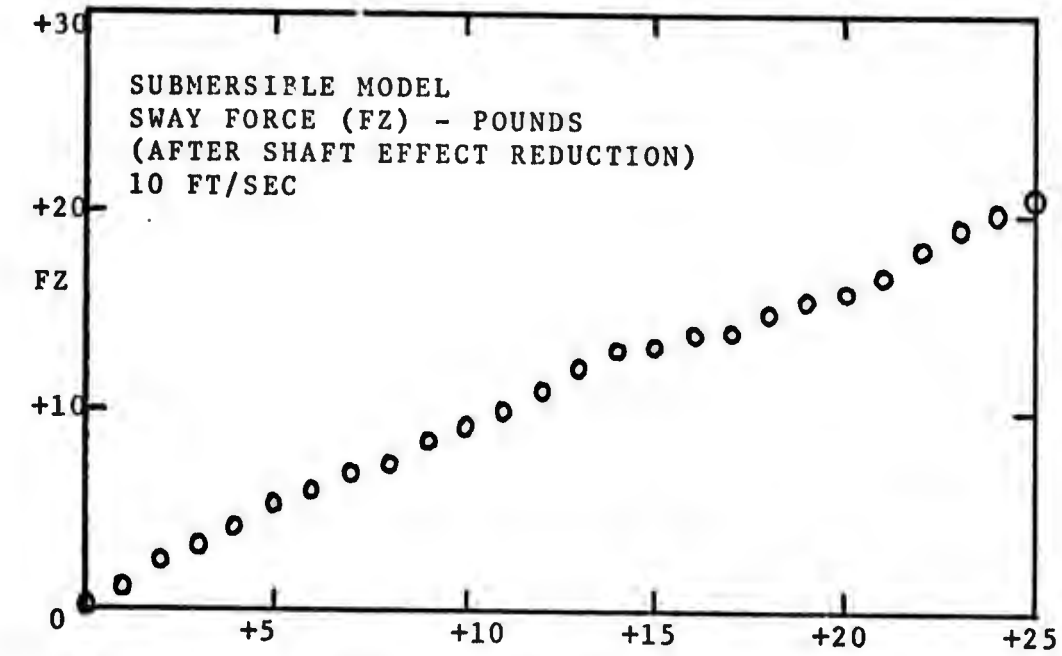
+30
SUBMERSIBLE MODEL
SWAY FORCE (FZ) - POUNDS
(AFTER SHAFT EFFECT REDUCTION)
10 FT/SEC
+20
FZ
+10
0
+5
+10
+15
+20
+25
Angle of Attack- (Degrees-Yaw)

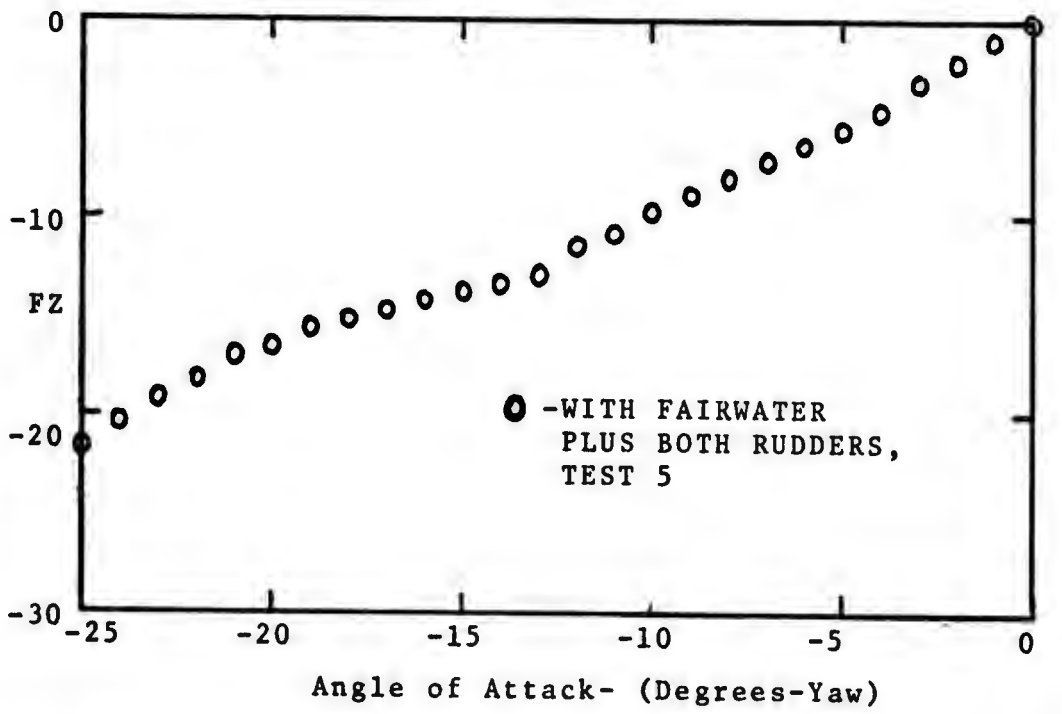
0
-10
FZ
-20
-30
-25
-20
-15
-10
-5
0
-WITH FAIRWATER
PLUS BOTH RUDDERS,
TEST 5
Angle of Attack- (Degrees-Yaw)

Figure 26

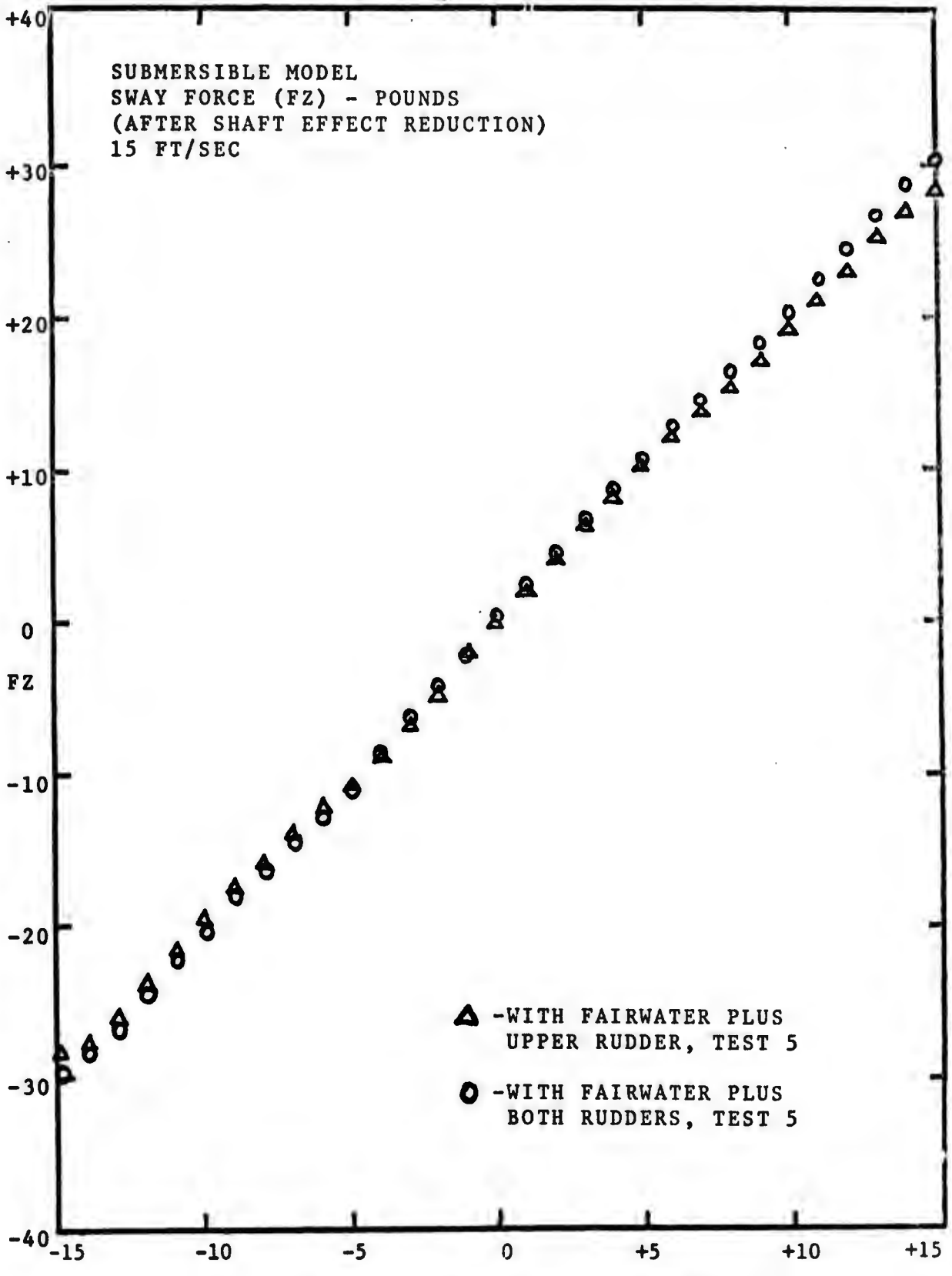
SUBMERSIBLE MODEL
SWAY FORCE (FZ) - POUNDS
(AFTER SHAFT EFFECT REDUCTION)
15 FT/SEC
+40
+30
+20
+10
0
FZ
-10
-20
-30
-40
-15
-10
-5
0
+5
+10
+15
-WITH FAIRWATER PLUS UPPER RUDDER, TEST 5
-WITH FAIRWATER PLUS BOTH RUDDERS, TEST 5
Angle of Attack- (Degrees-Yaw)

Figure 27

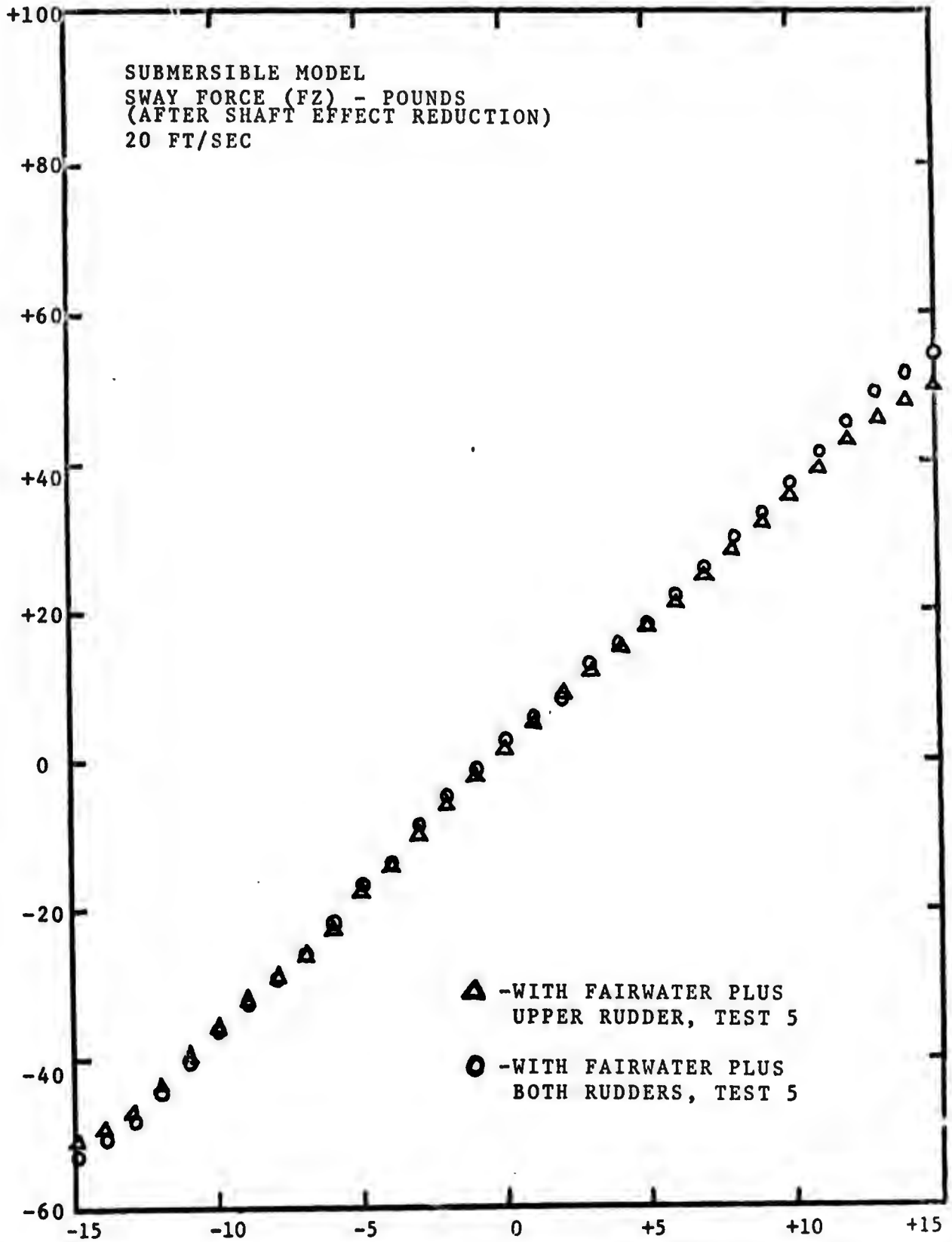
SUBMERSIBLE MODEL
SWAY FORCE (FZ) - POUNDS
(AFTER SHAFT EFFECT REDUCTION)
20 FT/SEC
+100
+80
+60
+40
+20
0
-20
-40
-60
-15
-10
-5
0
+5
+10
+15
-WITH FAIRWATER PLUS UPPER RUDDER, TEST 5
-WITH FAIRWATER PLUS BOTH RUDDERS, TEST 5
Angle of Attack- (Degrees-Yaw)

Figure 28

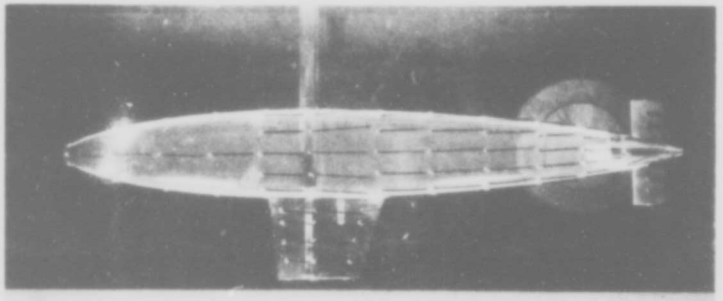

a. When submersible is parallel to water tunnel flow, α = 0 degrees

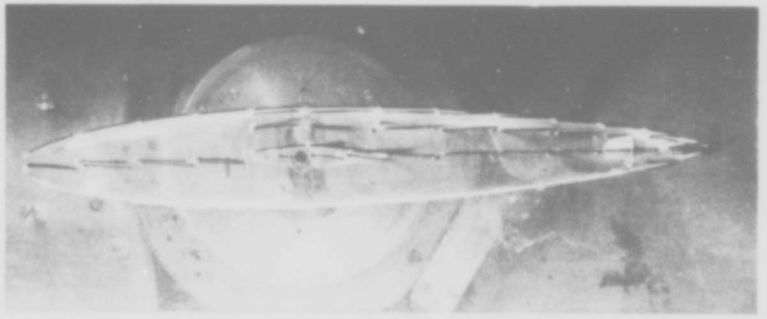

b. When submersible is parallel to water tunnel flow, α = 0 degrees

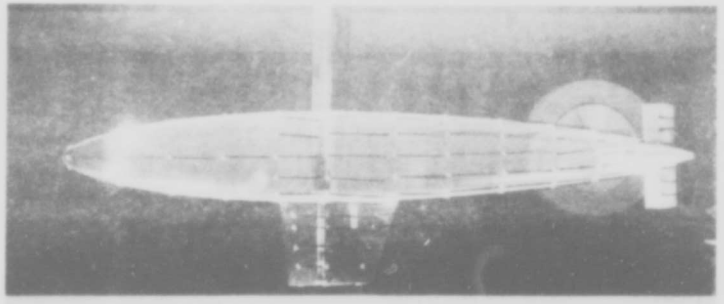

c. When α = 5 degrees

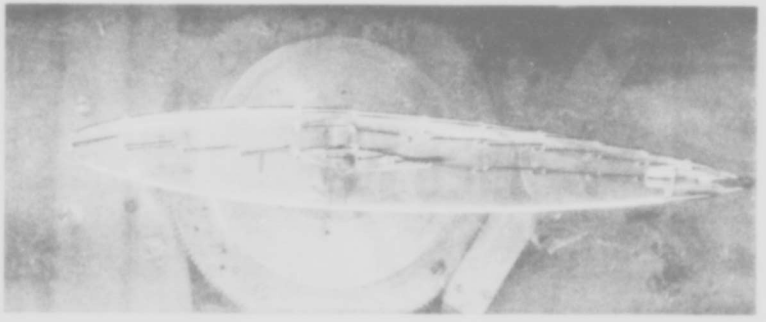

d. When α = 5 degrees

(Note: α = Yaw angle)

Figure 29 Submersible model with flow visualization (Tufted)

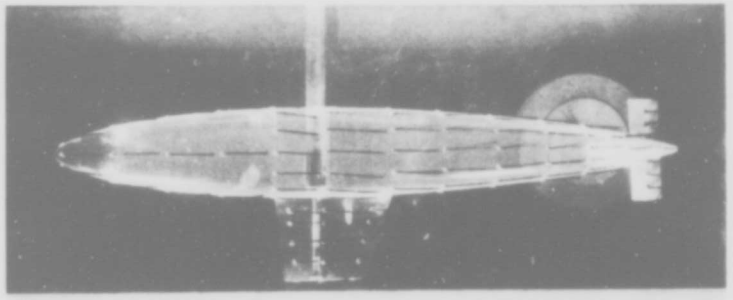

a. When α = 10 degrees

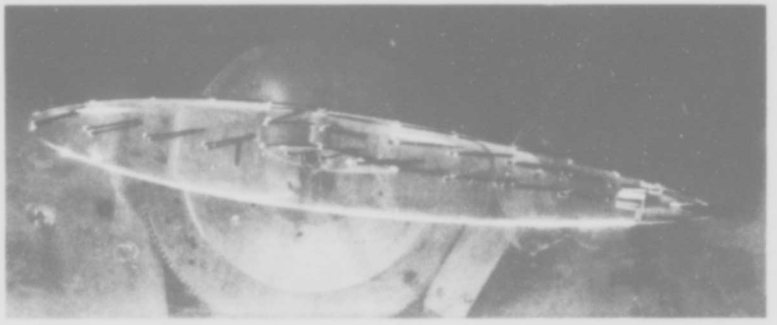

b. When α = 10 degrees

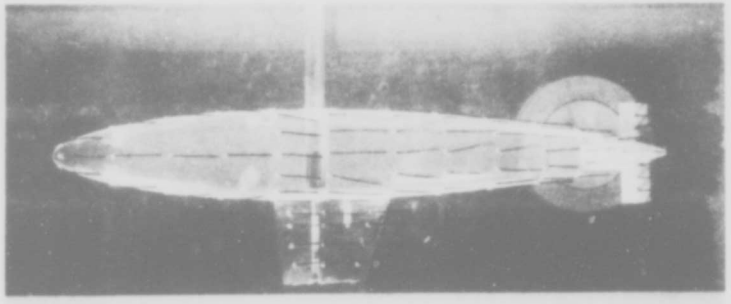

c. When α = 15 degrees

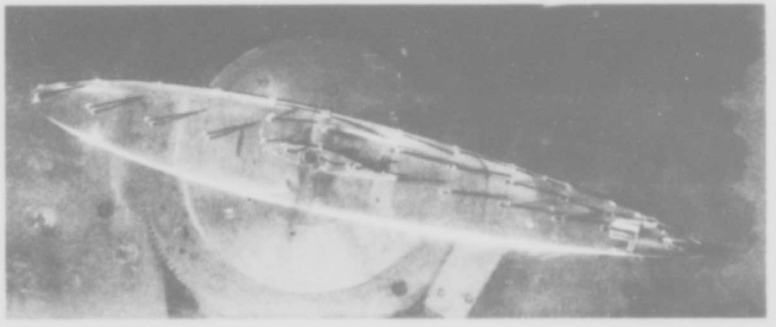

d. When α = 15 degrees

Figure 30 Submersible model with flow visualization (Tufted)

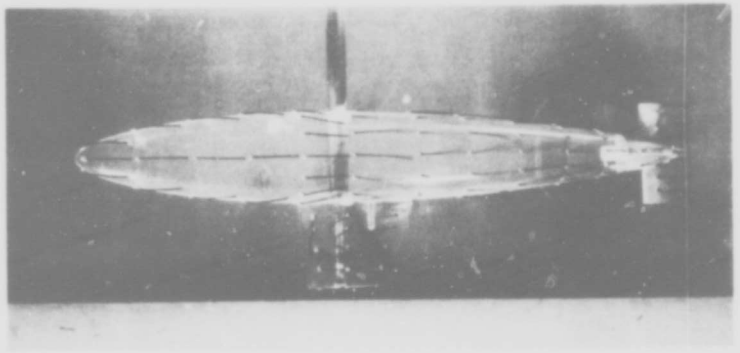

a. Separation on fairwater, but not on either of the rudders, when α = 16.5 degrees.

b. Separation on fairwater, but not on either of the rudders, when α = 16.5 degrees.

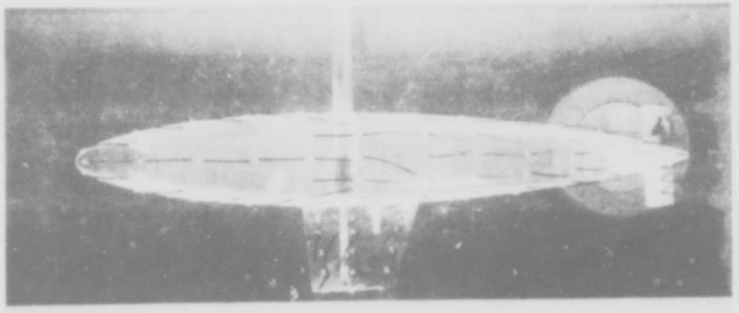

c. Separation on fairwater and one rudder, other rudder still effective, when α = 20 degrees.

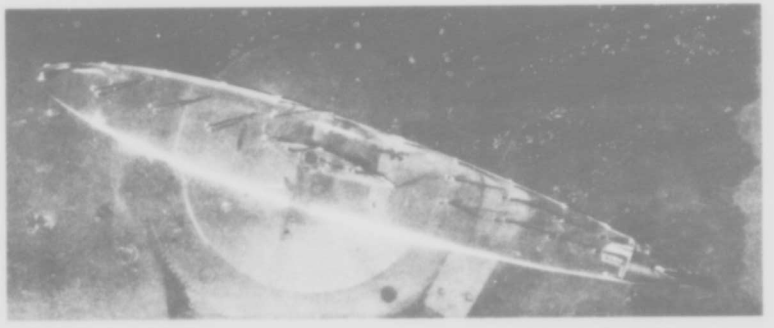

d. Separation on fairwater and one rudder, other rudder still effective, when α = 20 degrees.

Figure 31 Submersible model with flow visualization (Tufted)

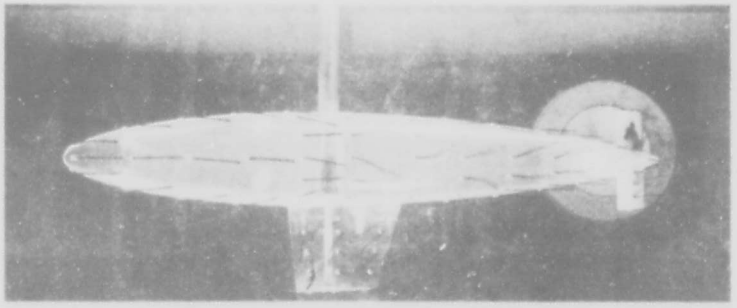

a. Separation on fairwater and one rudder, other rudder still effective, when α = 25 degrees.

b. Separation on fairwater and one rudder, other rudder still effective, when α = 25 degrees.

c. Separation on all three lifting surfaces is experienced (see backflow), when α = 29 degrees.

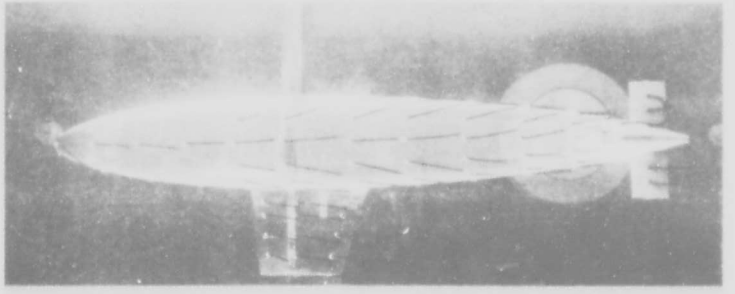

d. Flow when α = -15 degrees; tangle on one rudder resulted from a previous test run.

Figure 32 Submersible model with flow visualization (Tufted)

ROLL MOMENT (MX)

The roll moment on a submerged body of revolution at an angle of yaw, with and without appendages, is a direct result of the side forces (FZ) previously reported and the relative location of their concentrations with respect to a reference point. For an actual submersible, the reference point would be the center of gravity, which would be below the body axis of symmetry. The reference point for the model tested was at the origin of the coordinate system, which is on the body axis of symmetry.

1. Shaft Effect

The roll moment obtained on the base shaft decreased with an increasing angle of yaw and increasing flow velocity in a linear fashion, see Figure 33. When a linear result was approximated, the slopes of the lines formed were:

A. Slope = -7 in. lb/10 degrees = -.7 in. lb/degree, for a velocity of 15 ft/sec.

B. Slope = -13.5 in. lb/10 degrees = -1.35 in. lb/degrees, for a velocity of 20 ft/sec.

2. Model Results

Model configuration 1 (clean hull) is symmetrical in all respects, unlike an actual submersible of comparable configuration, whose center of gravity is below the body axis, for

roll stability. This caused an experimental result of zero roll moment for the clean hull at all angles of yaw and all velocities evaluated, see Figures 34 and 35. In actuality, a roll moment would occur on a submersible, due to the asymmetry described above. This fact is reflected in the results of all subsequent configurations, in the form of a difference in total magnitude of roll moment.

With the addition of the fairwater (configuration 2), an increasing roll moment is encountered with both increasing flow velocity and increasing angle of yaw, see Figures 34 and 35. The increase was approximately linear with the following slopes:

A. Slope = 28 in. lb/10 degrees = 2.8 in. lb/degree, for a velocity of 15 ft/sec.

B. Slope = 54 in. lb/10 degrees = 5.4 in. lb/degree, for a velocity of 20 ft/sec.

A decrease in the magnitude of the roll moment and a reversal of slope was noticeable when the model was placed in a yaw angle of about 15 degrees. This was caused by the separation on the fairwater, and the resulting loss of side force (lift component).

Configuration 3 (with fairwater and upper rudder) produced very little change in the roll moment on the model, see Figures 36 and 37. This is a result of a decrease in the effective angle of yaw on the rudder by the perturbations in

the flow due to the fairwater and its shedded wake, see Figures 29, 30, 31 and 32 for flow visualization. A decrease in moment, caused by separation on the fairwater, was experienced again at about 15 degrees yaw angle.

Configuration 4 (with fairwater and both rudders) decreased the magnitude of the roll moment, but only slightly, see Figures 36 and 37. A greater reduction in roll moment should have been obtained for the lifting surface added, but as in configuration 3, the effective angle of yaw on the lifting surface (rudder) in question was reduced. In this case, the support shaft sheds a wake, which interacts with the in-flow velocity on the lower rudder. A similar loss of lift on the fairwater, as in configurations 2 and 3, was obtained for configuration 4.

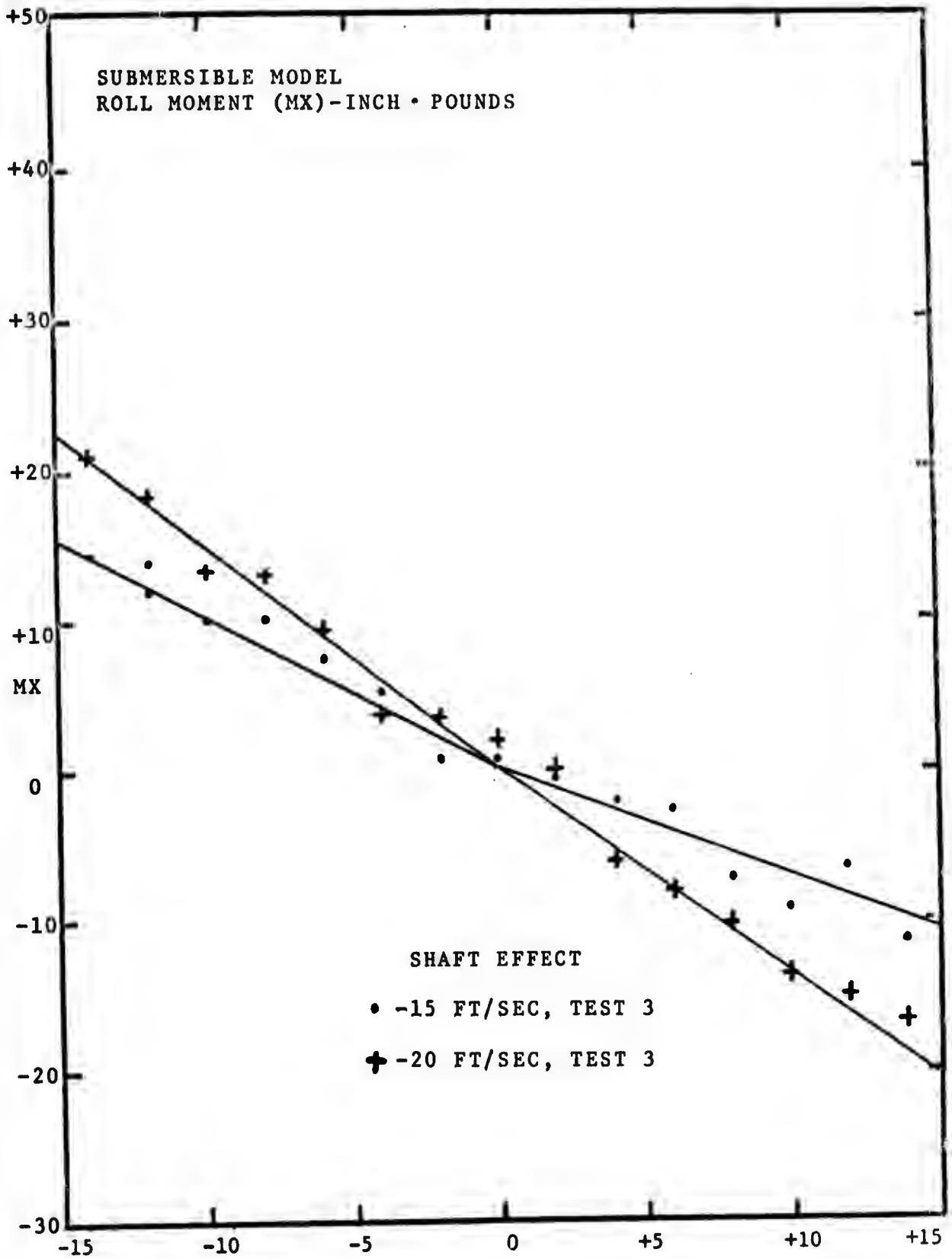
SUBMERSIBLE MODEL
ROLL MOMENT (MX)-INCH • POUNDS
+50
+40
+30
+20
+10
MX
0
-10
-20
-30
-15
-10
-5
0
+5
+10
+15
SHAFT EFFECT
• -15 FT/SEC, TEST 3
+ -20 FT/SEC, TEST 3
Angle of Attack- (Degrees-Yaw)

Figure 33

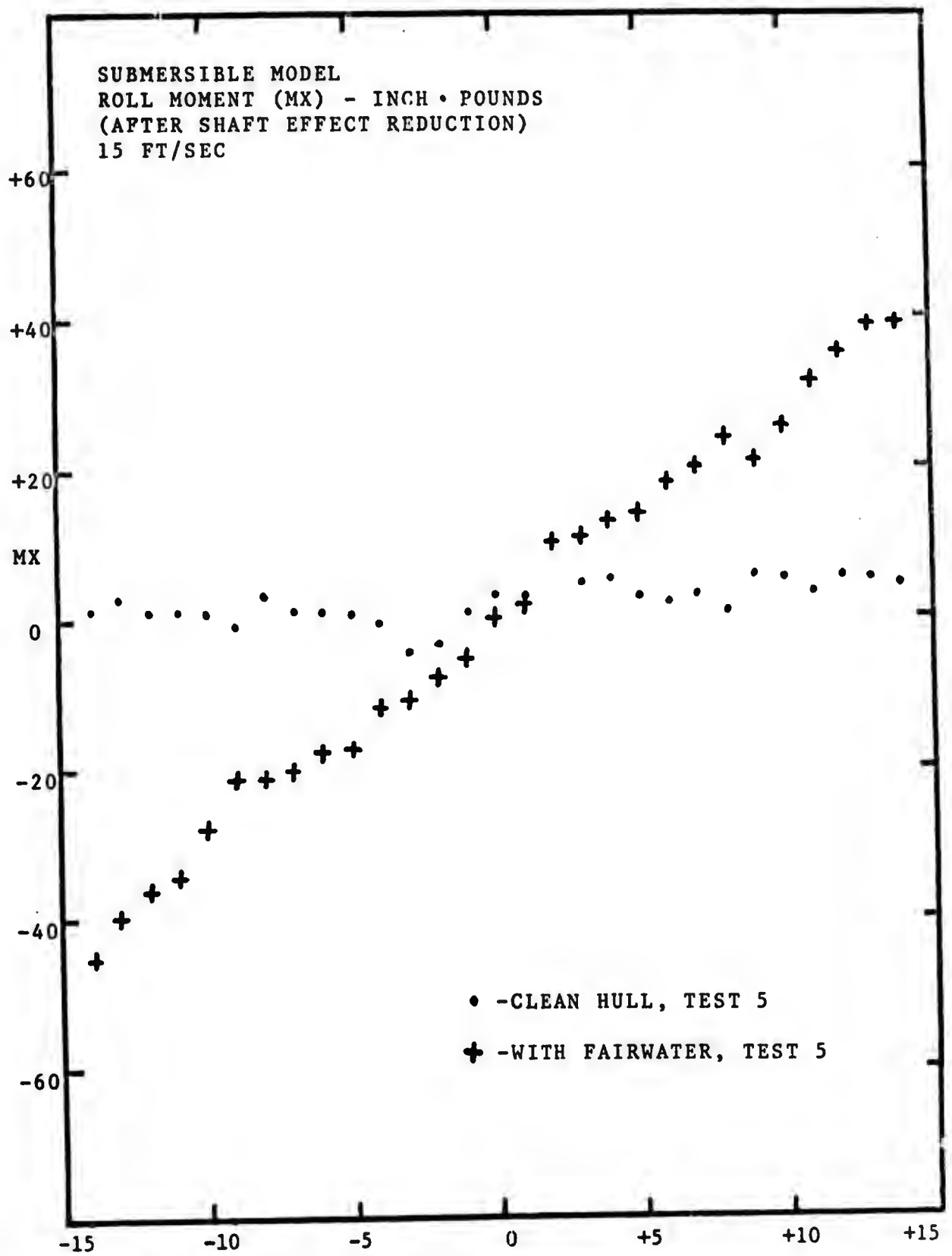
SUBMERSIBLE MODEL
ROLL MOMENT (MX) - INCH • POUNDS
(AFTER SHAFT EFFECT REDUCTION)
15 FT/SEC
+60
+40
+20
MX
0
-20
-40
-60
• -CLEAN HULL, TEST 5
+ -WITH FAIRWATER, TEST 5
-15
-10
-5
0
+5
+10
+15
Angle of Attack- (Degrees-Yaw)

Figure 34

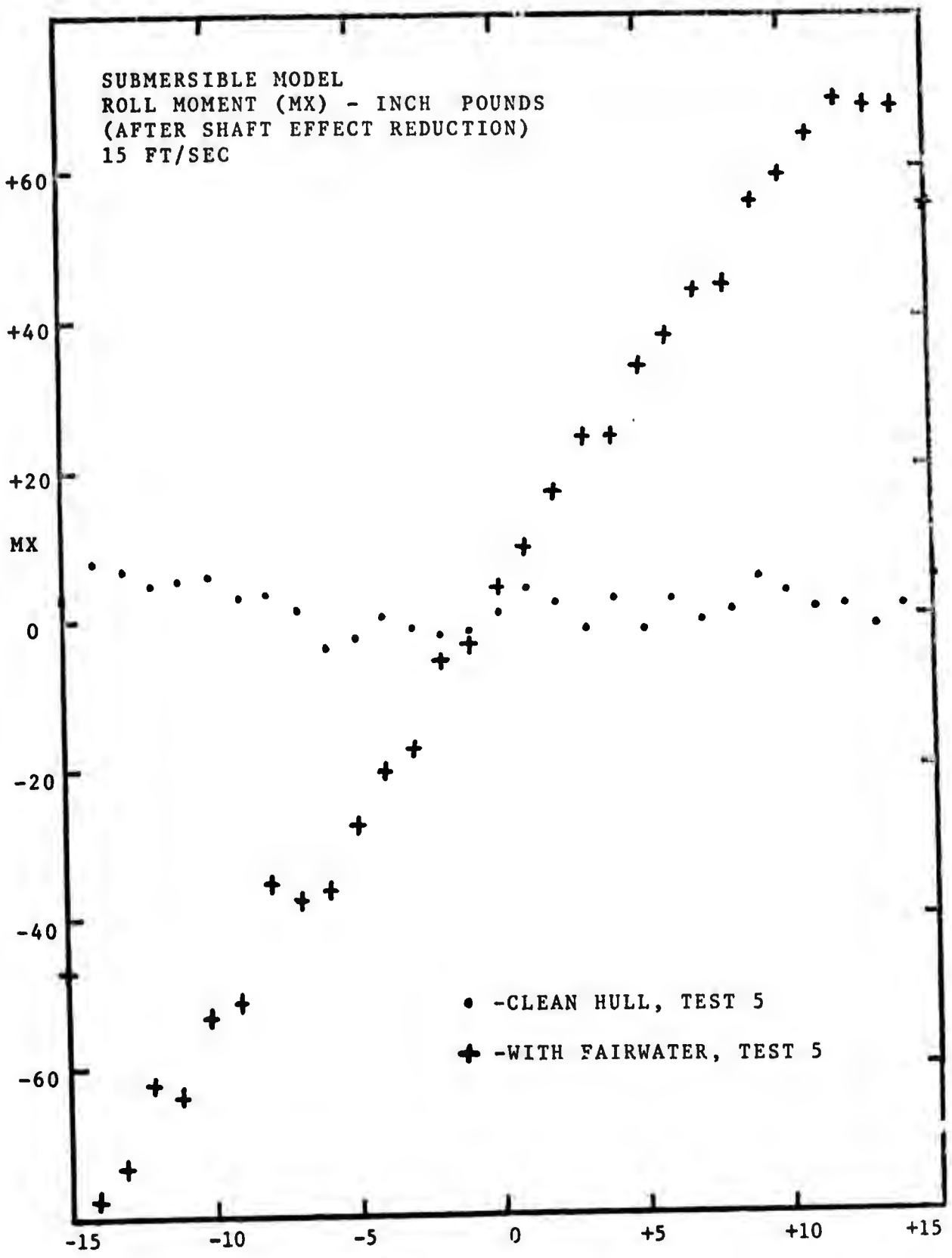
SUBMERSIBLE MODEL
ROLL MOMENT (MX) - INCH POUNDS
(AFTER SHAFT EFFECT REDUCTION)
15 FT/SEC
+60
+40
+20
MX
0
-20
-40
-60
-15
-10
-5
0
+5
+10
+15
• -CLEAN HULL, TEST 5
+ -WITH FAIRWATER, TEST 5
Angle of Attack- (Degrees-Yaw)

Figure 35

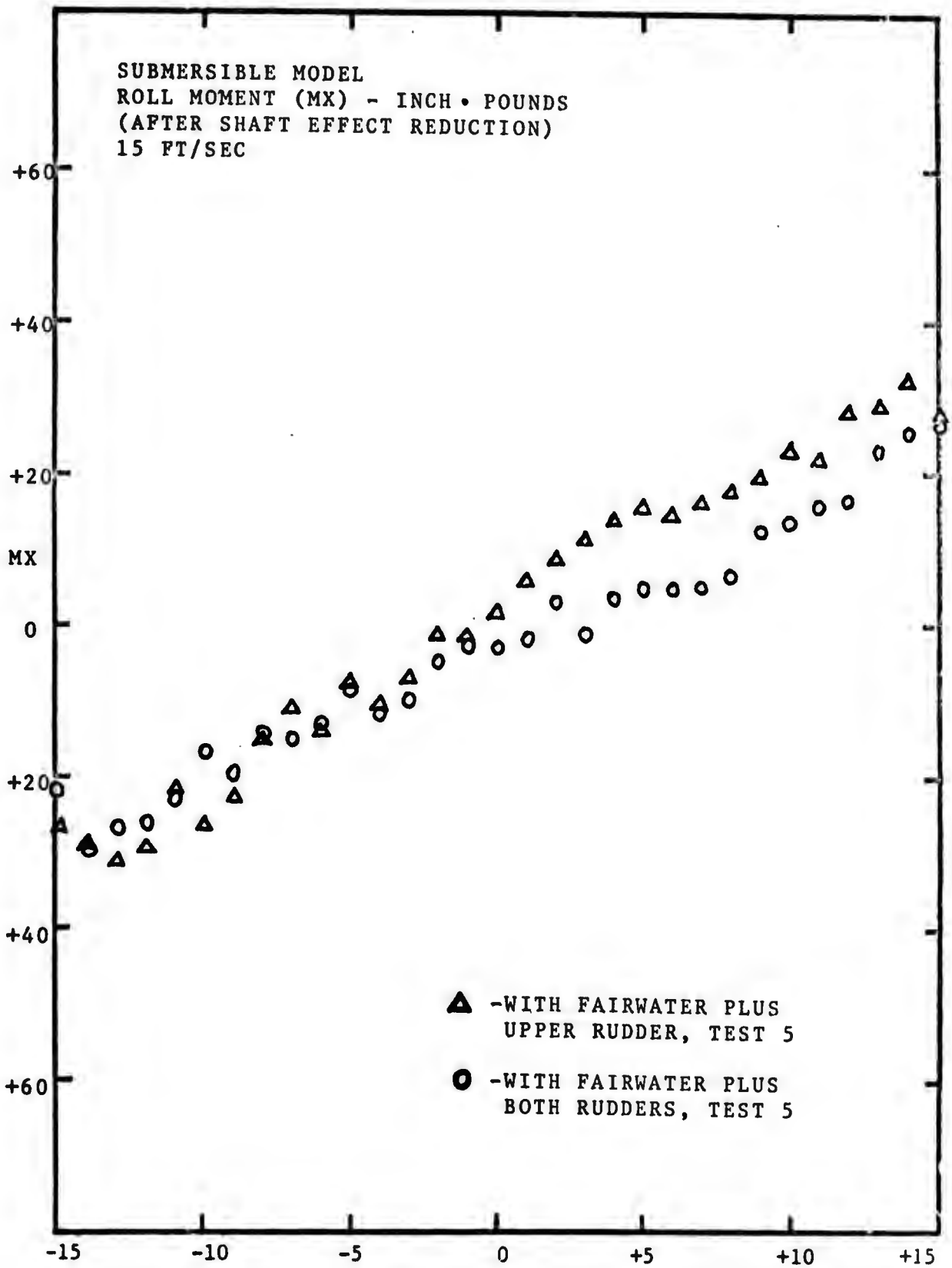
SUBMERSIBLE MODEL
ROLL MOMENT (MX) - INCH • POUNDS
(AFTER SHAFT EFFECT REDUCTION)
15 FT/SEC
+60
+40
+20
MX
0
+20
+40
+60
-15
-10
-5
0
+5
+10
+15
-WITH FAIRWATER PLUS UPPER RUDDER, TEST 5
-WITH FAIRWATER PLUS BOTH RUDDERS, TEST 5
Angle of Attack- (Degrees-Yaw)

Figure 36

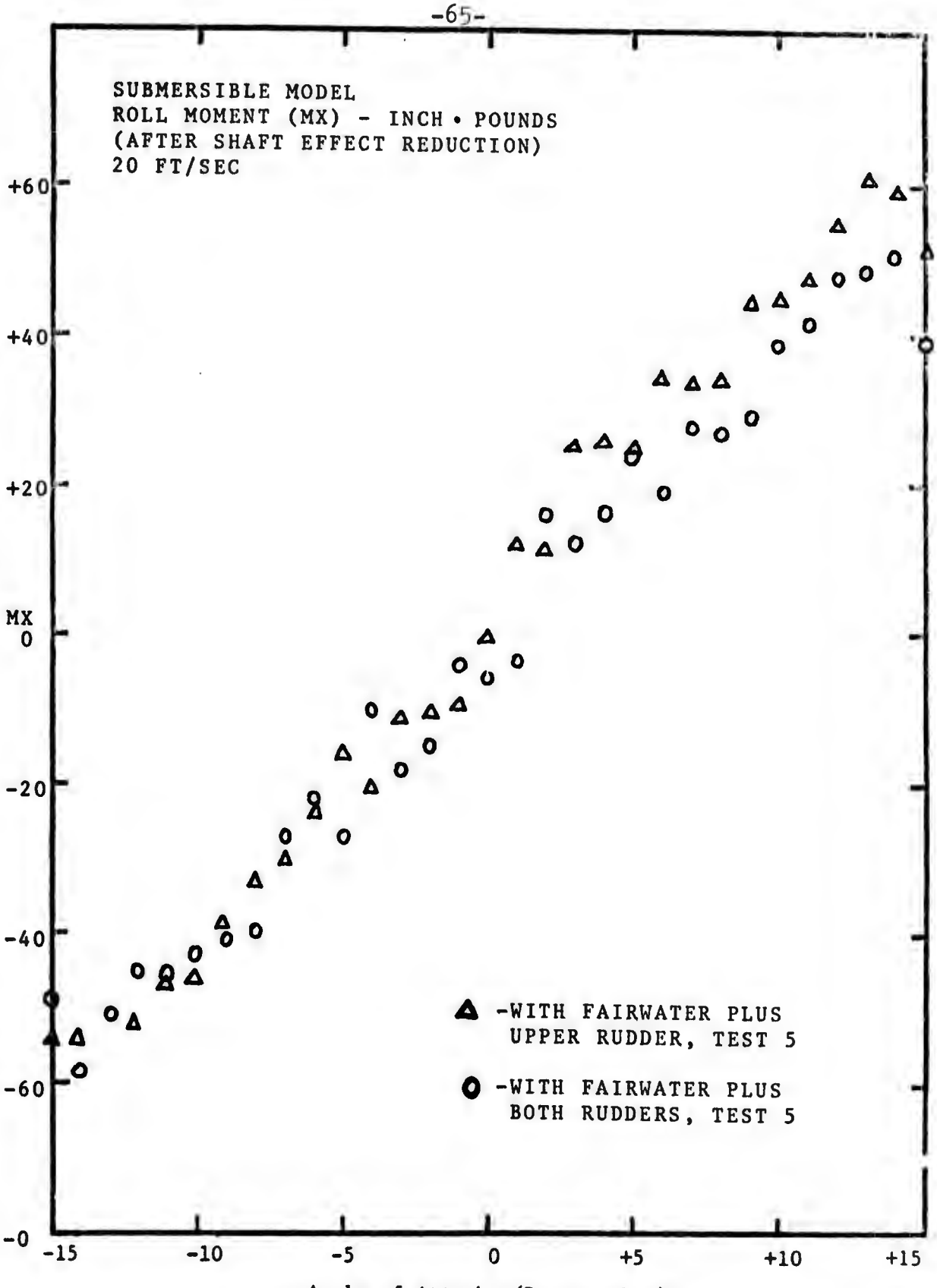
SUBMERSIBLE MODEL
ROLL MOMENT (MX) - INCH • POUNDS
(AFTER SHAFT EFFECT REDUCTION)
20 FT/SEC
+60
+40
+20
MX
0
-20
-40
-60
-0
-15
-10
-5
0
+5
+10
+15
-WITH FAIRWATER PLUS UPPER RUDDER, TEST 5
-WITH FAIRWATER PLUS BOTH RUDDERS, TEST 5
Angle of Attack- (Degrees-Yaw)

Figure 37

YAW MOMENT (MYO)

1. Shaft Effect

No shaft effect was, or should be, obtained for yaw moment, as this moment is measured about the shaft axis of symmetry.

2. Model Results

Configuration 1 (clean hull) produced a linear result that increased with increasing angle of yaw and flow velocity, see Figure 38. Yaw moment components resulted from form drag and changes in the cross flow pattern along the length of the model. The resulting slopes for the two velocities evaluated were:

A. Slope = 43 in. lb/10 degrees = 4.3 in. lb/degree, for 15 ft/sec,

B. Slope = 80 in. lb/10 degrees = 8.0 in. lb/degree, for 20 ft/sec.

When the fairwater (configuration 2) was added, there appears to be no effect until a yaw angle of 4 degrees is reached. Then, the yaw moment increases at a greater rate until the fairwater incurs separation (about 15 degrees yaw angle) and the yaw moment decreases until it reaches the magnitude obtained for the clean hull at that angle of yaw, see Figure 39.

When configuration 3 (with fairwater and upper rudder)

was tested, the magnitude of the yaw moment was decreased slightly due to the opposing yaw moment component from the upper rudder, see Figure 40. The yaw component from the rudder would have been larger if the fairwater had not caused any interaction, as previously described, to reduce the side force on the rudder. This configuration follows the same pattern as configuration 2; it incurs a rapid change in slope when the fairwater separates, but at a lower magnitude.

Configuration 4 (with fairwater and both rudders) produced a very powerful effect on reduction of yaw moment, see Figure 41. The side force developed by the addition of the lower rudder, combined with its moment arm, produces a yaw component that eventually supercedes that caused by the fairwater and forward portion of the body of revolution. When this model configuration was tested at an extreme yaw angle of 25 degrees, in both directions, and a flow velocity of 10 ft/sec, the resulting yaw moment was zero. The result for positive angles of yaw can be seen in Figure 42. Negative angles of yaw produced symmetrical results.

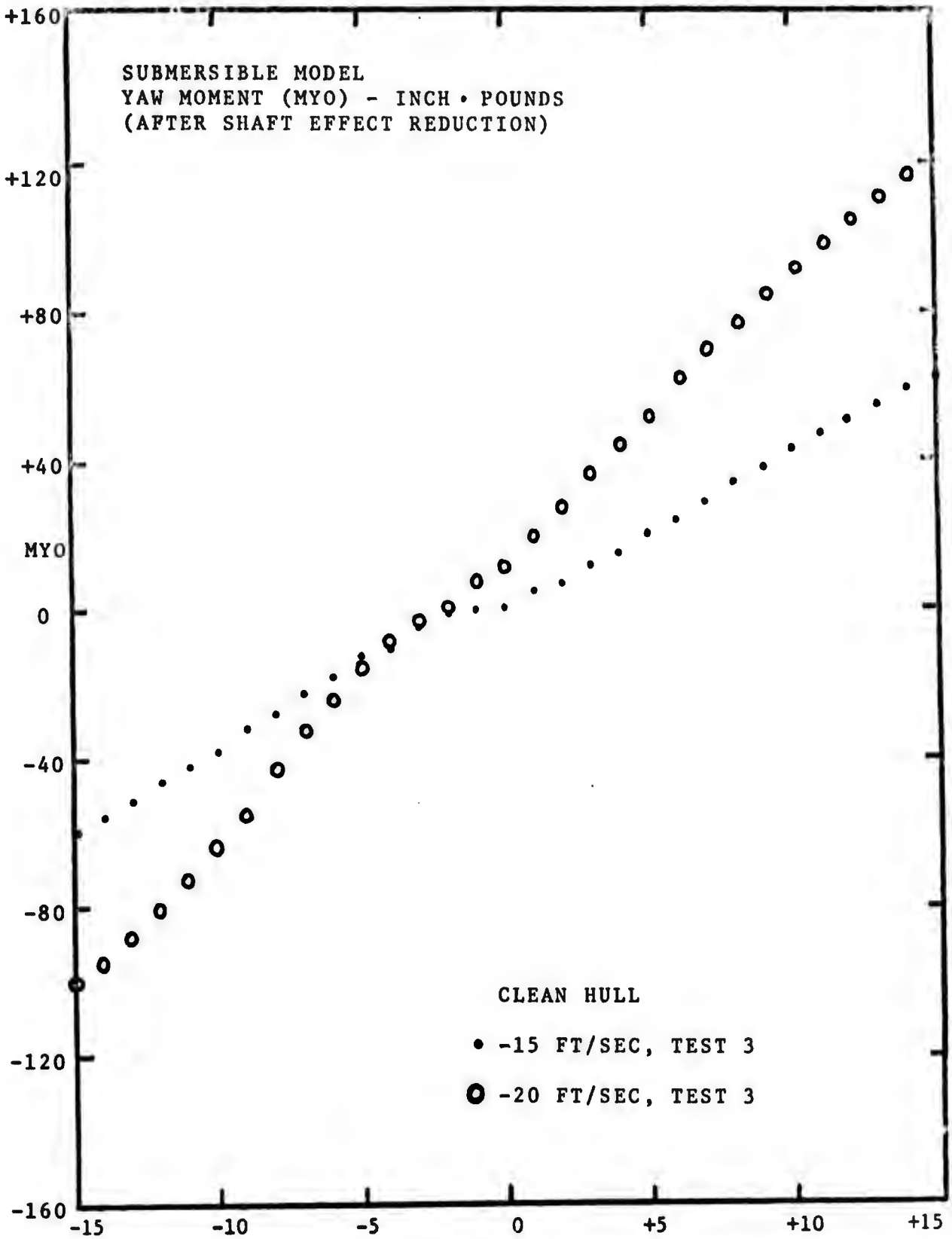
SUBMERSIBLE MODEL
YAW MOMENT (MYO) - INCH • POUNDS
(AFTER SHAFT EFFECT REDUCTION)
+160
+120
+80
+40
MYO
0
-40
-80
-120
-160
-15
-10
-5
0
+5
+10
+15
CLEAN HULL
• -15 FT/SEC, TEST 3
O -20 FT/SEC, TEST 3
Angle of Attack- (Degrees-Yaw)

Figure 38

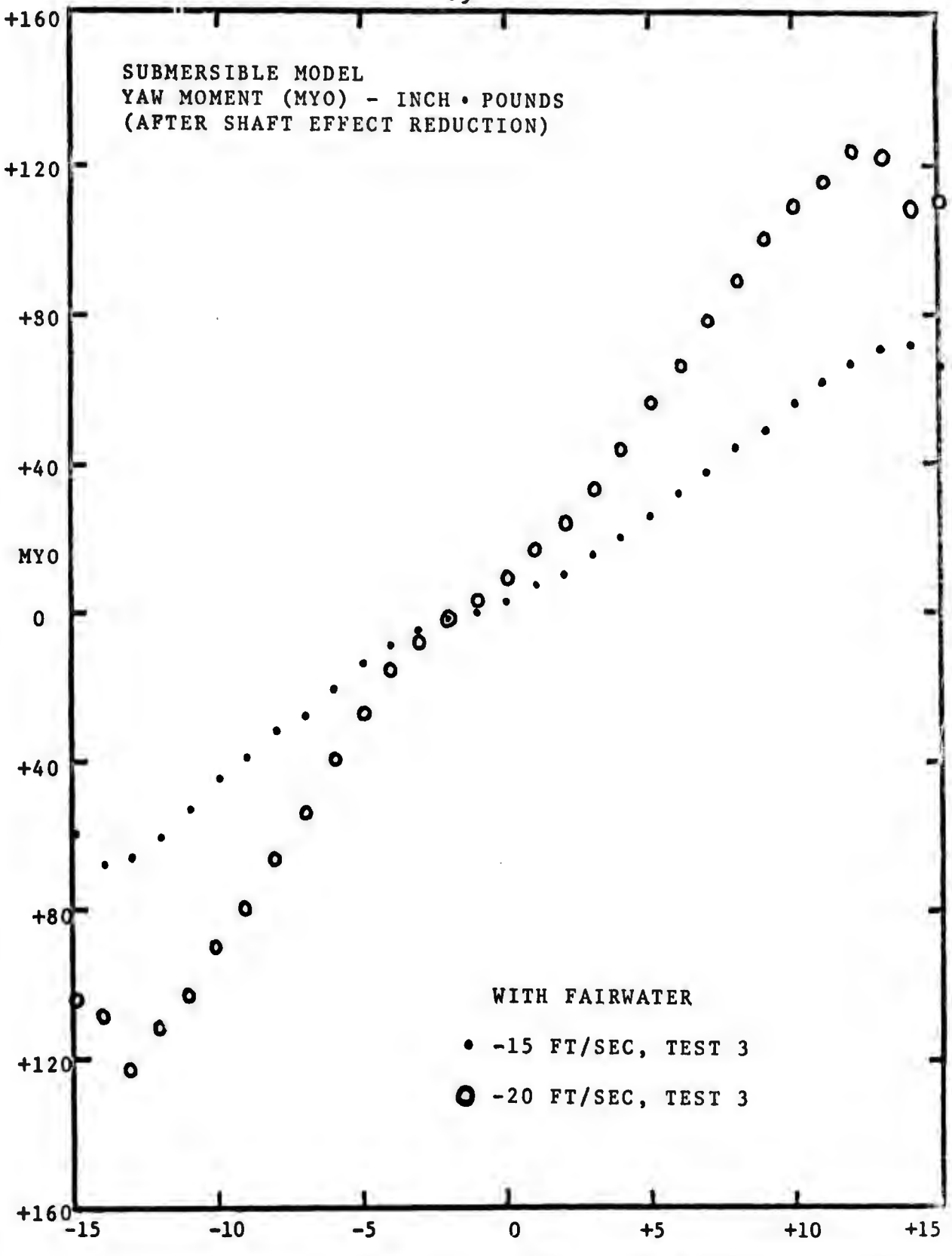
SUBMERSIBLE MODEL
YAW MOMENT (MYO) - INCH • POUNDS
(AFTER SHAFT EFFECT REDUCTION)
+160
+120
+80
+40
MYO
0
+40
+80
+120
+160
-15
-10
-5
0
+5
+10
+15
WITH FAIRWATER
• -15 FT/SEC, TEST 3
O -20 FT/SEC, TEST 3
Angle of Attack- (Degrees-Yaw)

Figure 39

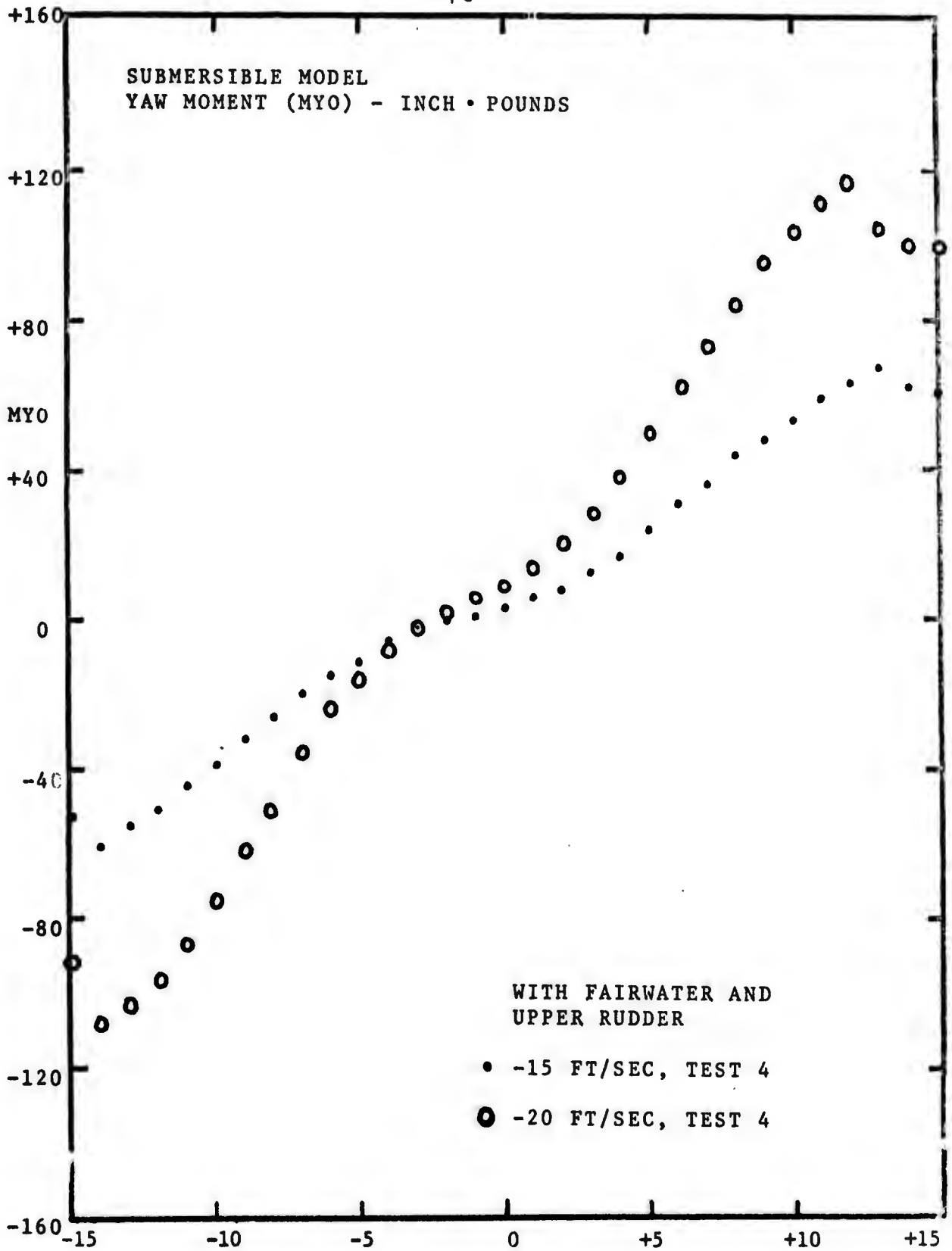
SUBMERSIBLE MODEL
YAW MOMENT (MYO) - INCH • POUNDS
+160
+120
+80
MYO
+40
0
-40
-80
-120
-160
-15
-10
-5
0
+5
+10
+15
WITH FAIRWATER AND
UPPER RUDDER
• -15 FT/SEC, TEST 4
O -20 FT/SEC, TEST 4
Angle of Attack- (Degrees-Yaw)

Figure 40

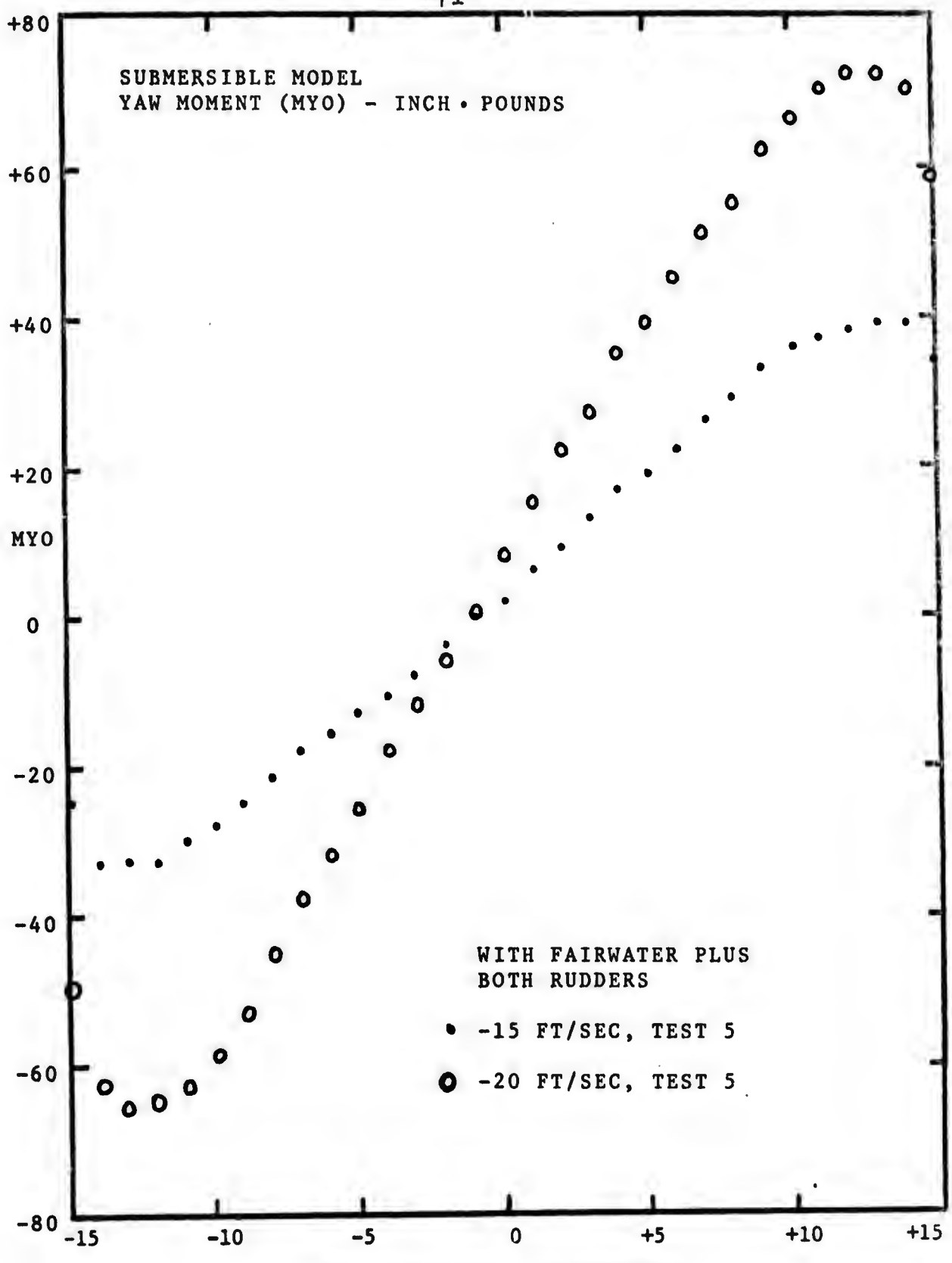
SUBMERSIBLE MODEL
YAW MOMENT (MYO) - INCH • POUNDS
+80
+60
+40
+20
MYO
0
-20
-40
-60
-80
-15
-10
-5
0
+5
+10
+15
WITH FAIRWATER PLUS
BOTH RUDDERS
-15 FT/SEC, TEST 5
-20 FT/SEC, TEST 5
Angle of Attack- (Degrees-Yaw)

Figure 41

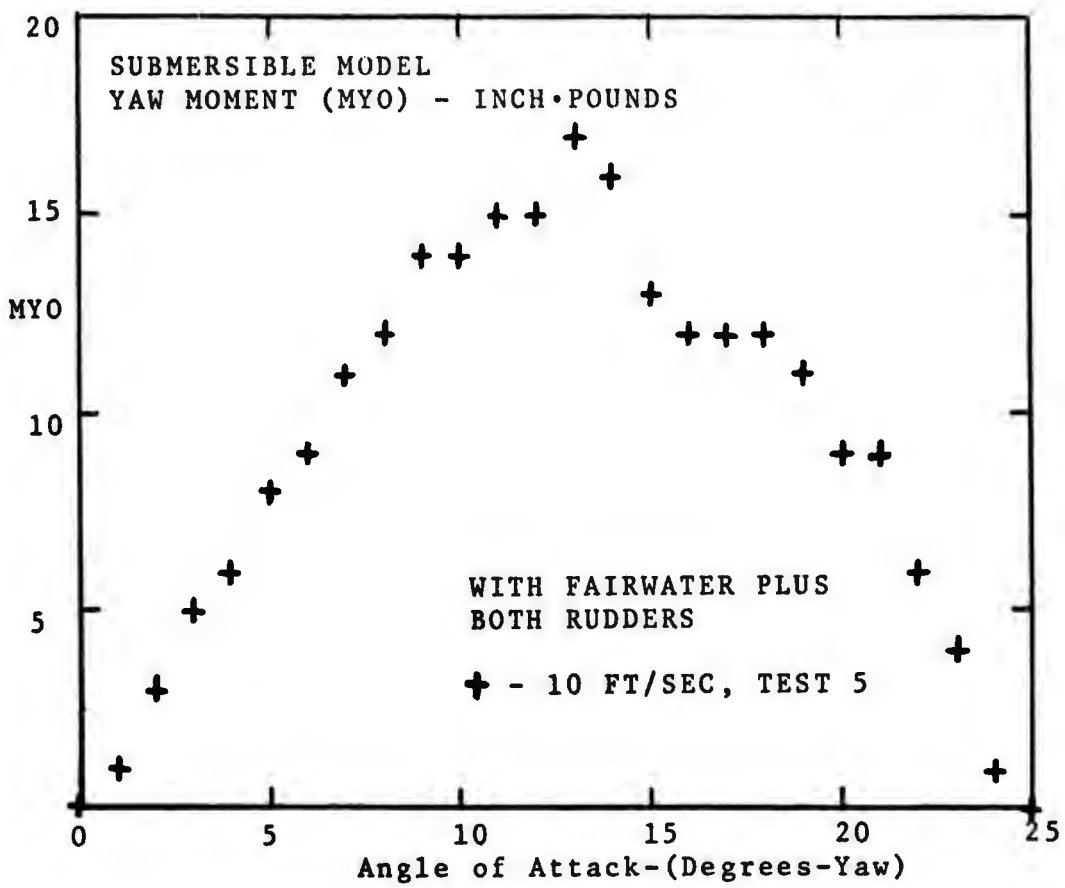
SUBMERSIBLE MODEL
YAW MOMENT (MYO) - INCH•POUNDS
MYO
20
15
10
5
0
5
10
15
20
25
Angle of Attack-(Degrees-Yaw)
WITH FAIRWATER PLUS
BOTH RUDDERS
+ - 10 FT/SEC, TEST 5

Figure 42

V. FAIRWATER MODEL EXPERIMENTAL RESULTS

The second set of experiments conducted in the M.I.T. Variable Pressure Water Tunnel consisted of testing the fairwater model, without control surfaces and then with control surfaces attached. The control surfaces were attached to the fairwater by means of a shaft through both the control surfaces and the fairwater. The shaft was used for transferring hydrodynamic forces and moments on the control surfaces to the fairwater, in effect, to the body of the submersible. To control and maintain particular angles of attack of the control surfaces, a guide pin was installed on each of the two separate control surfaces, between the location of the shaft and trailing edge. Guide holes were placed on each side of the fairwater for angles of attack to be evaluated, see Figure 7a. The particular angles of attack of the control surfaces (α') tested were: 0°, $\pm 5^\circ$, $\pm 10^\circ$, $\pm 15^\circ$, and $\pm 20^\circ$.

Six different tests (configurations) were conducted on the above model, and consisted of:

Test 1 - fairwater clean, no control surfaces, see Figure 7a;

Test 2 - fairwater, with control surfaces at $\alpha' = 0^\circ$, see figure 7b;

Test 3 - fairwater, with control surfaces at opposite angles of attack, $\alpha' = \pm 5^\circ$;

Test 4 - fairwater, with control surfaces at opposite angles of attack, $\alpha' = \pm 10^{o}$;

Test 5 - fairwater, with control surfaces at opposite angles of attack, $\alpha' = \pm 15^{o}$;

Test 6 - fairwater, with control surfaces at opposite angles of attack, $\alpha' = \pm 20^{o}$, see Figures 7c - e.

Each test considered fairwater angles of attack (α) from 0^{o} through stall on both sides of the fairwater, to cover the full spectrum of possible configurations, see Figure 43.

The purpose of these tests was to determine the hydrodynamic effect of using fairwater control surfaces independent of each other to generate side forces and moments to help alleviate the roll-moment (MZ) and side forces (FZ) caused by angle of attack (α) in yaw of the fairwater, which is the same as that of the submersible. These control surfaces are located as close as possible to the fairwater tip, contrary to usual practice on current submersible design.

These tests were developed into more meaningful results by transforming the side forces (FZ) and roll moments (MZ) of the fairwater to the center of an imaginary submersible, to evaluate only the effects of a fairwater and control surfaces on a submersible.

An imaginary submersible moment arm, in the vertical plane, was obtained by scaling the fairwater model with that of an actual submersible. The resulting roll moment:

Net Roll Moment = MX + (FZ)·(R),

where: MX = roll moment at fairwater base

FZ = side force at fairwater base

R = imaginary submersible moment arm = 6.3".

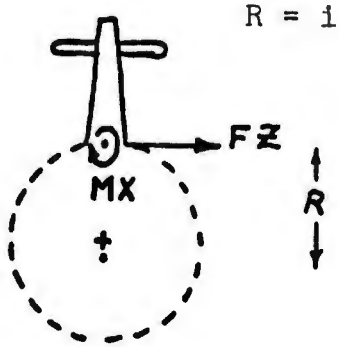

The results were: for an increasing angle of attack (α') of the control surfaces, the effective angle of attack (α) of the fairwater (submersible) in yaw is reduced. For a maximum angle of attack (α') of $\pm$ 20°, the reduction is approximately 4.5° for the first series of model test, see Figures 44 - 49.

This first series of tests of the fairwater used control surfaces with non-tapered tips. A second series of tests was performed with tapered end tips added, to alleviate some of the possible drag of the flat-ended configuration of the control surfaces. The results of this second series of tests showed an increase in desired effect, or a decrease in effective angle of attack of the fairwater from the first series of tests. This difference in the second test was approximately 2° beyond the first, see Figures 50 and 51.

Compatible results for lift (FZO - component perpendicular to tunnel flow) and drag (FXO - component parallel to

tunnel flow) on the fairwater model for the flat tip and tapered tip fairwater control surfaces are given in Figures 52 - 59, and Figures 60 - 63 respectively.

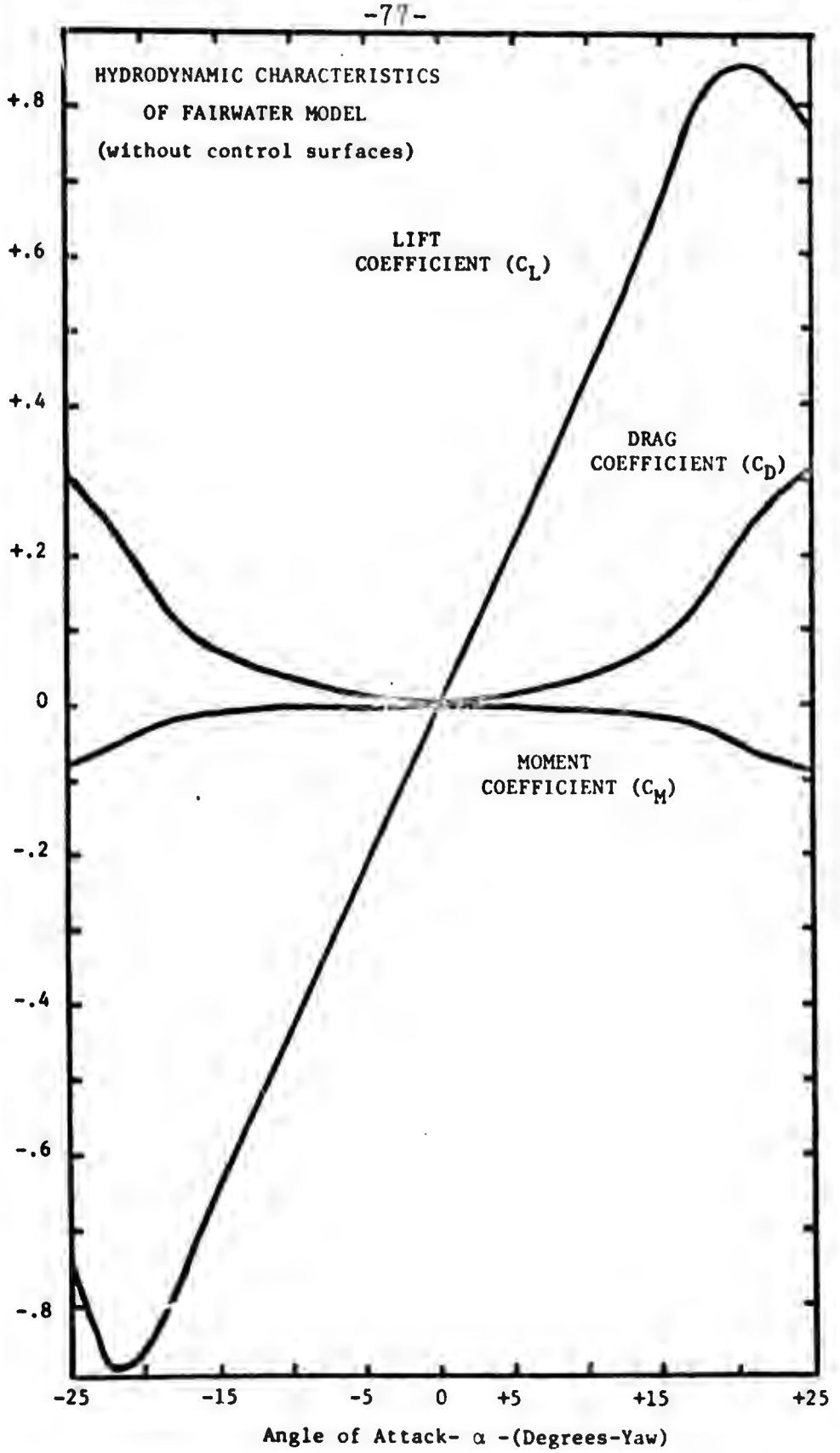
HYDRODYNAMIC CHARACTERISTICS
OF FAIRWATER MODEL
(without control surfaces)
LIFT
COEFFICIENT (C_L)
DRAG
COEFFICIENT (C_D)
MOMENT
COEFFICIENT (C_M)
+.8
+.6
+.4
+.2
0
-.2
-.4
-.6
-.8
-25
-15
-5
0
+5
+15
+25
Angle of Attack- α -(Degrees-Yaw)

Figure 43

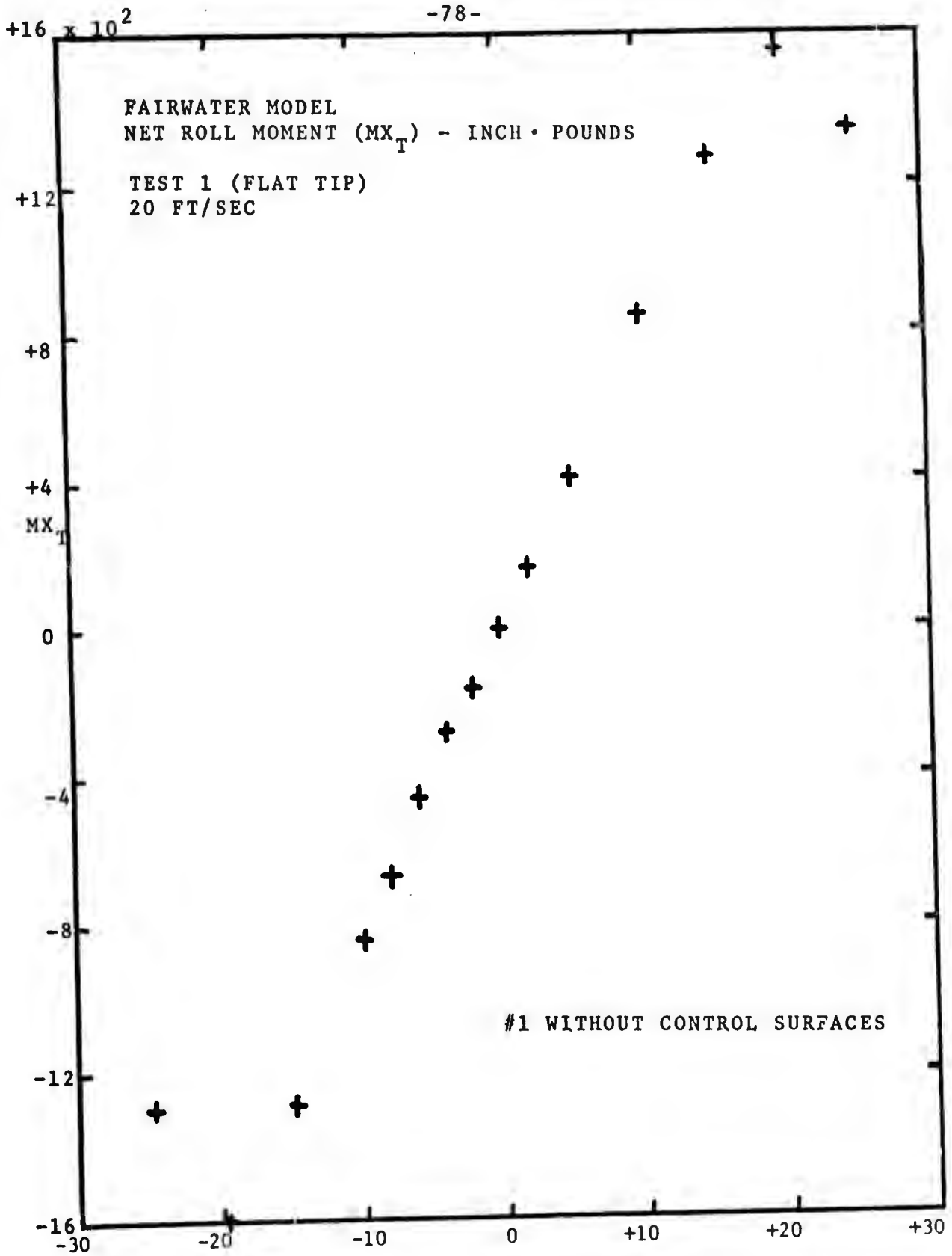
+16 x 10^2
FAIRWATER MODEL
NET ROLL MOMENT (MX_T) - INCH • POUNDS
TEST 1 (FLAT TIP)
20 FT/SEC
+12
+8
+4
MX_T
0
-4
-8
-12
-16
#1 WITHOUT CONTROL SURFACES
-30
-20
-10
0
+10
+20
+30
Angle of Attack- α -(Degrees-Yaw)

Figure 44

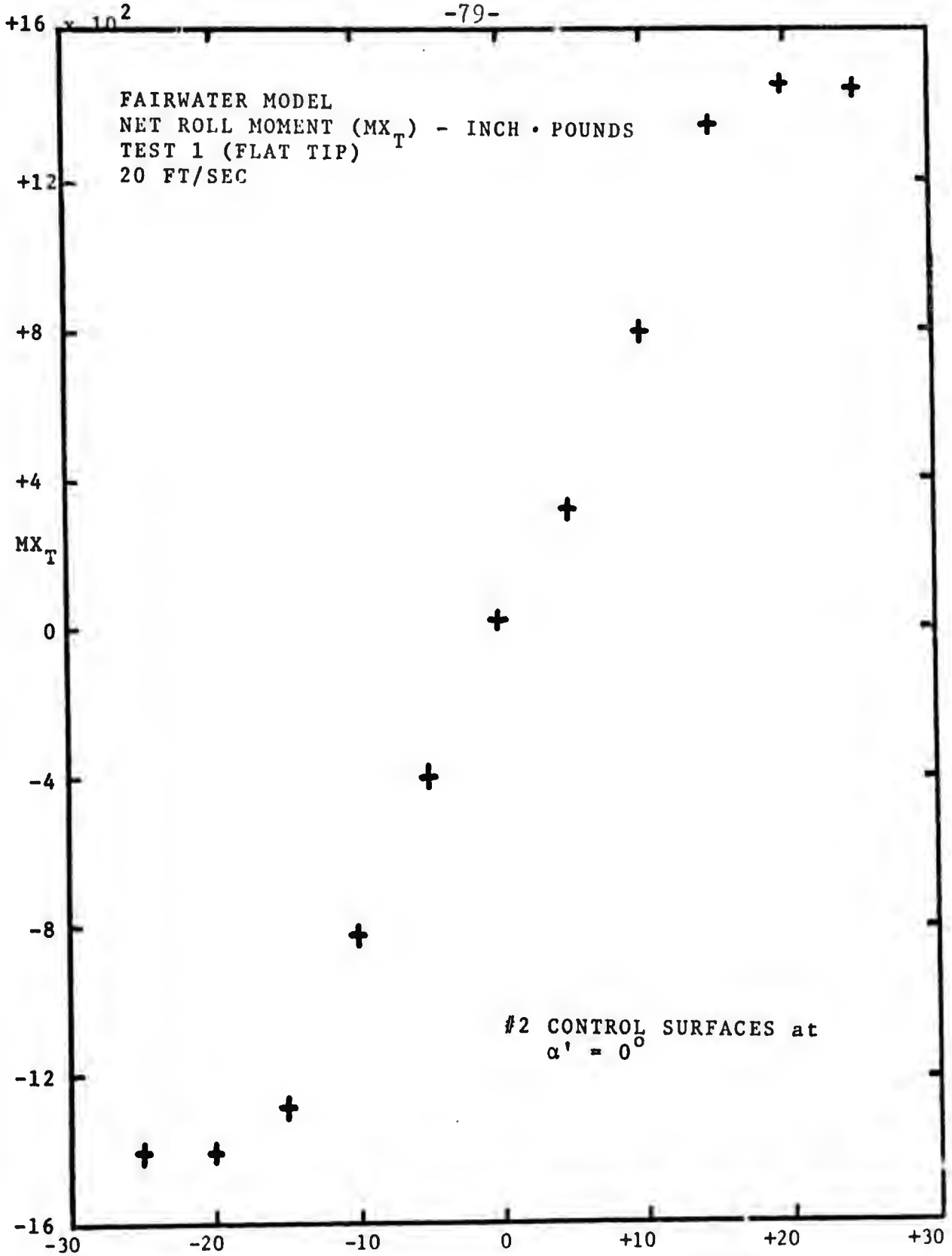
+16 x 10^2
+12
+8
+4
MX_T
0
-4
-8
-12
-16
-30
-20
-10
0
+10
+20
+30
FAIRWATER MODEL
NET ROLL MOMENT (MX_T) - INCH • POUNDS
TEST 1 (FLAT TIP)
20 FT/SEC
#2 CONTROL SURFACES at
α' = 0°
Angle of Attack- α -(Degrees-Yaw)

Figure 45

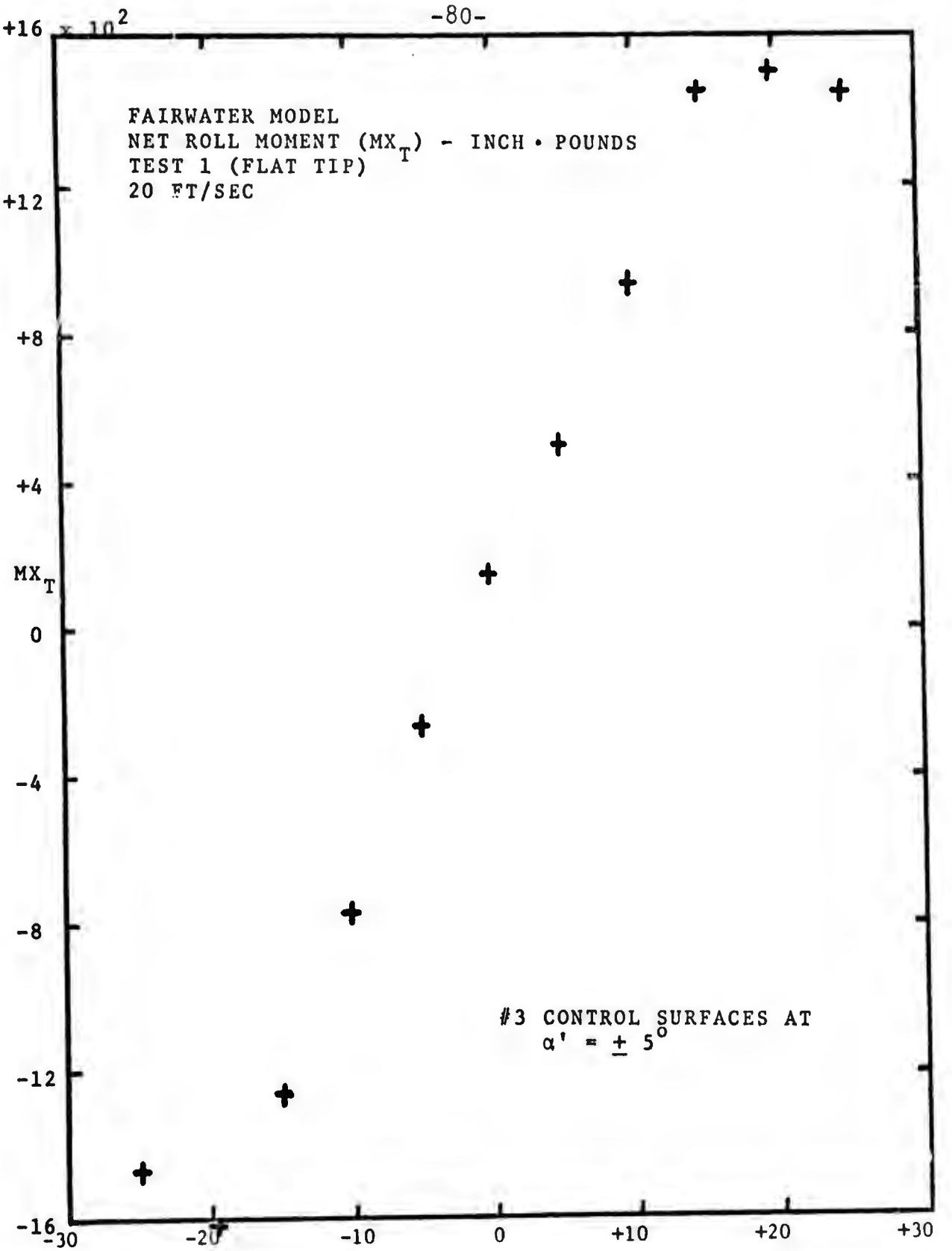
+16 x 10^2
FAIRWATER MODEL
NET ROLL MOMENT (MX_T) - INCH • POUNDS
TEST 1 (FLAT TIP)
20 FT/SEC
+12
+8
+4
MX_T
0
-4
-8
-12
-16
#3 CONTROL SURFACES AT
α' = ± 5°
-30
-20
-10
0
+10
+20
+30
Angle of Attack- α -(Degrees-Yaw)

Figure 46

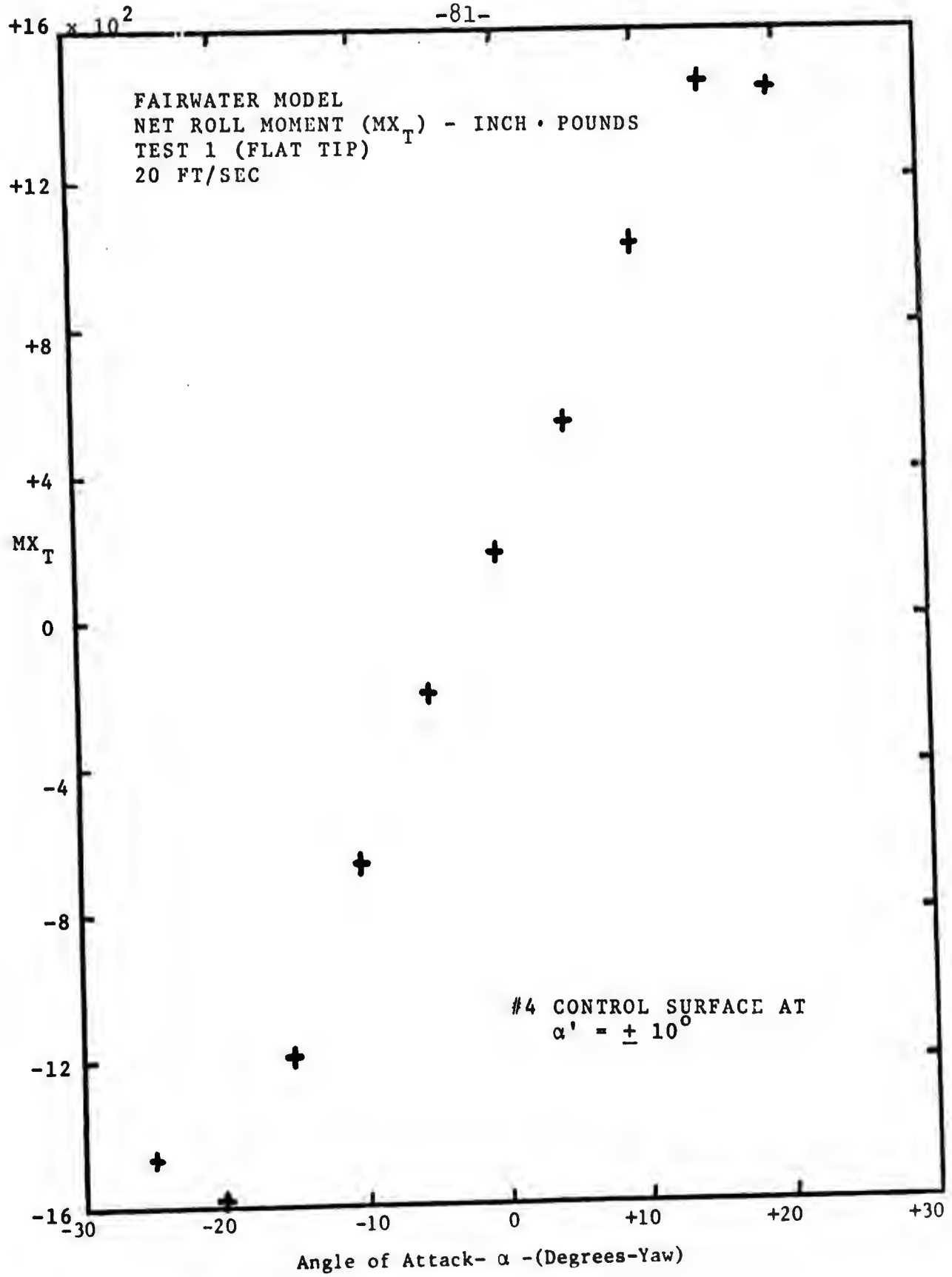
+16 x 10^2
FAIRWATER MODEL
NET ROLL MOMENT (MX_T) - INCH • POUNDS
TEST 1 (FLAT TIP)
20 FT/SEC
+12
+8
+4
MX_T
0
-4
-8
-12
-16
#4 CONTROL SURFACE AT
α' = ± 10°
-30
-20
-10
0
+10
+20
+30
Angle of Attack- α -(Degrees-Yaw)

Figure 47

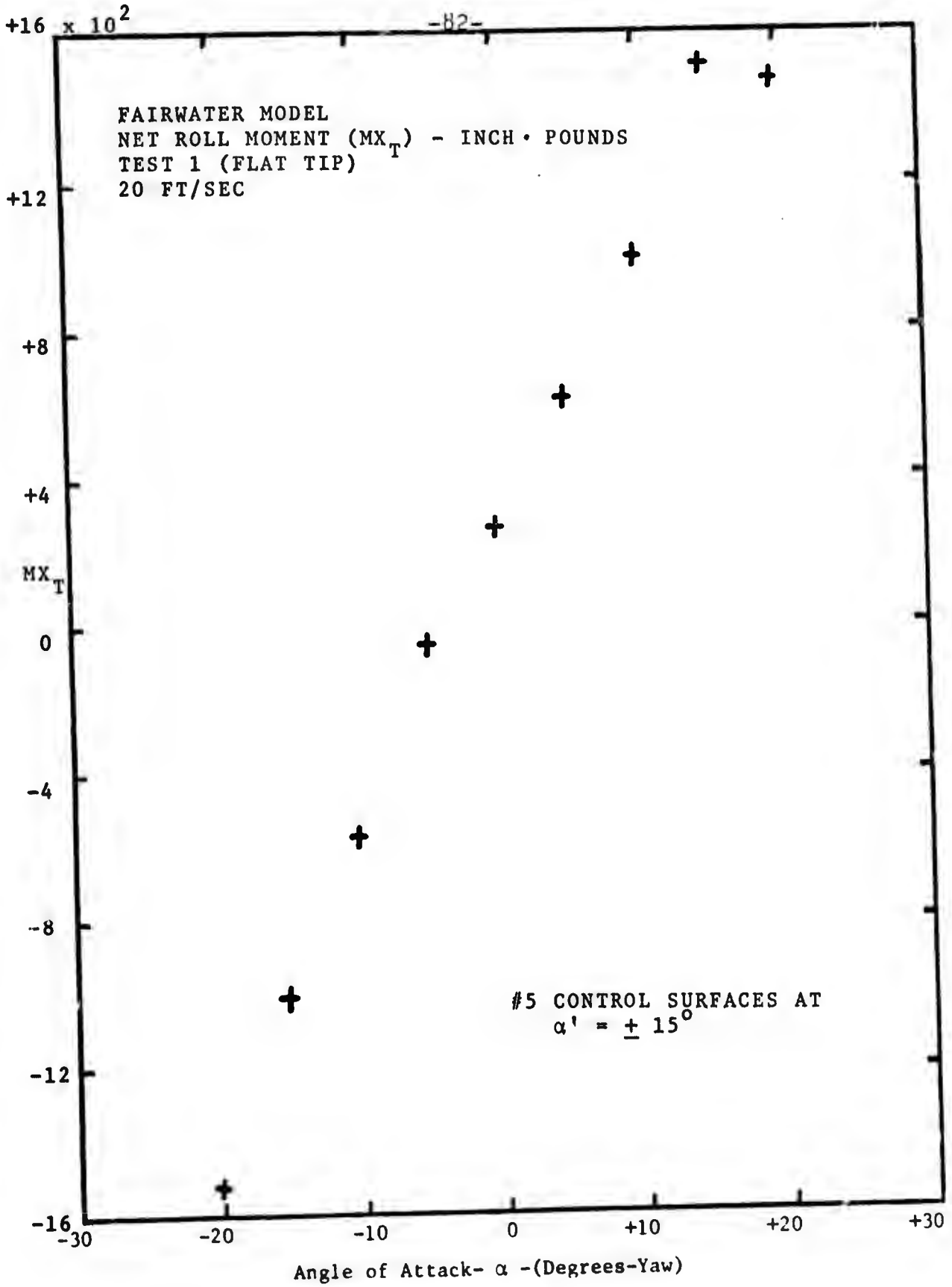
+16 x 10^2
FAIRWATER MODEL
NET ROLL MOMENT (MX_T) - INCH • POUNDS
TEST 1 (FLAT TIP)
20 FT/SEC
+12
+8
+4
MX_T
0
-4
-8
-12
-16
#5 CONTROL SURFACES AT
α' = ± 15°
-30
-20
-10
0
+10
+20
+30
Angle of Attack- α -(Degrees-Yaw)

Figure 48

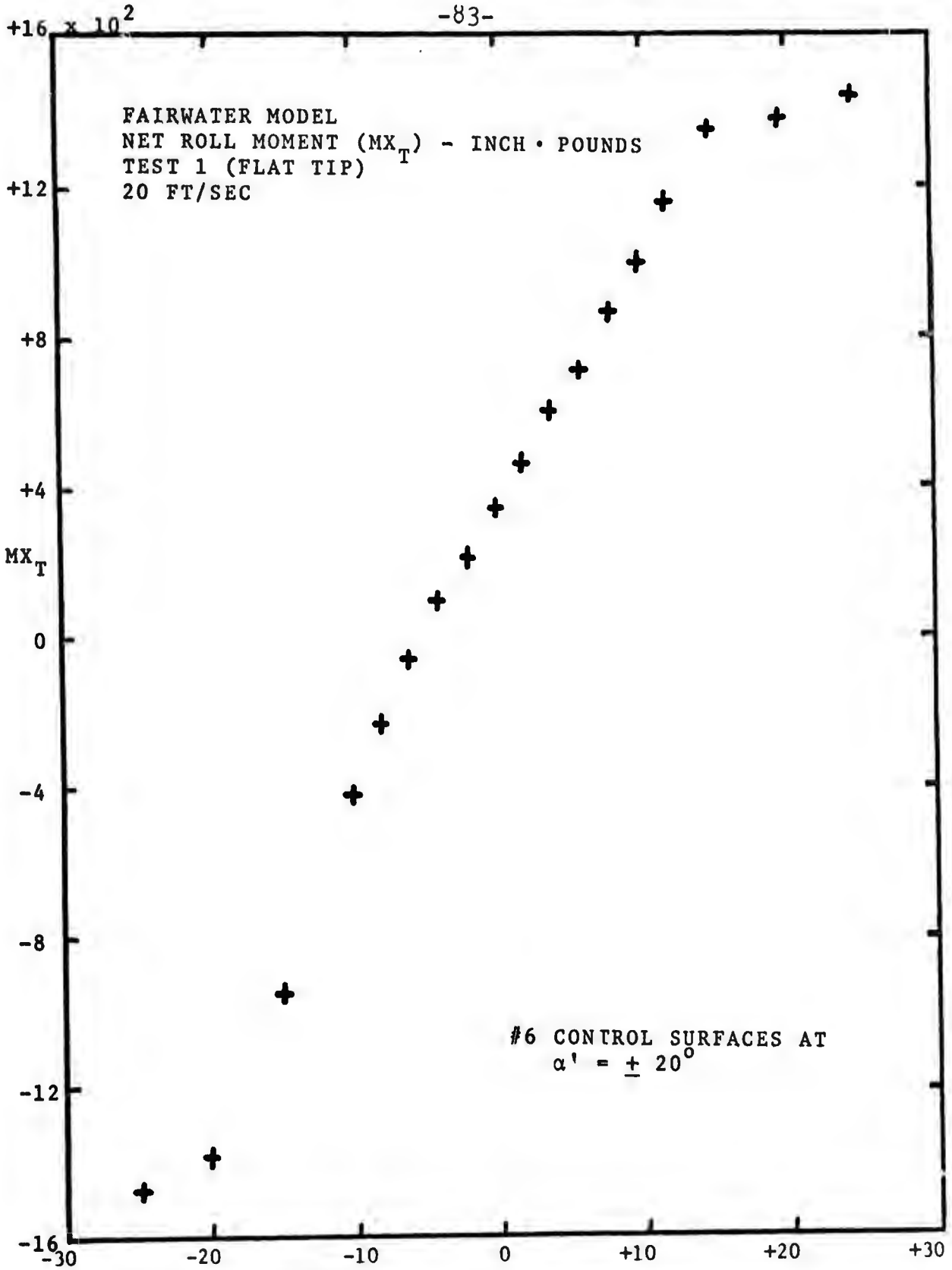
+16 x 10^2
FAIRWATER MODEL
NET ROLL MOMENT (MX_T) - INCH • POUNDS
TEST 1 (FLAT TIP)
20 FT/SEC
+12
+8
+4
MX_T
0
-4
-8
-12
-16
#6 CONTROL SURFACES AT
α' = ± 20°
-30
-20
-10
0
+10
+20
+30
Angle of Attack- α -(Degrees-Yaw)

Figure 49

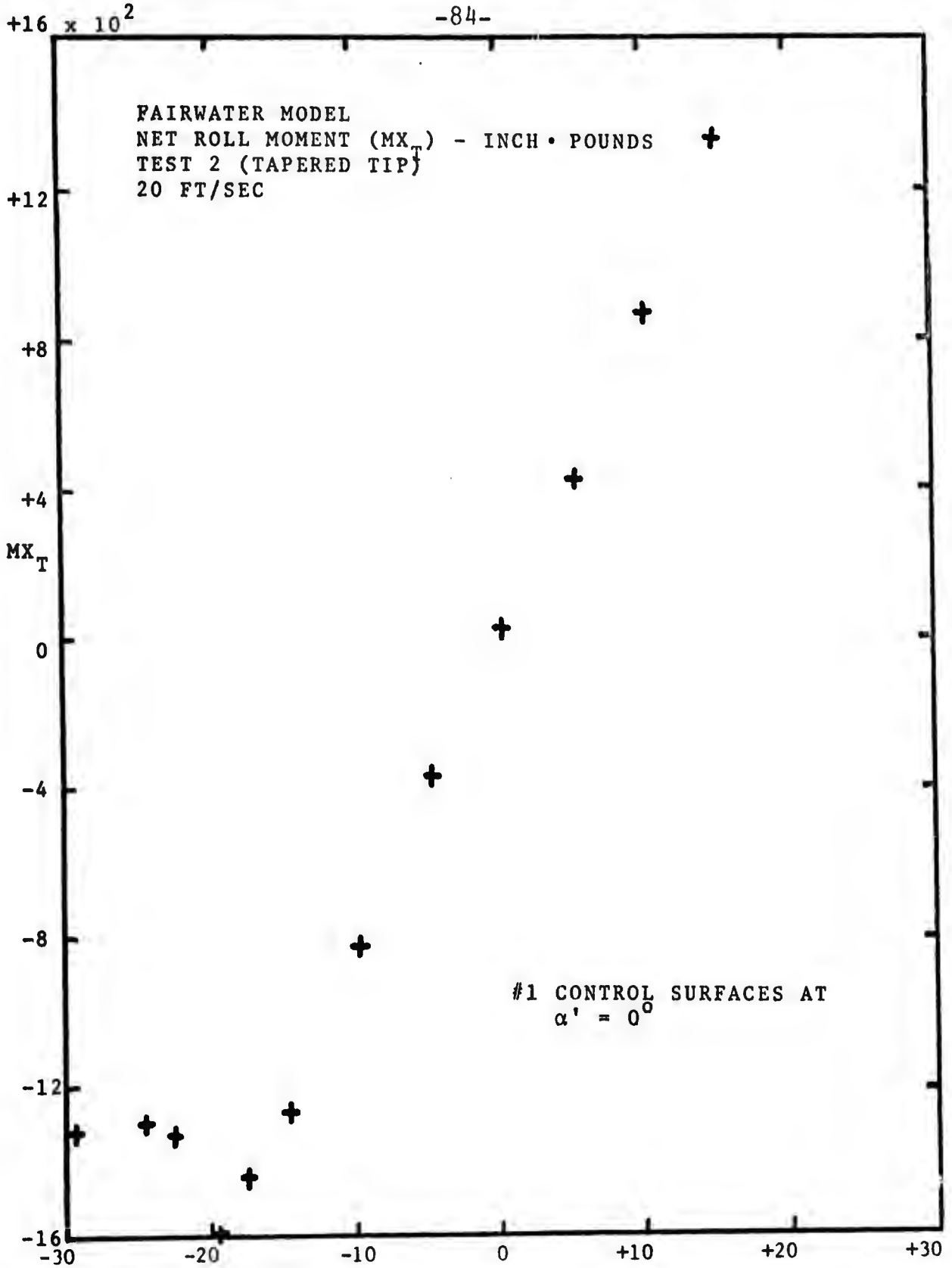
+16 x 10²
FAIRWATER MODEL
NET ROLL MOMENT (MX_T) - INCH • POUNDS
TEST 2 (TAPERED TIP)
20 FT/SEC
+12
+8
+4
MX_T
0
-4
-8
-12
-16
#1 CONTROL SURFACES AT
α' = 0°
-30
-20
-10
0
+10
+20
+30
Angle of Attack- α -(Degrees-Yaw)

Figure 50

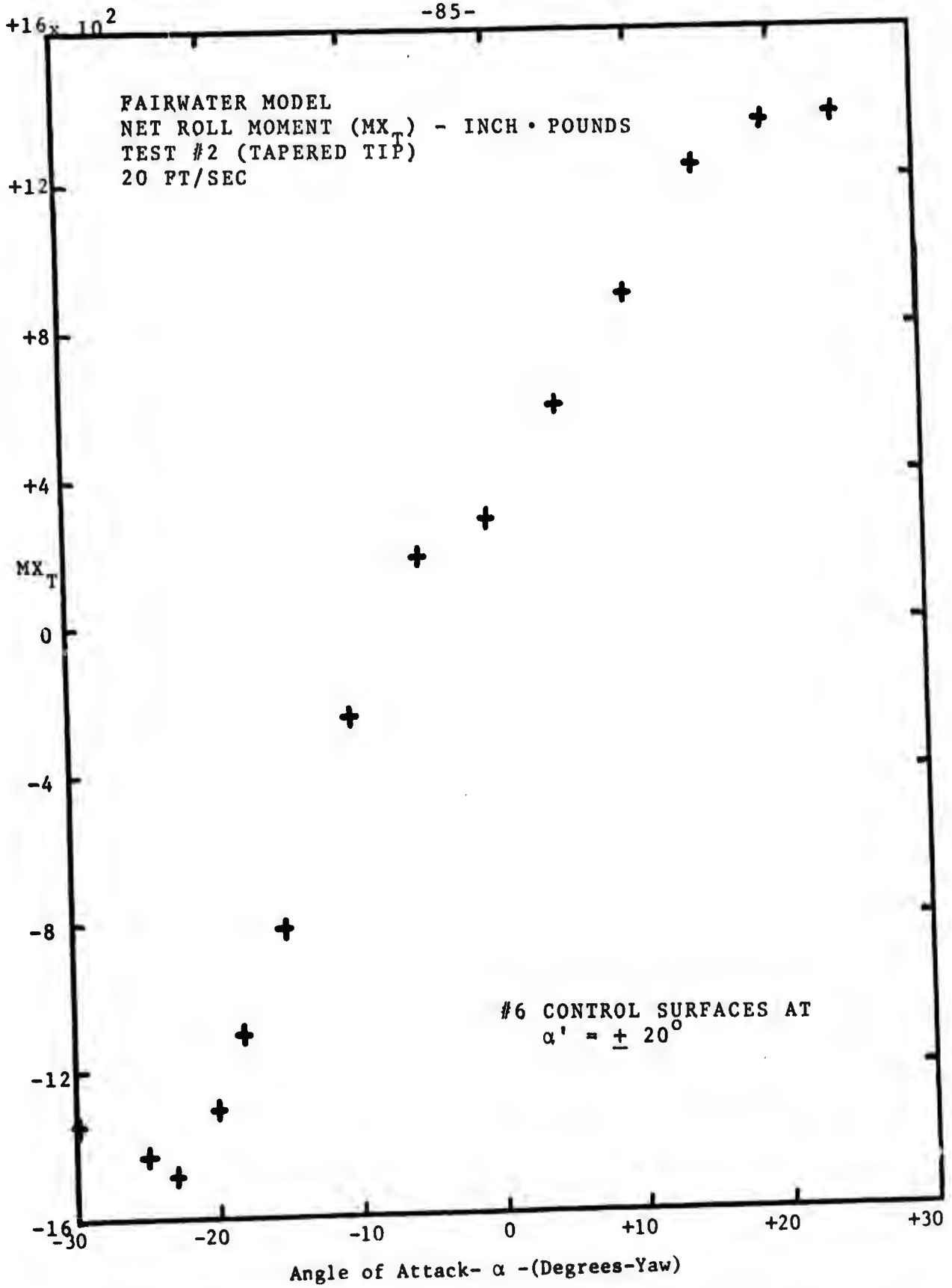
+16 x 10^2
FAIRWATER MODEL
NET ROLL MOMENT (MX_T) - INCH • POUNDS
TEST #2 (TAPERED TIP)
20 FT/SEC
+12
+8
+4
MX_T
0
-4
-8
-12
-16
#6 CONTROL SURFACES AT
α' = ± 20°
-30
-20
-10
0
+10
+20
+30
Angle of Attack- α -(Degrees-Yaw)

Figure 51

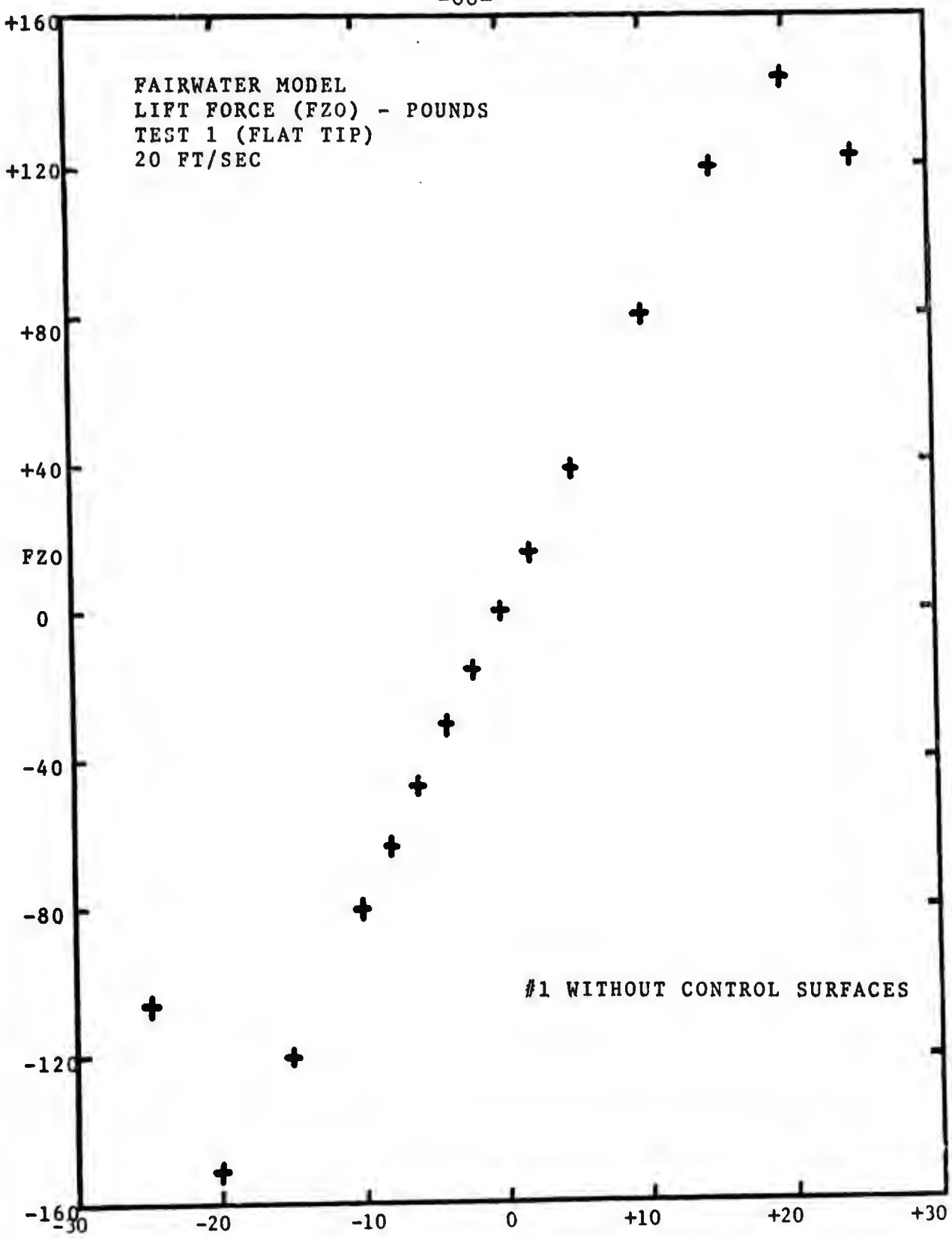
FAIRWATER MODEL
LIFT FORCE (FZO) - POUNDS
TEST 1 (FLAT TIP)
20 FT/SEC
#1 WITHOUT CONTROL SURFACES
+160
+120
+80
+40
FZO
0
-40
-80
-120
-160
-30
-20
-10
0
+10
+20
+30
Angle of Attack- α -(Degrees-Yaw)

Figure 52

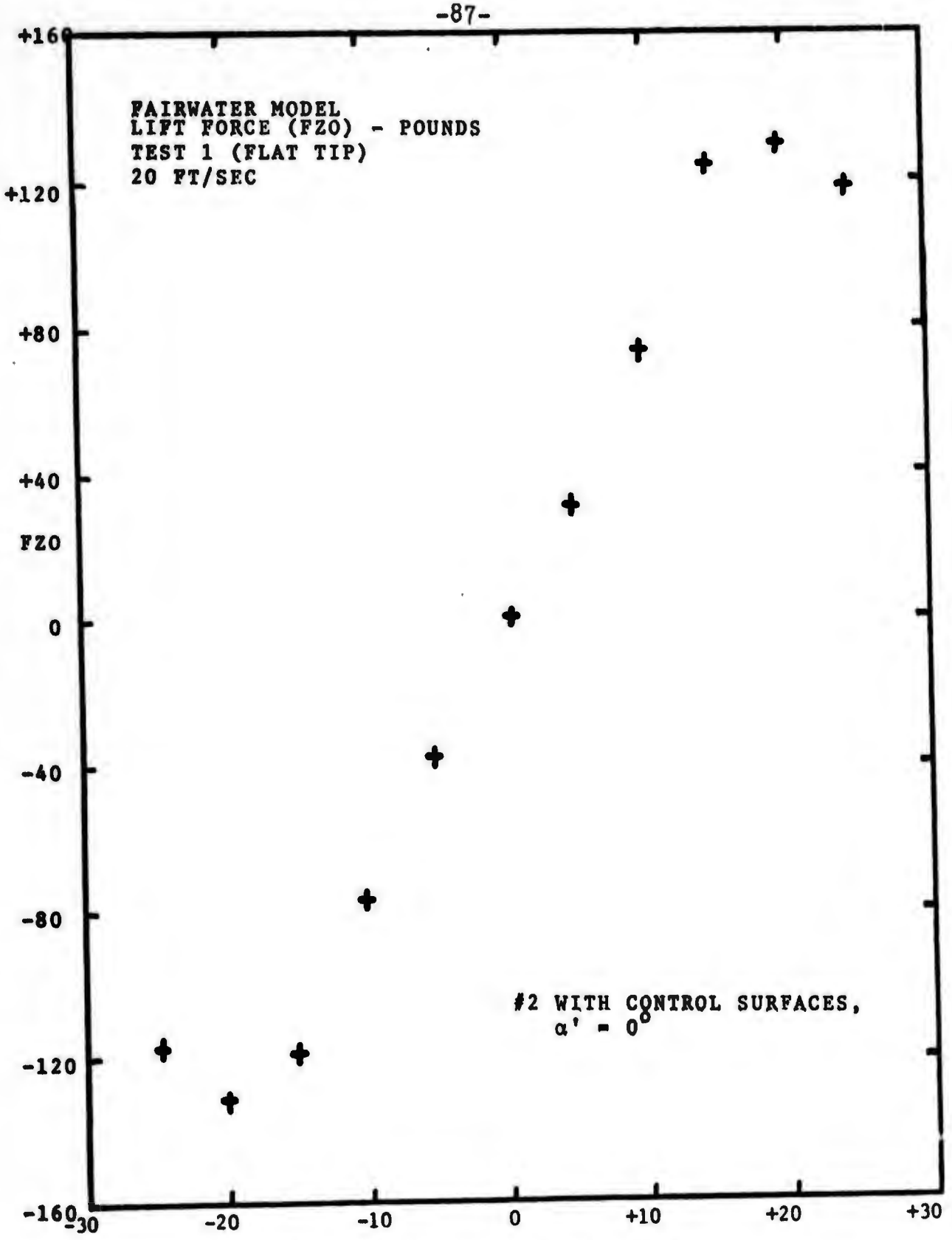
FAIRWATER MODEL
LIFT FORCE (FZO) - POUNDS
TEST 1 (FLAT TIP)
20 FT/SEC
+160
+120
+80
+40
FZO
0
-40
-80
-120
-160
#2 WITH CONTROL SURFACES,
α' = 0°
-30
-20
-10
0
+10
+20
+30
Angle of Attack- α -(Degrees-Yaw)

Figure 53

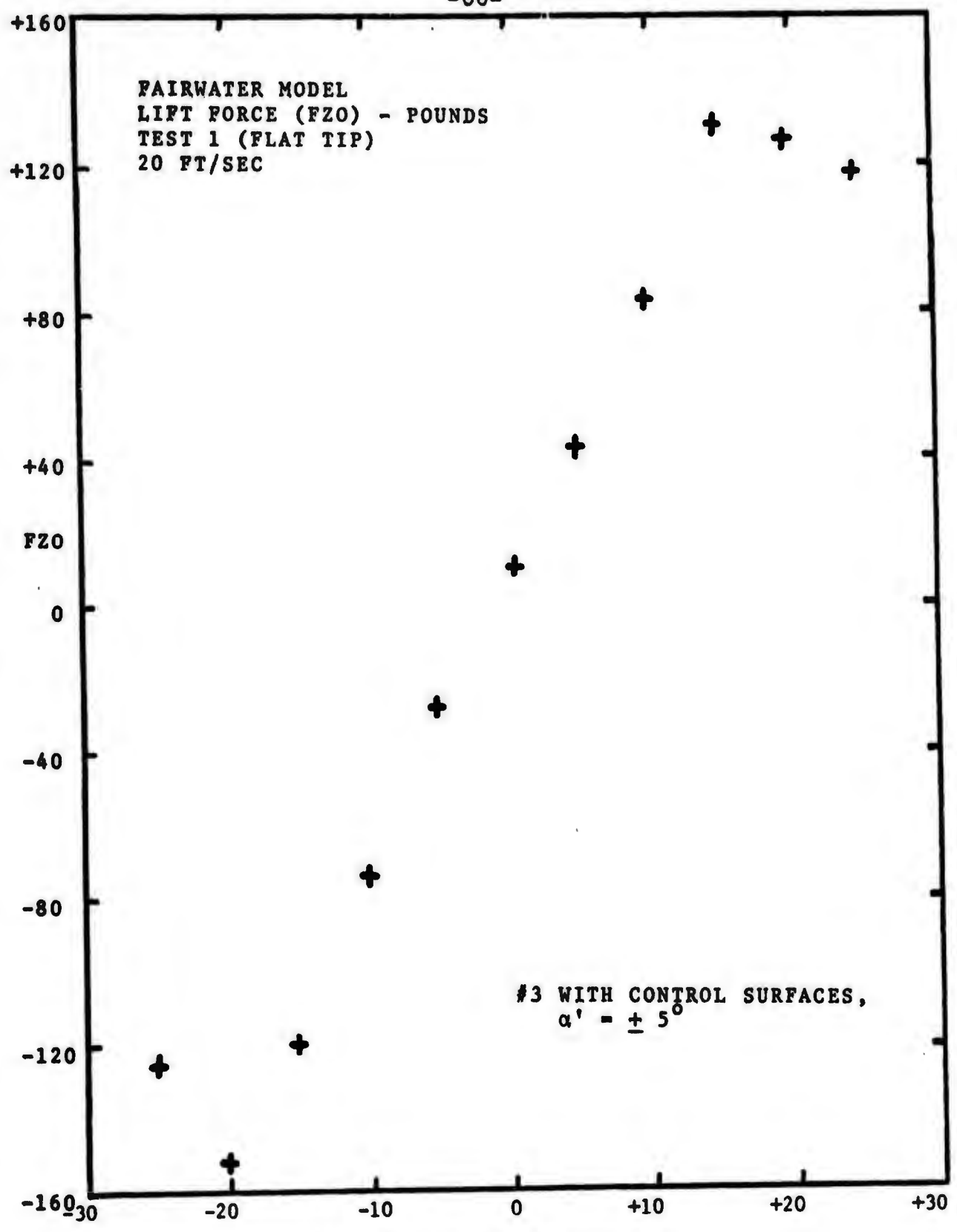
FAIRWATER MODEL
LIFT FORCE (FZO) - POUNDS
TEST 1 (FLAT TIP)
20 FT/SEC
#3 WITH CONTROL SURFACES,
α' = ± 5°
+160
+120
+80
+40
FZO
0
-40
-80
-120
-160
-30
-20
-10
0
+10
+20
+30
Angle of Attack- α -(Degrees-Yaw)

Figure 54

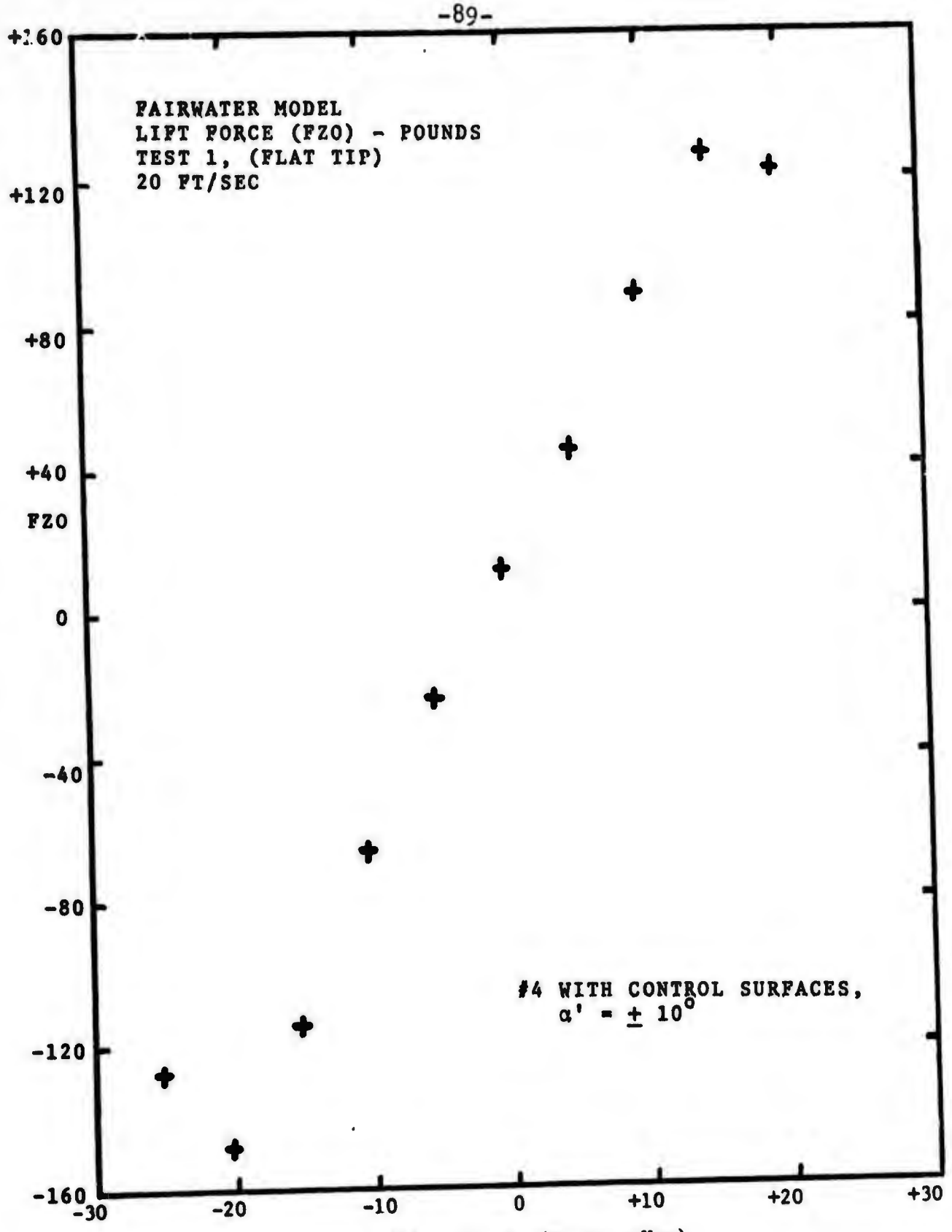
FAIRWATER MODEL
LIFT FORCE (FZO) - POUNDS
TEST 1, (FLAT TIP)
20 FT/SEC
#4 WITH CONTROL SURFACES,
α' = ± 10°
+160
+120
+80
+40
FZO
0
-40
-80
-120
-160
-30
-20
-10
0
+10
+20
+30
Angle of Attack- α -(Degrees-Yaw)

Figure 55

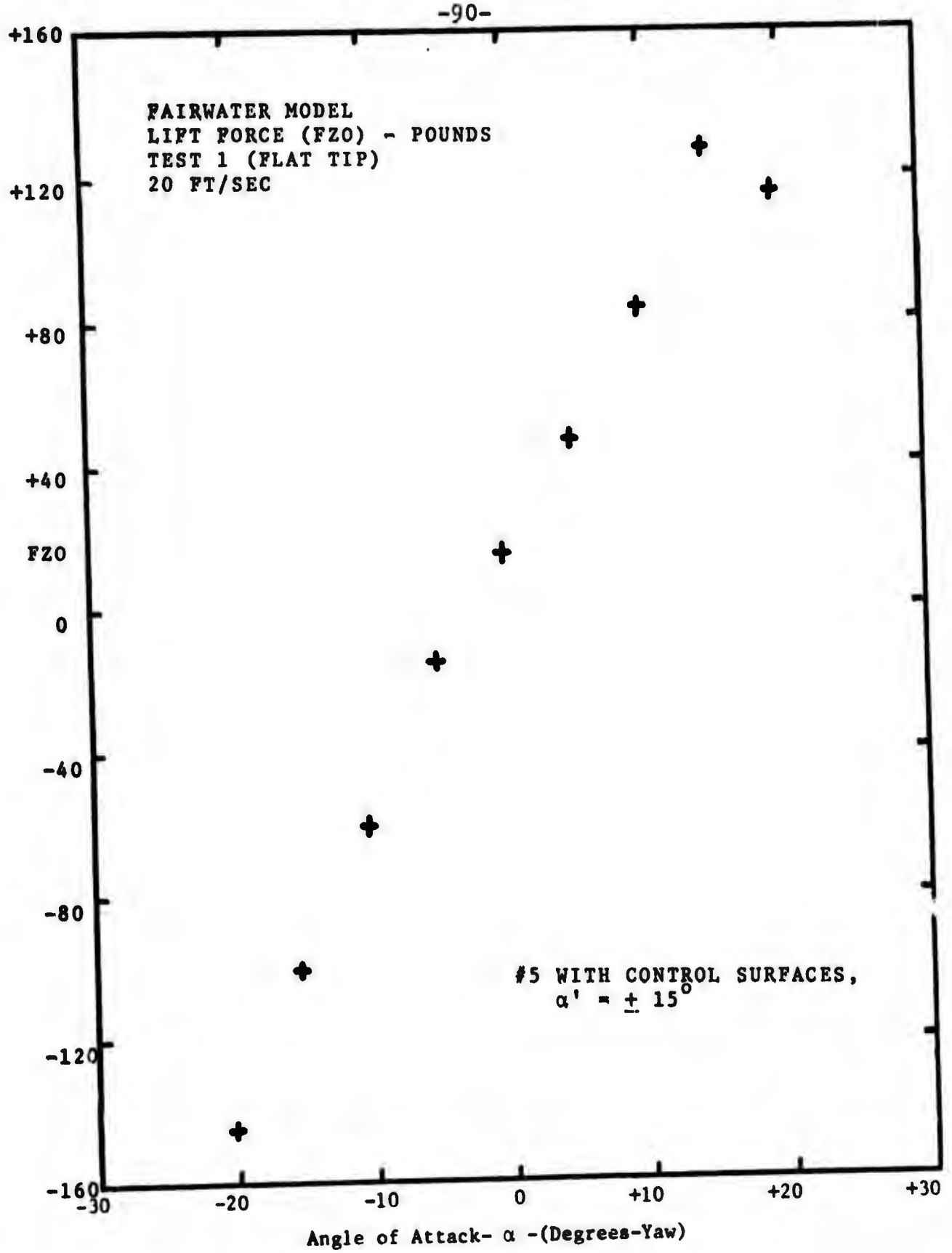
FAIRWATER MODEL
LIFT FORCE (FZO) - POUNDS
TEST 1 (FLAT TIP)
20 FT/SEC
#5 WITH CONTROL SURFACES,
α' = ± 15°
+160
+120
+80
+40
FZO
0
-40
-80
-120
-160
-30
-20
-10
0
+10
+20
+30
Angle of Attack- α -(Degrees-Yaw)

Figure 56

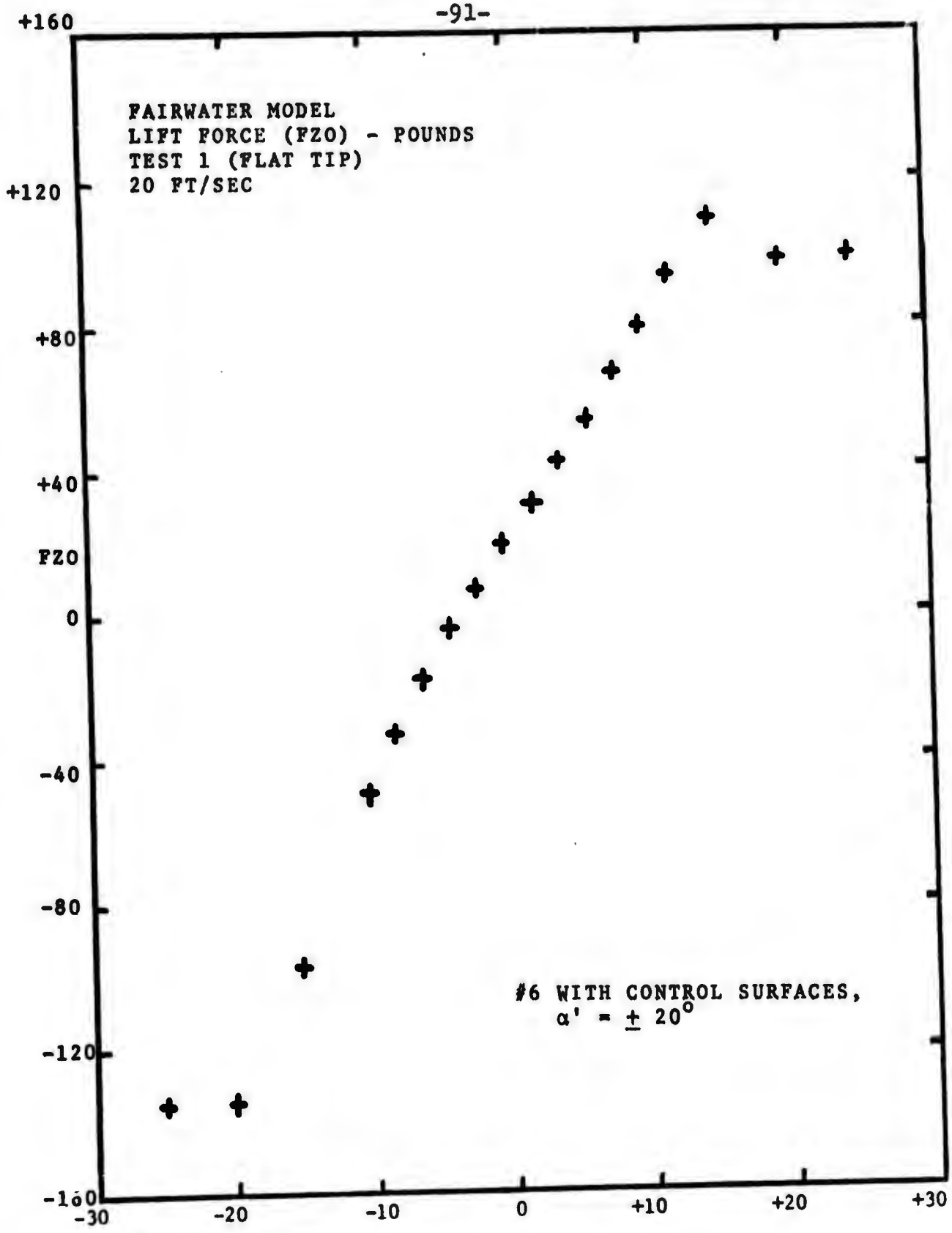
FAIRWATER MODEL
LIFT FORCE (FZO) - POUNDS
TEST 1 (FLAT TIP)
20 FT/SEC
+160
+120
+80
+40
FZO
0
-40
-80
-120
-160
-30
-20
-10
0
+10
+20
+30
#6 WITH CONTROL SURFACES,
α' = ± 20°
Angle of Attack- α -(Degrees-Yaw)

Figure 57

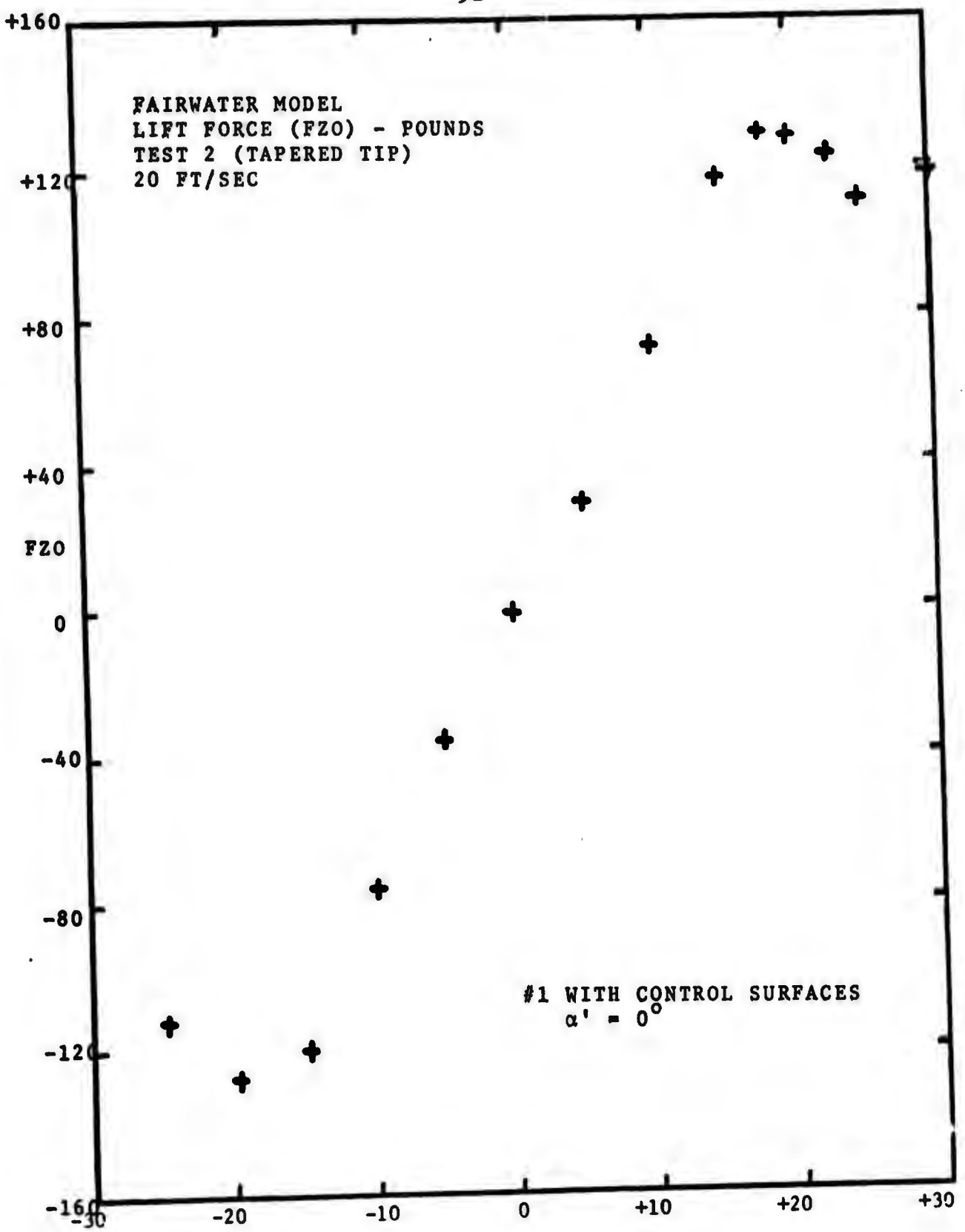
FAIRWATER MODEL
LIFT FORCE (FZO) - POUNDS
TEST 2 (TAPERED TIP)
20 FT/SEC
+160
+120
+80
+40
FZO
0
-40
-80
-120
-160
#1 WITH CONTROL SURFACES
α' = 0°
-30
-20
-10
0
+10
+20
+30
Angle of Attack- α -(Degrees-Yaw)

Figure 58

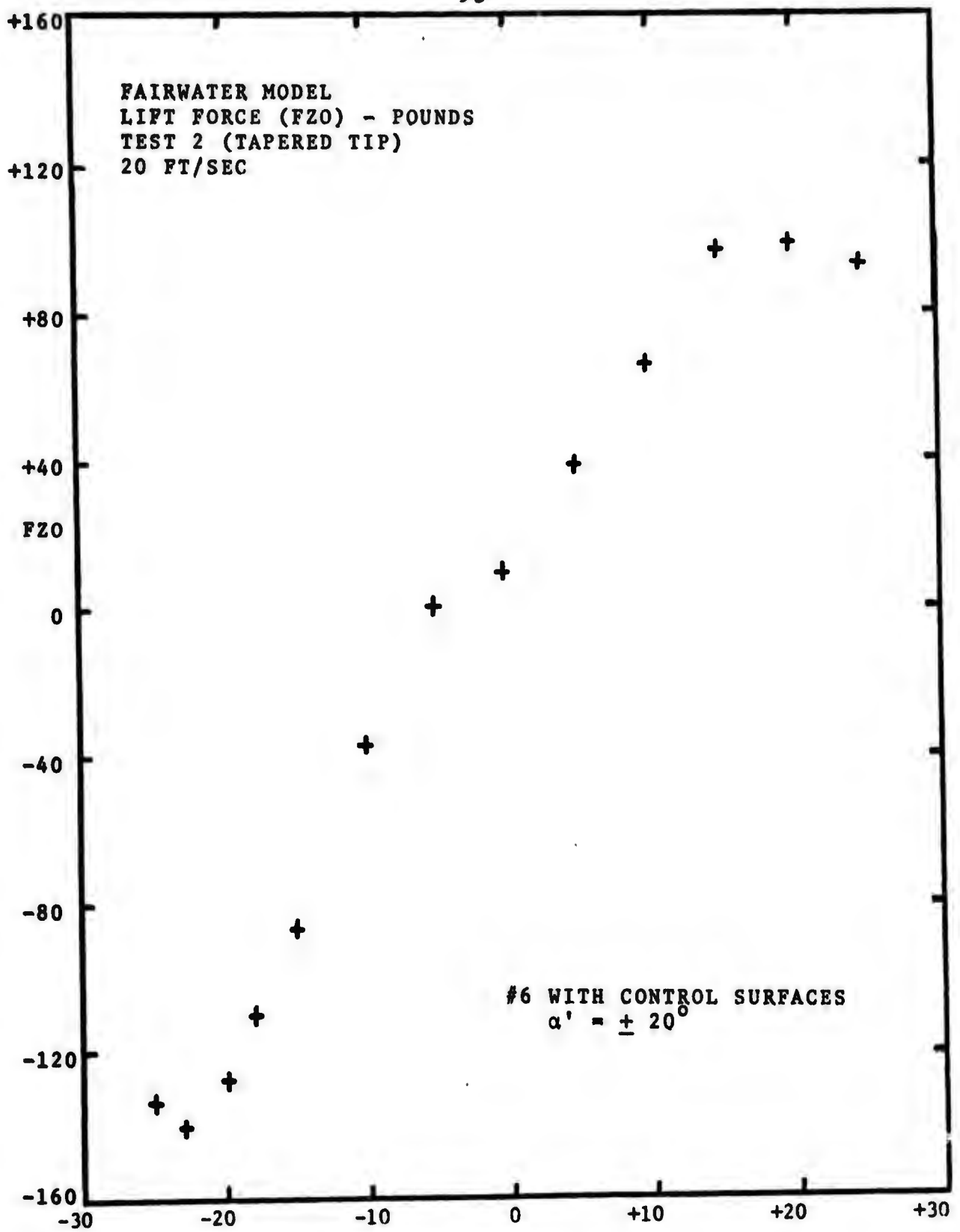
FAIRWATER MODEL
LIFT FORCE (FZO) - POUNDS
TEST 2 (TAPERED TIP)
20 FT/SEC
+160
+120
+80
+40
FZO
0
-40
-80
-120
-160
-30
-20
-10
0
+10
+20
+30
#6 WITH CONTROL SURFACES
α' = ± 20°
Angle of Attack- α -(Degrees-Yaw)

Figure 59

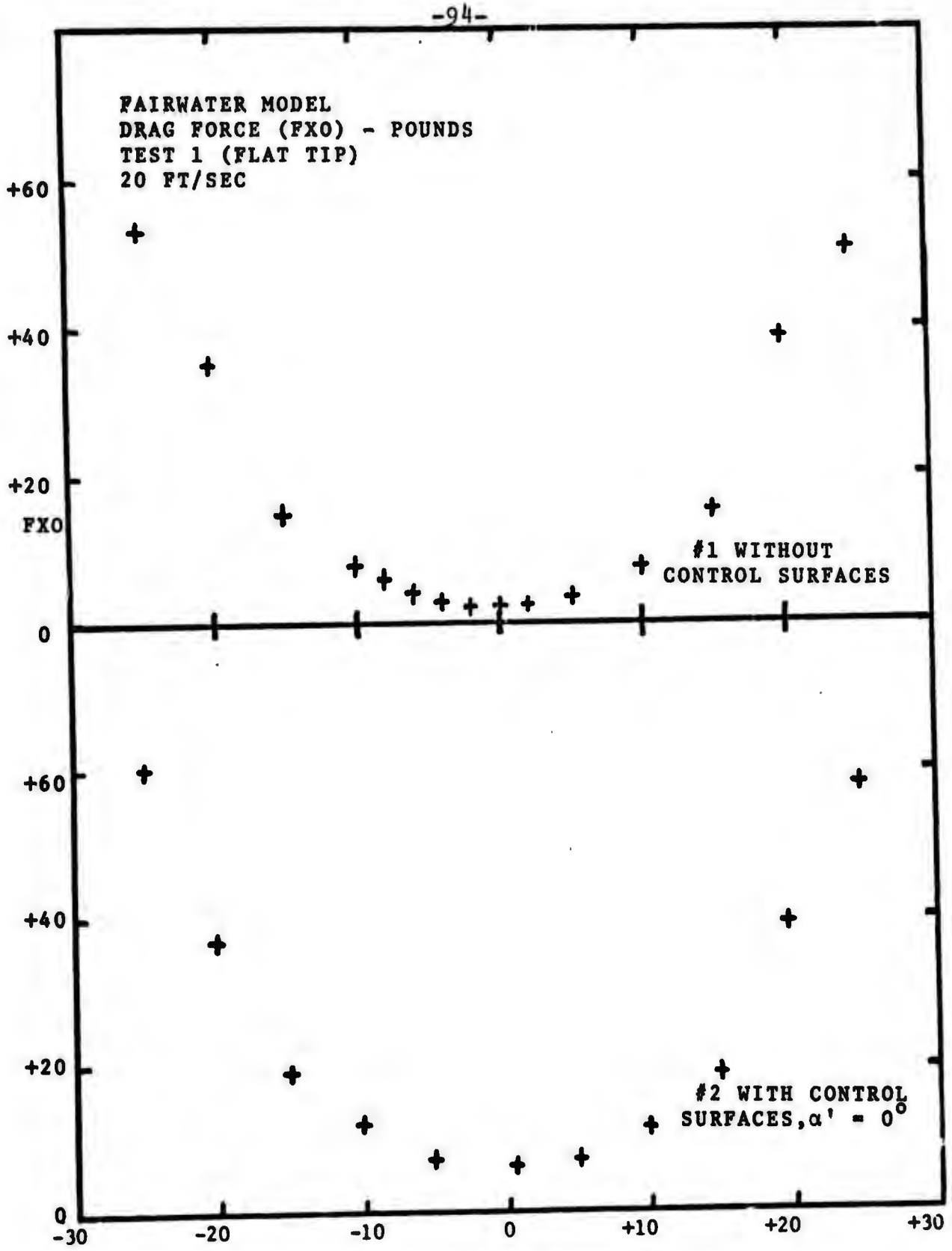
FAIRWATER MODEL
DRAG FORCE (FXO) - POUNDS
TEST 1 (FLAT TIP)
20 FT/SEC
+60
+40
+20
FXO
0
#1 WITHOUT
CONTROL SURFACES
+60
+40
+20
0
#2 WITH CONTROL
SURFACES, α' = 0°
-30
-20
-10
0
+10
+20
+30
Angle of Attack- α -(Degrees-Yaw)

Figure 60

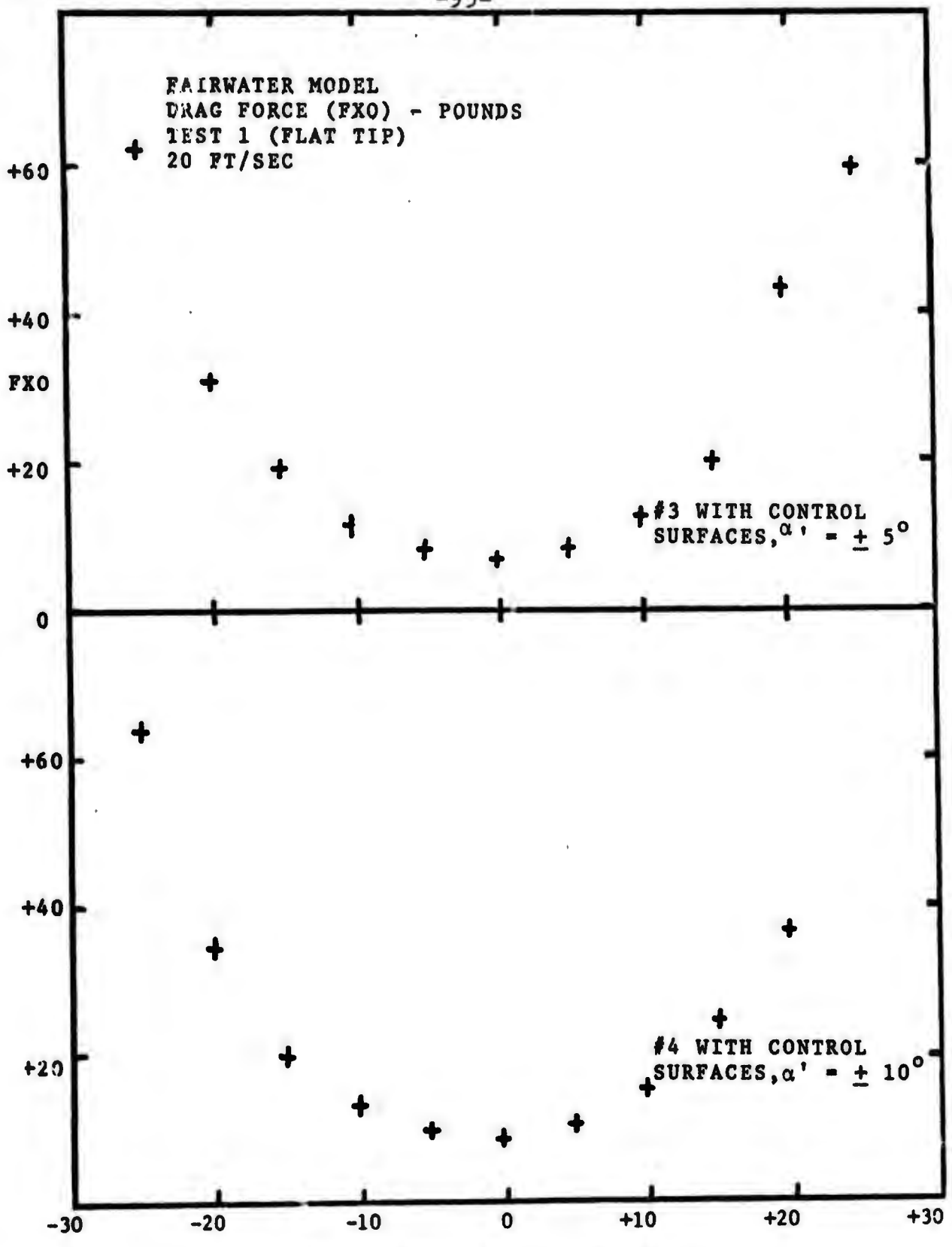
FAIRWATER MODEL
DRAG FORCE (FXO) - POUNDS
TEST 1 (FLAT TIP)
20 FT/SEC
#3 WITH CONTROL SURFACES, α' = ± 5°
#4 WITH CONTROL SURFACES, α' = ± 10°
FXO
+60
+40
+20
0
+60
+40
+20
-30
-20
-10
0
+10
+20
+30
Angle of Attack- α -(Degrees-Yaw)

Figure 61

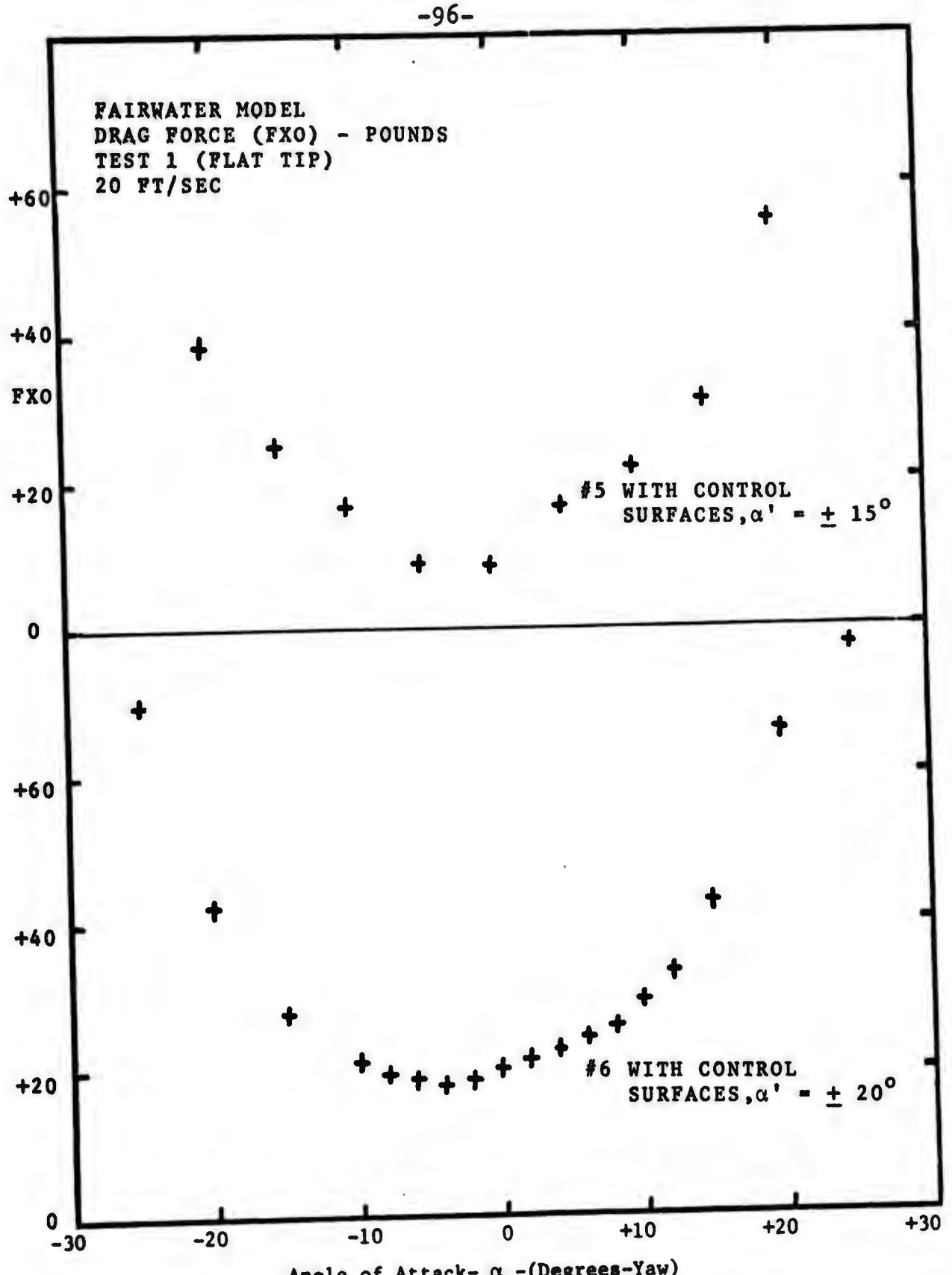
FAIRWATER MODEL
DRAG FORCE (FXO) - POUNDS
TEST 1 (FLAT TIP)
20 FT/SEC
+60
+40
FXO
+20
0
#5 WITH CONTROL SURFACES, α' = ± 15°
+60
+40
+20
0
#6 WITH CONTROL SURFACES, α' = ± 20°
-30
-20
-10
0
+10
+20
+30
Angle of Attack- α -(Degrees-Yaw)

Figure 62

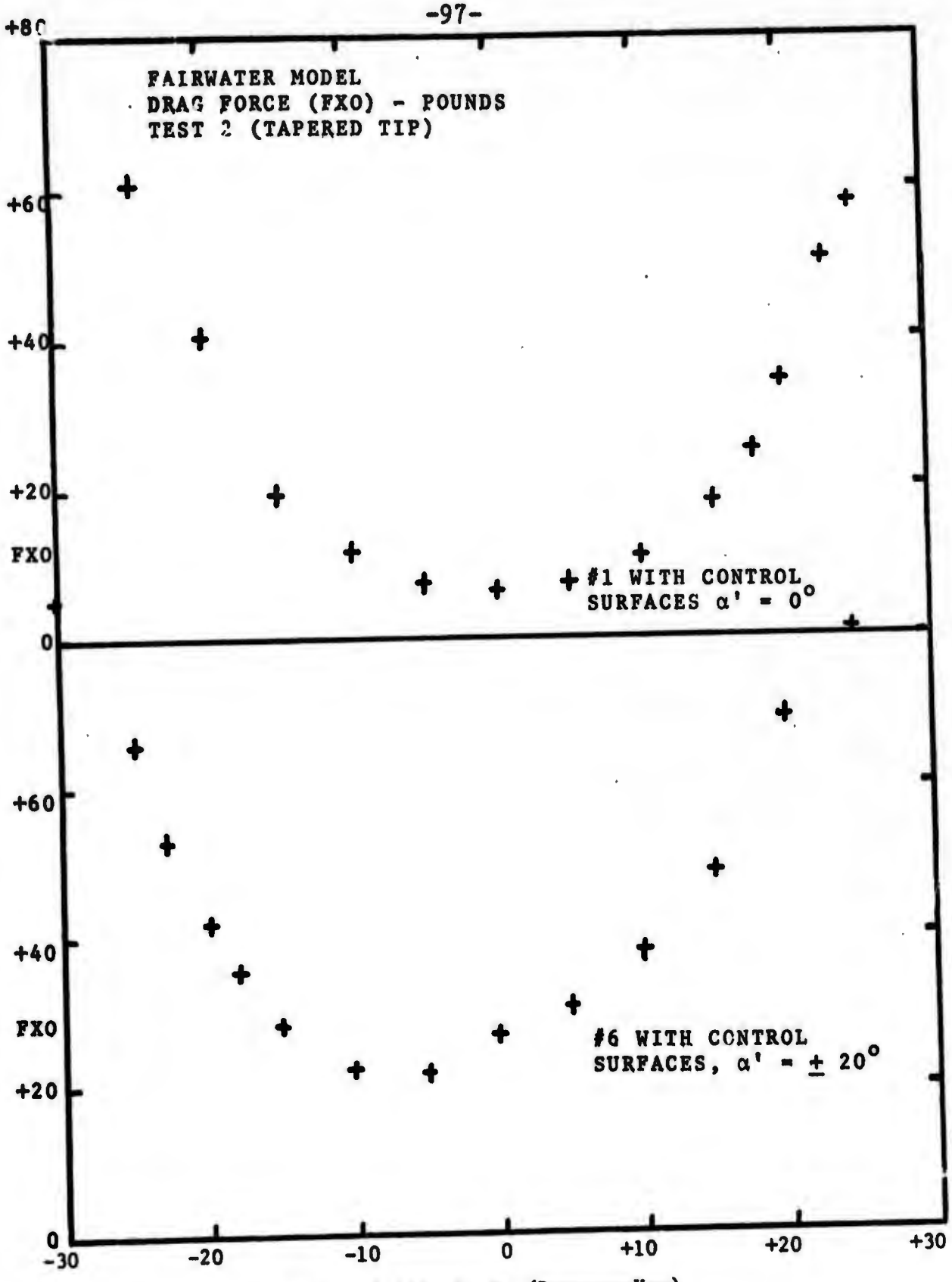
FAIRWATER MODEL
DRAG FORCE (FXO) - POUNDS
TEST 2 (TAPERED TIP)
+80
+60
+40
+20
FXO
0
#1 WITH CONTROL SURFACES α' = 0°
+60
+40
FXO
+20
0
#6 WITH CONTROL SURFACES, α' = ± 20°
-30
-20
-10
0
+10
+20
+30
Angle of Attack- α -(Degrees-Yaw)

Figure 63

VI. THEORETICAL BASIS FOR NUMERICAL MODEL

In developing a numerical method for predicting the flow characteristics, and eventually the forces and moments, on a submerged body of revolution, it was necessary to use potential flow as the basic theory. Therefore, simplifying assumptions of an ideal fluid were initially required of the flow: inviscid, incompressible, homogeneous, and irrotational. The submerged body, in this case a slender body of revolution, is approximately represented by the combination of two different appropriate distributions. To model the flow along the longitudinal body axis, a distribution of sources and sinks was constructed along this axis to form the closed body.

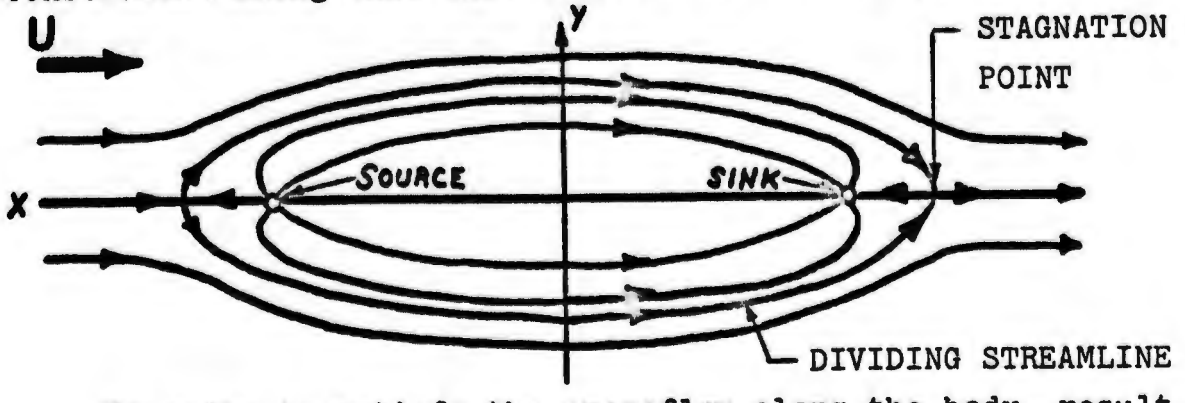

In order to satisfy the crossflow along the body, resulting from an angle of incidence between the body axis and free stream, a distribution of doublets was similarly placed along the body axis.

IDEAL FLUID FLOW:

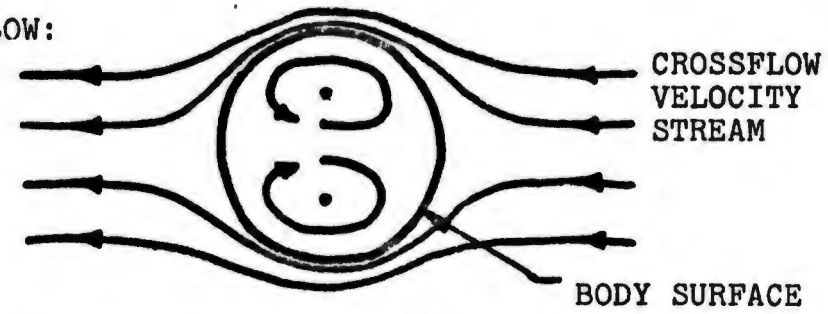

The basis of the approach used for lifting surface calculations was the linearized two-dimensional hydrofoil theory for a thin foil and the law of Biot-Savart, which is a governing relationship for an induced velocity in space by a three dimensional vortex.

Using the linearized two-dimensional hydrofoil theory for a thin foil with the required assumptions of no separation, and the Kutta condition imposed on the trailing edge, the lift force and moment resulting from the hydrodynamic pressure can be obtained. This result, Kutta-Joukowski theorem, states that for a two-dimensional body, moving with constant velocity in an unbounded inviscid fluid, the hydrodynamic pressure force (lift) is directed normal to the velocity vector and is equal to the product of the fluid density, velocity, and the circulation around the body.

$$L = \rho U \Gamma = \text{lift/unit length of span}$$

Circulation (Γ) is defined as the integrated tangential velocity around the closed contour, in this case a lifting surface, in a fluid. With the standard hydrodynamic reference

orientation used:

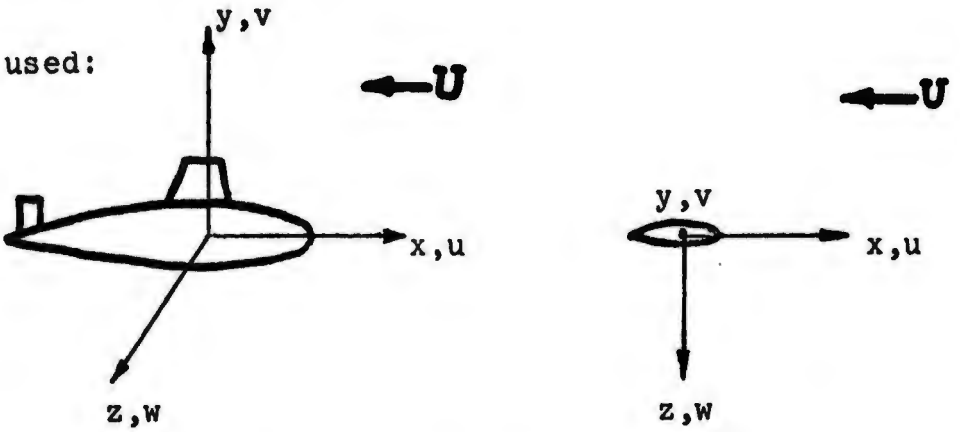

Circulation, $\Gamma = \oint u dx$, where

u = horizontal perturbation velocity component

U = free stream velocity component

The hydrodynamic moment about the y-axis is represented by the pressure integral:

$$M = \rho U \int u x dx$$

The coordinate system used during the experimental portion of this project required the above system to be rotated 180 degrees in the horizontal plane, to be compatible with the water tunnel construction and dynamometer program.

In order to satisfy the presence and the effects of lifting surface appendages (fairwater and rudders) and the discontinuity in pressure, pressure loading across these surfaces was modeled by a distribution of vorticity. The axis for each distribution of vorticity is on the center plane of the

representative lifting surface and normal to the incoming flow, and this vorticity is referred to as a bound vorticity distribution. To fulfill continuity of vorticity, an additional distribution of vorticity, whose axis is on the representative lifting surface and parallel to the incoming flow, was required. This latter distribution is referred to as trailing vortices, or more commonly, trailers. Trailing vortices extend to infinity in the wake formed behind each respective lifting surface, while the effects of the bound vortices are only experienced on the lifting surface itself.

The thickness of the lifting surfaces described above could be represented by a distribution of sources and sinks of appropriate strength, but were defined as being of zero thickness.

Effective Span of Lifting Surfaces

Since the lifting surfaces are each connected to the hull, essentially a curved ground board, an effective span length must be calculated for a valid modeling. This was accomplished using a relationship from Milne-Thomson (3), in which a distance from the body axis to the new effective base is generated. This distance is equal to the ratio of the actual hull radius, at the mid-point of the actual base of lifting surface, squared, divided by the maximum radial distance from

the body axis to the lifting surface tip.

FAIRWATER EXAMPLE:

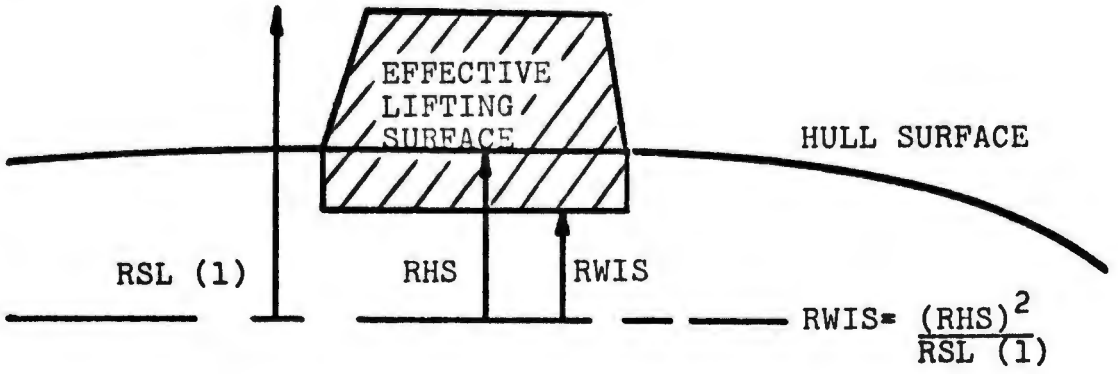

Effective Span of Fairwater = SPNS = RSL(1) - RWIS

The image system is based on the theory that when a pair of two dimensional vortices of equal and opposite strength are located on the same radial line, there is no normal induced velocity on a circle of radius RHS, if RSL is equal to the radius of the outer vortex, and RWIS the radius of the image vortex.

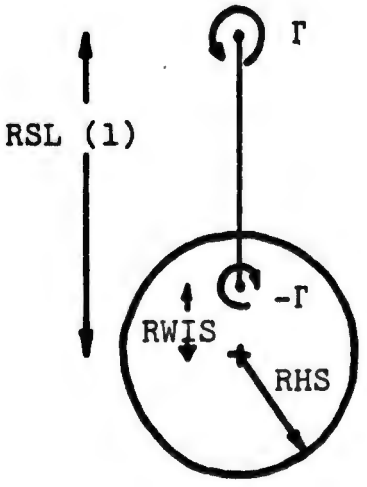

By using this image system for the fairwater and rudder(s), the solid boundary condition of the hull is satisfied.

The technique used, distribution of vorticity, is similar to a method developed by Falkner for lift distribution of wings (4, 5, 6, 7, 8). A continuous distribution of bound and trailing vortices is replaced by a discrete element approximation, in which a lattice of horse-shoe shaped discrete vortex lines are used. The lifting surface is divided into a series of finite rectangular elements in which the lift is considered to be constant within each element, and each element is a horse-shoe of the total lattice, see Figure 64. As the number of elements chordwise and spanwise is increased, the approximation to the actual surface is refined. The trailing vortex sheet formed is assumed, as a first approximation, to remain a flat sheet to infinity downstream while the sheet angle to the vehicle longitudinal axis is adjustable. A selected minimum number of control points are then systematically located chordwise and spanwise midway between vortices on each lifting surface. At the control points, the induced velocity by each horse-shoe lattice element is determined by integration using the Biot-Savart law:

$$\underset{(u,v,w)}{\bar{w}} = \frac{\Gamma}{4\pi} \int \frac{\overline{dl} \times \bar{S}}{S^3}$$

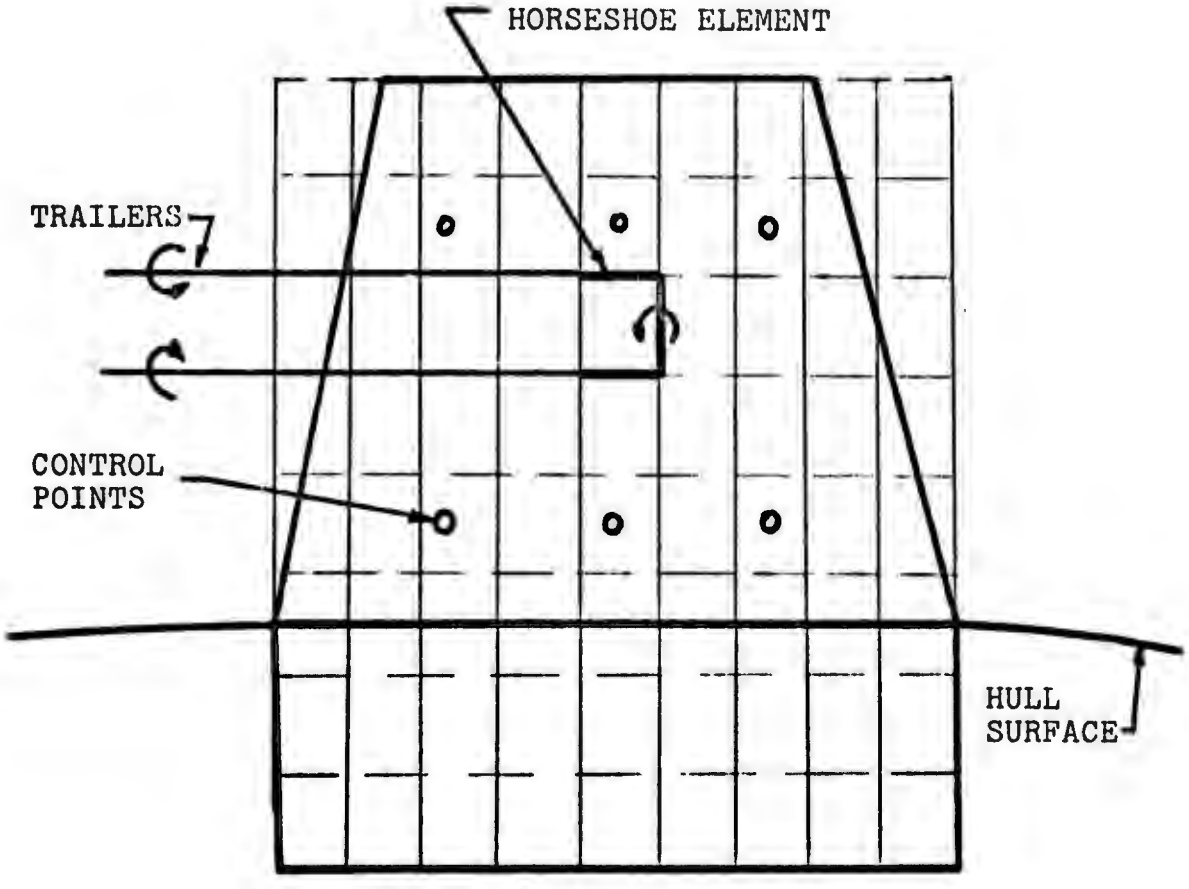

Figure 64 Vortex Lattice

where Γ = vortex strength

$\overline{S}$ = vector distance from vortex element to control point

$\overline{dl}$ = vector element of distance along the vortex

$\overline{w}$ = vector-induced velocity of an element.

The bound vortex strength of each element is first numerically solved using 2 modes of distribution spanwise and 2 modes chordwise; one of a flat plate and the other for camber over the various chord lengths along the length of the effective span.

To insure zero slope, but not necessarily zero value of the circulation at the actual hull surface, an approximated series form for the bound circulation was taken from Kerwin and Leopold (9). This series:

$$\text{nondimensional circulation} = G(q) = (1 - q^2)^{\frac{1}{2}} \sum_{j=1}^{J} a_j q^{(2j-2)}$$

$$\text{where } q = \frac{r - r_h}{1 - r_h}$$

r = radius of image vortex (RWIS,RWIR)

r_h = radius of hull (RHS,RHR)

a_j = unknown coefficient to be determined from modal distributions

Since the strength of a trailing vortex of an element is equal to the difference in bound circulation between adjacent bound vortices, as a vortex may not end in a fluid, the vortex strengths are readily calculated also.

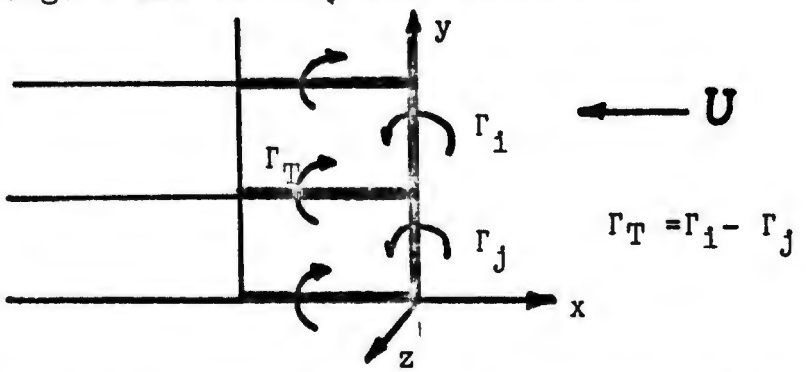

Using the law of Biot-Savart, and the bound vortex strengths just calculated, the induced velocities of each element on each of the control points of the lifting surface are calculated. Then, the same method is repeated for the induced velocities resulting from the trailing vortices.

The number of control points used should be a minimum, yet retain accuracy, to reduce the size of the resulting matrix of induced velocities that is eventually developed for each lifting surface, to reduce computation time. Although accuracy should be improved by a greater number of control points and smaller horse-shoe element size, a point of diminishing return will eventually occur, and care must be

taken not to allow the matrix, a set of simultaneous linear equations, to become too nearly singular to be solved numerically.

Since the bound and trailing vortices do not yield the total induced velocity on the lifting surface, the trailing wake of the surface in question, the hull, and other adjacent lifting surface wakes must also be considered and their effects combined.

The induced velocity on the control points from the wake of the surfaces is determined by the Biot-Savart law with respect to the control points. The induced velocity on the lifting surfaces from the hull results from the singularities used in developing the hull model and the potential flow around it. The sources and sinks do not cause any induced velocities, but the crossflow compensating doublet distribution along the body axis does contribute induced velocity normal to the lifting surfaces. These velocities are developed from the doublets distributed at the corresponding locations of the lifting surfaces with respect to the body axis. Their effects on the previously-designated control points are deduced by an equation which is a function of the crossflow velocity, and the ratio of body radius and perpendicular control point distance from body axis at corresponding points on the body axis. This relationship:

$$WDS = W(x) \frac{R^2}{YCP^2}$$

where:

WDS = induced velocity of doublet

R = body radius at XCP (long. location of control point)

YCP = vertical location of control point

W(x) = crossflow velocity

is the component normal to the lifting surface of the velocity due to a doublet in a uniform crossflow, and is found by differentiating the potential of the doublet (10).

The wake of each lifting surface connected to the body also produces induced velocities on all other lifting surfaces and the hull. The magnitude and relative importance of each induced velocity is based on the relative distance and location of the wakes with respect to the other surfaces, and is determined by the Biot-Savart law. In the numerical procedure developed for this project, (see Appendix D), the effect of the rudder wake on the fairwater is assumed to be negligible, because of its relative location, and was not considered.

The combined induced velocities at each control point of a particular lifting surface result in a set of simultaneous linear equations, a matrix of induced velocities, which relate:

(1) the modal vortex strength of the lattice elements to the lifting surface shape;

(2) wake effects;

(3) applicable effects of other lifting surfaces (wake, surface); and,

(4) the induced velocity of the hull doublet distribution, based on inflow velocity and yaw angle.

The different mode strengths for each lifting surface are then generated for subsequent development of force and moment calculation.

The hydrodynamic forces and moments on the hull result from induced velocity contributions of each lifting surface wake, the crossflow velocity, source and sink distribution, and doublet distribution.

As before, the induced velocity imposed by each wake on the hull is found by the Biot-Savart law, at each station along the body axis. This externally-induced velocity is combined with the crossflow, or sway, velocity to give a total externally-induced velocity at each station on the centerline.

The induced forces and moments at each station are derived using the above externally-induced velocities as a major governing parameter. Using a relationship from McCreight (11, 12) based on Lagally's theorem, the resulting force on a source distribution of constant strength per unit length along the body axis, when subjected to the above

externally-induced velocity, is equal to:

$$U\rho \sum_{1}^{NSTA} S'(M)W(M)$$

where:

U = free stream velocity

ρ = density of fluid

S'(M) = slope of hull surface at input point M;
M = station number

W(M) = externally induced velocity

NSTA = number of stations

The slope of the hull surface (S'), being a measure of the change in area per unit length, is also the source strength at the station in question. The moment due to the source distribution is found from the numerically-integrated product of the force at a station and distance from axial reference point.

Since the doublet distribution does not contribute a force when an induced velocity is imposed, we are only interested in its moment contributions. Using a method introduced

by von Karman (1930) for crossflow past airships and the assumptions:

1) uniform crossflow in the transverse plane; and,
2) body and flow radius do not change drastically along the body axis;

the crossflow effect can be represented by the flow past a circular cylinder in which the doublet strength is equal to:

$$\bar{\gamma}\,(x) = -\frac{1}{2}\,r^2\,(x)W(x)$$

where:

r(x) = body radius at cross-section
W(x) = externally induced velocity (crossflow)

Since the doublets with a vertical axis are in a horizontal uniform velocity stream U, the moment is equal to $-4\pi\rho\bar{\gamma}\,(x)$. When this moment is integrated over the length of the body axis the resulting integral is formed:

$$M = 2\,\pi\rho U\int_{x} r^2(x)W(X)dx$$

This is numerically approached by calculating the surface area at each station and knowing the crossflow velocity W(x) at each station.

Since the above two models, of sources and doublets, do not account for viscous effects - separation of flow around the body and crossflow drag -

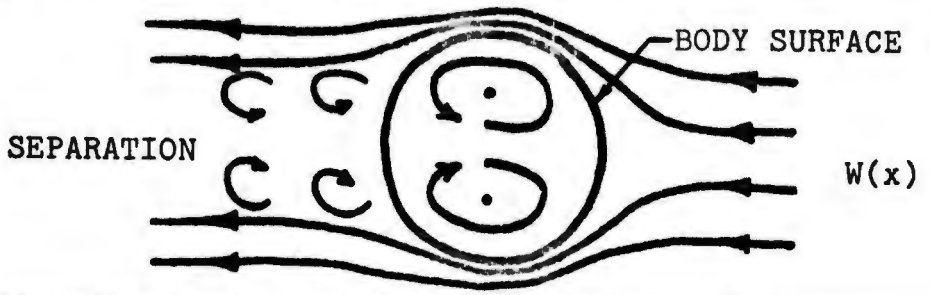

consideration and provisions must be made to compensate for this failure, as the effects are significant with respect to some of the hydrodynamic forces and resulting moments acting on a submerged body in the steady state case. A first approximation is made by adjusting with a linear distribution factor (FAC) along the portion of the body length aft of the coordinate system reference point. This adjustment is accomplished by a factor which increases the force and moment effect of the sinks, and decreases the moment due to the doublet distribution aft.

The forces on the lifting surfaces are found by numerically integrating the four spanwise modal circulation effects to obtain the circulation along the effective span, and, in accordance with the Kutta-Joukowski theorem, determine the lift (side force) caused by the fairwater and rudder(s) separately.

The moments resulting from these lifting surfaces are

determined from the numerically integrated product of the spanwise modal circulation effects and the appropriate chordwise moment arm, based on the center of pressures for the flat plate and camber modes along the chord.

The total force and moment experienced on the submerged body is obtained from the vector summation of each individual component calculated.

Total Side Force = Rudder(s) Side Force + Fairwater Side Force + Source Side Force

Total Moment = Rudder(s) Moment + Fairwater Moment + Source Moment + Doublet Moment

An attempt to model heave force and pitch moment is made by taking the induced circulation around the hull caused by the strength of the trailer-forming wake off the external portion of the actual fairwater span. The Kutta-Joukowski theorem again is used to determine the heave force and pitch moment.

VII. COMPARISON OF EXPERIMENTAL SUBMERSIBLE RESULTS

A. NSRDC Model Test

A model test was conducted at the Naval Ship Research and Development Center (NSRDC) to investigate the forces and moments on a submerged body of revolution for various rudder aspect ratios. The final results of this investigation have not been completed, and only preliminary results of the clean hull configuration were comparable with these experimental results. Lateral force coefficients and yawing moment coefficients were calculated and plotted for all submersible model configurations for comparison when the final NSRDC results are available, see Figures 65 - 71. The clean hull results obtained for this experiment were about 40 per cent higher for lateral coefficients, but showed only minor differences for yawing moment coefficients.

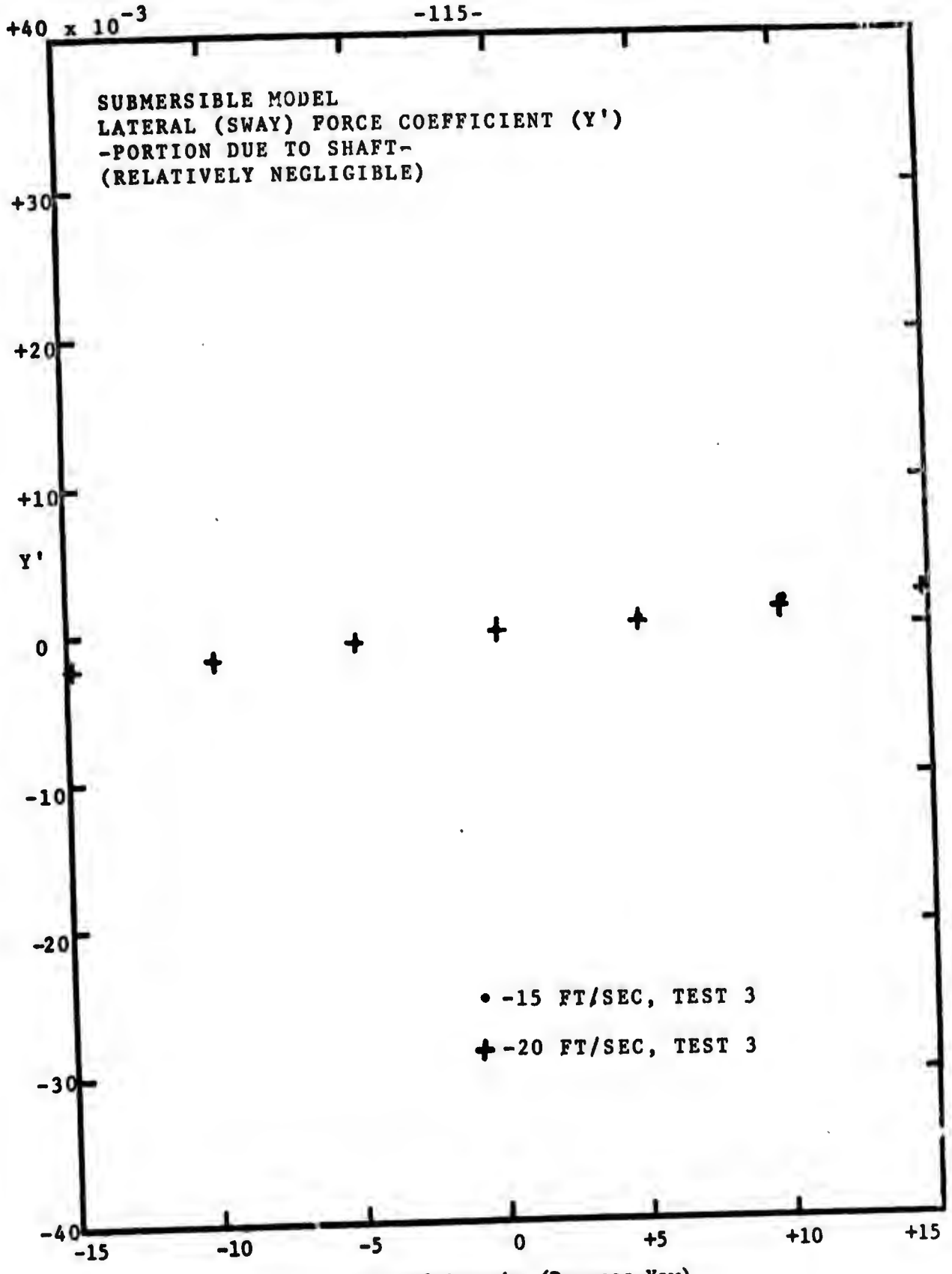
+40 x 10-3
SUBMERSIBLE MODEL
LATERAL (SWAY) FORCE COEFFICIENT (Y')
-PORTION DUE TO SHAFT-
(RELATIVELY NEGLIGIBLE)
+30
+20
+10
Y'
0
-10
-20
-30
-40
-15
-10
-5
0
+5
+10
+15
• -15 FT/SEC, TEST 3
+ -20 FT/SEC, TEST 3
Angle of Attack- (Degrees-Yaw)

Figure 65

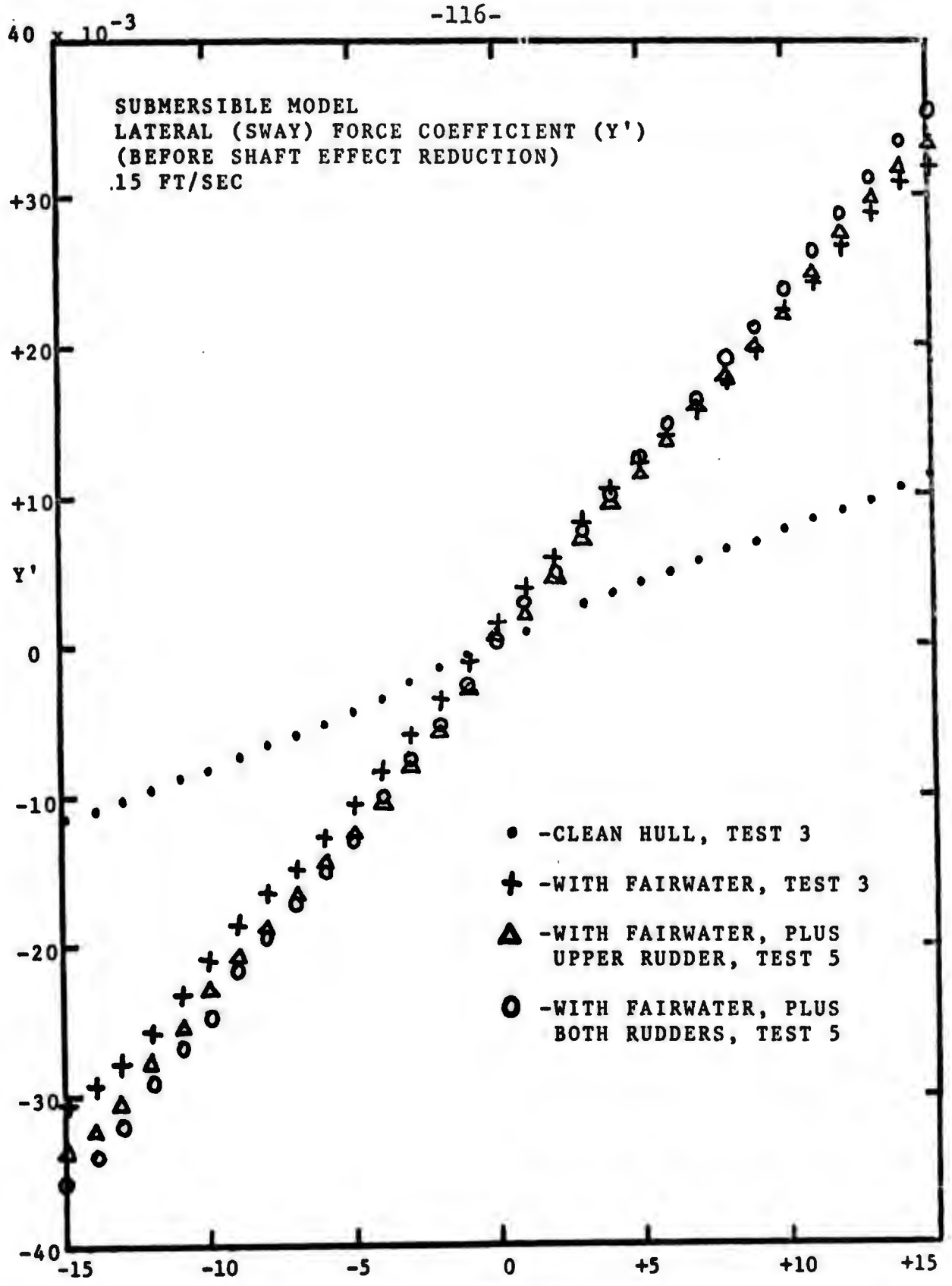
40 x 10-3
SUBMERSIBLE MODEL
LATERAL (SWAY) FORCE COEFFICIENT (Y')
(BEFORE SHAFT EFFECT REDUCTION)
.15 FT/SEC
+30
+20
+10
Y'
0
-10
-20
-30
-40
-15
-10
-5
0
+5
+10
+15
• -CLEAN HULL, TEST 3
+ -WITH FAIRWATER, TEST 3
△ -WITH FAIRWATER, PLUS UPPER RUDDER, TEST 5
O -WITH FAIRWATER, PLUS BOTH RUDDERS, TEST 5
Angle of Attack- (Degrees-Yaw)

Figure 66

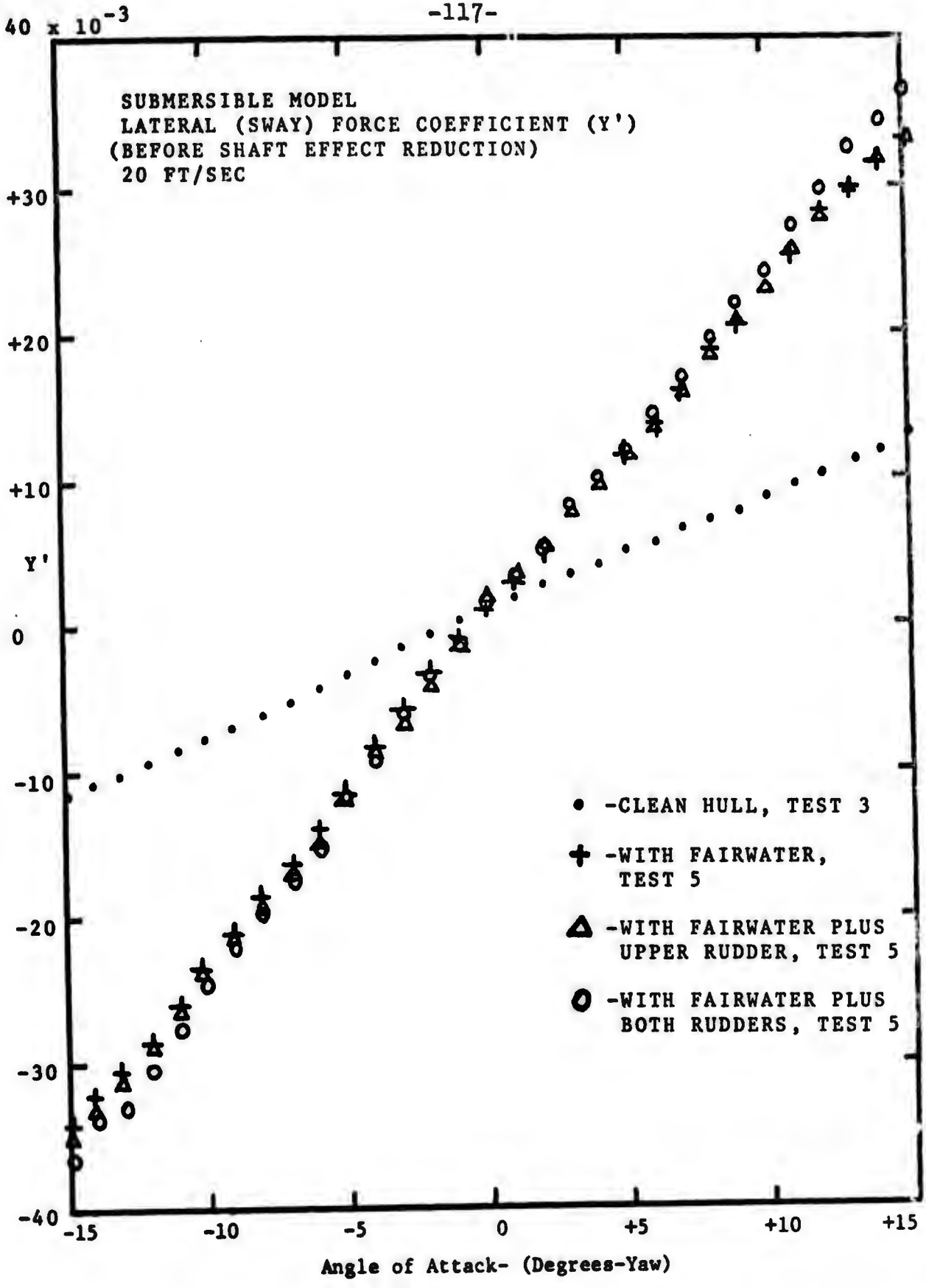
40 x 10-3
SUBMERSIBLE MODEL
LATERAL (SWAY) FORCE COEFFICIENT (Y')
(BEFORE SHAFT EFFECT REDUCTION)
20 FT/SEC
+30
+20
+10
Y'
0
-10
-20
-30
-40
-15
-10
-5
0
+5
+10
+15
Angle of Attack- (Degrees-Yaw)
-CLEAN HULL, TEST 3
-WITH FAIRWATER, TEST 5
-WITH FAIRWATER PLUS UPPER RUDDER, TEST 5
-WITH FAIRWATER PLUS BOTH RUDDERS, TEST 5

Figure 67

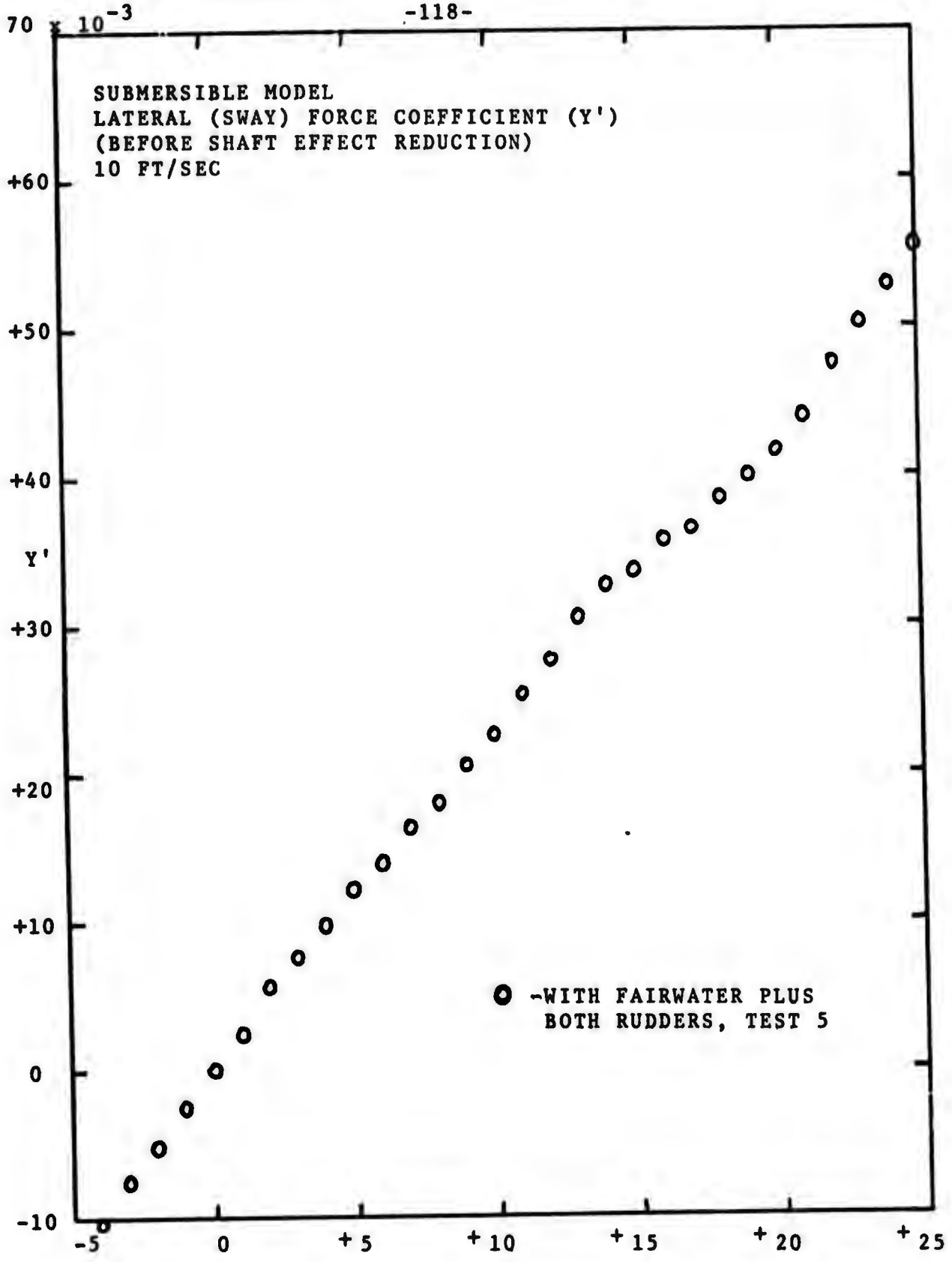
70 x 10-3
SUBMERSIBLE MODEL
LATERAL (SWAY) FORCE COEFFICIENT (Y')
(BEFORE SHAFT EFFECT REDUCTION)
10 FT/SEC
+60
+50
+40
Y'
+30
+20
+10
0
-10
-5
0
+5
+10
+15
+20
+25
-WITH FAIRWATER PLUS
BOTH RUDDERS, TEST 5
Angle of Attack- (Degrees-Yaw)

Figure 68

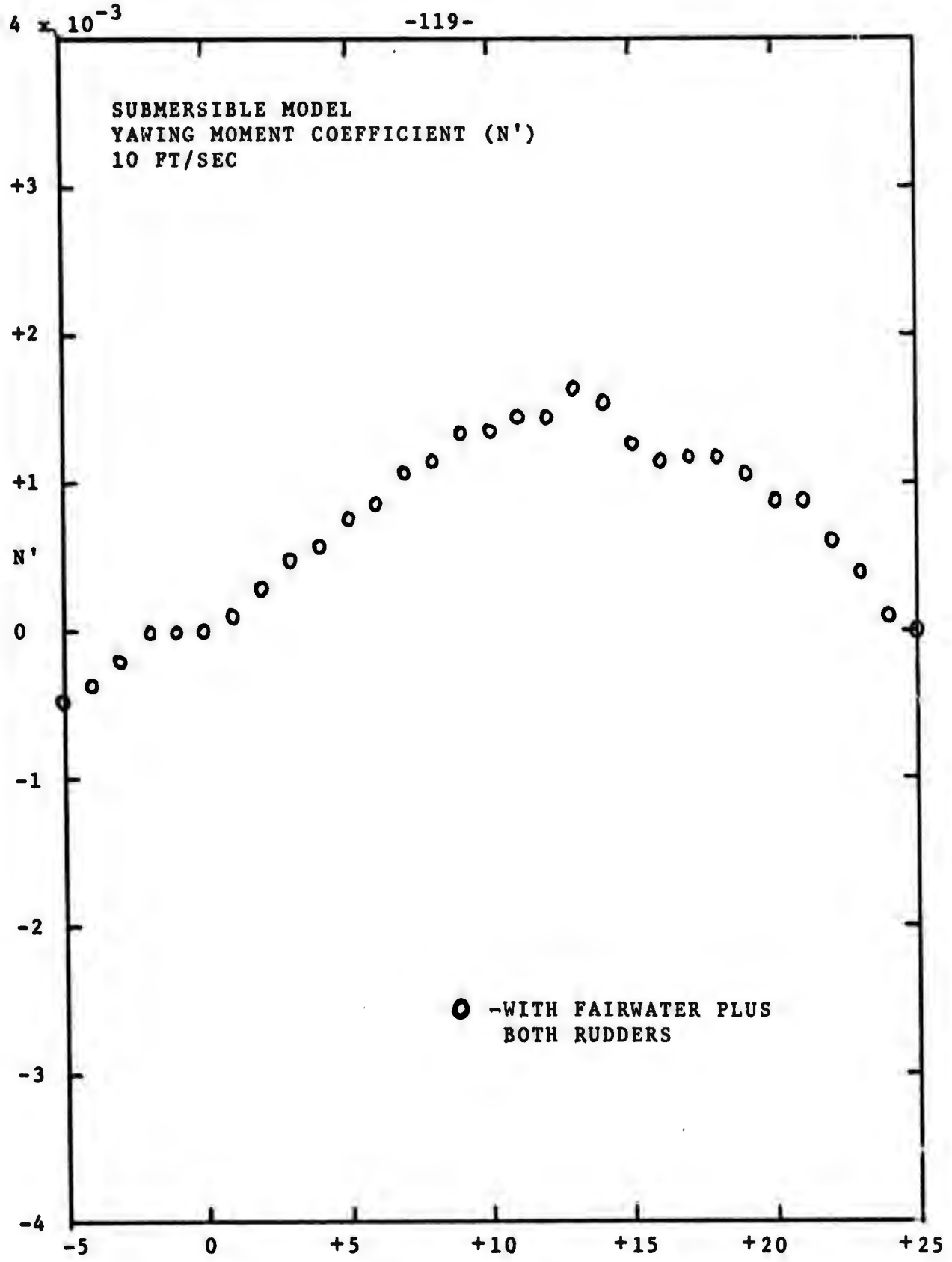
4 x 10^-3
SUBMERSIBLE MODEL
YAWING MOMENT COEFFICIENT (N')
10 FT/SEC
+3
+2
+1
N'
0
-1
-2
-3
-4
-5
0
+5
+10
+15
+20
+25
-WITH FAIRWATER PLUS
BOTH RUDDERS
Angle of Attack - (Degrees-Yaw)

Figure 69

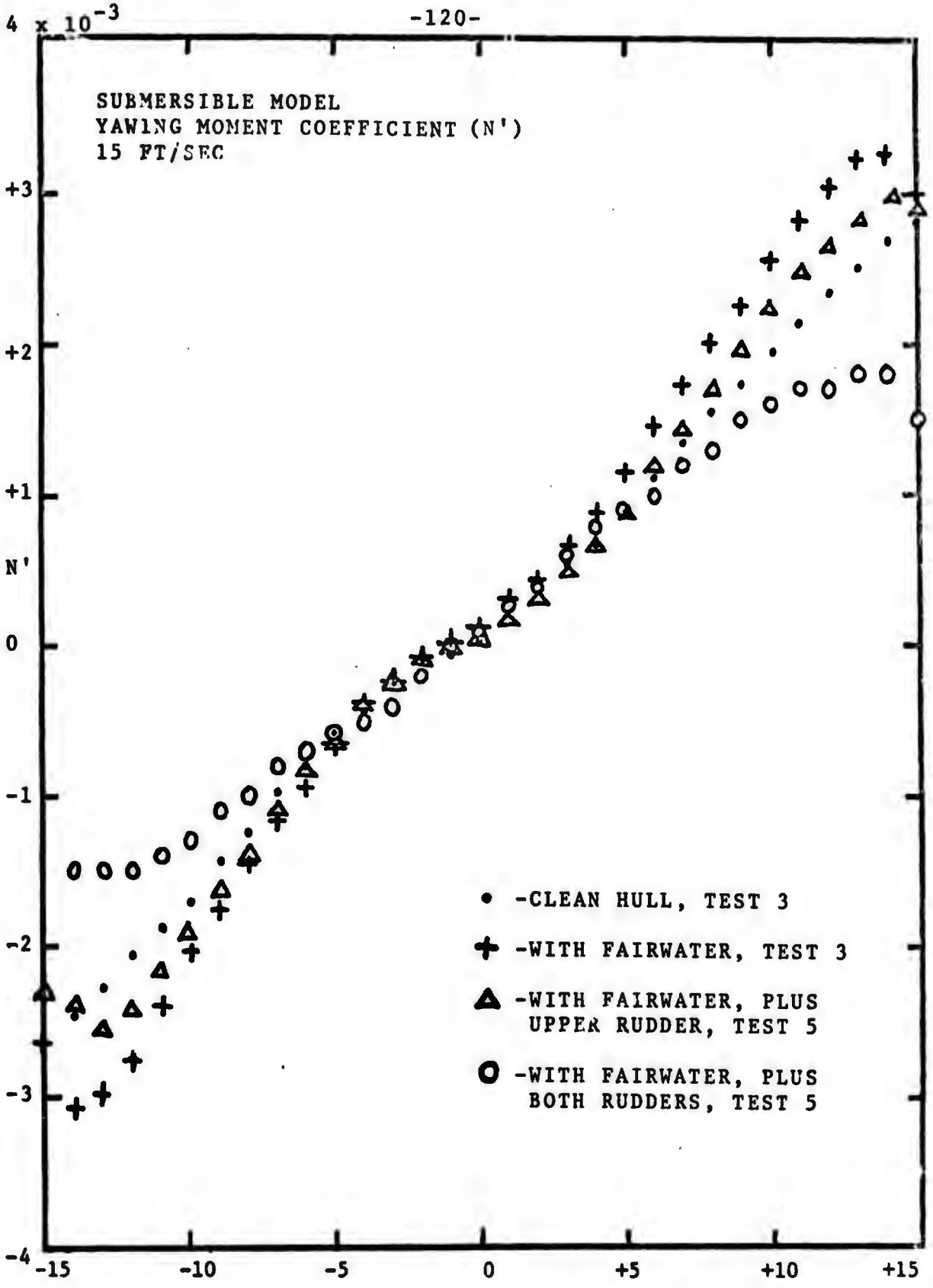
4 x 10-3
SUBMERSIBLE MODEL
YAWING MOMENT COEFFICIENT (N')
15 FT/SEC
+3
+2
+1
N'
0
-1
-2
-3
-4
-15
-10
-5
0
+5
+10
+15
• -CLEAN HULL, TEST 3
+ -WITH FAIRWATER, TEST 3
△ -WITH FAIRWATER, PLUS UPPER RUDDER, TEST 5
O -WITH FAIRWATER, PLUS BOTH RUDDERS, TEST 5
Angle of Attack- (Degrees-Yaw)

Figure 70

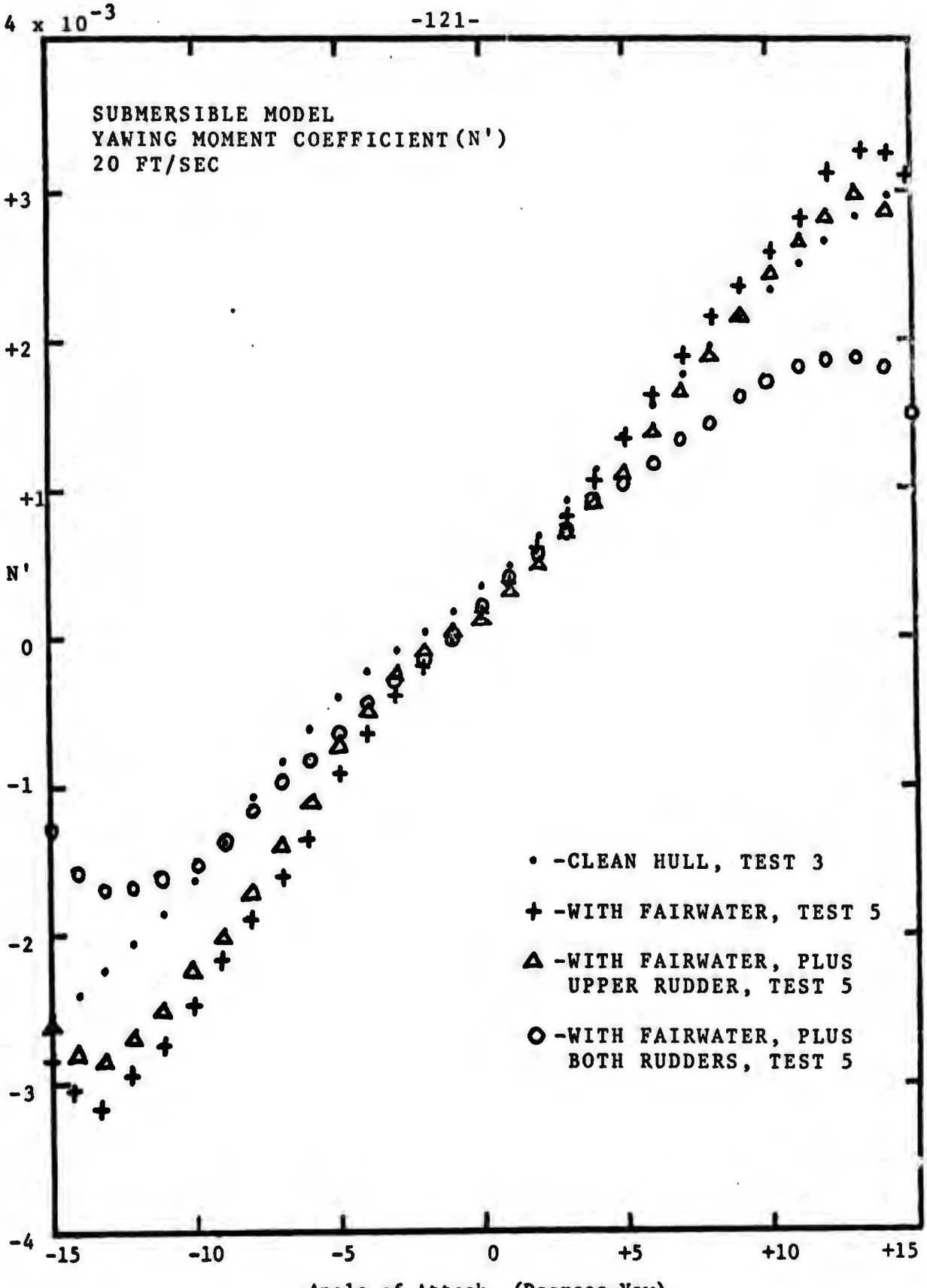
4 x 10^-3
SUBMERSIBLE MODEL
YAWING MOMENT COEFFICIENT (N')
20 FT/SEC
+3
+2
+1
N'
0
-1
-2
-3
-4
-15
-10
-5
0
+5
+10
+15
Angle of Attack- (Degrees-Yaw)
• -CLEAN HULL, TEST 3
+ -WITH FAIRWATER, TEST 5
△ -WITH FAIRWATER, PLUS UPPER RUDDER, TEST 5
○ -WITH FAIRWATER, PLUS BOTH RUDDERS, TEST 5

Figure 71

B. Newman-Rodriguez Results

Theoretical results obtained by Dr. J. N. Newman and Neptune Rodriguez from an investigation of a linearized low aspect ratio slender body theory are presented for comparison with experimental results, see Figures 72 and 73, taken from (13).

$$\text{Lift Coefficient} = C_L = \frac{L}{\rho\, b_o^2 U^2 \alpha\pi}$$

where:

L = lift force, perpendicular to flow

ρ = fluid density

b_o = radial distance to tip of fairwater

U = flow velocity

α = yaw angle.

Configuration 2 (with fairwater)

$$\frac{r_o}{b_o} = .354$$

$$\frac{b_t}{b_o} = 0$$

C_L (experimental) = .433, using Figure 74

C_L (Newman-Rodriguez) = .375

Configuration 3 (with fairwater and upper rudder)

$$\frac{r_o}{b_o} = .354$$

$$\frac{b_t}{b_o} = .417$$

C_L (experimental) = .445, using Figure 75

C_L (Newman-Rodriguez) = .270

Configuration 4 (with fairwater and both rudders)

$$\frac{r_o}{b_o} = .354$$

$$\frac{b_t}{b_o} = .417$$

C_L (experimental) = .497, using Figure 76

C_L (Newman-Rodriguez) = .475

The greater difference in lift coefficients for configuration 3 results from the fact that the downwash from the fairwater, although decreasing the effective angle of attack of the rudder, does not cause the flow to become parallel to the body axis. In the linear theory, the trailing vortex sheet passes directly over the upper rudder, thereby decreasing the

rudder angle of attack. Experimentally and in the numerical model, the trailing vortex system misses the rudder.

Therefore, more lift is generated by the rudder than would appear in the linearized theory used by Newman and Rodriguez.

The experimental and theoretical values of C_L are actually in better agreement than presented, since the experimental lift coefficients calculated included a minor component of lift resulting from the support shaft, which was not deducted before calculation.

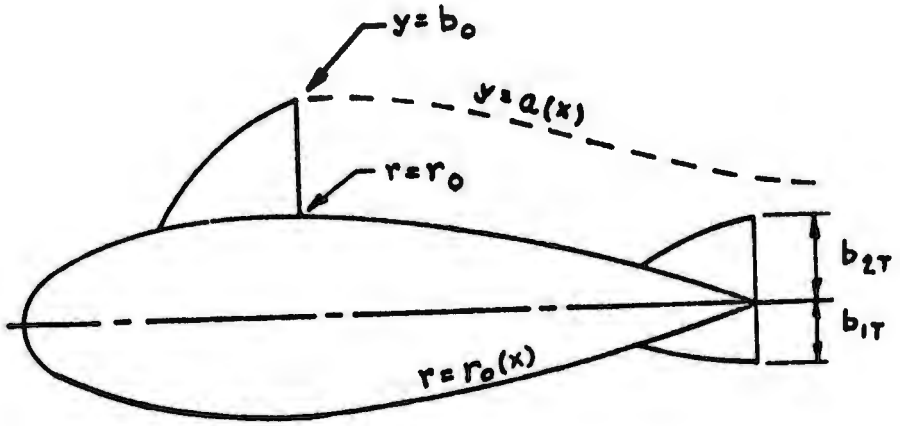

The axi-symmetric body with asymmetric tail fins and one upstream fin.

Figure 72

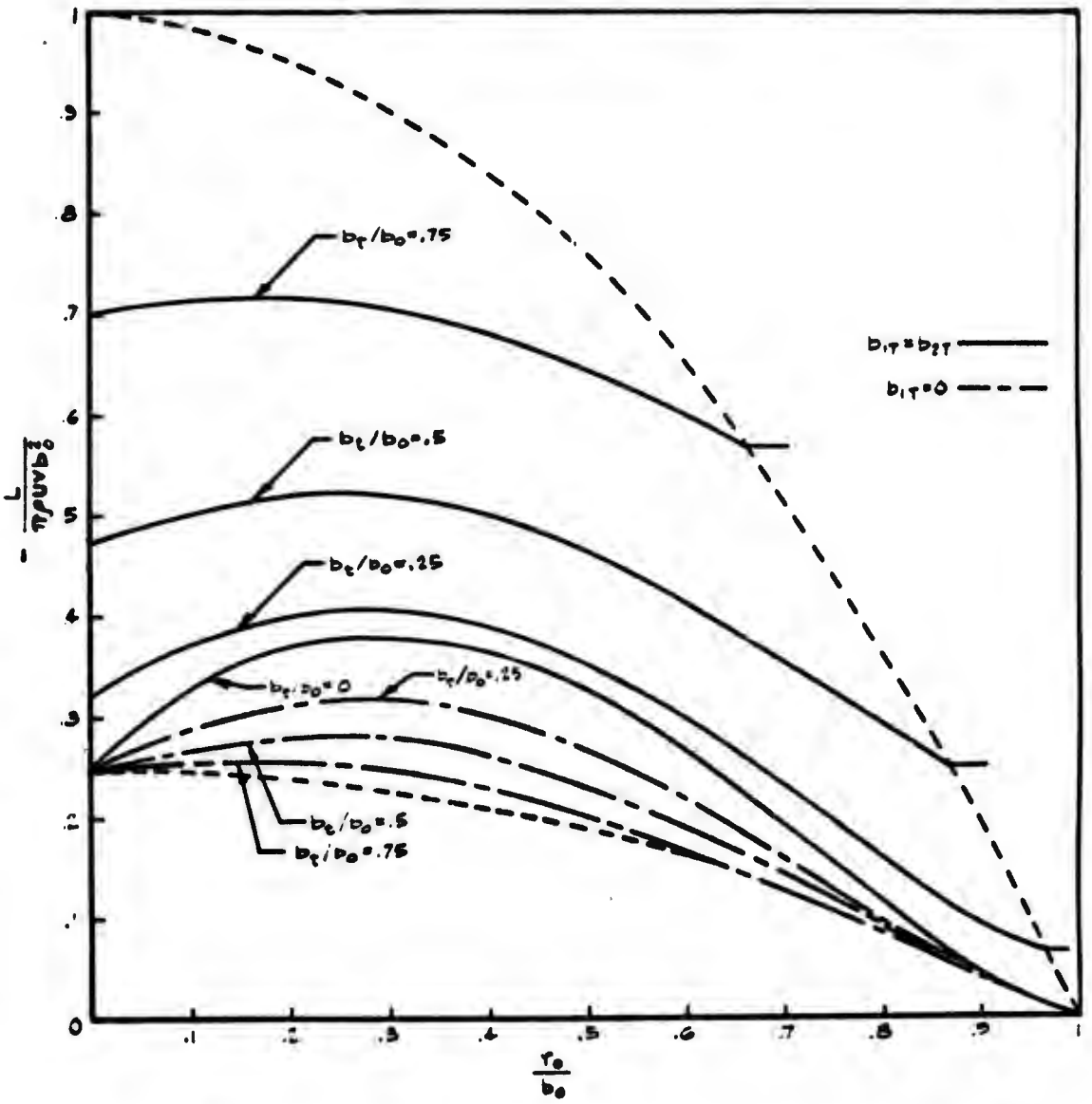

Lift coefficient of the axi-symmetric body with asymmetric fins shown in Figure 72 The upper family of curves (———) are for a symmetric tail configuration ($b_{1T} = b_{2T}$) , and the lower family of curves (——— – ———) are for a single upper tail fin ($b_{1T} = 0$) . The curve $b_{2T}/b_0 = 0$ is for a body without tail fins. Note that the symmetric tail fin carries a positive lift force, whereas the upper tail fin experiences a negative lift force due to the effects of downwash.

Figure 73

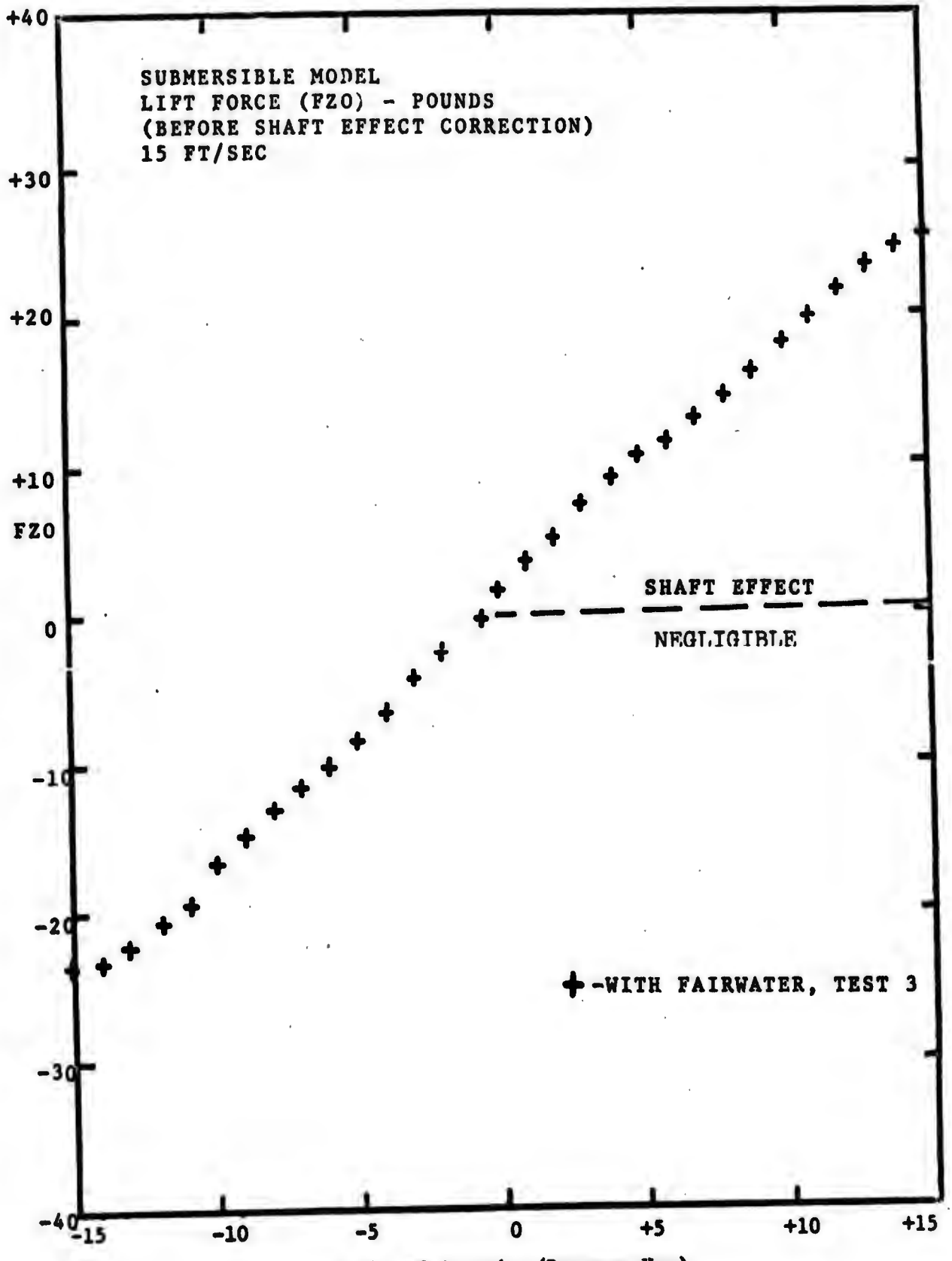
SUBMERSIBLE MODEL
LIFT FORCE (FZO) - POUNDS
(BEFORE SHAFT EFFECT CORRECTION)
15 FT/SEC
+40
+30
+20
+10
FZO
0
-10
-20
-30
-40
SHAFT EFFECT
NEGLIGIBLE
-WITH FAIRWATER, TEST 3
-15
-10
-5
0
+5
+10
+15
Angle of Attack- (Degrees-Yaw)

Figure 74

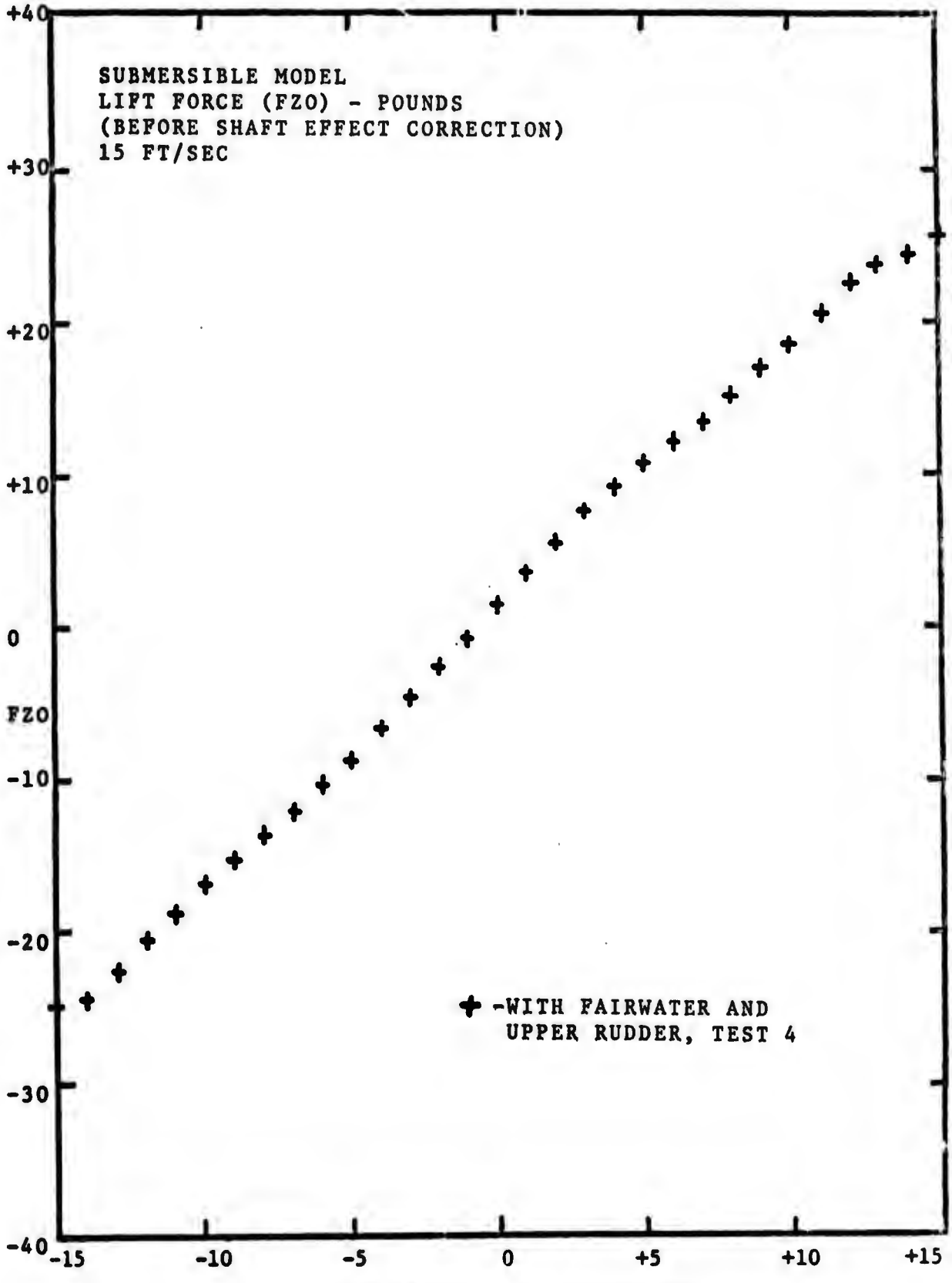
SUBMERSIBLE MODEL
LIFT FORCE (FZO) - POUNDS
(BEFORE SHAFT EFFECT CORRECTION)
15 FT/SEC
+40
+30
+20
+10
0
FZO
-10
-20
-30
-40
-15
-10
-5
0
+5
+10
+15
-WITH FAIRWATER AND
UPPER RUDDER, TEST 4
Angle of Attack- (Degrees-Yaw)

Figure 75

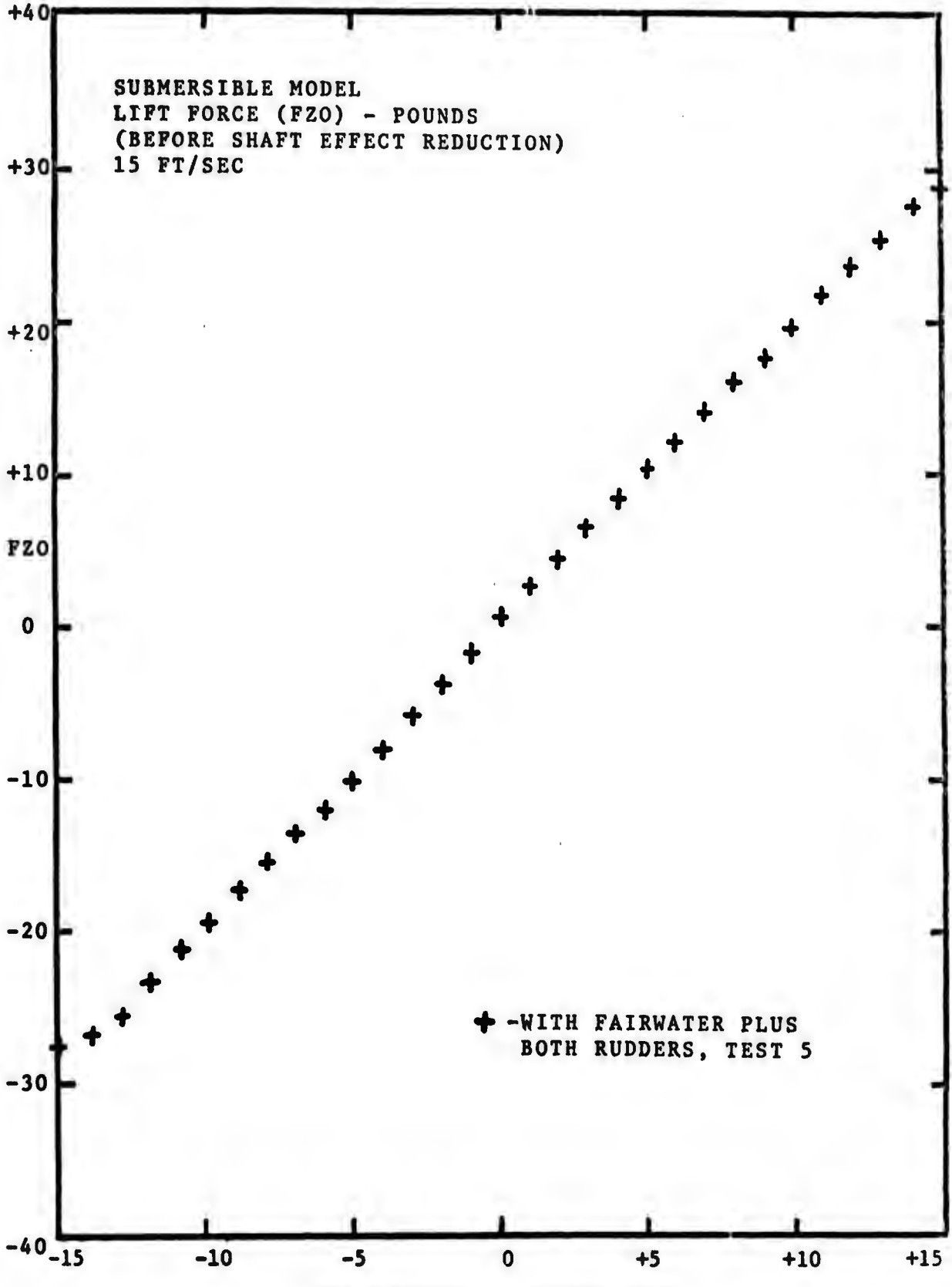
SUBMERSIBLE MODEL
LIFT FORCE (FZO) - POUNDS
(BEFORE SHAFT EFFECT REDUCTION)
15 FT/SEC
+40
+30
+20
+10
FZO
0
-10
-20
-30
-40
-15
-10
-5
0
+5
+10
+15
-WITH FAIRWATER PLUS
BOTH RUDDERS, TEST 5
Angle of Attack- (Degrees-Yaw)

Figure 76

C. Numerical Prediction

Numerical procedure results for a submersible with:

1. fairwater and upper rudder
2. Angle of yaw = 10 degrees
3. flow velocity = 15 ft/sec; therefore, free stream velocity = 14.77 ft/sec, side velocity = 2.6 ft/sec
4. wake angle = 10 degrees (free stream)

were:

Rudder side force	= 1.025 lb
Fairwater side force	= 11.754 lb
Source side force	= 1.394 lb
Total side force	= 14.173 lb

Rudder yaw moment	= 1.0947 ft·lb
Fairwater yaw moment	= -0.8960 ft·lb
Source yaw moment	= 7.2101 ft·lb
Doublet yaw moment	= -9.0152 ft·lb
Total yaw moment	= -1.064 ft·lb

Heave force on body	= -5.0780 lb
Pitch moment on body	= 3.5585 ft·lb

Comparable averaged experimental results were:

Test 4 results	Test 5 results	
18.0	19.0	Side force (FZ) lb
-3.75	-4.0	Yaw moment (MYO) ft·lb
-1.7	-2.7	Heave force (FYO) ft
3.0	7.0	Pitch moment (MZ) ft·lb

Numerical results were also compared with preliminary results from NSRDC for the base hull configurations. Bare hull configuration for the numerical program was accomplished by reducing the span length of the fairwater and rudder, measured from the body axis of symmetry to the radius of the hull surface at the appropriate points on the hull. The results were:

Rudder side force	= 0.012 lb
Fairwater side force	= 0.003 lb
Source side force	= 2.990 lb
Total side force (FZ)	= 3.004 lb

No side force should result from fairwater or rudder; therefore,

Total side force (FZ) = 2.99 lb

Rudder yaw moment	= 0.0134
Fairwater yaw moment	= 0.0000
Source yaw moment	= 8.5134
Doublet yaw moment	= -9.7262
Total yaw moment	= -1.1994

No moment should result from fairwater or rudder; therefore,

Total yaw moment (MYO) = -1.2128 ft lb

Since

$$Y' = \frac{-FZ}{\frac{1}{2}\rho U^2 L^2} = \text{Lateral Force Coefficient}$$

$$N' = \frac{MYO}{\frac{1}{2}\rho U^2 L^3} = \text{Yaw Moment Coefficient}$$

where ρ = fluid density

U = free stream velocity

L = model length

Y'(numerical) $= -3.41 \times 10^{-3}$

N'(numerical) $= -.679 \times 10^{-3}$ (needs a greater doublet strength correction aft of the fairwater)

Comparable results for NSRDC and this investigation were:

NSRDC	Experimental
$Y' = -3.5 \times 10^{-3}$	$Y' = -5.92 \times 10^{-3}$
$N' = -1.9 \times 10^{-3}$	$N' = -1.8 \times 10^{-3}$

VIII. CONCLUSION

The purpose of this project was to investigate hull-control surface interactions on submerged bodies, to include the effects imposed on the body by the fairwater and rudders, when the body is at a constant yaw angle.

It has been shown through experimental and numerical models, and flow visualization, that the addition of a non-symmetric appendage (fairwater) on a symmetrical body of revolution has a significant effect on the hull and the control surfaces (rudders) located downstream.

The fairwater, besides being a lifting surface and generating a side (sway) force when at an angle of yaw, also induces a circulation around the hull of a submersible. When this circulation and a sway velocity are combined, a lift is generated on the hull. These asymmetric forces then produce moments around each of the three coordinate axes and cross-coupling moments. The fairwater was also instrumental in decreasing the effective angle of attack of the upper rudder, located on the same side and downstream of it. The trailing vortex sheet, shed from the fairwater, induced velocities on this rudder and effectively changed the direction of fluid flow meeting the rudder. This change in flow direction was readily seen during the flow visualization experiments.

The upper and lower rudders produced relatively minor

effects on the forces and moments at small angles of yaw. Only at high angles of yaw, when the fairwater and support-shaft downwashes were least effective on the rudders, did the side (sway) force of the rudders combine with the extended moment arm to produce a major effect. Investigation of the effects of the rudders on the body of revolution, without the fairwater, is needed for a more complete analysis.

The numerical model considered the effects of the fairwater and although requiring refinement, the initial results are comparable with experimental results obtained during this investigation.

LIST OF REFERENCES

1. Department of Naval Architecture and Marine Engineering, Massachusetts Institute of Technology, Technical Proposal to The General Hydrodynamics Research Program, NSRDC; "Hull-Control Surface Interactions on Submerged Bodies," Submitted March 1971.

2. E. S. Arentzen, Capt. USN and Philip Mandel, "Naval Architectural Aspects of Submarine Design," paper presented at Annual Meeting, SNAME, New York, New York, November 17 - 18, 1960.

3. L. M. Milne-Thomson, Theoretical Hydrodynamics, Fourth Edition, the Macmillan Company, New York, New York, 1960.

4. V. M. Falkner, "The Calculation of Aerodynamic Loading on Surfaces of Any Shape," Aeronautical Research Committee R & M No. 1910, 1943.

5. V. M. Falkner, "The Solution of Lifting-Plane Problems by Vortex Lattice Theory," Aeronautical Research Council, R & M No. 2591, 1947.

6. V. M. Falkner, "The Scope and Accuracy of Vortex Lattice Theory," Aeronautical Research Council, R & M No. 2740, 1952.

7. J. E. Kerwin, "The Solution of Propeller Lifting Surface Problems by Vortex Lattice Methods," Report, Department of Naval Architecture and Marine Engineering, M.I.T., Cambridge, Mass., June 1961.

8. D. E. Cummings, "Vortex Interaction in a Propeller Wake," Report No. 68-12, Department of Naval Architecture and Marine Engineering, M.I.T., Cambridge, Mass., June 1968.

9. J. E. Kerwin and R. Leopold, "A Design Theory for Subcavitating Propellers," paper presented at Annual Meeting, SNAME, New York, New York, November 12 - 13, 1964.

10. F. B. Hildebrand, Advanced Calculus for Applications, Prentice-Hall, Inc., Englewood Cliffs, New Jersey, 1962.

11. W. R. McCreight, "Force and Moment on a Slender Body of Revolution Moving in Water of Finite Depth," M. S. Thesis, M.I.T., Cambridge, Mass., June 1970.

12. W. R. McCreight, "Heave Force and Pitching Moment on a Submerged Body of Revolution in Finite Depth," Report No. 70-7, Department of Naval Architecture and Marine Engineering, M.I.T., Cambridge, Mass., June 1970.

13. J. N. Newman and T. Y. Wu, "A Generalized Slender-Body Theory For Fish-Like Forms," Journal of Fluid Mechanics, Volume 57, pp. 673-693, 1973.

14. C. O. Horton, "Design and Construction of a System for Measurement of Unsteady Propeller Forces," Naval Engineer Thesis, Department of Naval Architecture and Marine Engineering, M.I.T., Cambridge, Mass, June 1970.

15. T. Brockett, "Minimum Pressure Envelopes for Modified NACA - 66 Sections With NACA a = 0.8 Camber and BuShips Type I and Type II Sections," Report 1780, DTMB, Washington, D. C., February 1966.

OTHER REFERENCES CONSULTED

J. P. Comstock (editor), Principles of Naval Architecture, Society of Naval Architects and Marine Engineers, New York, New York, 1967.

R. F. Elliott, "Experiments on a Slender Body of Revolution Moving Near a Wall," M. S. Thesis, Department of Naval Architecture and Marine Engineering, M.I.T., Cambridge, Mass., 1969.

J. N. Newman, Marine Hydrodynamics, (Lecture Notes), Revised Edition, Department of Naval Architecture and Marine Engineering, M.I.T., Cambridge, Mass. 1971.

B. Thwaites (editor), Incompressible Aerodynamics, Oxford University Press, Oxford, England, 1960.

APPENDIX A

THE M.I.T.

VARIABLE PRESSURE WATER TUNNEL

APPENDIX A

THE M.I.T. VARIABLE PRESSURE WATER TUNNEL (14)

The M.I.T. Variable Pressure Water Tunnel was built in 1938 - 39, and provided a significant advance in propeller and model test facilities at that time. Since then, several modifications have been made to the tunnel to extend its useful life, to make it more convenient to use, and to give it additional capabilities in keeping with current research needs.

General Features

The tunnel is a closed-return type and is approximately a 24-foot diameter square in shape. See Figure A-1. It occupies parts of the first and second floors of Building 3 on the M.I.T. campus. The smallest internal diameter is approximately 30 inches, but this gradually widens to a 60-inch maximum before narrowing again to enter the test section. The tunnel cross-section is circular except at the test section and in the tapered transition section. The transition section narrows the 60-inch circular cross-section to the 20-inch square test section.

Testing Facilities

The tunnel can provide water velocities in the test

section up to 33 ft/sec and maintain any selected internal pressure from atmospheric (760mm Hg) down to approximately 140 mm Hg.

The test section is accessible via any of four identical removable plexiglas windows. The windows are 2.0 inches thick by 13 7/16 in. by 41 15/16 in. high and cover access holes measuring 41 15/16 by 13 7/16 in. The windows are readily cut or drilled and are thus ideal for mounting experiments. The dynamometer apparatus used allows measuring six-degrees-of-freedom forces on lifting surfaces, such as rudders or hydrofoils. Fittings are installed in the windows to accept Pitot tubes at several locations.

The tunnel may also be operated with a free surface to test-surface piercing hydrofoils or to simulate a miniature towing tank for small ship model testing.

Impeller Drive Systems

A 100 HP motor drives three DC generators. One of these, a 60 KW shunt-wound generator, provides power for the 75 HP DC impeller drive motor. The second, a 30 KW shunt-wound DC generator, provides power for the 40 HP propeller drive motor. The third is a 3 KW compound-wound DC generator and provides excitation for the other two DC generators.

A variable resistance vernier control system provides close control of impeller RPM.

A device attached to the impeller drive shaft provides a 60 pulse per revolution output. The signal is fed to a Hewlett-Packard 5212A electronic counter. By using 60 pulses per revolution, the counter reads directly in RPM instead of RPS.

Water Flow

A four-bladed bronze impeller is used to provide water flow. It is located in the lower level horizontal run in the 30-inch diameter section. It is immediately followed by straightening vanes to remove rotation from the water.

Each 90° bend has several thin stainless steel turning vanes with a non-symmetrical cross-section developed from airfoil theory. The vanes have a low power loss and the resoluting turbulence generated by rounding the corners is fine-patterned and on the order of the turning vane spacing.

The 30-inch diameter widens out to 60 inches to slow the water velocity and further reduce turbulence. After rounding a 90° bend, the water is passed through a honeycomb of one-inch diameter plastic tubes and 2 sections of metal screens.

The 60-inch diameter is then smoothly constricted to flow through the 20-inch square test section. The section area reduction is 7.07. The constriction speeds up the flow velocity and at the same time stretches out any remaining turbulence. A smooth flow pattern results.

The Variable Pressure System

Any pressure in the range of atmospheric to 140 mm Hg can be maintained by the vacuum pump. The lower limit is dictated by the vapor pressure of water and small air leaks in the tunnel. Water vapor pressure at 60° F is 135 mm Hg.

Suction from the vacuum pump is taken at three points on the tunnel: (1) from the vacuum dome; (2) from the manhole cover over the 60-inch horizontal section; and (3), at the last 90° bend before entering the honeycomb.

If the tunnel is completely filled with water, some water may be sucked into the vacuum line to the pump. This is trapped in a receiver tank. Suction by the pump is taken from the top of the tank, while a drain line is provided at the bottom of the tank. The drain line drops 35 feet and is kept below water level in the building basement.

The vacuum system is the primary means of removing dissolved gases from the tunnel water. Dissolved oxygen is chemically removed for corrosion protection of the mild steel walls, and other gases are removed by keeping the tunnel at reduced pressure for several hours. If this is not done, dissolved gases form bubbles at reduced pressure and obscure the viewing of experiments in the test section.

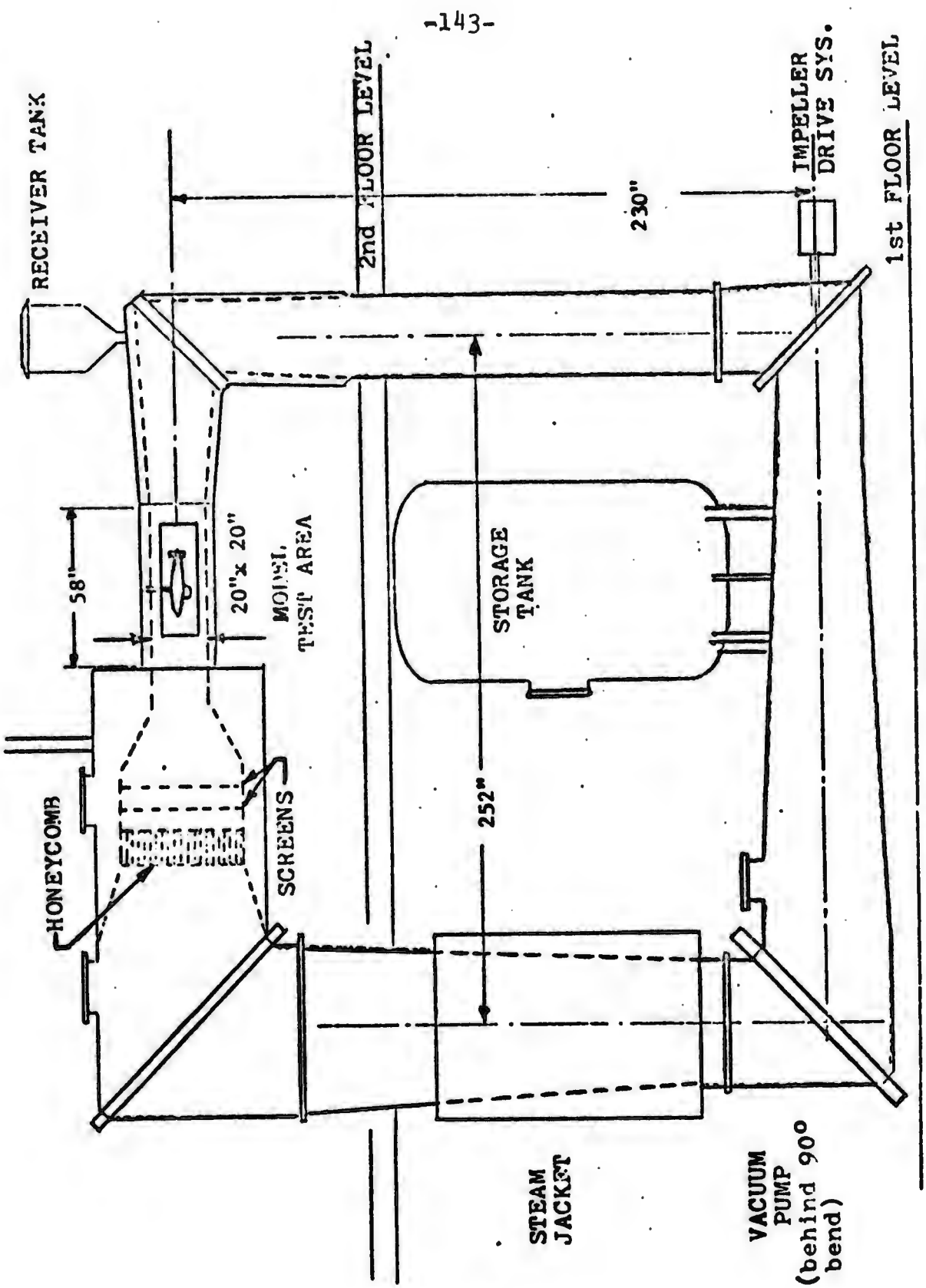
RECEIVER TANK
2nd FLOOR LEVEL
230"
IMPELLER DRIVE SYS.
1st FLOOR LEVEL
58"
20"x 20"
MODEL TEST AREA
STORAGE TANK
HONEYCOMB
SCREENS
252"
STEAM JACKET
VACUUM PUMP (behind 90° bend)
M.I.T. VARIABLE PRESSURE WATER TUNNEL

Figure A-1

APPENDIX B

DYNAMOMETER PROGRAM USED

FOR

EXPERIMENTAL MODEL TESTS

```
C      DYNAMOMETER PROGRAM USED TO EVALUATE THE FORCES AND MOMENT ON THE          PGM10001
C      SUBMERSIBLE AND FAIRWATER MODELS (EXPERIMENTAL)                            PGM10002
C      MK4 RUDDER DYNAMOMETER DATA REDUCTION PROGRAM   KERWIN/LEWIS    MAY 72     PGM10003
       INTEGER RS,S,BLANK                                                        PGM10004
       REAL MX,MAG,MYG,MZ,MZC,MFLAP                                              PGM10005
       DIMENSION IDENT(18),ZM(2),ZI(6,2,2),ZF(2),NTAP(32),NFLD(32),ANGM(3        PGM10006
      12),ANGL(32),S(32,6),R(32,7),DZI(6,2),CL(32),CD(32),CM(32),CPL(32),        PGM10007
      2CY(32),CMF(32),VC(5),VE(5),FM(2),C(6),CLD(32),CLSQ(32),RN(32),SI(3        PGM10008
      32),CC(32)                                                                 PGM10009
       DATA VC/4.11447,2.63068,0.9016,0.6214,4.7361/,VE/.49353,.5,.4724,0        PGM10010
      1.90038,.5/,RS/'R'/,BLANK/' '/                                             PGM10011
       READ(5,104)(C(N),N=1,6),TWIST,SHAFT                                       PGM10012
  104  FORMAT(8F10.5)                                                            PGM10013
    1  READ(5,103)(IDENT(N),N=1,18)                                              PGM10014
  103  FORMAT(18A4)                                                              PGM10015
       READ(5,100) DF,NRT,NTT,AREA,SPAN,AC,XAC,ZAC,FMC                           PGM10016
  100  FORMAT(F5.1,I5,I6,F10.2,F9.1,F9.3,F9.3,F10.2,F9.5)                        PGM10017
       IF(AREA.LE.0) GO TO 99                                                    PGM10018
       RHO=1.9374-0.00028*NTT                                                    PGM10019
       SCALE=1.000952-13.3E-6*NRT                                                PGM10020
       FM(1)=1.4675-.00071*NRT                                                   PGM10021
       FM(2)=24.5334-.00230*NRT                                                  PGM10022
       WRITE(6,200)(IDENT(N),N=1,18)                                             PGM10023
  200 FORMAT('1',17X,'FLAPPED RUDDER INPUT DATA'/1X,18A4/5X,'DF',5X,'TR'         PGM10024
     1,4X,'TT',5X,'AREA',6X,'SPAN',4X,'C-MAC',4X,'X-MAC',14X,'ZAC',6X,'F         PGM10025
     2MC')                                                                       PGM10026
       WRITE(6,100) DF,NRT,NTT,AREA,SPAN,AC,XAC,ZAC,FMC                          PGM10027
       READ(5,101)(ZM(K),((ZI(M,L,K),L=1,2),M=1,6),ZF(K),K=1,2)                  PGM10028
  101  FORMAT(I5.0,12X,F5.0,F4.0,F5.0,F4.0,F5.0,F4.0,F5.0,F4.0,F5.0,F4.0,        PGM10029
     1F5.0,F4.0,F9.0)                                                           PGM10030
       WRITE(6,201)                                                              PGM10031
  201  FORMAT('     ZERO READINGS BEFORE AND AFTER'/' ANGM 1-N    1-R    2-N     PGM10032
     1    2-R   3-N   3-R    4-N    4-R    5-N    5-R    6-N    6-R    FLAP')   PGM10033
       WRITE(6,204)(ZM(K),((ZI(M,L,K),L=1,2),M=1,6),ZF(K),K=1,2)                 PGM10034
  204  FORMAT(2(F4.0,4(2X,F4.0),2(1X,F4.0),6(2X,F4.0),1X,F6.0/))                 PGM10035
       WRITE(6,212)(C(N),N=1,6),TWIST ,SHAFT                                     PGM10036
```

```
 212 FORMAT('     CELL LBS/COUNT  1=',F7.5,' 2=',F7.5,' 3=',F7.5,' 4=',F      PGM10037
    17.5,' 5=',F7.5,' 6=',F7.5,/'     TWIST=',F7.1,'    SHAFT DIA.=',F7.2    PGM10038
    2,' IN.')                                                                PGM10039
      WRITE(6,202)                                                           PGM10040
 202  FORMAT( /'     INPUT DATA AS RECORDED'/'  TF  ANOM ANGLE    S     1     PGM10041
    1 S     2    S     3    S     4    S     5    S     6        FLAP')      PGM10042
      DO 2 J=1,32                                                            PGM10043
      JT=J-1                                                                 PGM10044
      READ(5,102) NTAP(J),NFLD(J),ANOM(J),ANGL(J),(S(J,M),R(J,M),M=1,6),     PGM10045
    1R(J,7)                                                                  PGM10046
 102  FORMAT(I4,I1,F5.0,F6.1,3X,A1,F8.2,A1,F8.2,A1,F8.2,A1,F8.2,A1,F8.2,     PGM10047
    1A1,F8.2,F7.0)                                                           PGM10048
      IF(ANOM(J).LE.0.0) GO TO 3                                             PGM10049
 2    WRITE(6,203) NTAP(J),NFLD(J),ANOM(J),ANGL(J),(S(J,M),R(J,M),M=1,6)     PGM10050
    1,R(J,7)                                                                 PGM10051
 203  FORMAT(I3,I1,F6.0,F6.1,3X,6(A1,F6.0,2X),F7.0)                          PGM10052
      GO TO 99                                                               PGM10053
 3    BUG=1.0/(JT-1)                                                         PGM10054
      DZM=(ZM(2)-ZM(1))*BUG                                                  PGM10055
      DO 4 M=1,6                                                             PGM10056
      DO 4 L=1,2                                                             PGM10057
 4    DZI(M,L)=(ZI(M,L,2)-ZI(M,L,1))*BUG                                     PGM10058
      DZF=(ZF(2)-ZF(1))*BUG                                                  PGM10059
      DO 5 J=1,JT                                                            PGM10060
      IF(J.EQ.1) GO TO 6                                                     PGM10061
      IF(NTAP(J).EQ.0) NTAP(J)=NTAP(J-1)                                     PGM10062
      IF(NFLD(J).EQ.0) NFLD(J)=NFLD(J-1)                                     PGM10063
 6    BUG=J-1                                                                PGM10064
      ANOM(J)=ANOM(J)-ZM(1)-BUG*DZM                                          PGM10065
      RAT=(ANGL(J)-100.0)*0.0174532                                          PGM10066
      SI(J)=SIN(RAT)                                                         PGM10067
      CO(J)=COS(RAT)                                                         PGM10068
      ANGL(J)=ANGL(J)-ZAC                                                    PGM10069
      DO 7 M=1,6                                                             PGM10070
      IF(S(J,M).EQ.BLANK) S(J,M)=S(J-1,M)                                    PGM10071
      IF(S(J,M).EQ.RS) GO TO 8                                               PGM10072
```

```
      R(J,M)=R(J,M)-ZI(M,1,1)-BUG*DZI(M,1)                                  PGM10073
      GO TO 7                                                               PGM10074
8     R(J,M)=-R(J,M)+ZI(M,2,1)+BUG*DZI(M,2)                                 PGM10075
7     CONTINUE                                                              PGM10076
5     R(J,7)=R(J,7)-ZF(1)-BUG*DZF                                           PGM10077
      WRITE(6,205)(NTAP(J),NFLD(J),ANOM(J),ANGL(J),(R(J,M),M=1,6),R(J,7)    PGM10078
     1,J=1,JT)                                                              PGM10079
205   FORMAT(///'     INPUT DATA CORRECTED FOR ZERO READINGS AND SIGNS'//(I PGM10080
     13,11,F6.0,F7.2,2X,6F9.2,F7.0))                                        PGM10081
      WRITE(6,207)(IDEN1(N),N=1,18)                                         PGM10082
207   FORMAT('1  **FLAPPED RUDDER DATA REDUCTION**'//1X,18A4//3X,'   ALP    PGM10083
     1HA      FX-LB     FZ-LB   MX-INLB   MZ-INLB    FXU-LB    FYU-LB    PGM10084
     2 MXU-INLB MYU-INLB MZU-INLB MYUFLAP-INLB VEL-FPS')                    PGM10085
      BEAR=AC/(12*3.9739*EXP(67.6632/NTT))                                  PGM10086
      DO 9 J=1,JT                                                           PGM10087
      I=NTAP(J)                                                             PGM10088
      IF(I.LT.1.OR.I.GT.5) GO TO 99                                         PGM10089
      K=NFLD(J)                                                             PGM10090
      IF(K.LT.1.OR.K.GT.2) GO TO 99                                         PGM10091
      BUG=VE(I)                                                             PGM10092
      V=(ANOM(J)*FM(K)*SCALE/(VC(I)*RHO))**BUG                              PGM10093
      FYHAFT=0.00327*SHAFT**2*V**2                                          PGM10094
      FBOX1=C(1)*R(J,1)                                                     PGM10095
      FBOX2=C(2)*R(J,2)                                                     PGM10096
      FBOX3=C(3)*R(J,3)                                                     PGM10097
      FBOX4=C(4)*R(J,4)+FYHAFT*0.41477                                      PGM10098
      FBOX5=C(5)*R(J,5)+FYHAFT*0.41477                                      PGM10099
      FBOX6=C(6)*R(J,6)+FYHAFT*0.17045                                      PGM10100
      FX=-FBOX3                                                             PGM10101
      FY=-FBOX4-FBOX5-FBOX6                                                 PGM10102
      FZ=-FBOX1-FBOX2                                                       PGM10103
      MX=14.725*(FBOX1+FBOX2)+6.062*(FBOX5-FBOX4)                           PGM10104
      MY=-18.0*FBOX2                                                        PGM10105
      MZ=17.054*FBOX6-14.725*FBOX3-5.5*(FBOX4+FBOX5)                        PGM10106
      FXU=FX*CU(J)+FZ*SI(J)                                                 PGM10107
      FYU=FY                                                                PGM10108
```

```
      FZU=FZ*CU(J)-FX*SI(J)                                                  PGM10109
      MXU=MX*CU(J)+MZ*SI(J)                                                  PGM10110
      MYU=MY                                                                 PGM10111
      MZU=MZ*CU(J)-MX*SI(J)                                                  PGM10112
      MFLAP=R(J,7)*FMC                                                       PGM10113
      ANGL(J)=ANGL(J)+MYU/TWIST                                              PGM10114
      WRITE(6,206) ANGL(J),FX,FZ,MX,MZ,FXL,FYU,FZU,MXU,MYU,MZU,MFLAP,V      PGM10115
  206  FORMAT(11F9.2,F13.2,F8.2)                                             PGM10116
      RVS=0.5*RHO*AREA*V**2/144.0                                            PGM10117
      CL(J)=FZU/RVS                                                          PGM10118
      CLSQ(J)=CL(J)**2                                                       PGM10119
      CD(J)=FXU/RVS                                                          PGM10120
      CLD(J)=CL(J)/CD(J)                                                     PGM10121
      CM(J)=(MYU+FZ*XAC)/RVS/AC                                              PGM10122
      CPL(J)=(MXU/FZU)/SPAN                                                  PGM10123
      CY(J)=FYU/RVS                                                          PGM10124
      RN(J)=V*CLAR                                                           PGM10125
9     CMF(J)=MFLAP/RVS/AC                                                    PGM10126
      WRITE(6,208)(IDENT(N),N=1,18)                                          PGM10127
  208  FORMAT('1  **FLAPPED RUDDER DATA IN NON-DIMENSIONAL FORM**'//3X18A    PGM10128
     14///'    ALPHA     CL       CD       CM       CPL      CY       L/D     CMF      C     PGM10129
     2LSQ   RN*10**-6')                                                      PGM10130
      WRITE(6,209)(ANGL(J),CL(J),CD(J),CM(J),CPL(J),CY(J),CLD(J),CMF(J),     PGM10131
     1CLSQ(J),RN(J),J=1,JT)                                                  PGM10132
  209 FORMAT(F8.2,F7.3,F8.4,5F7.3,F8.4,F8.3)                                 PGM10133
      DO 15 J=1,JT                                                           PGM10134
      ANGL(J)=ANGL(J)+0.01962*AREA*CL(J)                                     PGM10135
      CD(J)=CD(J)+0.0003425*AREA*CL(J)**2                                    PGM10136
   15  CLD(J)=CL(J)/CD(J)                                                    PGM10137
      WRITE(6,211)                                                           PGM10138
  211  FORMAT(///'     ABOVE DATA CORRECTED FOR TUNNEL INTERFERENCE'         PGM10139
     1 //'    ALPHA     CL       CD       CM       CPL      CY       L/D     CMF      C     PGM10140
     2LSQ   RN*10**-6')                                                      PGM10141
      WRITE(6,209)(ANGL(J),CL(J),CD(J),CM(J),CPL(J),CY(J),CLD(J),CMF(J),     PGM10142
     1CLSQ(J),RN(J),J=1,JT)                                                  PGM10143
      GO TO 1                                                                PGM10144
```

```
99    STOP                                                    PGM10145
      END                                                     PGM10146
```

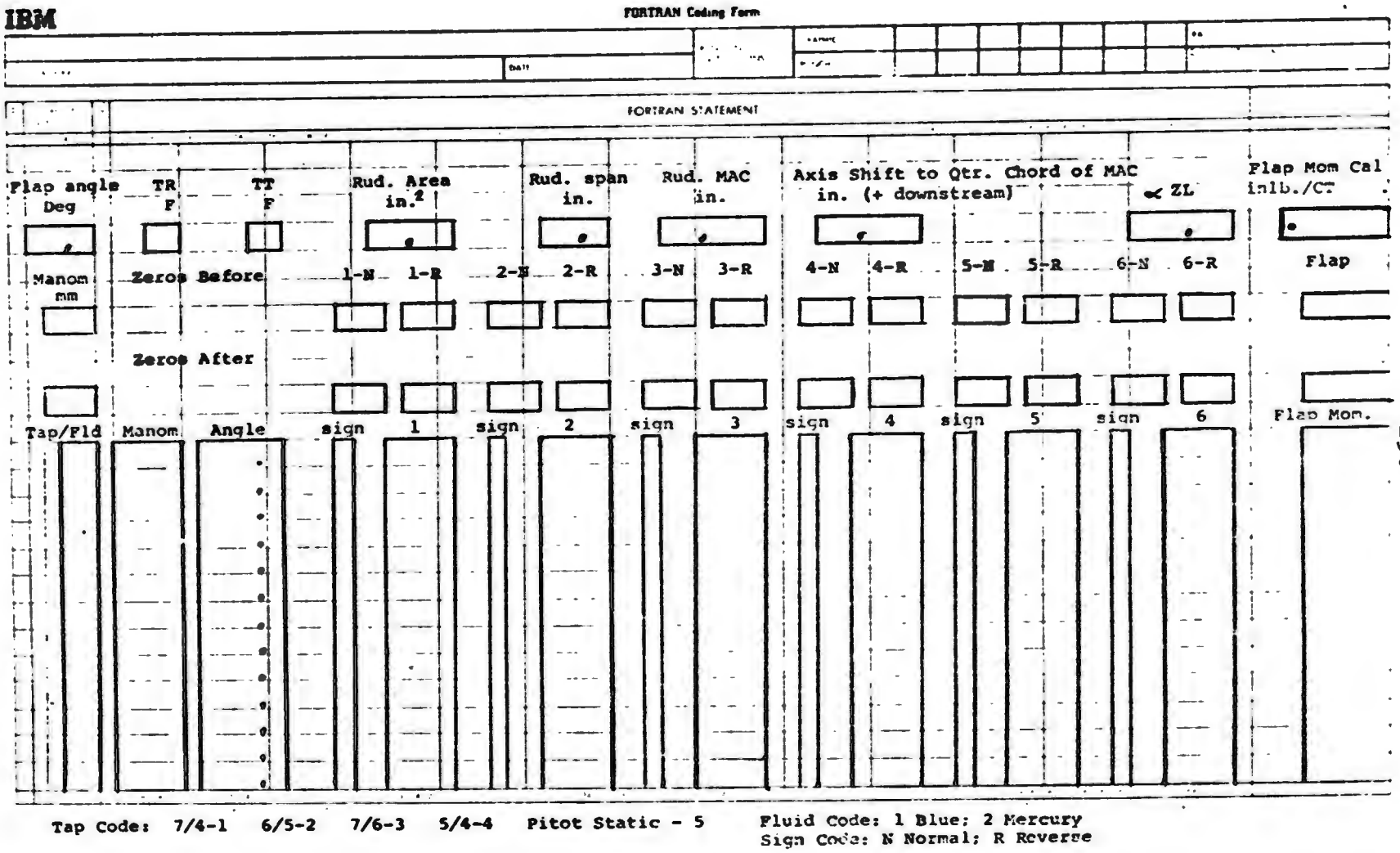

Figure B-1 Sample Data Sheet

```
C     SAMPLE DATA DECK FOR SUBMERSIBLE MODEL                                      PGM10001
          SUB WITH FAIRWATER, UPPER & LOWER RUDDERS 10 FT/SEC                     PGM10002
 0.0   75    81     62.06      3.5    24.600    0.0               97.60    .0     PGM10003
 00                100 100   50  50   50  50  100 100   50  50   50  50         PGM10004
 00                100 100   50  50   50  51  100 100   50  50   50  50         PGM10005
 11   626   96.6  N    110  N    50 R     77 N    136 R     49 R     64         PGM10006
      625   95.6       121       51       77      148       52       63         PGM10007
      624   94.6       130       53       77      160       55       63         PGM10008
      626   93.6       142       55       76      175       58       62         PGM10009
      627   92.6       153       56       76      185       60       62         PGM10010
      626   91.6       162       56       76      200       63       62         PGM10011
      627   90.6       169       56       75      210       66       61         PGM10012
```

Sample Results

FLAPPED RUDDER INPUT DATA
SUB WITH FAIRWATER, UPPER & LOWER RUDDERS 10 FT/SEC

DF	TR	TT	AREA	SPAN	C-MAC	X-MAC	ZAC	FMC
0.0	75	81	62.06	3.5	24.600	0.0	97.60	0.0

ZERO READINGS BEFORE AND AFTER

ANOM	1-N	1-R	2-N	2-R	3-N	3-R	4-N	4-R	5-N	5-R	6-N	6-R	FLAP
0.	100.	100.	50.	50.	50.	50.	100.	100.	50.	50.	50.	50.	0.
0.	100.	100.	50.	50.	50.	51.	100.	100.	50.	50.	50.	50.	0.

CELL LBS/COUNT 1=0.09926 2=0.05000 3=0.20030 4=0.10050 5=0.48970 6=0.20490
TWIST= 323.7 SHAFT DIA.= 0.75 IN.

INPUT DATA AS RECORDED

TF	ANOM	ANGLE	S	1	S	2	S	3	S	4	S	5	S	6	FLAP
11	626.	96.6	N	110.	N	50.	R	77.	N	136.	R	49.	R	64.	0.
00	625.	95.6		121.		51.		77.		148.		52.		63.	0.
00	624.	94.6		130.		53.		77.		160.		55.		63.	0.
00	626.	93.6		142.		55.		76.		175.		58.		62.	0.
00	627.	92.6		153.		56.		76.		185.		60.		62.	0.
00	626.	91.6		162.		56.		76.		200.		63.		62.	0.
00	627.	90.6		169.		58.		75.		210.		66.		61.	0.

INPUT DATA CORRECTED FOR ZERO READINGS AND SIGNS

11	626.	-1.00	10.00	0.0	-27.00	36.00	1.00	-14.00	0.
11	625.	-2.00	21.00	1.00	-26.83	48.00	-2.00	-13.00	0.
11	624.	-3.00	30.00	3.00	-26.67	60.00	-5.00	-13.00	0.
11	626.	-4.00	42.00	5.00	-25.50	75.00	-8.00	-12.00	0.
11	627.	-5.00	53.00	6.00	-25.33	85.00	-10.00	-12.00	0.
11	626.	-6.00	62.00	6.00	-25.17	100.00	-13.00	-12.00	0.
11	627.	-7.00	69.00	8.00	-24.00	110.00	-16.00	-11.00	0.

FLAPPED RUDDER DATA REDUCTION

SUB WITH FAIRWATER, UPPER & LOWER RUDDERS 10 FT/SEC

ALPHA	FX-LB	FZ-LB	MX-INLB	MZ-INLB	FXO-LB	FYO-LB	FZO-LB	MXO-INLB	MYO-INLB	MZO-INLB	MYOFLAP-INLB	VEL-FPS
-1.00	5.41	-0.99	-4.35	16.39	5.46	-1.43	-0.67	-5.31	0.0	16.11	0.0	10.30
-2.00	5.37	-2.13	-3.75	20.31	5.52	-1.38	-1.72	-5.30	0.0	19.97	0.0	10.29
-3.01	5.34	-3.13	-5.34	20.74	5.61	-1.11	-2.61	-7.27	-2.00	20.15	0.0	10.28
-4.01	5.11	-4.42	-4.37	20.66	5.57	-1.36	-3.82	-6.65	-4.00	20.04	0.0	10.30
-5.02	5.07	-5.56	0.41	20.08	5.75	-1.38	-4.86	-2.18	-5.00	19.96	0.0	10.31
-6.02	5.04	-6.45	-4.48	19.45	5.93	-1.42	-5.65	-7.27	-5.00	18.59	0.0	10.30
-7.02	4.81	-7.25	-7.77	21.12	5.93	-1.16	-6.37	-11.12	-7.00	19.57	0.0	10.31

FLAPPED RUDDER DATA IN NON-DIMENSIONAL FORM

SUB WITH FAIRWATER, UPPER & LOWER RUDDERS 10 FT/SEC

ALPHA	CL	CD	CM	CPL	CY	L/D	CMF	CLSQ	RN*10**-6
-1.00	-0.015	0.1234	0.0	2.265	-0.032	-0.123	0.0	0.0002	2.304
-2.00	-0.039	0.1251	0.0	0.882	-0.031	-0.311	0.0	0.0015	2.302
-3.01	-0.059	0.1273	-0.002	0.795	-0.025	-0.465	0.0	0.0035	2.300
-4.01	-0.086	0.1259	-0.004	0.497	-0.031	-0.686	0.0	0.0075	2.304
-5.02	-0.110	0.1298	-0.005	0.128	-0.031	-0.846	0.0	0.0120	2.306
-6.02	-0.128	0.1341	-0.005	0.368	-0.032	-0.953	0.0	0.0163	2.304
-7.02	-0.144	0.1338	-0.006	0.499	-0.026	-1.074	0.0	0.0207	2.306

ABOVE DATA CORRECTED FOR TUNNEL INTERFERENCE

ALPHA	CL	CD	CM	CPL	CY	L/D	CMF	CLSQ	RN*10**-6
-1.02	-0.015	0.1234	0.0	2.265	-0.032	-0.123	0.0	0.0002	2.304
-2.05	-0.039	0.1251	0.0	0.882	-0.031	-0.311	0.0	0.0015	2.302
-3.08	-0.059	0.1274	-0.002	0.795	-0.025	-0.465	0.0	0.0035	2.300
-4.12	-0.086	0.1261	-0.004	0.497	-0.031	-0.686	0.0	0.0075	2.304
-5.15	-0.110	0.1300	-0.005	0.128	-0.031	-0.844	0.0	0.0120	2.306
-6.17	-0.128	0.1344	-0.005	0.368	-0.032	-0.953	0.0	0.0163	2.304
-7.20	-0.144	0.1342	-0.006	0.499	-0.026	-1.071	0.0	0.0207	2.306

APPENDIX C

NUMERICAL PROGRAM TO GENERATE OFFSETS FOR CONSTRUCTION OF FOIL SHAPES

```
C     MILLING GEOMETRY FOR DEVELOPING LIFTING SURFACES FROM EXP. MODELS
C     GEOMETRY INPUT,DRILL DIAMETER,SPACING IN X,SPACING IN Y.
      DIMENSION XCIN(27),YCIN(27)
      READ(5,100) A,B,C,D,E,F,G,H
      WRITE(6,100) A,B,C,D,E,F,G,H
      READ(5,101) (XCIN(I),I=1,27)
      WRITE(6,101) (XCIN(I),I=1,27)
      READ(5,101) (YCIN(I),I=1,27)
      WRITE(6,101) (YCIN(I),I=1,27)
      K=1
  100 FORMAT(8F10.5)
  101 FORMAT((8F10.5))
C     LEADING HALF
      YCEN=F/2.0
      XCEN=0.0-F/2.0
    1 XOUT=XCEN+F/2.0
      IF(K.EQ.2)XOUT=XCEN-F/2.0
      YOUT=YCEN-F/2.0
C     CHECK AT XOUT & YOUT
      SH=A-YOUT
      CH=B-C*YOUT
      TK=D-E*YOUT
      XTBL=XOUT-SH
      XTBLND=XTBL/CH
      IF(XTBLND .LT.0.0 .OR.XTBLND .GT.1.0)GO TO 4
      CEN=SPLINE (XTBLND,XCIN,YCIN,27)
      DF=DEAD TK
      DF=1.0-DF
      WRITE(6,102)XCEN,YCEN,XOUT,YOUT,DF
  102 FORMAT(5F10.3)
    4 XCEN=XCEN+G
      IF(XCEN .GT.4.5)GO TO 2
      GO TO 1
    2 CONTINUE
      XCEN= . -F/2.
C     DO BACK HALF
```

```
      IF (K .EQ.2) STOP                                                 PGM20037
      K=2                                                               PGM20038
      XCEN=F/2.0                                                        PGM20039
      XC=N=0.0*F/2.0                                                    PGM20040
      WRITE(6,103)                                                      PGM2  41
  103 FORMAT(//,' BACK HALF')                                           PGM20042
      GO TO 1                                                           PGM20043
      END                                                               PGM20044
C     FILLIN  PARABOLIC INTERPOLATION                                   PGM20045
C     FINDS Y(X) FROM TABLE OF                                          PGM2  46
C     AR(M) AND OR(M) CONTAINING NO POINTS.                             PGM20047
      FUNCTION FILLIN(X,AR,OR,NO)                                       PGM20048
      DIMENSION AR(2),OR(2)                                             PGM20049
      ANTRA(X1,X2,X3,X,Y1,Y2,Y3)=Y1*(X-X2)*(X-X3)/((X1-X2)*(X1-X3))+    PGM20050
     1 Y2*(X-X1)*(X-X3)/((X2-X1)*(X2-X3))+Y3*(X-X1)*(X-X2)/((X3-X1)     PGM2  51
     2 *(X3-X2))                                                        PGM20052
      IF(X-AR(1))  1,3,2                                                PGM20053
    3 Y=OR(1)                                                           PGM20054
      GO TO 99                                                          PGM20055
    1 Y=ANTRA(AR(1),AR(2),AR(3),X,OR(1),OR(2),OR(3))                    PGM2  56
      GO TO 99                                                          PGM20057
    2 IF(X-AR(2))1,6,5                                                  PGM20058
    4 Y=OR(2)                                                           PGM2  59
      GO TO 99                                                          PGM20060
    5 DO 7 I=2,NO                                                       PGM2  61
      M=I                                                               PGM20062
      IF(X-AR(I))8,9,7                                                  PGM20063
    6 Y=OR(I)                                                           PGM2  64
      GO TO 99                                                          PGM20065
    7 CONTINUE                                                          PGM20066
    8 Y=ANTRA(AR(M-2),AR(M-1),AR(M),X,OR(M-2),OR(M-1),OR(M))            PGM20067
   99 FILLIN=Y                                                          PGM20068
      RETURN                                                            PGM2  69
      END                                                               PGM20070
```

```
C     SAMPLE DATA DECK FOR NACA (6(MOD) & A=.8 CAMBER                                   PGM20001
 .[illegible]  4.45     .0000    1.0000   .0000    .2500    .1       .1                 PGM20002
0.0      .005     .0075    .0125    .025     .05      .075     .1                 PGM20003
 .15      .2       .25      .3       .35      .4       .45      .5                 PGM20004
 .55      .6       .65      .7       .75      .8       .85      .9                 PGM20005
 .95      .975     1.0                                                              PGM20006
 .[illegible]  .0665    .0812    .1044    .1466    .2066    .2525    .2907              PGM20007
 .3521    .4000    .4363    .4637    .4832    .4952    .5       .4962              PGM20008
 .4846    .4653    .4383    .4035    .3612    .3111    .2532    .1877              PGM20009
 .1143    .0743    .0333                                                            PGM20010
```

PAGE 3

APPENDIX D

NUMERICAL MODEL OF A SUBMERSIBLE BODY OF REVOLUTION WITH LIFTING SURFACE APPENDAGES

```
C       NUMERICAL MODEL OF A SUBMERSIBLE BODY OF REVOLUTION WITH LIFTING        PGM30001
C       SURFACE APPENDAGES, TO DETERMINE THE HYRODYNAMIC FORCES AND             PGM30002
C       MOMENTS AND THEIR INTERACTIONS.                                         PGM30003
        COMMON ALPHA,ALR,AUX(12),AR(5),AUX2(6),C,CHOR(20),CSA,CMSS1(7),CHO      PGM30004
       1KK1(30),CMSK1(7)                                                        PGM30005
        COMMON DELX,DELTA(2),DBT1,DELC1,DBCP,DCX,DBTK1                          PGM30006
        COMMON GS(30,8),G1,G2,GWKS1(31),GTK(31),GTF(31),GBVS1(31,20,3,2),G      PGM30007
       1K(30,8),GBVK1(30,20,3,2)                                                PGM30008
        COMMON I,IPIV(6),IPI(3),IHCL,J,JM,L(6),IER,EPS,ISP(35)                  PGM30009
        COMMON NSTA,NTS,NBSC,NCPS,NCPC,NBS,NHS,NHLFT,NMIA,PI,PIINV,DPIINV,      PGM30010
       1N                                                                       PGM30011
        COMMON RHO,RIN(21),RSL(2),RROD(2),RHS,RWTS,RHR,RHS2,RHR2,RWTR,RF,R      PGM30012
       1T,RMSS1(32),RILHS(32,7),RFR,RTR,RILHS(32)                               PGM30013
        COMMON SINV(21),SPNS,SPNR,SLEF,STEF,SGG,SX,SY,SZ,S32,SIA,SILHS(32,      PGM30014
       1 7),SPRM(21),SLEER,SLTER                                                PGM30015
        COMMON THETA,TVSS1(31,20,3,2),TEN(32,4),TVSK1(31,20,3,2)                PGM30016
        COMMON UU,VZB(8,4,3,2),VZT(8,4,3,2),VZW(8,4,3,2),VZBK1(8,4,3,2),VZ      PGM30017
       1TK1(8,4,3,2),VZWK1(8,4,3,2),VZ                                          PGM30018
        COMMON WFS,WBSS1(8,4),WWS1K1(31),WBSK1(8,4),WS1K1(8,4),WTF(31,21),      PGM30019
       1WTR(31,21),W(21)                                                        PGM30020
        COMMON XIN(21),XLET(2),XLEB(2),XTET(2),XTLB(2),XLE1R(2),XLEBR(2),X      PGM30021
       1TE1R(2),XTEBR(2),XBVS1(20),XLE,XTE,XCPS1(8,4),XB,XBVK1(20),XCPK1(8      PGM30022
       2,4)                                                                     PGM30023
        COMMON YTKS1(31),YBS1(30),YCPS1(8),Y,YWKS1(31,21),YBUNK(31),YTBK1(      PGM30024
       1 31),YBK1(30),YCPK1(8),ZWKS1                                            PGM30025
        REAL LENGTH                                                             PGM30026
  100   FORMAT(I4,5X,3F10.4)                                                    PGM30027
  101   FORMAT((8F10.5))                                                        PGM30028
  102   FORMAT(9F10.5)                                                          PGM30029
  103   FORMAT(8F10.3)                                                          PGM30030
  104   FORMAT(2F10.4)                                                          PGM30031
  105   FORMAT(4I5)                                                             PGM30032
C       INPUT HULL AND FLOW PROPERTIES                                          PGM30033
        NSM=2                                                                   PGM30034
        READ (5,100)NSTA,UU,WFS,RHO                                             PGM30035
        READ (5,101)(XIN(J),J=1,NSTA)                                           PGM30036
```

```
      READ (5,101)(RIN(J),J=1,NSTA)                                     PGM30037
      DELX=XIN(1)-XIN(2)                                                PGM30038
      PI=3.14159                                                        PGM30039
      PIINV=1.0/PI                                                      PGM30040
      QPIINV=0.25*PIINV                                                 PGM30041
      DO 1 J=1,NSTA                                                     PGM30042
    1 SINV(J)=PI*RIN(J)**2                                              PGM30043
C     INPUT FIN PROPERTIES                                              PGM30044
      DO 2 J=1,2                                                        PGM30045
    2 READ (5,102) RSL(J),XLET(J),XLEB(J),XTET(J),XTEB(J)               PGM30046
C     INPUT RUDDER PROPERTIES                                           PGM30047
      DO 3 J=1,2                                                        PGM30048
    3 READ(5,103 ) RROD(J),XLETR(J),XLEBR(J),XTETR(J),XTEBR(J),DELTA(J) PGM30049
C     INPUT WAKE SHEDDING ANGLES                                        PGM30050
      READ (5,104) ALPHA,ALR                                            PGM30051
      IF(ALPHA.EQ.0.9999) ALPHA=WFS/UO                                  PGM30052
      IF(ALR.EQ.0.9999)    ALR=WFS/UO                                   PGM30053
C     INPUT GRID SIZES                                                  PGM30054
      READ (5,105) NTS,NBSC,NCPS,NCPC                                   PGM30055
C     CALCULATE SPAN OF FIN                                             PGM30056
      DUMX=0.5*(XLEB(1)+XTEB(1))                                        PGM30057
      RHS=FILLI (DUMX,XIN,RIN,NSTA)                                     PGM30058
      RHS2=RHS*RHS                                                      PGM30059
      RWIS=RHS2/RSL(1)                                                  PGM30060
      SPNS=RSL(1)-RWIS                                                  PGM30061
C     CALCULATE RUDDER SPAN                                             PGM30062
      DUMX=0.5*(XLEBR(1)+XTEBR(1))                                      PGM30063
      RHR=FILLI (DUMX,XIN,RIN,NSTA)                                     PGM30064
      RHR2=RHR*RHR                                                      PGM30065
      RWIR=RHR2/RROD(1)                                                 PGM30066
      SPNR=RROD(1)-RWIR                                                 PGM30067
C     TRAILING VORTEX RADII ON FIN 1                                    PGM30068
      DBT1=SPNS/FLOAT(NTS-1)                                            PGM30069
      YTRS1(1)=RWIS                                                     PGM30070
      DO 4 N=2,NTS                                                      PGM30071
    4 YTRS1(N)=YTRS1(N-1)+DBT1                                          PGM30072
```

```
      WRITE(6,120)(YTRS1(N),N=1,NTS)                                    PGM30073
  120 FORMAT(' TRAILER RADII ON SAIL',/,(16F7.3))                       PGM30074
C     CALCULATE MIDPOINT RADII ON SAIL 1                                PGM30075
      YBS1(1)=YTRS1(1)+DBT1*0.5                                         PGM30076
      NBS=NTS-1                                                         PGM30077
      DO 5 N=2,NBS                                                      PGM30078
    5 YBS1(N)=YBS1(N-1)+DBT1                                            PGM30079
C     CALCULATE X VALUE OF BOUND VORTEX LINES ON SAIL 1                 PGM30080
      XBVS1(1)=XLEB(1)                                                  PGM30081
      NBS=NBSC-1                                                        PGM30082
      DELC1=(XLEB(1)-XTEB(1))/FLOAT(NBS)                                PGM30083
      DO 6 M=2,NBSC                                                     PGM30084
    6 XBVS1(M)=XBVS1(M-1)-DELC1                                         PGM30085
      WRITE(6,121)(XBVS1(M),M=1,NBSC)                                   PGM30086
  121 FORMAT(' X LOCATION OF BOUND VORTEX LINES ON SAIL',/,(16F7.2))    PGM30087
C     LOCATE SAIL 1 CONTROL POINTS SPANWISE                             PGM30088
      DBCP=(RSL(1)-RHS)/FLOAT(NCPS+1)                                   PGM30089
      YCPS1(1)=RHS+DBCP                                                 PGM30090
      DO 7 N=1,NBS                                                      PGM30091
      N=N                                                               PGM30092
      IF(YCPS1(1).GT.YBS1(N).AND.YCPS1(1).LE.YBS1(N+1)) GO TO 8         PGM30093
    7 CONTINUE                                                          PGM30094
    8 YCPS1(1)=YBS1(N)                                                  PGM30095
      NRLFT=NBS-N                                                       PGM30096
      IHUL=FLOAT(NRLFT)/FLOAT(NCPS)                                     PGM30097
      DO 9 N=2,NCPS                                                     PGM30098
    9 YCPS1(N)=YCPS1(N-1)+IHUL*DBT1                                     PGM30099
C     CONTROL POINT SPACING CHORDWISE                                   PGM30100
      RF=FILLI (XLEB(1),XIN,RIN,NSTA)                                   PGM30101
      RT=FILLI (XTEB(1),XIN,RIN,NSTA)                                   PGM30102
      SLEF=(XLEB(1)-XLET(1))/(RSL(1)-RF)                                PGM30103
      STEF=(XTEB(1)-XTET(1))/(RSL(1)-RT)                                PGM30104
      DO 10 N=1,NCPS                                                    PGM30105
      Y=YCPS1(N)                                                        PGM30106
      XLE=XLEB(1)-SLEF*(Y-RF)                                           PGM30107
      XTE=XTEB(1)-STEF*(Y-RT)                                           PGM30108
```

```
      C=XLE-XTE                                                          PGM30139
      DCX=C/FLOAT(NCPC+1)                                                PGM30140
      XCPSI(N,1)=XTE+DCX                                                 PGM30141
      DO 11 M=1,NHS                                                      PGM30142
      M=M                                                                PGM30143
      IF(XCPSI(N,1).LT.XBVSI(M).AND.XCPSI(N,1).GE.XBVSI(M+1))GO TO 12    PGM30144
   11 CONTINUE                                                           PGM30145
   12 XCPSI(N,1)=XBVSI(M)-0.5*DELCI                                      PGM30146
      DO 13 M=2,NCPC                                                     PGM30147
      XCPSI(N,M)=XCPSI(N,M-1)+DCX                                        PGM30148
      DO 13 JM=1,NHS                                                     PGM30149
      JM=JM                                                              PGM30150
      IF(XCPSI(N,M).LT.XBVSI(JM).AND.XCPSI(N,M).GE.XBVSI(JM+1))XCPSI(N,M PGM30151
     1)=XBVSI(JM)-0.5*DELCI                                              PGM30152
   13 CONTINUE                                                           PGM30153
   10 CONTINUE                                                           PGM30154
      DO 123 N=1,NCPS                                                    PGM30155
  123 WRITE(6,122)(YCPSI(N),(XCPSI(N,M),M=1,NCPC))                       PGM30156
  122 FORMAT(' YCP=',F10.3,'XCP=',4F7.3)                                 PGM30157
C     SOUND VORTEX STRENGTHS FOR SAIL 1 UNIT MODES                       PGM30158
      DO 14 N=1,NBS                                                      PGM30159
      XLE=XLEB(1)-SLEF*(YBSI(N)-RF)                                      PGM30160
      IF(XLE.GT.XLEB(1)) XLE=XLEB(1)                                     PGM30161
      XTE=XTEB(1)-STEF*(YBSI(N)-RT)                                      PGM30162
      IF(XTE.LT.XTEB(1)) XTE=XTEB(1)                                     PGM30163
      CHOR(N)=XLE-XTE                                                    PGM30164
      Q=(YBSI(N)-RHS)/(RSL(1)-RHS)                                       PGM30165
      SQQ=(1.0-Q*Q)**0.5                                                 PGM30166
      DO 15 NSP=1,NSM                                                    PGM30167
   15 GS(N,NSP)=SQQ*Q**(2*NSP-2)                                         PGM30168
      GSUM1=0.0                                                          PGM30169
      GSUM2=0.0                                                          PGM30170
      G1=0.0                                                             PGM30171
      G2=0.0                                                             PGM30172
      DO 14 M=1,NBSC                                                     PGM30173
      XD=XLE+.5*DELCI                                                    PGM30174
```

```
      IF(XBVS1(M) .GT. XD) GO TO 16                                     PGM30145
      XT=XTE-.5*DELC1                                                   PGM30146
      IF( XBVS1(M).LT. XT ) GO TO 16                                    PGM30147
      XT=XTE+.5*DELC1                                                   PGM30148
      IF( XBVS1(M) .LT. XT) GO TO 951                                   PGM30149
      GO TO 952                                                         PGM30150
  951 THETA=PI                                                          PGM30151
      GO TO 955                                                         PGM30152
  952 CONTINUE                                                          PGM30153
      GO TO 17                                                          PGM30154
   16 G1=0.0                                                            PGM30155
      G2=0.0                                                            PGM30156
      GO TO 18                                                          PGM30157
   17 COSX=      (1.-2.*(XLE-XBVS1(M)+DELC1*.5)/CHOR(N))                PGM30158
      THETA=ARCOS(COSX)                                                 PGM30159
  850 FORMAT(' COSX=',F20.8,' THETA=',F20.5)                            PGM30160
  955 G1=(THETA+SIN(THETA))*PIINV -GSUM1                                PGM30161
      G2=2.*PIINV*(THETA*.5-SIN(2.*THETA)*.25)-GSUM2                    PGM30162
      GSUM1=GSUM1+G1                                                    PGM30163
      GSUM2=GSUM2+G2                                                    PGM30164
   18  DO 14 NSP=1,NSM                                                  PGM30165
      GBVS1(N,M,NSP,1)=G1*GS(N,NSP)                                     PGM30166
   14 GBVS1(N,M,NSP,2)=G2*GS(N,NSP)                                     PGM30167
      DO 124 NSP=1,NSM                                                  PGM30168
  124 WRITE(6,125) NSP,(GS(N,NSP),N=1,NBS)                              PGM30169
  125 FORMAT(' MODE',I2,(16F7.3))                                       PGM30170
      NCUT=IFIX(FLOAT(NTS)/2.)                                          PGM30171
      WRITE(6,126) NCUT,(GBVS1(NCUT,M,1,1),M=1,NBSC)                    PGM30172
  126 FORMAT(' N=',I2,'CIRC MODE 1,1',(12F7.5))                         PGM30173
C     CALCULATE TRAILER STRENGTH ON SAIL 1                              PGM30174
      NMIN=NTS-1                                                        PGM30175
      DO 19 NSP=1,NSM                                                   PGM30176
      DO 19 MCR=1,2                                                     PGM30177
      IVSS1(1,1,NSP,MCR)=GBVS1(1,1,NSP,MCR)                             PGM30178
      DO 20 M=2,NBSC                                                    PGM30179
      IVSS1(1,M,NSP,MCR)=GBVS1(1,M,NSP,MCR)+IVSS1(1,M-1,NSP,MCR)        PGM30180
```

```
 20    CONTINUE                                                          PGM30181
       DO 21 N=2,NMIN                                                    PGM30182
       TVSS1(N,1,NSP,MCR)=GBVS1(N,1,NSP,MCR)-GBVS1(N-1,1,NSP,MCR)        PGM30183
       DO 21 M=2,NBSC                                                    PGM30184
       TVSS1(N,M,NSP,MCR)=TVSS1(N,M-1,NSP,MCR)+GBVS1(N,M,NSP,MCR)-GBVS1(N PGM30185
      1-1,M,NSP,MCR)                                                     PGM30186
 21    CONTINUE                                                          PGM30187
       TVSS1(NTS,1,NSP,MCR)=-GBVS1(NBS,1,NSP,MCR)                        PGM30188
       DO 19 M=2,NBSC                                                    PGM30189
 19    TVSS1(NTS,M,NSP,MCR)=TVSS1(NTS,M-1,NSP,MCR)-GBVS1(NBS,M,NSP,MCR)  PGM30190
       WRITE(6,128) TVSS1(1,1,1,1),TVSS1(1,NBSC,1,1),TVSS1(NTS,1,1,1),T  PGM30191
      1VSS1(NTS,NBSC,1,1)                                                PGM30192
 128   FORMAT(' TRAILERS FOR UNIT MODE(1,1) AT BASE(LE,TE) AND TIP(LE,TE) PGM30193
      1',4F10.4)                                                         PGM30194
C      VELOCITY ON S1 DUE TO S1 BOUND VORTEX SYSTEM                      PGM30195
       DO 22 NCP=1,NCPS                                                  PGM30196
       DO 22 MCP=1,NCPC                                                  PGM30197
       DO 22 NSP=1,NSM                                                   PGM30198
       DO 22 MCR=1,2                                                     PGM30199
       VZB(NCP,MCP,NSP,MCR)=0.0                                          PGM30200
       VZT(NCP,MCP,NSP,MCR)=0.0                                          PGM30201
       VZW(NCP,MCP,NSP,MCR)=0.0                                          PGM30202
       VZBR1(NCP,MCP,NSP,MCR)=0.0                                        PGM30203
       VZTR1(NCP,MCP,NSP,MCR)=0.0                                        PGM30204
 22    VZWR1(NCP,MCP,NSP,MCR)=0.0                                        PGM30205
       DO 23 NCP=1,NCPS                                                  PGM30206
       DO 23 MCP=1,NCPC                                                  PGM30207
       DO 23 N=1,NBS                                                     PGM30208
       DO 23 M=1,NBSC                                                    PGM30209
       SX=XBVS1(M)-XCPS1(NCP,MCP)                                        PGM30210
       SY=YBS1(N)-YCPS1(NCP)                                             PGM30211
       S32=SQRT(SX*SX+SY*SY)**3                                          PGM30212
       VZ=QPIINV/S32*(DBT1*SX)                                           PGM30213
       DO 23 NSP=1,NSM                                                   PGM30214
       DO 23 MCR=1,2                                                     PGM30215
 23    VZB(NCP,MCP,NSP,MCR)=VZB(NCP,MCP,NSP,MCR)+VZ*GBVS1(N,M,NSP,MCR)   PGM30216
```

```
      NMID=IFIX(FLOAT(NCPS)/2.)                                          PGM30217
      WRITE(6,129)XCPS1(NMID,NCPC),YCPS1(NMID),VZB(NMID,NCPC,1,1)        PGM30218
  129 FORMAT(' VEL AT CP X=',F7.3,' Y=',F7.3,F20.4 ,' DUE TO MODE 1,1 BO PGM30219
     1UND VORTICES')                                                     PGM30220
C     VELOCITY ON SAIL 1 DUE TO SAIL 1 TRAILERS                          PGM30221
      DO 24 NCP=1,NCPS                                                   PGM30222
      DO 24 MCP=1,NCPC                                                   PGM30223
      DO 24 N=1,NTS                                                      PGM30224
      SY=YTRS1(N)-YCPS1(NCP)                                             PGM30225
      DO 24 M=1,NMS                                                      PGM30226
      SX=0.5*(XBVS1(M)+XBVS1(M+1))-XCPS1(NCP,MCP)                        PGM30227
      S32=SQRT(SX*SX+SY*SY)**3                                           PGM30228
      VZ=QPIINV/S32*SY*(XBVS1(M+1)-XBVS1(M))                             PGM30229
      DO 24 NSP=1,NSM                                                    PGM30230
      DO 24 MCR=1,2                                                      PGM30231
   24 VZT(NCP,MCP,NSP,MCR)=VZT(NCP,MCP,NSP,MCR)+VZ*TVSS1(N,M,NSP,MCR)    PGM30232
C     VELOCITY ON SAIL 1 DUE TO SAIL 1 WAKE                              PGM30233
      SIA=SIN(ALPHA)                                                     PGM30234
      CSA=COS(ALPHA)                                                     PGM30235
      XB=XBVS1(NBSC)                                                     PGM30236
      DO 25 NCP=1,NCPS                                                   PGM30237
      DO 25 MCP=1,NCPC                                                   PGM30238
      DO 25 N=1,NTS                                                      PGM30239
      RS=((XCPS1(NCP,MCP)-XB)*SIA)**2+(YTRS1(N)-YCPS1(NCP))**2           PGM30240
      R=SQRT(RS)                                                         PGM30241
      QS=(XCPS1(NCP,MCP)-XB)**2+(YTRS1(N)-YCPS1(NCP))**2                 PGM30242
      Q=SQRT(QS)                                                         PGM30243
      QV=QPIINV/R*((XB-XCPS1(NCP,MCP))/Q*CSA+1.0)                        PGM30244
      IF(YTRS1(N).GT.YCPS1(NCP)) QV=-QV                                  PGM30245
      VZ=QV*CSA                                                          PGM30246
      DO 25 NSP=1,NSM                                                    PGM30247
      DO 25 MCR=1,2                                                      PGM30248
   25 VZW(NCP,MCP,NSP,MCR)=VZW(NCP,MCP,NSP,MCR)+VZ*TVSS1(N,NBSC,NSP,MCR) PGM30249
      WRITE(6,130)VZT(NMID,NCPC,1,1),VZW(NMID,NCPC,1,1)                  PGM30250
  130 FORMAT(' VEL AT SAME POINT DUE TO TRAILERS ON BLADE=',F15.4,' AND  PGM30251
     1WAKE=',F15.4,' DUE TO UNIT MODE 1,1')                              PGM30252
```

```
C       VELOCITY ON SAIL 1 DUE TO HULL                                          PGM30253
        DO 26 NCP=1,NCPS                                                        PGM30254
        DO 26 MCP=1,NCPC                                                        PGM30255
        R=FILLI(XCPS1(NCP,MCP),XIN,RIN,NSTA)                                    PGM30256
 26     WDSS1(NCP,MCP)=WFS*R*R/(YCPS1(NCP)**2)                                  PGM30257
        WRITE(6,131)WDSS1(NMID,NCPC)                                            PGM30258
 131    FORMAT(' VELOCITY AT SAME POINT DUE TO HULL=',F15.5)                    PGM30259
C       GET RFS FOR EACH CP                                                     PGM30260
        I=1                                                                     PGM30261
        DO 27 NCP=1,NCPS                                                        PGM30262
        DO 27 MCP=1,NCPC                                                        PGM30263
        RHSS1(I)=-WFS-WDSS1(NCP,MCP)                                            PGM30264
        WRITE(6,601) I,RHSS1(I)                                                 PGM30265
 601    FORMAT(I4,F40.10)                                                       PGM30266
 27     I=I+1                                                                   PGM30267
        IMAX=NCPS*NCPC                                                          PGM30268
C       GET LEFT HAND SIDE FOR EACH CP                                          PGM30269
        I=1                                                                     PGM30270
        DO 28 NCP=1,NCPS                                                        PGM30271
        DO 28 MCP=1,NCPC                                                        PGM30272
        J=1                                                                     PGM30273
        DO 89 MCR=1,2                                                           PGM30274
        DO 89 NSP=1,NSM                                                         PGM30275
        S1LHS(I,J)=VZW(NCP,MCP,NSP,MCR)+VZT(NCP,MCP,NSP,MCR)+VZB(NCP,MCP,N      PGM30276
      1SP,MCR)                                                                  PGM30277
        WRITE(6,602) I,J,S1LHS(I,J)                                             PGM30278
 602    FORMAT(2I4,F40.10)                                                      PGM30279
 89     J=J+1                                                                   PGM30280
 28     I=I+1                                                                   PGM30281
        DO 900 K=1,IMAX                                                         PGM30282
 900    S1LHS(K,5)=RHSS1(K)                                                     PGM30283
        EPS=.0001                                                               PGM30284
        CALL GLSQ(S1LHS,CMSS1,ISP,IMAX,4,BUG,EPS,EPS)                           PGM30285
C                                                                               PGM30286
        WRITE(6,132) (CMSS1(J),J=1,4)                                           PGM30287
 132    FORMAT(' MODE STRENGTHS ON SAIL=',6F10.5)                               PGM30288
```

```
C       VELOCITY AT R1 DUE TO S1 WAKE                                    PGM30289
        DO 29 MS=1,NSTA                                                  PGM30290
        MS=MS                                                            PGM30291
        IF(XIN(MS).LT.XTEB(1)) GO TO 30                                  PGM30292
   29   CONTINUE                                                         PGM30293
   30   NSTS=MS                                                          PGM30294
        DO 31 MS=NSTS,NSTA                                               PGM30295
        MS=MS                                                            PGM30296
        IF(XIN(MS).LT.XLEBR(1)) GO TO 32                                 PGM30297
   31   CONTINUE                                                         PGM30298
   32   NSTE=MS                                                          PGM30299
        DO 33 N=1,NTS                                                    PGM30300
   33   YWKS1(N,NSTS)=YTRS1(N)                                           PGM30301
        NSTEM=NSTE-1                                                     PGM30302
        DO 34 MS=NSTS,NSTEM                                              PGM30303
        CONST=-    .5*PIINV*(SINV(MS)-SINV(MS+1))                        PGM30304
        DO 34 N=1,NTS                                                    PGM30305
        YWKS1(N,MS+1)=YWKS1(N,MS)+CONST/YWKS1(N,MS)                      PGM30306
        IF(YWKS1(N,MS+1).LT.RIN(MS+1))YWKS1(N,MS+1)=RIN(MS+1)*YTRS1(N)/RHS PGM30307
   34   CONTINUE                                                         PGM30308
        WRITE(6,133)(YWKS1(NOUT,MS),MS=NSTS,NSTEM)                       PGM30309
  133   FORMAT(' TYPICAL TRAILER CONTRACTION TRAJECTORY',12F7.3)         PGM30310
        ZWKS1=ALPHA*(XTEB(1)-XLEBR(1))                                   PGM30311
        DO 35 N=1,NTS                                                    PGM30312
        GWKS1(N)=0.0                                                     PGM30313
        J=1                                                              PGM30314
        DO 35 MCR=1,2                                                    PGM30315
        DO 35 NSP=1,NSM                                                  PGM30316
        GWKS1(N)=GWKS1(N)+CMSS1(J)*1VSS1(N,NBSC,NSP,MCR)                 PGM30317
   35   J=J+1                                                            PGM30318
        WRITE(6,134)(GWKS1(N),N=1,NTS)                                   PGM30319
  134   FORMAT(' REAL WAKE TRAILER STRENGTHS FROM SAIL 1',/,(1X,16F7.3)) PGM30320
        DO 36 N=1,NBS                                                    PGM30321
        YBOMR(N)=.5*(YWKS1(N,NSTE)+YWKS1(N+1,NSTE))                      PGM30322
        WWS1R1(N)=0.0                                                    PGM30323
        DO 36 NV=1,NTS                                                   PGM30324
```

```
      R=SQRT(ZWKS1**2+(YDUMR(N)-YWKS1(NV,NSTE))**2)                    PGM30325
      VEL=GWKS1(NV)*.5*PIINV/R                                         PGM30326
   30 WWS1R1(N)=WWS1R1(N)+VEL*(YDUMR(N)-YWKS1(NV,NSTE))/R              PGM30327
      WRITE(6,135)(WWS1R1(N),N=1,NBS)                                  PGM30328
  135 FORMAT(' RAW VELOCITY ON RUDDER DUE TO SAIL',/,(1X,16F7.3))      PGM30329
C     FIT WITH POLYNOMIAL                                              PGM30330
      RMIN=FILL1(XLEBR(1),XIN,RIN,NSTA)                                PGM30331
      DO 628 N=1,NBS                                                   PGM30332
      NO=N                                                             PGM30333
      IF(YDUMR(N) .GT. RMIN) GO TO 629                                 PGM30334
  628 CONTINUE                                                         PGM30335
  629 NRN=NBS-NO+1                                                     PGM30336
      DO 37 N=1,NRN                                                    PGM30337
      TEN(N,1)=1.0                                                     PGM30338
      TEN(N,2)=YDUMR(N+NO-1)                                           PGM30339
      TEN(N,4)=WWS1R1(N+NO-1)                                          PGM30340
   37 TEN(N,3)=TEN(N,2)**2                                             PGM30341
      L2=1                                                             PGM30342
      EPS=.0001                                                        PGM30343
      CALL GLSQ(TEN,AR,ISP,NRN,3,BUG,.0001,.0001)                      PGM30344
      WRITE(6,136)(AR(J),J=1,3)                                        PGM30345
  136 FORMAT(' POLYNOMIAL COEFFICIENTS FOR RUDDER VEL DUE TO SAIL',3F10.PGM30346
     1 5)                                                              PGM30347
C     GRID SETUP ON R1                                                 PGM30348
      DBTR1=SPNR/FLOAT(NBS)                                            PGM30349
      YTRR1(1)=RWIR                                                    PGM30350
      DO 38 N=2,NTS                                                    PGM30351
   38 YTRR1(N)=YTRR1(N-1)+DBTR1                                        PGM30352
      WRITE(6,140)(YTRR1(N),N=1,NTS)                                   PGM30353
  140 FORMAT(' TRAILER RADII ON R1',/,(16F7.3))                        PGM30354
      YBR1(1)=YTRR1(1)+0.5*DBTR1                                       PGM30355
      DO 39 N=2,NBS                                                    PGM30356
   39 YBR1(N)=YBR1(N-1)+DBTR1                                          PGM30357
      XBVR1(1)=XLEBR(1)                                                PGM30358
      DELCR1=(XLEBR(1)-XTEBR(1))/FLOAT(NHS)                            PGM30359
      DO 40 M=2,NBSC                                                   PGM30360
```

```
40    XBVR1(M)=XBVR1(M-1)-DELCR1                                          PGM30361
      WRITE(6,141)(XBVR1(M),M=1,NBSC)                                     PGM30362
141   FORMAT(' X LOCATION OF BOUND VORTEX LINES ON R1',/,(10F7.2))        PGM30363
      DELCPR=(RROD(1)-RHR)/FLOAT(NCPS+1)                                  PGM30364
      YCPR1(1)=RHR+DELCPR                                                 PGM30365
      DO 41 N=1,NBS                                                       PGM30366
      N=N                                                                 PGM30367
      IF(YCPR1(1).GT.YBR1(N).AND.YCPR1(1).LE.YBR1(N+1)) GO TO 42          PGM30368
41    CONTINUE                                                            PGM30369
42    YCPR1(1)=YBR1(N)                                                    PGM30370
      NRLFT=NBS-N                                                         PGM30371
      IHUL=FLOAT(NRLFT)/FLOAT(NCPS)                                       PGM30372
      DO 43 N=2,NCPS                                                      PGM30373
43    YCPR1(N)=YCPR1(N-1)+IHUL*DBTR1                                      PGM30374
      RFR=FILLI(XLEBR(1),XIN,RIN,NSTA)                                    PGM30375
      RTR=FILLI(XTEBR(1),XIN,RIN,NSTA)                                    PGM30376
      SLEBR=(XLEBR(1)-XLETR(1))/(RROD(1)-RFR)                             PGM30377
      SLTER=(XTEBR(1)-XTETR(1))/(RROD(1)-RTR)                             PGM30378
      DO 44 N=1,NCPS                                                      PGM30379
      Y=YCPR1(N)                                                          PGM30380
      XLER=XLEBR(1)-SLEBR*(Y-RFR)                                         PGM30381
      XTER=XTEBR(1)-SLTER*(Y-RTR)                                         PGM30382
      CR=XLER-XTER                                                        PGM30383
      DCXR=CR/FLOAT(NCPC+1)                                               PGM30384
      XCPR1(N,1)=XTER+DCXR                                                PGM30385
      DO 45 MC=1,NRS                                                      PGM30386
      MC=MC                                                               PGM30387
      IF(XCPR1(N,1).LT.XBVR1(MC).AND.XCPR1(N,1).GE.XBVR1(MC+1))GO TO 46   PGM30388
45    CONTINUE                                                            PGM30389
46    XCPR1(N,1)=(XBVR1(MC)+XBVR1(MC+1))*0.5                              PGM30390
      DO 44 M=2,NCPC                                                      PGM30391
      XCPR1(N,M)=XCPR1(N,M-1)+DCXR                                        PGM30392
      DO 47 MC=1,NRS                                                      PGM30393
      MC=MC                                                               PGM30394
      IF(XCPR1(N,M).LT.XBVR1(MC).AND.XCPR1(N,M).GE.XBVR1(MC+1))GO TO 44   PGM30395
47    CONTINUE                                                            PGM30396
```

```
 44   XCPR1(N,M)=0.5*(XBVR1(MC)+XBVR1(MC+1))                          PGM30397
      DO 143 N=1,NCPS                                                 PGM30398
 143  WRITE(6,142)(YCPR1(N),(XCPR1(N,M),M=1,NCPC))                    PGM30399
 142  FORMAT(' YCP=',F10.3,' XCP=',4F7.2)                             PGM30400
C     BOUND VORTEX STRENGTHS ON R1 FOR UNIT MODES                     PGM30401
      DO 46 N=1,NBS                                                   PGM30402
      XLER=XLEBR(1)-SLLER*(YBR1(N)-RFR)                               PGM30403
      IF(XLER.GT.XLEBR(1)) XLER=XLEBR(1)                              PGM30404
      XTER=XTEBR(1)-SLTER*(YBR1(N)-RTR)                               PGM30405
      IF(XTER.LT.XTEBR(1)) XTER=XTEBR(1)                              PGM30406
      CHORR1(N)=XLER-XTER                                             PGM30407
      Q=(YBR1(N)-RHR)/(RROOT(1)-RHR)                                  PGM30408
      SQQ=SQRT(1.0-Q*Q)                                               PGM30409
      DO 47 NSP=1,NSM                                                 PGM30410
 47   BR1(N,NSP)=SQQ*Q**(2*NSP-2)                                     PGM30411
      G1=0.0                                                          PGM30412
      G2=0.0                                                          PGM30413
      GSUM1=0.0                                                       PGM30414
      GSUM2=0.0                                                       PGM30415
      DO 48 M=1,NBSC                                                  PGM30416
      XD=XLER+.5*DELCR1                                               PGM30417
      IF(XBVR1(M) .GT. XC ) GO TO 50                                  PGM30418
      XT=XTER-.5*DELCR1                                               PGM30419
      IF(XBVR1(M) .LT. XT) GO TO 50                                   PGM30420
      XT=XTER+.5*DELCR1                                               PGM30421
      IF(XBVR1(M) .LT. XT) GO TO 953                                  PGM30422
      GO TO 954                                                       PGM30423
 953  THETA=PI                                                        PGM30424
      GO TO 956                                                       PGM30425
 954  CONTINUE                                                        PGM30426
      GO TO 51                                                        PGM30427
 50   G1=0.0                                                          PGM30428
      G2=0.0                                                          PGM30429
      GO TO 52                                                        PGM30430
 51   COSX=      (1.0-2.0*(XLER-XPVR1(M)+.5*DELCR1)/CHORR1(N))        PGM30431
      THETA=ARCOS(COSX)                                               PGM30432
```

```
 950  G1=(THETA+SIN(THETA))*PIINV -GSUM1                                PGM30433
      G2=2.0*PIINV*(THETA*0.5-SIN(2.0*THETA)*0.25)  -GSUM2              PGM30434
      GSUM1=GSUM1+G1                                                    PGM30435
      GSUM2=GSUM2+G2                                                    PGM30436
 52   DO 46 NSP=1,NSM                                                  PGM30437
      GBVR1(N,M,NSP,1)=G1*GR(N,NSP)                                     PGM30438
 46   GBVR1(N,M,NSP,2)=G2*GR(N,NSP)                                     PGM30439
      DO 144 NSP=1,NSM                                                  PGM30440
 144  WRITE(6,145) NSP,(GR(N,NSP),N=1,NBS)                              PGM30441
 145  FORMAT(' MODE',I2,(16F7.3))                                       PGM30442
      WRITE(6,146) NOUT,(GBVR1(NOUT,M,1,1),M=1,NBSC)                    PGM30443
 146  FORMAT(' N=',I2,' CIRC MODE 1,1',(12F7.5))                        PGM30444
      DO 53 NSP=1,NSM                                                   PGM30445
      DO 53 MCR=1,2                                                     PGM30446
      TVSR1(1,1,NSP,MCR)=GBVR1(1,1,NSP,MCR)                             PGM30447
      DO 54 M=2,NBSC                                                    PGM30448
 54   TVSR1(1,M,NSP,MCR)=TVSR1(1,M-1,NSP,MCR)+GBVR1(1,M,NSP,MCR)       PGM30449
      DO 55 N=2,NMIN                                                    PGM30450
      TVSR1(N,1,NSP,MCR)=GBVR1(N,1,NSP,MCR)-GBVR1(N-1,1,NSP,MCR)        PGM30451
      DO 55 M=2,NBSC                                                    PGM30452
 55   TVSR1(N,M,NSP,MCR)=TVSR1(N,M-1,NSP,MCR)+GBVR1(N,M,NSP,MCR)-GBVR1(N PGM30453
     1-1,M,NSP,MCR)                                                     PGM30454
      TVSR1(NTS,1,NSP,MCR)=-GBVR1(NBS,1,NSP,MCR)                        PGM30455
      DO 53 M=2,NBSC                                                    PGM30456
 53   TVSR1(NTS,M,NSP,MCR)=TVSR1(NTS,M-1,NSP,MCR)-GBVR1(NBS,M,NSP,MCR)  PGM30457
      WRITE(6,148) TVSR1(1,1,1,1),TVSR1(1,NBSC,1,1),TVSR1(NTS,1,1,1),TVS PGM30458
     1R1(NTS,NBSC,1,1)                                                  PGM30459
 148  FORMAT(' TRAILERS FOR UNIT MODE(1,1) AT BASE(LE,TE) AND TIP(LE,TL) PGM30460
     1 ',4F10.4)                                                        PGM30461
C     VELOCITIES ON R1                                                  PGM30462
      DO 56 NCP=1,NCPS                                                  PGM30463
      DO 56 MCP=1,NCPC                                                  PGM30464
      DO 56 N=1,NBS                                                     PGM30465
      DO 56 M=1,NBSC                                                    PGM30466
      SX=XBVR1(M)-XCPR1(NCP,MCP)                                        PGM30467
      SY=YBR1(N)-YCPR1(NCP)                                             PGM30468
```

```
      S32=SQRT(SX*SX+SY*SY)**3                                          PGM30469
      VZ=QPIINV/S32*(DBTR1*SX)                                          PGM30470
      DO 56 NSP=1,NSM                                                   PGM30471
      DO 56 MCR=1,2                                                     PGM30472
56    VZBR1(NCP,MCP,NSP,MCR)=VZBR1(NCP,MCP,NSP,MCR)+VZ*GBVR1(N,M,NSP,MCR PGM30473
     1)                                                                 PGM30474
      WRITE(6,149)XCPR1(NMID,NCPC),YCPR1(NMID),VZBR1(NMID,NCPC,1,1)     PGM30475
149   FORMAT(' VEL AT CP X=',F7.2,' Y=',F7.3,F20.4,' DUE TO MODE 1,1 BOU PGM30476
     1ND VORTICES')                                                     PGM30477
      DO 57 NCP=1,NCPS                                                  PGM30478
      DO 57 MCP=1,NCPC                                                  PGM30479
      DO 57 N=1,NTS                                                     PGM30480
      SY=YTKR1(N)-YCPR1(NCP)                                            PGM30481
      DO 57 M=1,NHS                                                     PGM30482
      SX=0.5*(XBVR1(M)+XBVR1(M+1))-XCPR1(NCP,MCP)                       PGM30483
      S32=SQRT(SX*SX+SY*SY)**3                                          PGM30484
      VZ=QPIINV/S32*SY*(XBVR1(M+1)-XBVR1(M))                            PGM30485
      DO 57 NSP=1,NSM                                                   PGM30486
      DO 57 MCR=1,2                                                     PGM30487
57    VZTR1(NCP,MCP,NSP,MCR)=VZTR1(NCP,MCP,NSP,MCR)+VZ*TVSR1(N,M,NSP,MCR PGM30488
     1)                                                                 PGM30489
      SIAR=SIN(ALR)                                                     PGM30490
      CSAR=COS(ALR)                                                     PGM30491
      XBR=XBVR1(NBSC)                                                   PGM30492
      DO 56 NCP=1,NCPS                                                  PGM30493
      DO 56 MCP=1,NCPC                                                  PGM30494
      DO 56 N=1,NTS                                                     PGM30495
      RSR=((XCPR1(NCP,MCP)-XBR)*SIAR)**2+(YTKR1(N)-YCPR1(NCP))**2       PGM30496
      RR=SQRT(RSR)                                                      PGM30497
      QSR=(XCPR1(NCP,MCP)-XBR)**2+(YTKR1(N)-YCPR1(NCP))**2              PGM30498
      QR=SQRT(QSR)                                                      PGM30499
      QVR=QPIINV/RR*((XBR-XCPR1(NCP,MCP))/QR*CSAR+1.0)                  PGM30500
      IF(YTKR1(N).GT.YCPR1(NCP))QVR=-QVR                                PGM30501
      VZ=QVR*CSAR                                                       PGM30502
      DO 56 NSP=1,NSM                                                   PGM30503
      DO 58 MCR=1,2                                                     PGM30504
```

```
 50   VZWR1(NCP,MCP,NSP,MCR)=VZWR1(NCP,MCP,NSP,MCR)+VZ*TVSR1(N,NDSC,NSP,   PGM00503
     1MCR)                                                                 PGM00506
      WRITE(6,150)VZTR1(NMID,NCPC,1,1),VZWR1(NMID,NCPC,1,1)                PGM00507
 150  FORMAT(' VEL AT SAME POINT DUE TO TRAILERS ON BLADE=',F15.4,' AND    PGM00508
     1WAKE=',F15.4,' DUE TO UNIT MODE 1,1')                                PGM00509
C     VELOCITY ON R1 DUE TO HULL                                           PGM00510
      DO 59 NCP=1,NCPS                                                     PGM00511
      DO 59 MCP=1,NCPC                                                     PGM00512
      R=FILLI(XCPR1(NCP,MCP),XIN,RIN,NSTA)                                 PGM00513
 59   WDSR1(NCP,MCP)=WFS*R**2/(YCPR1(NCP)**2)                              PGM00514
      WRITE(6,151)WDSR1(NMID,NCPC)                                         PGM00515
 151  FORMAT(' VELOCITY AT SAME POINT DUE TO HULL=',F15.5)                 PGM00516
C     VELOCITY AT R1 DUE TO S1 AT CONTROL POINTS                           PGM00517
      DO 60 NCP=1,NCPS                                                     PGM00518
      R=YCPR1(NCP)                                                         PGM00519
      D=AR(1)+AR(2)*R+AR(3)*R*R                                            PGM00520
      DO 60 MCP=1,NCPC                                                     PGM00521
 60   WS1R1(NCP,MCP)=D                                                     PGM00522
C     CALCULATE LHS FOR RUDDER                                             PGM00523
      I=1                                                                  PGM00524
      DO 61 NCP=1,NCPS                                                     PGM00525
      DO 61 MCP=1,NCPC                                                     PGM00526
      J=1                                                                  PGM00527
      DO 62 MCR=1,2                                                        PGM00528
      DO 62 NSP=1,NSM                                                      PGM00529
      R1LHS(I,J)=VZWR1(NCP,MCP,NSP,MCR)+VZTR1(NCP,MCP,NSP,MCR)+VZBR1(NCP   PGM00530
     1,MCP,NSP,MCR)                                                        PGM00531
      WRITE(6,602) I,J,R1LHS(I,J)                                          PGM00532
 62   J=J+1                                                                PGM00533
 61   I=I+1                                                                PGM00534
C     CALCULATE RHS FOR RUDDER                                             PGM00535
      I=1                                                                  PGM00536
      DO 63 NCP=1,NCPS                                                     PGM00537
      DO 63 MCP=1,NCPC                                                     PGM00538
      R1RHS(I)=DELTA(1)*UO-WFS-WS1R1(NCP,MCP)-WDSR1(NCP,MCP)               PGM00539
      WRITE(6,602) I,R1RHS(I)                                              PGM00540
```

```
 63   I=I+1                                                              PGM30541
      EPS=.0001                                                          PGM30542
      DO 901 K=1,IMAX                                                    PGM30543
 901  R1LHS(K,J)=R1RHS(K)                                                PGM30544
      CALL GLSQ(R1LHS,CMSR1,ISP,IMAX,4,BUG,EFS,EPS)                      PGM30545
      WRITE(6,152)(CMSR1(J),J=1,4)                                       PGM30546
 152  FORMAT(' MODE STRENGTHS ON R1  =',6F10.5)                          PGM30547
C     GET TOTAL WAKE TRAILER STRENGTHS                                   PGM30548
      DO 66 N=1,NTS                                                      PGM30549
      GTR(N)=0.0                                                         PGM30550
      GTF(N)=0.0                                                         PGM30551
      J=1                                                                PGM30552
      DO 66 MCR=1,2                                                      PGM30553
      DO 66 NSP=1,NSM                                                    PGM30554
      GTR(N)=GTR(N)+TVSR1(N,NBSC,NSP,MCR)*CMSR1(J)                       PGM30555
      GTF(N)=GTF(N)+TVSS1(N,NBSC,NSP,MCR)*CMSS1(J)                       PGM30556
 66   J=J+1                                                              PGM30557
C     VELOCITY ON CL DUE TO FIN WAKE                                     PGM30558
      DO 64 N=1,NTS                                                      PGM30559
      N=N                                                                PGM30560
      IF(YTRS1(N).GT.RHS)GO TO 64                                        PGM30561
 64   CONTINUE                                                           PGM30562
 64   NOUT=N                                                             PGM30563
      NIN=N-1                                                            PGM30564
      DO 65 N=NOUT,NTS                                                   PGM30565
      Y=YTRS1(N)                                                         PGM30566
      YSQ=Y*Y                                                            PGM30567
      DO 65 M=1,NSTA                                                     PGM30568
      CPI=XIN(M)-XB                                                      PGM30569
      CPI=CPI       /SQRT(YSQ+(XIN(M)-XB)**2)                            PGM30570
 65   WTF(N,M)=(CPI-1.0)*CPIINV/Y*GTF(N)                                 PGM30571
C     VELOCITY ON CL DUE TO RUDDER WAKE                                  PGM30572
      DO 67 N=1,NTS                                                      PGM30573
      N=N                                                                PGM30574
      IF(YTRR1(N).GT.RHS) GO TO 68                                       PGM30575
 67   CONTINUE                                                           PGM30576
```

```
 66   NOUTR=N                                                          PGM30577
      NINR=N-1                                                         PGM30578
      DO 69 N=NOUTR,NTS                                                PGM30579
      Y=YTRKI(N)                                                       PGM30580
      YSQ=Y*Y                                                          PGM30581
      DO 69 M=1,NSTA                                                   PGM30582
      CPI=XIN(M)-XBR                                                   PGM30583
      CPI=CPI       /SQRT(YSQ+(XIN(M)-XBR)**2)                         PGM30584
 69   WTR(N,M)=(CPI-1.0)*CPIINV/Y*GTR(N)                               PGM30585
C     TOTAL VELOCITY AT STATION M ON CL                                PGM30586
      DO 70 M=1,NSTA                                                   PGM30587
      W(M)=WFS                                                         PGM30588
      DO 71 N=NOUT,NTS                                                 PGM30589
 71   W(M)=W(M)+WTF(N,M)                                               PGM30590
      DO 70 N=NOUTR,NTS                                                PGM30591
 70   W(M)=W(M)+WTR(N,M)                                               PGM30592
      WRITE(6,193)(W(M),M=1,NSTA)                                      PGM30593
 193  FORMAT(' VELOCITY ON CL DUE TO FIN,RUDDER,FREE STR',/,(12F7.3))  PGM30594
C     GET SLOPE AT INPUT POINTS                                        PGM30595
      DO 72 M=1,NSTA                                                   PGM30596
 72   SPRM(M)=SPIL(XIN(M),XIN,SINV,NSTA)                               PGM30597
      WRITE(6,194)(SPRM(M),M=1,NSTA)                                   PGM30598
 194  FORMAT(' SLOPE AT INPUT POINTS',/,(12F7.2))                      PGM30599
C     FORCES + MOMENTS DUE TO CIRC AROUND HULL DUE TO FIN              PGM30600
      NSDUM=NSTA-1                                                     PGM30601
      NTSH=NOUT-1                                                      PGM30602
      GAMMA=0.0                                                        PGM30603
      DO 81 N=1,NTSH                                                   PGM30604
 81   GAMMA=GAMMA+GTF(N)                                               PGM30605
      SIY=0.0                                                          PGM30606
      SIN=0.0                                                          PGM30607
 83   DO 82 M=1,NSDUM                                                  PGM30608
      IF(XIN(M).GE.XTEB(1)) GO TO 82                                   PGM30609
      SIY=SIY+RHO*W(M)*GAMMA*DELX                                      PGM30610
      SIN=SIN+RHO*W(M)*GAMMA*DELX*XIN(M)                               PGM30611
 82   CONTINUE                                                         PGM30612
```

```
      SIY=SIY+0.5*RHO*W(NSTA)*GAMMA*DELX                                PGM30613
      SIM=SIM+0.5*RHO*W(NSTA)*GAMMA*DELX*XIN(NSTA)                      PGM30614
C     GET FORCES + MOMENTS DUE TO SOURCES ON CL                         PGM30615
      SOURZ=0.5*DELX*W(1)*RHO*UO*SPRM(1)                                PGM30616
      SOURM=-SOURZ*XIN(1)                                               PGM30617
      SOURZ=SOURZ+0.5*DELX*W(NSTA)*RHO*UO*SPRM(NSTA)*2                  PGM30618
      SOURM=SOURM-0.5*DELX*W(NSTA)*RHO*UO*SPRM(NSTA)*XIN(NSTA)*2        PGM30619
      LENGTH=XIN(1)-XIN(NSTA)                                           PGM30620
      DO 75 M=2,NSOUM                                                   PGM30621
      IF(XIN(M).GE.0.0)    FAC=1.0                                      PGM30622
      IF(XIN(M).LT.0.0)    FAC=1.0-2.*(XIN(M)/LENGTH)                   PGM30623
      SOURZ=SOURZ+DELX*W(M)*RHO*UO*SPRM(M)*FAC                          PGM30624
 75   SOURM=SOURM-DELX*W(M)*RHO*UO*SPRM(M)*XIN(M)*FAC                   PGM30625
C     MOMENT DUE TO DOUBLETS                                            PGM30626
      DOUM=-DELX*W(1)*RHO*UO*SINV(1)                                    PGM30627
      DOUM=DOUM-DELX*W(NSTA)*RHO*UO*SINV(NSTA)*.5                       PGM30628
      DO 74 M=2,NSOUM                                                   PGM30629
      IF(XIN(M).GE.0.0)    FAC=1.0                                      PGM30630
      IF(XIN(M).LT.0.0)    FAC=1.0+2.*(XIN(M)/LENGTH)                   PGM30631
 74   DOUM=DOUM-2.0*DELX*W(M)*RHO*UO*SINV(M)*FAC                        PGM30632
C     FORCE AND MOMENT ON FIN                                           PGM30633
      SIZ=0.0                                                           PGM30634
      SIM=0.0                                                           PGM30635
      DO 77 N=1,NBS                                                     PGM30636
      SIZ=SIZ+RHO*UO*DBT1*(GS(N,1)*(CMSSI(1)+CMSSI(3))+GS(N,2)*(CMSSI(2)PGM30637
     1+CMSSI(4)))                                                       PGM30638
      XLE=XLEB(1)-SLEF*(YBSI(N)-RF)                                     PGM30639
      IF(XLE.GT.XLEB(1))    XLE=XLEB(1)                                 PGM30640
      XCP1=XLE-.25*CHOR(N)                                              PGM30641
      XCP2=XLE-.50*CHOR(N)                                              PGM30642
 77   SIM=SIM+RHO*UO*DBT1*(CMSSI(1)*XCP1*GS(N,1)+CMSSI(3)*XCP2*GS(N,1)+CPGM30643
     1MSSI(2)*XCP1*GS(N,2)+CMSSI(4)*XCP2*GS(N,2))                       PGM30644
C     FORCE AND MOMENT ON RUDDER                                        PGM30645
      RIZ=0.0                                                           PGM30646
      RIM=0.0                                                           PGM30647
      DO 50 N=1,NBS                                                     PGM30648
```

```
      R1Z=R1Z+RHO*UU*DBTR1*(GR(N,1)*(CMSR1(1)+CMSR1(3))+GR(N,2)*(CMSR1(2
     1)+CMSR1(4)))                                                      PGM30050
      XLE=XLEBR(1)-SLLER*(YBR1(N)-RFR)                                  PGM30051
      IF(XLE.GT.XLEB(1))   XLE=XLEB(1)                                  PGM30052
      XCP1=XLE-0.25*CHORR1(N)                                           PGM30053
      XCP2=XLE-0.5J*CHORR1(N)                                           PGM30054
 80   R1M=R1M+RHO*UU*DETR1*(CMSR1(1)*XCP1*GR(N,1)+CMSR1(3)*XCP2*GR(N,1)+PGM30055
     1CMSR1(2)*XCP1*GR(N,2)+CMSR1(4)*XCP2*GR(N,2))                      PGM30056
C     TOTAL FORCE AND MOMENT                                            PGM30057
      R1Z=-R1Z                                                          PGM30058
      S1Z=-S1Z                                                          PGM30059
      FZDIR=R1Z+S1Z+SOURZ                                               PGM30060
      ZDIRM=R1M+S1M+SOURM+DOUM                                          PGM30061
      WRITE(6,106) NSTA,UU,WFS,RHO                                      PGM30062
 106  FORMAT('1 NO. OF STATIONS ',I4,' FREE STREAM FORWARD SPEED ',F8.3,PGM30063
     1' SWAY VELOCITY ',F8.3,' WATER DENSITY ',F8.4)                    PGM30064
      WRITE(6,250) (XIN(J),J=1,NSTA)                                    PGM30065
 250  FORMAT(' XIN ', (8F10.5))                                         PGM30066
      WRITE(6,251) (RIN(J),J=1,NSTA)                                    PGM30067
 251  FORMAT(' RIN ',(8F10.5))                                          PGM30068
      WRITE(6,252) ALPHA,ALR,DELTA(1)                                   PGM30069
 252  FORMAT(' WAKE AND RUDDER ANGLES ', 3F20.5)                        PGM30070
      WRITE(6,253) RSL(1),RRUD(1)                                       PGM30071
 253  FORMAT(' SAIL AND RUDDER TIP RADII ',2F20.5)                      PGM30072
      WRITE(6,107) R1Z,S1Z,SOURZ,FZDIR                                  PGM30073
 107  FORMAT(' RUDDER SIDE FORCE ',F10.3,' FIN SIDE FORCE ',F10.3,' SOUR PGM30074
     1CE SIDE FORCE ',F10.3,' TOTAL SIDE FORCE ',F10.3)                 PGM30075
      WRITE(6,108)R1M,S1M,SOURM,DOUM,ZDIRM                              PGM30076
 108  FORMAT(' R1    MOMENT',F11.4,' FIN MOMENT',F11.4,' SOURCE MOMENT',PGM30077
     1F11.4,' DOUBLET MOMENT',F11.4,' TOTAL MOMENT',F11.4)              PGM30078
      WRITE(6,109)S1Y,S1R                                               PGM30079
 109  FORMAT(' HEAVE FORCE ON HULL',F11.4,' PITCH MOMENT',F11.4)        PGM30080
      STOP                                                              PGM30081
      END                                                               PGM30082
```

```
      FUNCTION SPIL(X,XI,YI,NO)                                          PGM30001
C     THIS WORKS ONLY FOR DECENDING VALUES OF X WITH INDEX               PGM30002
      DIMENSION XI(2),YI(2)                                              PGM30003
      DYDX(X,X1,X2,X3,Y1,Y2,Y3)=Y1*(2.*X-(X2+X3))/((X1-X2)*(X1-X3))+Y2*( PGM30004
     12.*X-(X1+X3))/((X2-X1)*(X2-X3))+Y3*(2.*X-(X1+X2))/((X3-X1)*(X3-X2) PGM30005
     2)                                                                  PGM30006
      IF(X.GT.XI(3)) GO TO 1                                             PGM30007
      IF(X.LT.XI(NO-2)) GO TO 2                                          PGM30008
      GO TO 3                                                            PGM30009
1     Y=DYDX(X,XI(3),XI(2),XI(1),YI(3),YI(2),YI(1))                      PGM30010
      GO TO 99                                                           PGM30011
2     Y=DYDX(X,XI(NO),XI(NO-1),XI(NO-2),YI(NO),YI(NO-1),YI(NO-2))        PGM30012
      GO TO 99                                                           PGM30013
3     DO 4 I=3,NO                                                        PGM30014
      I=I                                                                PGM30015
      IF(X.LE.XI(I).AND.X.GT.XI(I+1))  GO TO 5                           PGM30016
4     CONTINUE                                                           PGM30017
5     Y=DYDX(X,XI(I+1),XI(I),XI(I-1),YI(I+1),YI(I),YI(I-1))              PGM30018
99    SPIL=Y                                                             PGM30019
      RETURN                                                             PGM30020
      END                                                                PGM30021
```

```
      FUNCTION FILLI(X,XI,YI,NC)                                        PGM30001
C     FITS ONLY FOR DECENDING VALUES OF X                               PGM30002
      DIMENSION XI(2),YI(2)                                             PGM30003
      A(X1,X2,X3,X,Y1,Y2,Y3)=Y1*(X-X2)*(X-X3)/((X1-X2)*(X1-X3))+Y2*(X-X1 PGM30004
     1)*(X-X3)/((X2-X1)*(X2-X3))+Y3*(X-X1)*(X-X2)/((X3-X1)*(X3-X2))     PGM30005
      IF(X-XI(1))2,3,1                                                  PGM30006
    3 Y=YI(1)                                                           PGM30007
      GO TO 99                                                          PGM30008
    1 Y=A(XI(3),XI(2),XI(1),X,YI(3),YI(2),YI(1))                        PGM30009
      GO TO 99                                                          PGM30010
    2 IF(X-XI(2))5,6,4                                                  PGM30011
    6 Y=YI(2)                                                           PGM30012
      GO TO 99                                                          PGM30013
    5 DO 7 I=3,NC                                                       PGM30014
      M=I                                                               PGM30015
      IF(X-XI(I))7,9,8                                                  PGM30016
    9 Y=YI(I)                                                           PGM30017
      GO TO 99                                                          PGM30018
    7 CONTINUE                                                          PGM30019
    8 Y=A(XI(M-2),XI(M-1),XI(M),X,YI(M-2),YI(M-1),YI(M))                PGM30020
   99 FILLI=Y                                                           PGM30021
      RETURN                                                            PGM30022
      END                                                               PGM30023
```

```
      SUBROUTINE GLSQ(A,X,IL,N,M,ALPHA,E1,E2)                          0454 PGM30001
C     GLSQ SUBROUTINE ********************************                0453 PGM30002
      DIMENSION A( 32, 21),X(1),IL(1)                                  0455 PGM30003
      MM=M+1                                                           0456 PGM30004
      LL=1                                                             0457 PGM30005
      DO 60 J=1,MM                                                     0458 PGM30006
 60   IL(J)=0                                                          0459 PGM30007
      I=1                                                              0460 PGM30008
      DO 3 K=1,MM                                                      0461 PGM30009
      II=I+1                                                           0462 PGM30010
      DO 4 J=II,N                                                      0463 PGM30011
      IF(ABS(A(J,K))-E1)4,4,6                                          0464 PGM30012
 6    T1=SQRT((A(J,K))**2+(A(I,K))**2)                                 0465 PGM30013
      S=A(J,K)/T1                                                      0466 PGM30014
      C=A(I,K)/T1                                                      0467 PGM30015
      DO 5 L=K,MM                                                      0468 PGM30016
      T2=C*A(I,L)+S*A(J,L)                                             0469 PGM30017
      A(J,L)=-S*A(I,L)+C*A(J,L)                                        0470 PGM30018
 5    A(I,L)=T2                                                        0471 PGM30019
      LL=LL+1                                                          0472 PGM30020
 4    CONTINUE                                                         0473 PGM30021
      IF(ABS(A(I,K))-E2)3,3,8                                          0474 PGM30022
 8    IL(K)=I                                                          0475 PGM30023
      I=I+1                                                            0476 PGM30024
 3    CONTINUE                                                         0477 PGM30025
      X(MM)=-1.0                                                       0478 PGM30026
      II=M                                                             0479 PGM30027
      DO 35 I=1,M                                                      0480 PGM30028
 35   X(I)=0.0                                                         0481 PGM30029
      DO 30 J=1,M                                                      0482 PGM30030
      IF(IL(II))30,30,31                                               0483 PGM30031
 31   S=0.0                                                            0484 PGM30032
      LL=II+1                                                          0485 PGM30033
      I=IL(II)                                                         0486 PGM30034
      DO 32 K=LL,MM                                                    0487 PGM30035
 32   S=S+A(I,K)*X(K)                                                  0488 PGM30036
```

```
      A(II)=-S/A(I,II)                                          0489 PGM30037
30    II=II-1                                                   0490 PGM30038
      IF(IL(MM))50,51,50                                        0491 PGM30039
51    ALPHA=0.0                                                 0492 PGM30040
      GO TO 52                                                  0493 PGM30041
50    I=IL(MM)                                                  0494 PGM30042
      ALPHA=A(I,MM)                                             0495 PGM30043
52    RETURN                                                    0496 PGM30044
      END                                                       0497 PGM30045
```

```
C     SAMPLE DATA DECK FOR NUMERICAL PREDICTION OF FORCES AND MOMENTS
  13      14.772     2.606      2.0
.833       .666       .500       .333       .166       .000      -.166      -.333
-.500      -.666      -.833     -1.000     -1.166
.000       .077       .110       .133       .143       .147       .143       .136
.124       .106       .086       .059       .023
.414       .115       .141      -.153      -.242
.172      -1.051     -1.051     -1.150     -1.150      0.0
.1746      .1746
   24   12    4     4
```

PGM30001
PGM30002
PGM30003
PGM30004
PGM30005
PGM30006
PGM30007
PGM30008
PGM30009
PGM30010
PGM30011
PGM30012
PGM30013

Sample Results

```
TRAILER RADII ON SAIL
 0.052  0.068  0.083  0.099  0.115  0.131  0.146  0.162  0.176  0.194  0.209  0.225  0.241  0.257  0.272  0.288
 0.304  0.320  0.335  0.351  0.367  0.383  0.398  0.414
X LOCATION OF BOUND VORTEX LINES ON SAIL
  0.14   0.11   0.07   0.04   0.00  -0.03  -0.07  -0.10  -0.14  -0.17  -0.21  -0.24
YCP=      0.186XCP= -0.155 -0.085 -0.016  0.054
YCP=      0.233XCP= -0.155 -0.085 -0.016  0.054
YCP=      0.280XCP= -0.123 -0.051  0.019  0.089
YCP=      0.327XCP= -0.120 -0.051  0.019  0.089
MODE 1  0.940  0.964  0.978  0.989  0.996  1.000  1.000  0.996  0.989  0.979  0.965  0.946  0.924  0.898  0.866  0.833
 0.787  0.737  0.673  0.608  0.522  0.411  0.241
MODE 2  0.100  0.085  0.042  0.022  0.006  0.001  0.001  0.006  0.021  0.041  0.067  0.099  0.135  0.174  0.216  0.259
 0.303  0.337  0.366  0.383  0.383  0.342  0.227
A=120IMC MODE 1.10.1.2273.2270.38.13276.0.09857.0.37612.0.06344.0.05171.0.041530.031950.021800.008650.0
TRAILERS FOR UNIT MODE(1,1) AT BASE(LE,TE) ARE TIP(LE,TE)    0.2548    0.9438    0.0     -0.2409
VEL AT CP X=  0.054 Y=  0.233                       0.6326 DUE TO MODE 1.1 BOUND VORTICES
VEL AT SAME POINT DUE TO TRAILERS ON BLADE=         1.0670 AND WAKE=         0.1165 DUE TO UNIT MODE 1.1
VELOCITY AT SAME POINT DUE TO HULL=       1.02842
  1                    -4.16160325
  2                    -4.21490360
  3                    -4.23745352
  4                    -4.22367469
  5                    -3.59496307
  6                    -3.62372020
  7                    -3.64307690
  8                    -3.63441544
  9                    -3.50299167
 10                    -3.31968403
 11                    -3.32174015
 12                    -3.30967143
 13                    -3.11042742
 14                    -3.12865162
 15                    -3.13015747
 16                    -3.12131802
  1   1                   2.76626535
  1   2                  -0.76061244
  1   3                   2.60401330
  1   4                  -0.65107627
  2   1                   2.59244023
  2   2                  -0.65341637
  2   3                   1.7402214
  2   4                  -0.54470137
  3   1                   2.55104207
  3   2                  -0.50726533
  3   3                   0.61420461
  3   4                  -0.36530263
  4   1                   2.11530081
  4   2                  -0.42931678
  4   3                  -0.59783752
  4   4                  -0.20464323
  5   1                   2.66060925
  5   2                  -0.31105327
  5   3                   2.7855824
  5   4                  -0.20860153
  6   1                   2.50543308
  6   2                  -0.20132349
  6   3                   1.6123985
  6   4                  -0.2656855
  7   1                   2.30079365
```

```
 7   2                    -0.215182074
 7   3                     0.022293937
 7   4                    -0.210557401
 8   1                     2.03610611
 8   2                    -0.112904787
 8   3                    -0.146735106
 8   4                    -0.155145943
 9   1                     2.57711601
 9   2                     0.565520452
 9   3                     2.45953759
 9   4                     0.471244574
10   1                     2.39547253
10   2                     0.525353965
10   3                     1.41722775
10   4                     0.254606461
11   1                     2.14677620
11   2                     0.451386771
11   3                     0.361610267
11   4                     0.057244U624
12   1                     1.85092545
12   2                     0.493062473
12   3                    -0.045337153
12   4                    -0.141653511
13   1                     2.65626575
13   2                     1.92453937
13   3                     2.67560249
13   4                     1.76107788
14   1                     2.44221306
14   2                     1.74654660
14   3                     1.56670330
14   4                     1.11560345
15   1                     2.14625249
15   2                     1.50512123
15   3                     0.447343111
15   4                     0.460063593
16   1                     1.97851849
16   2                     1.36300617
16   3                    -0.022360125
16   4                    -0.150032776
MODE STRENGTHS ON SAIL=  -1.79975   0.53597   0.44123  -0.25192
TYPICAL TRAILER CONTRACTION TRAJECTORY  0.225  0.216  0.210  0.199  0.190
REAL WAKE TRAILER STRENGTHS FROM SAIL 1
 -1.261 -0.332 -0.326 -0.319 -0.013 -0.007 -0.000  0.006  0.013  0.019  0.026  0.032  0.039  0.046  0.053  0.060
  0.065  0.077  0.087  0.099  0.116  0.142  0.205  0.272
RAW VELOCITY ON RUDDER DUE TO SAIL
 -0.363 -0.617 -0.647 -0.676 -0.726 -1.001 -1.274 -1.379 -1.416 -1.419 -1.393 -1.349 -1.289 -1.215 -1.129 -1.031
 -0.921 -0.801 -0.671 -0.535 -0.396 -0.259 -0.130
POLYNOMIAL COEFFICIENTS FOR RUDDER VEL DUE TO SAIL  -0.96565  -5.94720  21.66938
TRAILER RADII ON R1
 0.009  0.016  0.023  0.030  0.037  0.044  0.051  0.058  0.065  0.072  0.080  0.087  0.094  0.101  0.108  0.115
 0.122  0.129  0.136  0.144  0.151  0.158  0.165  0.172
X LOCATION OF BOUND VORTEX LINES ON R1
 -1.05  -1.06  -1.07  -1.08  -1.09  -1.10  -1.10  -1.11  -1.12  -1.13  -1.14  -1.15
YCP=     0.002 XCP=  -1.13  -1.11  -1.09  -1.07
YCP=     0.063 XCP=  -1.13  -1.11  -1.05  -1.07
YCP=     0.104 XCP=  -1.13  -1.11  -1.09  -1.07
YCP=     0.126 XCP=  -1.13  -1.11  -1.05  -1.07
MODE 1  0.981  0.996  0.998  0.999  1.000  0.996  0.992  0.984  0.973  0.959  0.942  0.921  0.897  0.869  0.836  0.799
 0.756  0.707  0.649  0.581  0.498  0.391  0.229
MODE 2  0.038  0.023  0.008  0.001  0.000  0.005  0.015  0.031  0.051  0.076  0.105  0.139  0.175  0.213  0.251  0.289
```

```
 0.324  0.354  0.376  0.385  0.375  0.331  0.217
N=12 CIRC MODE 1,10.240200.174940.114140.067440.070720.058510.046730.040340.032660.025110.016720.00384
TRAILERS FOR UNIT MODE(1,1) AT BASE(LE,TE) AND TIP(LE,TE)     0.2642     0.9806   -0.0617   -0.2290
VEL AT CP X=  -1.07 Y=  0.085                 0.0422 DUE TO MODE 1,1 BOUND VORTICES
VEL AT SAME POINT DUE TO TRAILERS ON BLADE=         1.0701 AND WAKE=          0.5561 DUE TO UNIT MODE 1,1
VELOCITY AT SAME POINT DUE TO HULL=         3.73504
   1   1                          0.97260380
   1   2                         -0.99501944
   1   3                          6.04307384
   1   4                         -0.62805460 7
   2   1                          0.66171578
   2   2                         -0.69597821 2
   2   3                          4.10459709
   2   4                         -0.70105544 7
   3   1                          6.33108010
   3   2                         -0.75218510 0
   3   3                          1.34676519
   3   4                         -0.55874654 3
   4   1                          5.92332322
   4   2                         -0.56059275 8
   4   3                         -1.39094405
   4   4                         -0.43174272 8
   5   1                          0.35770615
   5   2                         -0.12009026 2
   5   3                          0.20440360
   5   4                         -0.01426300 83
   6   1                          6.11121655
   6   2                         -0.07726016 87
   6   3                          3.70006532
   6   4                         -0.15345265 4
   7   1                          5.61735134
   7   2                         -0.00205487 01
   7   3                          1.11465767
   7   4                         -0.26175741 4
   8   1                          5.47436508
   8   2                          0.10421836 4
   8   3                         -1.46913624
   8   4                         -0.42119652 6
   9   1                          5.96180420
   9   2                          1.37450551
   9   3                          5.87084304
   9   4                          1.36567334
  10   1                          5.72471714
  10   2                          1.32416821
  10   3                          3.47001171
  10   4                          0.06351275 2
  11   1                          5.43667412
  11   2                          1.20601873
  11   3                          1.04646208
  11   4                          0.23995331 8
  12   1                          5.09266308
  12   2                          1.20529366
  12   3                         -1.30686516
  12   4                         -0.32419600 80
  13   1                          5.03133240
  13   2                          3.47222241
  13   3                          5.49050672
  13   4                          3.25860430
  14   1                          5.38217068
  14   2                          3.22205508
```

```
14    3                          3.29458237
14                               2.15015796
15    1                          5.66565285
15    2                          2.95771434
15    3                          1.07602692
15    4                          1.02097034
16    1                          4.67159081
16    2                          2.66221333
16    3                         -1.12376404
16    4                         -0.08860026621
 1                          -2.04045486
 2                          -2.23243715
 3                          -2.44159565
 4                          -2.00618347
 5                          -1.60545230
 6                          -1.77160166
 7                          -1.86725656
 8                          -2.01142653
 9                          -1.48252201
10                          -1.54576555
11                          -1.62362085
12                          -1.70168972
13                          -1.38558368
14                          -1.43190392
15                          -1.48249531
16                          -1.53675276
MODE STRENGTHS OF RI  =  -0.37983   0.12165   0.11383  -0.14017
VELOCITY ON CL DUE TO FIN,RUDDER,FREE STR
 2.591  2.565  2.577  2.561  2.533  2.474  2.356  2.191  2.076  2.022  1.992  1.963
 1.933
SLOPE AT INPUT POINTS
 -0.11  -0.11  -0.11  -0.08  -0.04   0.0    0.03   0.05   0.06   0.08   0.08   0.06
  0.05
```

```
NO. OF STATIONS   13 FREE STREAM FORWARD SPEED   14.772 SWAY VELOCITY    2.000 WATER DENSITY   2.0000
XIN    0.83300   0.66600   0.50000   0.33300   0.16600   0.0      -0.16600  -0.33300
 -0.50000  -0.66600  -0.83300  -1.00000  -1.16600
RIN    0.0        0.07700   0.11000   0.13300   0.14300   0.14700   0.14300   0.13600
  0.12400   0.11000   0.08000   0.05900   0.02300
WAKE AND RUDDER ANGLES                    0.17400                    0.17400            0.0
SAIL AND RUDDER TIP RADII                     0.41400                    0.17200
RUDDER SIDE FORCE        1.025 FIN SIDE FORCE     11.754 SOURCE SIDE FORCE       1.394 TOTAL SIDE FORCE     14.173
RI    MOMENT      1.0947 FIN MOMENT    -0.6900 SOURCE MOMENT     7.2161 DOUBLET MOMENT    -9.0152 TOTAL MOMENT    -1.0064
HEAVE FORCE ON HULL    -5.0780 PITCH MOMENT      3.5545
```